University of California
Santa Barbara

# Quantum Operators in Gravity: from Geometric Entropies to Group-Averaged Observables

A dissertation submitted in partial satisfaction
of the requirements for the degree

Doctor of Philosophy
in
Physics

by

Molly Elizabeth Kaplan

Committee in charge:

Professor Donald Marolf, Chair
Professor Xi Dong
Professor Xiao Luo

September 2024

The Dissertation of Molly Elizabeth Kaplan is approved.

---

Professor Xi Dong

---

Professor Xiao Luo

---

Professor Donald Marolf, Committee Chair

August 2024

Quantum Operators in Gravity: from Geometric Entropies to Group-Averaged Observables



by

Molly Elizabeth Kaplan

*Dedicated to Michael, Sammie, Haley, and my parents—for their unconditional love and support.*

## Acknowledgements

Firstly, thank you to my advisor, Don Marolf, for his endless guidance. At the start of graduate school I was new to high energy theory, and I will never forget how he welcomed me to the field with open arms, always happy to explain even the most basic concepts. Thank you for sharing your wealth of knowledge with all your PhD students. I particularly appreciated your enthusiasm and encouragement of my art of science projects.

Secondly, I would like to thank my collaborators: Jesse Held, Zhencheng Wang, Jieqiang Wu, Xuyang Yu, and Ying Zhao. Thanks especially to Jesse for many hours spent at Old Town Coffee, puzzling through wormhole calculations, and to Ying Zhao for her mentorship. I would also like to thank my other colleagues from UCSB and beyond: Ben Concepcion, Elliott Gesteau, David Grabovsky, Brianna Grado-White, Sergio Hernandez Cuenca, George Hulsey, Maciej Kolanowski, Xiaoyi Liu, Quim Lorens, Alexey Milekhin, Kyle Ritchie, Jon Sorce, Marija Tomasevic, Diandian Wang, Wayne Weng, etc.

Thirdly, thank you to my support network, without whom I could not have made it through graduate school. Thank you to the WiSE and WAGMIP communities; the close friends I made through physics (Rémi Boros, Merrell Brzeczek, Aria Chaderjian, Joe Costello, Kelsey Delk, Jemma Fendley, Paarth Gulati, Rimika Jaiswal, Yonna Kim, Amara McCune, Brad Price, Mathilde Papillon, Otis the Dog, Toshi Parmar, Kailey Schwab, Kathlynn Simotas, Tonda Sojka, Millie Vergara, and Michael Zimet); the triathlon community (Abby Bertics, Chris Cheney, Kat Copeland, Jean Chen, Dixon Atkins, Arturo Juan, Kaitlyn Mullin, Elana Muzzy, Liz Schauer, Johanna Schubert, Zsófia Szegletes, Rohan Thomas, and Alex Zele); and the FSH community, especially the Johnsons.

In addition to the communities above, I would like to give special thanks to Megan

Newsome and Alex Molenaar, who became family throughout my time at UCSB. Thank you to my therapist, Clorinda Rossi-Shewan, for helping me navigate the emotions that come with a PhD program. And thank you to my partner's family—Marian, Lauren, and Brielle—for supporting us both throughout graduate school, and for constantly inspiring me with their intelligence, hard work, and compassion.

My parents have always been my biggest cheerleaders, and I do not know how I can thank them enough for their unending support. They are a primary reason I ended up graduate school: my love of math was fostered early on by my dad, while my mom fostered in me a lifelong love of learning. I would also like to thank my sister, Haley, for being my best friend and my inspiration for completing my PhD. It was truly a gift getting to spend two years at UCSB with you, and I am so proud of all you have accomplished.

Lastly, thank you to Sammie the Dog, the best boy in the world, and to my partner, Dr. Michael Choquer. Meeting you was the highlight of graduate school, and since then your kindness and love have buoyed me on the most difficult of days. When I spent months searching for a missing minus sign, or when the stress of postdoctoral applications became too much, you were always by my side. Your future is so bright, and I cannot wait to live that future together.

# Curriculum Vitæ

Molly Elizabeth Kaplan

## Education

| | |
|---|---|
| 2024 | Ph.D. in Physics (Expected), University of California, Santa Barbara. |
| 2022 | M.A. in Physics, University of California, Santa Barbara. |
| 2019 | B.S. in Physics and Mathematics, Massachusetts Institute of Technology |

## Publications

1. J. Held, M. Kaplan, D. Marolf, and J. qiang Wu, *Link-area commutators in ads$_3$ area-networks*, arXiv:2401.0248 [1]
2. M. Kaplan, *The action of geometric entropy in topologically massive gravity*, *Journal of High Energy Physics* **2023** (Dec., 2023) 106, [arXiv:2308.0976] [2]
3. M. Kaplan and D. Marolf, *The action of HRT-areas as operators in semiclassical gravity*, *Journal of High Energy Physics* **2022** (aug, 2022) [arXiv:2203.0427] [3]
4. M. Kaplan, D. Marolf, Z. Yu, and Y. Zhao, "De Sitter quantum gravity and the emergence of local algebras." to appear [4]
5. J. Held, M. Kaplan, D. Marolf, and Z. Wang, "Do Euclidean Wormhole Saddles Contribute to the Factorization Problem?." to appear [5]

**Abstract**

Quantum Operators in Gravity: from Geometric Entropies to Group-Averaged Observables

by

Molly Elizabeth Kaplan

In this thesis, we first study the action of Hubeny-Rangamani-Takayanagi (HRT) area operators on the covariant phase space of classical solutions in Einstein-Hilbert gravity. We find that this action is a boundary-condition-preserving kink transformation, which introduces a relative boost between the entanglement wedges on either side of the HRT-surface but preserves the asymptotically Anti-de Sitter (AdS) boundary conditions. We then perform a similar analysis for the "geometric entropy", i.e. the bulk dual to boundary entanglement entropy, in topologically massive gravity (TMG). Here, the geometric entropy is given by the HRT-area plus an anomalous contribution. We find that the action of this geometric entropy on the covariant phase space of classical solutions agrees precisely with the action of HRT-area operators in Einstein-Hilbert gravity.

In Einstein-Hilbert gravity, we show that HRT-areas do not generally commute. This poses an obstruction to constructing random tensor networks (RTNs), which are most analogous to fixed-area states of the bulk quantum gravity theory, with mutually commuting HRT-areas. We probe the severity of such obstructions in pure $AdS_3$ Einstein-Hilbert gravity by constructing networks whose links are codimension-2 extremal-surfaces and by explicitly computing semiclassical commutators of the associated link-areas. We find a simple 4-link network for which all link-areas commute, but the algebra generated by the link-areas of more general networks tends to be non-Abelian.

In the final chapter, we switch gears and explore perturbative quantum gravity around

de Sitter space, where gauge-invariant observables cannot be localized and, instead, local physics can arise only through certain relational constructions. In particular, we describe a class of gauge-invariant observables which, under appropriate conditions, provide good approximations to certain algebras of local fields. Our results suggest that, near any minimal $S^d$ in $dS_{d+1}$, this approximation can be accurate only over regions in which the corresponding global time coordinate $t$ spans an interval of order $\Delta t \lesssim \ln G^{-1}$. In contrast, however, we find that the approximation can be accurate over arbitrarily large regions of global $\mathrm{dS}_{d+1}$ so long as those regions are located far to the future or past of such a minimal $S^d$. This in particular includes arbitrarily large parts of any static patch.

# Contents

# Chapter 1

# Introduction

Physics has born witness to many paradigm shifts throughout history. Just over a hundred years ago the theory of general relativity upended Newtonian gravity, and, over the past century, quantum mechanics has been reconciled with special relativity, producing quantum field theory. Still eluding us, however, is a theory of quantum gravity—the weaving together of general relativity and quantum mechanics—which promises to transform our current understanding of the nature of spacetime.

Despite the great difficulty of formulating a theory of quantum gravity, there has been much progress made in recent years, even just over the course of my PhD. One of the most fundamental advances during this time was a potential resolution to the long-standing black hole information paradox: black holes radiate [6] and can eventually radiate away into a thermal gas, losing information about the initial state of the black hole and violating quantum-mechanical unitarity. In [7, 8, 9], a resolution was found in which unitarity was restored. In particular, in [9], the calculation proceeded by introducing special types of wormholes into a calculation of the black hole's entropy (the "replica trick"). These wormholes can be thought of as a calculational tool, but there was also progress made over the last five years in understanding the stability and relevance of

physical wormholes, in, e.g., [10, 11, 12, 13, 14, 15, 16, 17, 18, 19]. There has also been significant progress made in understanding, for example, low-dimensional gravitational theories (see [20] and references therein, especially [21, 22, 23, 24, 25, 26, 27] among many others); the application of tensor networks to holography (e.g., [28, 29, 30, 31, 32, 33]), as will be reviewed in Section 1.1.2; and, most recently, algebras of observables in different gravitational backgrounds, as in, for example, [34, 35, 36, 37, 38, 39, 40, 41, 42, 43, 44, 45, 46]. This list is non-exhaustive, but gives a flavor of the amount of growth the field has seen in recent years.

In this thesis, I present my work about different types of quantum operators in gravitational backgrounds. We first focus on the area operator, or more generally the "geometric entropy" operator. To understand why these geometric entropies are important, we will introduce in Section 1.1 the Anti-de Sitter/Conformal Field Theory (AdS/CFT) correspondence, where, in the semiclassical limit of AdS/CFT, entropies of boundary regions are described by this geometric entropy operator. In Chapters 2-4, we explore the properties of this operator, studying commutators with this operator and the way that the operator acts on semiclassical bulk geometries. The goal is to provide new (and more geometric) tools with which to study entropy in quantum gravity.

Though the bulk of my work takes place in Anti de Sitter space, Chapter 5 of this thesis is about quantum operators in de Sitter (dS) space. We will investigate the Hilbert space of observables in dS, which must be defined relative to some reference state and where we must carefully consider the effect of gauge symmetries in spacetime. We seek to understand where the states in the observable Hilbert space can no longer be described by the framework of QFT in curved spacetime, i.e. where leading-order quantum gravitational effects become important. This gives important intuition behind the physics of quantum operators in perturbative gravity about a dS background, with potential implications for the study of quantum operators in cosmology. To preface this work, in Section

1.2 we will take a brief look into the importance and challenges of quantum gravity in dS.

## 1.1 The Holographic Principle

The holographic principle is a proposal that the information contained in a region of spacetime is completely reproduced on the boundary of that region. This principle is known to be true for certain spacetime regions in (quantum) gravity. For example, it has been known since the 1970s that the entropy of a black hole is given by the area of its horizon: $S_{BH} = \frac{A}{4G}$ [47, 6]. It was then conjectured that the holographic principle should hold more generally [48, 49, 50]. A few years later came a concrete instance of this principle, in which [51] conjectured a duality between an eleven-dimensional theory of quantum gravity and a particular limit of a matrix quantum mechanics. Soon after came the AdS/CFT correspondence [52], which is of vast importance to our field as it is the only UV-complete theory of quantum gravity.

Starting with some number $N$ of D3-branes, [52] showed that one can take a large $N$ and small string coupling limit to either get Type IIB string theory in $\mathrm{AdS}_5 \times S^5$, or $\mathcal{N} = 4$ supersymmetric Yang-Mills, a conformally invariant gauge theory. AdS is a spacetime with an asymptotic boundary, and we can think of the CFT as being contained on this boundary. This correspondence has also been shown to hold for AdS and CFTs in other dimensions, and is expected to hold in general for $\mathrm{AdS}_{d+1}$ (times some hypersphere) dual to $\mathrm{CFT}_d$. This is especially motivated by the fact that the isometry group of $\mathrm{AdS}_{d+1}$ is the same as the conformal group in one lower dimension. The conjecture is also expected to hold for general string coupling and $N$, though we often taken the large $N$ limit, where Newton's constant $G$ goes to zero. This gives us semiclassical gravity, where we treat spacetime as classical but quantize any matter fields present. In this thesis we

consider the semiclassical gravity approximation, or, in Chapter 5, we take the further approximation of QFT in curved spacetime.

The Hilbert spaces of the theories on both sides of the duality should match, $\mathcal{H}_{AdS} = \mathcal{H}_{CFT}$, but this does not a priori tell us which elements within each Hilbert space should be equivalent. However, it has been shown that there is a dictionary between bulk fields in AdS—or correlators of these fields—and (correlators of) boundary CFT operators, though the boundary operators can only be reconstructed using bulk fields in certain regions of spacetime [53, 54, 55, 56, 57, 58, 59, 60]. Additionally, like the Bekenstein-Hawking entropy of black holes, it has been well established that there is a more general duality between boundary entanglement entropies and areas of surfaces in the bulk theory, which we will review shortly. Relatedly, another important tool for understanding the mapping between spacetime geometry and boundary entanglement are tensor networks, which we discuss in more detail below.

### 1.1.1 Geometric Entropies

The duality between bulk areas and boundary entropies started with the Ryu-Takayanagi (RT) formula. Restricting to a time-symmetric slice of AdS, we have a boundary subregion $R$, and a family of bulk surfaces which are anchored to the boundaries of $R$ and are homologous to $R$. If we use $\gamma$ to label the bulk surface with minimal area, then the RT formula states that the entanglement entropy of $R$ is directly proportional to the area of $\gamma$ [61, 62]:

$$S[R] = \frac{A[\gamma]}{4G}. \tag{1.1}$$

See Figure 1.1 for a diagram of an example $R$ and $\gamma$.

The RT formula was then made covariant in the Hubeny-Rangamani-Takayanagi (HRT) formula [63], in which we are no longer restricted to one achronal slice $\Sigma$ of AdS.

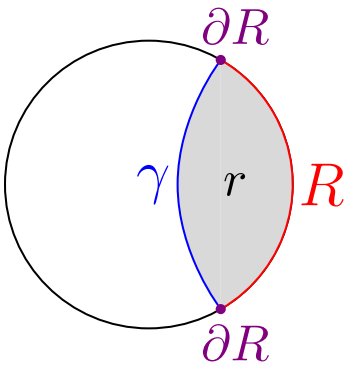


Figure 1.1: For $R$ on the boundary of an $AdS_3$ constant-time slice, the RT surface is given by $\gamma$, the surface with minimal area that is anchored to $\partial R$. The surface $\gamma$ divides the slice into two regions, and we label the region between $\gamma$ and the boundary as $r$.

Now, we find the surface $\gamma$ by minimizing the surface's area over some $\Sigma$ containing $R$, then maximizing its area with respect to different $\Sigma$ [64]. Thus, the HRT surface is called an extremal surface. The RT formula was proven by [65], using the same replica trick we mentioned earlier, and in [66] the authors used a Lorentzian version of this trick to prove the HRT formula.

If we are more careful, it turns out that the entanglement entropy of a boundary subregion is not simply given by the area of an extremal surface. Instead, there are quantum corrections to this formula, given by the entanglement entropy of quantum fields in the region $r$, bounded by $\gamma$ and $R$ (as shown in Figure 1.1). There are also so-called "Wald-like" corrections, which will be important when we consider a higher-derivative theory of gravity in Chapter 3. In [67] the authors showed $S[R]$ is dual to the area of the extremal surface plus these quantum corrections; this was then revised in [68], where it was shown that one must take the extremization *after* the quantum corrections are included.

In this paper, and especially in Chapter 3, we will often call the bulk dual to boundary entanglement entropy the "geometric entropy." In situations where the quantum

corrections are unimportant, we will instead refer to these bulk duals as HRT-areas.

### 1.1.2 Tensor Networks

Tensor networks (TNs) have played an important role across many disciplines in physics and beyond. In our field, they can be used to model the AdS/CFT correspondence. There have been many types of TNs that have been used to model AdS/CFT (see, e.g., [69, 70, 71, 72]), but they all follow a version of the RT formula called the "Swingle bound" [73, 74] where there exists a minimum area bulk graph that bounds the entanglement entropy of a boundary subregion. TNs also have similar quantum error correction properties to AdS/CFT, where bulk operators are protected from errors by their encoding in the CFT.

Despite the similarities between tensor networks and the AdS/CFT correspondence, [75] noted there is a potential obstruction to taking TN models too seriously: TNs have a flat entanglement spectrum, i.e. their Renyi entropies $S_n(\rho) = -\frac{1}{n-1}\log \mathrm{Tr}(\rho^n)$ for any quantum state $\rho$ are independent of $n$. This is not what is expected for typical gravitational states. There are, however, less typical gravitational states that do have a flat entanglement spectrum, as shown by [76, 77]. These are fixed-area states, where the area of a surface in the bulk (e.g., an RT-surface) has been fixed to a certain value. Taking this relationship between TNs and fixed-area states seriously, as in [78, 28], one can construct a network of surfaces on a Cauchy slice, which then serves as the dual graph to a tensor network. Each leg of the TN corresponds to a contracted index, determined by the (exponential of) the area of the corresponding dual surface.

A drawback of this construction is that we must specify the area of many surfaces at once, and this will not always be possible: if we take the area of these surfaces to be a quantum operator, there may be nontrivial commutation relations between areas of

different surfaces. The commutation relation between two HRT-areas will be computed in Chapter 2. Then, in Chapter 4, we look at the commutation relations of more general surfaces in gravity, particularly ones that make an intersecting network of surfaces that could be used to define a tensor network. We find that these commutation relations indeed pose a significant hurdle to constructing area networks.

## 1.2 Quantum Gravity without Holography

In Chapter 5, we will no longer rely on the AdS/CFT correspondence, and will instead consider quantum operators in de Sitter (dS) space. Though quantum gravity in dS is not as well understood as quantum gravity in AdS, it is much more relevant to our own universe. In the distant past, our universe underwent a period of exponential expansion, called inflation, which is well-modelled by dS. Additionally, our universe's cosmological constant is positive [79], indicating that we are approaching a de Sitter-like phase in the future. It is thus important to understand quantum gravity in dS, despite the fact that we do not have a well-established holographic principle in dS.

Though there have been many attempts to apply the holographic principle to de Sitter [80, 81, 82, 83, 84, 85, 86, 87, 88, 89, 90, 91, 92], there has yet to be a widely accepted, string-theory derived proposal for a non-gravitational dual to dS space. The lack of a timelike boundary makes this especially difficult. Furthermore, besides the absence of a holographic principle, there are other hurdles to overcome in understanding quantum gravity in de Sitter. Whether one can construct dS vacua in string theory remains an open question [93, 94, 95], though there has been recent progress constructing candidate vacua [96]. Additionally, a form of Gauss's Law applies in perturbative gravity about dS: since dS has compact Cauchy surfaces, there is nowhere for flux to escape, and so the charges associated with the spacetime symmetries must vanish. This then means

states have to be invariant under these symmetries, but since the symmetry group is non-compact this leaves only the vacuum state.

Moreover, if we wish to consider a Hilbert space of observers and observables in de Sitter, we run into two issues. The first is that dS observers cannot be separated from the gravitational system (this is unlike in AdS when we can take observers to live on the boundary, in the non-gravitating region). Second, at late times in dS, a virtual observer can thermally fluctuate into existence and make an observation. This is called the Boltzmann brain phenomenon [97, 98, 99, 100], and it means local observables are not well defined as the Boltzmann brains will cause their two-point functions to diverge [101, 102].

In Chapter 5, we introduce a framework that avoids many of these hurdles. To create dS invariant states besides the vacuum, we use a technique called group averaging. Additionally, we include an observer in our framework, and we make the observer non-local to avoid the Boltzmann brain problem. Our research is part of a renewed interest in the field to understand quantum observables in de Sitter and cosmology [39, 45, 46, 103].

## 1.3 Outline

In Chapter 2, we study HRT-area operators and their action on the surrounding spacetime. It has been previously proposed that this action generates a transformation which, roughly speaking, boosts the entanglement wedge on one side of the HRT surface relative to the entanglement wedge on the other side. We give a sharp argument for a precise result of this form in a general theory of Einstein-Hilbert gravity minimally coupled to matter, taking appropriate care with asymptotically Anti-de Sitter (AdS) boundary conditions. The result agrees with direct computations of commutators involving HRT areas in pure 2+1 dimensional Einstein-Hilbert gravity on spacetimes asymptotic to pla-

nar AdS. We also clarify the sense in which this transformation is singular in the deep UV when the HRT-surface is anchored to an asymptotically AdS boundary.

Then, in Chapter 3, we consider geometric entropies in topologically massive gravity (TMG), a higher-derivative theory which is the gravitational dual to a chiral boundary CFT. Due to the presence of a gravitational anomaly in TMG, the geometric entropy is no longer simply the Hubeny-Rangamani-Takayanagi (HRT) area; instead, it is given by the HRT area plus an anomalous contribution. We study the action of this geometric entropy on the covariant phase space of classical solutions for TMG with matter fields whose action is algebraic in the metric. We show that the action agrees precisely with the action of HRT-area operators in Einstein-Hilbert gravity given in Chapter 2. Furthermore, we show our result to be consistent with direct computations of semiclassical commutators of geometric entropies in pure TMG spacetimes asymptotic to planar AdS, as computed in [104].

In Chapter 4, we build on the results of Chapter 2, in which we showed area operators do not necessarily commute. As reviewed above, standard random TNs are most analogous to fixed-area states of the bulk quantum gravity theory, in which quantum fluctuations have been suppressed for the area of the corresponding HRT surface. This is due to their flat entanglement spectra when discussing a given boundary region $R$ and its complement $\bar{R}$. However, such TNs have flat entanglement spectra for all choices of $R, \bar{R}$, while quantum fluctuations of multiple HRT-areas can be suppressed only when the corresponding HRT-area operators mutually commute. We probe the severity of such obstructions in pure $AdS_3$ Einstein-Hilbert gravity by constructing networks whose links are codimension-2 extremal-surfaces and by explicitly computing semiclassical commutators of the associated link-areas. Since $d = 3$, codimension-2 extremal-surfaces are geodesics, and codimension-2 'areas' are lengths. We find a simple 4-link network defined by an HRT surface and a Chen-Dong-Lewkowycz-Qi [105] constrained HRT surface for

which all link-areas commute. However, the algebra generated by the link-areas of more general networks tends to be non-Abelian. One such non-Abelian example is associated with entanglement-wedge cross sections and may be of more general interest.

Chapter 5 is quite different from the rest of this thesis, as we switch from considering Anti-de Sitter to de Sitter. In de Sitter (dS), observers cannot be treated as separate from the rest of spacetime, and hence observables are inextricably linked to their observers. We emphasize here that observers must also be treated using QFT. We then explore how well spaces of states and observables, each defined relative to a QFT observer, approximate standard non-gravitating QFT in a fixed dS background. We take into account that perturbative gravity in global dS requires states to be invariant under the dS isometries. This, however, leaves too few states, and so we build a new Hilbert space using group averaging. We study 1+1 dS with a one-particle observer in each static patch, where the observers lie on a minimal $S^1$. In this context we find that QFT in curved space is only a good approximation in a spacetime volume proportional to 1/G. Adding additional particles along a timelike path does not seem to increase the size of this "good" region, and we find similar results in general dimensions. However, if we consider regions far to the future or past of a minimal $S^d$ in $\mathrm{dS}_{d+1}$, then we find that the approximation can be accurate over arbitrarily large regions of global $\mathrm{dS}_{d+1}$.

Finally, Appendix G details two artistic projects related to my research, both submitted to UCSB CSEP's Art of Science competition. The first, *A Wormhole Lullaby*, is a painting and musical composition following some of the calculations computing the entropy of a black hole in [9]. The second, *The Dance of the Qutrits*, is a painting and musical composition on the three qutrit code [106], which is a simple quantum error correcting code.

## 1.4 Permissions and Attributions

1. The content of Chapter 2 and Appendix A is the result of a collaboration with Donald Marolf, and has previously appeared in the Journal of High Energy Physics [3]. It is reproduced here with the permission of the International School of Advanced Studies (SISSA): `http://jhep.sissa.it/jhep/help/JHEP/CR_OA.pdf`.

2. The content of Chapter 3 has previously appeared in the Journal of High Energy Physics [2]. It is reproduced here with the permission of the International School of Advanced Studies (SISSA): `http://jhep.sissa.it/jhep/help/JHEP/CR_OA.pdf`.

3. The content of Chapter 4 and Appendices B, C and D is the result of a collaboration with Jesse Held, Donald Marolf, and Jie-qiang Wu, and has been accepted to appear in the Journal of High Energy Physics [1]. It is reproduced here with the permission of the International School of Advanced Studies (SISSA): `http://jhep.sissa.it/jhep/help/JHEP/CR_OA.pdf`.

4. The content of Chapter 5 is a work-in-progress, and is the result of collaboration with Donald Marolf, Xuyang Yu, and Ying Zhao.

# Chapter 2

# The Action of HRT-Areas as Operators in Semiclassical Gravity

## 2.1 Introduction

A fundamental aspect of gauge-gravity duality is the relation between gauge theory entropies and the areas of codimension-2 bulk extremal surfaces described by the Ryu-Takayanagi (RT) correspondence [61, 62] and its covariant Hubeny-Rangamani-Takayanagi (HRT) generalization [63]. The quantity $A_{HRT}[R]$ defined by computing the area of the HRT surface associated with an appropriate boundary region $R$ may thus be expected to be of great interest in the bulk theory, even without reference to the gauge theory dual.

At the classical level in the bulk, we can think of this $A_{HRT}[R]$ as a function on the space of solutions or, equivalently, on either the canonical or covariant phase space. At the quantum level, it should define a corresponding quantum operator. The purpose of this work is to better explore the commutation relations of such operators, either with themselves or with other objects of interest. We will work at leading order in the bulk

semiclassical approximation, where such commutators are described by Poisson brackets, or equivalently by Peierls brackets [107] up to the usual factor of $i$.

There is in fact a lengthy history of suggestions that taking brackets with $A_{HRT}[R]$ should generate a transformation closely related to the boost symmetry of a Rindler wedge in Minkowski space. Indeed, long before the days of gauge/gravity duality it was noted in various contexts that the area of black hole horizons seemed to generate such transformations; see especially [108], but similar observations are implicit in [109, 110, 111].

Later, in the context of gauge/gravity duality, analogous suggestions for general HRT-areas $A_{HRT}[R]$ were motivated in [112, 113, 44, 114, 115] by comparison with modular Hamiltonians, as the latter are again known to act as boosts in appropriate circumstances; see in particular [116] and [105]. In many cases this analogy was based on the Jafferis-Lewkowycz-Maldacena-Suh (JLMS) relation explicitly relating bulk areas to modular Hamiltonians in the gauge theory [117]. Furthermore, in a parallel series of developments, various related results [118, 119, 120] were established in contexts where boundary conditions are imposed at finite-distance boundaries. In particular, when the boundary is an appropriate bifurcate null surface, the area of the bifurcation surface is known to generate a boost-like symmetry of the associated gravitational system.

Nevertheless, despite the long list of closely related results and arguments given above, it appears that a direct analysis of the action of $A_{HRT}[R]$ on the gravitational phase space has yet to be performed. Here we are explicitly interested in the case where the relevant HRT surface $\gamma_R$ is determined dynamically and lives in the interior of the system, as opposed to being specified by hand to live on a finite-distance boundary. Our work will fill this gap and then study the implications for simple commutators involving HRT-areas.

In doing so, we will also give proper consideration to the asymptotically AdS boundary conditions that are of primary interest in the RT and HRT correspondences. In partic-

ular, in the presence of an asymptotically AdS boundary, the area of a codimension-2 surface anchored to the boundary will generally diverge. In order to discuss finite quantities, in that context we use $A_{HRT}$ below to denote the renormalized HRT-area given by introducing a cutoff $\epsilon$, subtracting an appropriate covariant counterterm from the naive area, and then sending $\epsilon \to 0$. Since the counter-term is a $c$-number, this object generates the same Hamiltonian flow as the naive (unrenormalized) HRT-area. One should also be aware that, as a result of this renormalization, in even boundary dimensions our $A_{HRT}$ will transform anomalously under conformal transformations. In contrast, when the boundary anchors are the empty set, no renormalization is needed and we use $A_{HRT}$ to denote the naive area of the HRT surface.

We begin in section 2.2 with a direct computation of the flow generated by $A_{HRT}[R]$ using the canonical formalism of Einstein-Hilbert gravity with arbitrary minimally coupled matter. We study the action of this flow on the initial data on a Cauchy slice $\Sigma$ that runs through the HRT surface $\gamma_R$, showing that it leaves the induced metric unchanged and that it shifts one component of the extrinsic curvature by a delta-function at $\gamma_R$. This result was predicted in [114, 115], where it was argued to correspond to an operation that, in an appropriate sense, boosts the entanglement wedge of $R$ relative to that of the complementary region $\bar{R}$. As a result, on such Cauchy surfaces HRT-area flow also agrees in the bulk with the 'kink transformation' introduced in [115], though (as we review) the two act differently in both the past and future of the HRT surface $\gamma_R$.

The above results and relations are then used in section 2.3 to derive explicit formulae for the action of HRT-area flow on the $AdS_3$ Poincaré vacuum, and in particular to study the action on the boundary stress tensor and on other HRT areas evaluated on that solution. A particular result is that, while an explicit such flow can be defined for any HRT surface $\gamma_R$, the flow turns out to cause the total energy to diverge when $\gamma_R$ has non-trivial anchors on the AdS boundary. This is a concrete manifestation of the UV

issues foreshadowed in [113, 44, 114].

For comparison, section 2.4 then provides an independent computation of the associated commutators evaluated on general solutions of pure 2+1 Einstein-Hilbert gravity asymptotic to Poincaré $AdS_3$. Instead of using the canonical commutation relations in the bulk, this latter approach is based on the fact that the above solutions can be constructed by acting on the Poincaré vacuum with boundary conformal transformations. From this it follows that any observable can be expressed in terms of the boundary stress tensor, so that the stress tensor algebra can be used to compute general commutators. We close with some final comments and future directions in section 2.5.

## 2.2 HRT-area flow as a boundary-condition-preserving kink transformation

We now derive the Hamiltonian flow generated by HRT-area operators by directly computing Poisson/Peierls brackets in asymptotically $AdS_D$ Einstein-Hilbert gravity. In the rest of this work we refer to such brackets as "semiclassical commutators" despite the lack of a factor of $i = \sqrt{-1}$. The commutators for which such computations are straightforward will in fact describe the effect of HRT-flow on certain Cauchy data for the solution, whence the action on the full solution is to be determined by solving the equations of motion. We thus begin by studying the effect on the desired Cauchy data in section 2.2.1. Section 2.2.2 then addresses details of the boundary conditions which determine the full solution. Finally, section 2.2.3 will discuss the relation to the kink transformation of [115], which will be useful in deriving further explicit results in section 2.3.

As usual, we take the HRT surface $\gamma_R$ to be defined by some region $R$ on the asymp-

totically $\mathrm{AdS}_D$ boundary. In particular, $R$ is an achronal surface on the boundary and $\gamma_R$ is a codimension-2 extremal surface in the bulk that is anchored to the boundary $\partial R$ of $R$. Since $\gamma_R$ is an HRT surface, it is in fact the smallest such extremal surface satisfying the homology constraint of [121]. The area of $\gamma_R$ thus defines a function on the space of solutions that we may call $A_{HRT}[R]$.

Equivalently, we may think of $A_{HRT}[R]$ as a function on the covariant or canonical gravitational phase space. To maximize accessibility to most readers, we will take the canonical perspective below. Since our argument in this section is based solely on the canonical commutation relations of Einstein-Hilbert gravity, all results in this section remain valid in the presence of arbitrary minimally-coupled matter fields.

### 2.2.1 HRT-area flow on a Cauchy surface containing $\gamma_R$

The object $A_{HRT}[R]$ is of course fully determined by the spacetime metric $g$. However, in practice it can useful to evaluate $A_{HRT}[R]$ in two steps, first finding the extremal surface $\gamma_R$ and then computing the area of $\gamma_R$. In reference to this two-step process, we will write $A_{HRT}[R] = A[\gamma_R, g]$. In particular, in this way we can think of $A_{HRT}[R]$ as a special case of a more general functional $A[\gamma, g]$ which would compute the area of an arbitrary surface $\gamma$, and where $A_{HRT}$ is obtained from $A[\gamma, g]$ by choosing $\gamma = \gamma_R$ as defined by the given metric $g$. We can make this very explicit by writing

$$A_{HRT}[R] = A[\gamma, g]|_{\gamma=\gamma_R[g]}. \tag{2.1}$$

The fact that $\gamma_R$ is an extremal surface means that, if we fix the spacetime metric $g$

and vary $A[\gamma, g]$ with respect to $\gamma$, the result vanishes when evaluated at $\gamma = \gamma_R$:

$$\left.\frac{\delta A[\gamma, g]}{\delta \gamma}\right|_{\gamma=\gamma_R[g]} = 0. \tag{2.2}$$

The relation (2.2) will enter in a critical way into our derivation of HRT-area flow below. The key point that allows it to be useful is that semiclassical commutators are defined by the Poisson Bracket (or equivalently by the Peierls Bracket [107]), which satisfies the Leibniz rule

$$\{B, C\} = B_{,I} C_{,J} \{\zeta^I, \zeta^J\}, \tag{2.3}$$

where the $\zeta^I$ are any set of coordinates on phase space and where $B_{,I}$ and $C_{,J}$ denote appropriate (perhaps functional) derivatives of $B, C$ with respect to such coordinates. Setting $B = A_{HRT}[R]$, we may evaluate its $\zeta^I$ derivatives by first separately varying $A[\gamma, g]$ with respect to $\gamma$ and $g$ and then using the chain rule to relate variations of $\gamma$ and $g$ to variations of the $\zeta^I$. We thus write

$$\frac{\delta}{\delta \zeta^I} A_{HRT}[R] = \left.\frac{\delta A[\gamma, g]}{\delta \gamma}\right|_{\gamma=\gamma_R[g]} \frac{\delta \gamma_R[g]}{\delta \zeta^I} + \left.\frac{\delta A[\gamma, g]}{\delta g}\right|_{\gamma=\gamma_R[g]} \frac{\delta g}{\delta \zeta^I}. \tag{2.4}$$

The notation implies an appropriate summation over the degrees of freedom associated with the surface $\gamma$ and the spacetime metric $g$. In particular, the last term in (2.4) includes both a sum over components of $g$ at each spacetime point and an integral over spacetime points.

Since the first term in (2.4) vanishes due to (2.2), we are left only with the second. This is precisely the statement that semiclassical commutators of $A_{HRT}$ can be computed as if the surface $\gamma_R$ were fixed and did not in fact depend on the phase space coordinates $\zeta^I$. In other words, it suffices to compute commutators with $A[\gamma, g]$ for some fixed $\gamma$ (say, given by certain coordinate conditions) and then to simply set $\gamma = \gamma_R$ at the

end of the calculation. Note that the final result after setting $\gamma = \gamma_R$ will describe a flow generated by a diffeomorphism-invariant observable, and will thus necessarily map solutions to solutions, even if this is not manifest in the intermediate steps. In particular, in the language of the Hamiltonian formalism, the final flow will necessarily preserve all constraints.

Indeed, since $\gamma_R$ is spacelike, in the canonical formalism we are free to simply suppose that we are given a Cauchy surface $\Sigma$ and a fixed submanifold $\gamma \subset \Sigma$. We may then take our phase space coordinates $\zeta^I$ to be the induced metric $h_{ij}$ on $\Sigma$ and the (undensitized) gravitational momentum $\Pi^{ij} = \frac{1}{16\pi G}(K^{ij} - Kh^{ij})$, where $K^{ij}$ is the extrinsic curvature of $\Sigma$ and $K = K^{ij}h_{ij}$. Such phase space coordinates have the standard Poisson Brackets

$$\begin{aligned} \{h_{kl}(x), h^{ij}(y)\} =& 0, \\ \{h_{kl}(x), \Pi^{ij}(y)\} =& \frac{1}{\sqrt{h(y)}} \delta^i_{(k}\delta^j_{l)}\delta^{(D-1)}(x-y), \end{aligned} \tag{2.5}$$

where $x^i$ (or equivalently $y^j$) denotes $D-1$ coordinates on $\Sigma$ and we have used the standard Dirac delta function in terms of the coordinates $x, y$.

Since we choose $\gamma \subset \Sigma$, our $A[\gamma, g]$ will be independent of $\Pi^{ij}$ and will depend only on $h_{ij}$. Thus $A[\gamma, g]$ commutes with $h_{ij}$ at leading order in the semiclassical expansion, and the leading semiclassical commutator of $A[\gamma, g]$ with any function is determined by $\{A[\gamma, g], \Pi^{ij}\}$, or equivalently by $\{A[\gamma, g], K^{ij}\}$. We shall keep only such leading-order terms below.

Let us consider the bracket with $K^{ij}$, as it will turn out to yield a geometric interpretation of the flow generated by $A_{HRT}[R]$. Using

$$K^{ij} = 16\pi G\left(\Pi^{ij} + \frac{1}{2-D}\Pi h^{ij}\right) \tag{2.6}$$

with $\Pi = \Pi^{ij} h_{ij}$, one finds

$$\begin{aligned}\{h_{kl}(x), K^{ij}(y)\} =& \frac{16\pi G}{\sqrt{h(y)}} \delta^{(D-1)}(x-y) \left( \delta^i_{(k} \delta^j_{l)} - \frac{1}{D-2} \delta^m_{(k} \delta^n_{l)} h_{mn}(y) h^{ij}(y) \right) \\ =& \frac{16\pi G}{\sqrt{h(y)}} \delta^{(D-1)}(x-y) \left( \delta^i_{(k} \delta^j_{l)} - \frac{1}{D-2} h_{kl}(y) h^{ij}(y) \right).\end{aligned} \tag{2.7}$$

We then need only combine this with a computation of derivatives of $A[\gamma, g]$ with respect to the induced metric. Proceeding in steps, we introduce the induced metric $q_{AB}$ on $\gamma$ and $D-2$ coordinates $w^A$ on $\gamma$ to write

$$A_{HRT} = \int_\gamma d^{D-2} w \sqrt{q(w)}. \tag{2.8}$$

Taking functional derivatives yields

$$\frac{\delta A_{HRT}}{\delta h_{kl}(x)} = \frac{1}{2} \int_\gamma d^{D-2} w \sqrt{q(w)} q^{AB}(w) \frac{\delta q_{AB}(w)}{\delta h_{kl}(x)}. \tag{2.9}$$

Now, since $q_{AB}(w) = \frac{\partial x^i}{\partial w^A} \frac{\partial x^j}{\partial w^B} h_{ij}(x)$ (with derivatives computed along $\gamma$), we can rewrite $q_{AB}$ as

$$\begin{aligned} q_{AB}(w) &= \int_\gamma d^{D-2} \tilde{w} \frac{\partial x^i}{\partial \tilde{w}^A} \frac{\partial x^j}{\partial \tilde{w}^B} h_{ij}(x(\tilde{w})) \delta^{(D-2)}_\gamma(w, \tilde{w}) \\ &= \int_\Sigma d^{D-1} x \frac{\partial x^i}{\partial \tilde{w}^A} \frac{\partial x^j}{\partial \tilde{w}^B} h_{ij}(x)\ \delta^{(D-2)}_\gamma(w, \tilde{w}(x))\ \delta_\Sigma(\gamma, x) \end{aligned} \tag{2.10}$$

where $\delta^{(D-2)}_\gamma(w, \tilde{w}(x))$ is a $\delta$-function on the HRT surface that satisfies

$$\int_\gamma d^{D-2} w\ f(w) \delta^{(D-2)}_\gamma(w, \tilde{w}) = f(\tilde{w}), \tag{2.11}$$

and where $\delta_\Sigma(\gamma, x)$ is a $\delta$-function on the Cauchy slice that localizes $x$ to the HRT surface according to $\int_\Sigma d^{D-1} x f(x) \delta_\Sigma(\gamma, x) = \int_\gamma d^{D-2} w f(x(w))$. We have also arbitrarily

extended $\tilde{w}$ and $\frac{\partial x^i}{\partial \tilde{w}^A}$ to smooth functions of the $x^i$ defined on all of $\Sigma$, though due to the delta-functions the result does not depend on the particular extension chosen. We thus find

$$\frac{\delta q_{AB}(w)}{\delta h_{kl}(x)} = \frac{\partial x^k}{\partial \tilde{w}^A}\frac{\partial x^l}{\partial \tilde{w}^B}\ \delta_\gamma^{(D-2)}(w, \tilde{w}(x))\ \delta_\Sigma(\gamma, x). \tag{2.12}$$

Finally, combining equations (2.7), (2.9) and (3.10) yields

$$\left\{\frac{A_{HRT}}{4G}, K^{ij}(x)\right\} = 2\pi\frac{\sqrt{q(\tilde{w}(x))}}{\sqrt{h(x)}}\delta_\Sigma(\gamma, x)\left(q^{AB}(\tilde{w}(x))\frac{\partial x^i}{\partial \tilde{w}^A}\frac{\partial x^j}{\partial \tilde{w}^B} - h^{ij}(x)\right) \tag{2.13}$$

$$= -2\pi\hat{\delta}_\Sigma(\gamma, x)\ \perp^i\perp^j\ . \tag{2.14}$$

where $\perp^i$ is the unit normal to $\gamma$ in $\Sigma$ and $\hat{\delta}_\Sigma(\gamma, x) = \frac{\sqrt{q(\tilde{w}(x))}}{\sqrt{h(x)}}\delta_\Sigma(\gamma, x)$ is a one-dimensional Dirac delta-function of the proper distance between $x$ and $\gamma$ measured along geodesics in $\Sigma$ orthogonal to $\gamma$.

Equation (2.13) is our main result. Since the Poisson Bracket with $h_{ij}$ vanishes, and since the right-hand-side of (2.13) is the same for all solutions when expressed in terms of proper distance, it is easy to integrate the above to yield the effect of a finite flow by a parameter $\lambda$. We see that the Hamiltonian flow generated by $A_{HRT}$ changes the initial data on any Cauchy surface $\Sigma$ that contains $\gamma$ by adding to the normal-normal component $K^{\perp\perp}$ of the extrinsic curvature a delta-function given by the right-hand-side of (2.13) multiplied by $\lambda$, but that this flow leaves unchanged both the induced metric $h_{ij}$ and all other components of $K^{ij}$.

The effect on the rest of the solution is then determined by the equations of motion. Note that since there is no change in the initial data on $\Sigma$ away from the HRT surface $\gamma_R$, causality then implies that there can be no change in the part of the solution within the entanglement wedge on either side of $\gamma_R$. Instead, the solution can change only within the past and future light cones of $\gamma_R$. In these regions, the change in the solution is

also influenced by boundary conditions. We thus now discuss the required boundary conditions in detail.

### 2.2.2 Boundary Conditions for HRT-area flow

The result (2.13) fully defines the flow generated by $A_{HRT}$. However, as is often the case, the precise connection to boundary conditions can be subtle. We thus take a moment to explore such issues here.

To this end, recall that (2.13) describes a flow within some particular notion of the gravitational phase space. We have described this phase space in terms of a Cauchy surface $\Sigma$. The bulk geometry and extrinsic curvature of $\Sigma$ are dynamical and so can change under HRT-area flow. But since $\Sigma$ represents a definite instant of time, in a context with an asymptotically AdS boundary $\partial\mathcal{M}$ on which the boundary metric has been fixed, the intersection $\partial\Sigma$ of $\Sigma$ with $\partial\mathcal{M}$ will remain fixed. This is in precise analogy with the familiar statement that the flow generated by a Hamiltonian on the phase space at $t = 0$ does not actually change the value of $t$ but, instead, changes the initial data in the manner dictated by time-translations. As a result, the boundary conditions require that neither the metric induced on $\partial\Sigma$ by the boundary metric nor the corresponding extrinsic curvature can change under the flow generated by $A_{HRT}$. And this must be true despite the transformation (2.13) of the initial data in the bulk.

The above may at first seem like a paradoxical state of affairs. However, any relation between the extrinsic curvature of the surface $\Sigma$ in the bulk $\mathcal{M}$ and the extrinsic curvature of $\partial\Sigma$ in the boundary $\partial\mathcal{M}$ will certainly depend on how $\partial\mathcal{M}$ is attached to $\mathcal{M}$. This allows extra degrees of freedom. In short, we believe that the situation is much like the famous issue discussed in [122, 123, 65] wherein one may have conical singularities in the bulk that end on smooth boundary metrics. We thus believe that there is an appropriate

sense in which HRT-area flow is a well-defined transformation. Indeed, we will show this explicitly below for spacetimes asymptotic to $AdS_3$, though we leave full discussion of the higher dimensional case for later work. In particular, the forthcoming work [124] will show that our issue is precisely equivalent to whether one can have Lorentz-signature bulk conical singularities in the presence of general smooth boundary metrics.

We also pause to warn the reader that, while we believe that HRT-area flow can be defined, there is a sense in which it will be rather singular in the UV. In particular, we will see in section 2.3 that in $AdS_3$ it leads to a boundary stress tensor that involves the square of a Dirac delta-function. The transformed solutions will thus have infinite energy. If we are inspired by [117] to think of $A_{HRT}/4G$ as the leading semiclassical term in the modular Hamiltonian of the dual CFT state, this UV-divergence is a concrete manifestation of the singular behavior predicted in [113] using results in algebraic quantum field theory. (Though see [125] for further comments.) As noted in [113] (and as further developed in [114, 115]), the UV behavior can be improved by simultaneously acting with a second transformation associated with the (right) vacuum modular Hamiltonian. Following [115], we refer to the combined smoother transformation as the 'kink transform,' whose details we describe below. See also the closely related discussions in [112] and [44].

### 2.2.3 Relation to the kink transformation

As a brief but useful aside, we now discuss the relation of the flow generated by $A_{HRT}$ to the kink transformation introduced in [115]. Indeed, the kink transformation was initially defined in [115] by using precisely the action (2.13) on Cauchy data, scaled by a factor that controls the amount of the transformation to be applied.[1] The transformation

[1] We will discuss such normalizations in appendix A. Performing a finite transformation by an amount $\lambda$ simply adds $\lambda$ times the left-hand-side of (2.13) to the extrinsic curvature. However, the astute reader

on solutions then followed by solving the equations of motion. However, for asymptotically AdS spacetimes the solution is unique only after boundary conditions have been fully specified, and the boundary conditions chosen to define the kink transformation in [115] turn out to differ from the HRT-area flow boundary conditions described in section 2.2.2. While the flow generated by $A_{HRT}$ preserves *any* boundary metric and leaves $\partial\Sigma$ invariant in $\partial\mathcal{M}$, the kink transform of [115] was fully defined only when the metric on $\partial\mathcal{M}$ has a Killing field $\xi_\partial$ that vanishes on the anchor set $\partial R$ of the HRT surface, and where $\xi_\partial$ acts locally as a boost about $\partial R$. In this setting the kink transformation was declared to leave the boundary metric invariant, and also to leave the surface $\partial\Sigma$ invariant in the region spacelike separated from $R$. However, in contrast to the HRT-area flow described above, the kink transformation moves the part of $\partial\Sigma$ in the domain of dependence of $R$. In particular, it shifts $\partial\Sigma$ toward the past along the orbits of $\xi_\partial$ by a Killing parameter $2\pi\lambda/\kappa$, where $\kappa$ is the surface gravity of $\xi_\partial$ at $\partial R$. In all cases below we take $D(R)$ to be the right wedge and describe the left wedge as $D(\bar{R})$ for some complimentary achronal surface $\bar{R}$ to $R$. See appendix A for verification of the above sign and normalization factors.

In the presence of the boundary Killing field $\xi_\partial$, the kink transformation differs from the flow generated by $A_{HRT}/4G$ only by whether or not $\partial\Sigma$ is distorted relative to the fixed boundary metric. We may thus refer to the flow generated by $A_{HRT}$ as a *boundary-condition preserving* kink transform. Again, because this flow preserves the boundary conditions precisely, it can be defined for any boundary metric. In particular, it does not require the existence of the boundary Killing field $\xi_\partial$ that was needed to define the original kink transform.

Since the above distortion involves a boost operation in the right ($R$) wedge but

will notice that the form of the normalization factor given in [115] is somewhat different. This difference in presentation will be discussed at the end of appendix A.

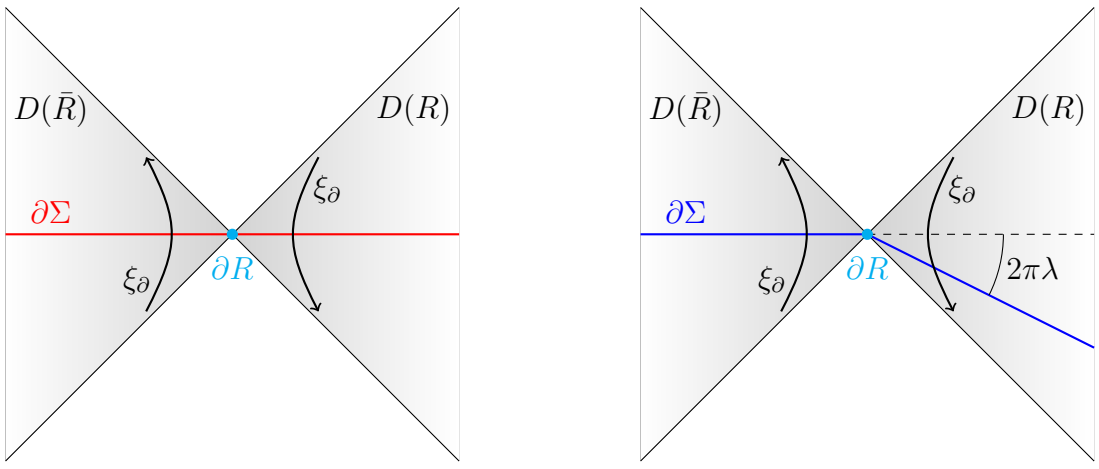


$(a)$ $(b)$

Figure 2.1: The conformal boundary of our spacetime, showing the domains of dependence $D(R)$ of $R$ and $D(\bar{R})$ of $\bar{R}$. The boundary metric has a Killing field $\xi_\partial$ that acts as a boost near $\partial R$. **(a)** The boundary $\partial\Sigma$ of a smooth bulk Cauchy surface $\Sigma$ in the original spacetime. The surface $\partial\Sigma$ and all boundary observables on that surface are preserved by the flow generated by $A_{HRT}R$. **(b)** The kink transformation with parameter $\lambda$ moves the part of $\partial\Sigma$ in $D(R)$ by sliding it toward the past along orbits of $\xi_\partial$ through a Killing parameter $2\pi\lambda/\kappa$. Near $\partial R$ this acts as a past-directed boost with rapidity $2\pi\lambda$.

trivial action in the left ($\bar{R}$) wedge, it was called a (boundary) one-sided boost in [115]. Note, however, that the action on observables in the future and past wedeges is again determined by solving the equations of motion. If we let $\mathcal{K}[\gamma]$ denote the generator of the kink transformation by $\lambda$, then we can define the difference $H_R := \frac{A_{HRT}}{4G} - \mathcal{K}[\gamma]$ to be ($2\pi$ times) the generator of the boundary one-sided boost (taken to generate flow toward the future in the right wedge). In the context of AdS/CFT, $H_R$ can be interpreted [115] as the right modular Hamiltonian of the Hartle-Hawking state[2] for the CFT associated with the boundary Killing field $\xi_\partial$. Furthermore, the term $\frac{A_{HRT}}{4G}$ was argued in [115] to correspond at leading order to the modular Hamiltonian of the boundary dual of the bulk spacetime. As a result, the kink transform was conjectured to be dual to a so-called Connes cocycle flow in the CFT (generated by the difference between the right modular Hamiltonian of the bulk state and the right modular Hamiltonian of the Hartle-Hawking state for $\xi_\partial$). Some refinements of this correspondence will be discussed in [125].

It is useful to note that, even in the absence of a bulk Killing field, the action of $A_{HRT}$ or $\mathcal{K}[\gamma]$ in the bulk can again be described in terms of a one-sided boost. This relationship was described in detail in [115], having been foreshadowed in [112, 113, 44, 114]. The essential point is to recall from [126] that the original solution can be reconstructed from four pieces of data: boundary conditions as defined by the boundary metric, the restriction of the solution to the left wedge, the restriction of the solution to the right wedge, and the way that affine parameters along the future and past null boundaries of each wedge are identified with those along the past and future null boundaries of the other wedge. The idea is that if we are given the last three, the remainder of the solution is uniquely determined by solving the equations of motion subject to the given boundary conditions (the first ingredient above).

[2]There will be cases where $H_R$ is unbounded below as a CFT operator. In such cases the Hartle-Hawking state is not well-defined, but the flow still exists. Such cases are the analogue of what occurs for Kerr black holes in asymptotically flat spacetimes.

The fourth piece of data above can be said to define the relative boost with which the two wedges are attached. The desired operation is then defined by changing these identifications in precisely the same way that they would be changed if there were an appropriate bulk Killing field, and if we were to transform the right wedge by flowing toward the past through a Killing parameter $2\pi\lambda/\kappa$ along the orbits of this Killing field. As verified in appendix A, on a Cauchy surface through $\gamma$ this generates precisely the desired transformation on initial data (2.13).

Again, the transformed initital data can be extended to a full solution by choosing boundary conditions and solving the equations of motion. And again, the result gives the flow generated by either $A_{HRT}/4G$ (if one preserves the way that each wedge attaches to the asymptotically AdS boundary), or by $\mathcal{K}[\gamma]$ (if there is a boundary Killing field $\xi_\partial$ and one flows the right wedge appropriately under $\xi_\partial$). In all cases the solution in the past and future of $\gamma$ is determined by solving the equations of motion with an appropriate choice of boundary conditions.[3]

## 2.3 Explicit results in vacuum Poincaré $AdS_3$

We will now use the above relations to give a simple geometric description of the flow generated by some $A_{HRT}[R]$ in pure 2+1 Einstein-Hilbert gravity (with negative cosmological constant but without matter) for spacetimes asymptotic to Poincaré $AdS_3$ that do not contain black holes. After deriving this description in section 2.3.1, explicit results for the action of the transformation on the boundary stress tensor and on other HRT-areas are given in sections 2.3.2 and 2.3.3.

[3]In particular, since the boundary metric is not dynamical, the boundary metric to the future and past of $\partial R$ cannot be determined by solving equations of motion. It must simply be specified by hand.

### 2.3.1 Representation as a boundary conformal transformation

Bulk spacetimes of the specified form are always diffeomorphic to Poincaré $AdS_3$. Let us thus focus on obtaining explicit results when the spacetime is exactly Poincaré $AdS_3$ with metric

$$ds^2 = \frac{1}{z^2}\left(-dt^2 + dx^2 + dz^2\right) = \frac{1}{z^2}\left(-dudv + dz^2\right). \tag{2.15}$$

Here we have set the AdS scale $\ell_{AdS}$ to one and introduced $u = t-x$ and $v = t+x$. Results for any other spacetime in the above class can then be obtained by applying an appropriate boundary conformal transformation. At least for infinitesimal such transformations, this generalization will be described in section 2.4.

Now, any two HRT surfaces in Poincaré $AdS_3$ are related by an $AdS_3$ isometry. Thus we may further simplify the discussion by taking the boundary region $R$ to be the half-line $x \in [0, \infty)$ at $t = 0$ on the boundary at $z = 0$. We will refer to this half-line as $R_0$. The HRT surface $\gamma_{R_0}$ is then the bulk geodesic given by $x = t = 0$ for all $z$.

The geodesic $\gamma_{R_0}$ is invariant under the manifest boost isometry $\xi = x\partial_t + t\partial_x$ in the $x, t$ plane, and it is clear that $\xi$ induces a related Killing field $\xi_\partial$ on the boundary at $z = 0$. This feature makes it easy to apply the kink transformation $\mathcal{K}[\gamma_{R_0}]$, as boosting the right wedge leaves invariant *all* data in that wedge. The kink transformation also leaves the boundary metric unchanged, though we remind the reader that it nevertheless 'moves each Cauchy surface with respect to that metric' as shown previously in figure 2.1. As a result, solving the equations of motion must precisely reproduce the original spacetime (2.15). We conclude that the action of $\mathcal{K}[\gamma_{R_0}]$ leaves Poincaré $AdS_3$ invariant.[4]

A similar conclusion clearly holds for Poincaré $AdS_d$ for any $d$. But what is special

[4]This is consistent with the conjecture of [115] that the kink transform is dual to the Connes cocycle flow generated by the difference between the one-sided modular Hamiltonian of the dual CFT state and the one-sided modular Hamiltonian of the CFT vacuum. Since Poincaré $AdS_3$ is dual to the CFT vacuum, the above difference clearly vanishes for this state and hence has trivial action. As usual, we refer the reader to [125] for further comments

about $d = 3$ is that we can also find a simple form for the transformation generated by the $H_R$ of section 2.2.3. Combining this with the above will then give a closed-form expression for the boundary-condition-preserving kink transformation defined by our HRT-area flow on Poincaré $AdS_3$.

To establish the desired result, recall first that $H_R$ generates a transformation that leaves invariant the boundary metric. And since all solutions to pure 2+1 Einstein-Hilbert gravity with such boundary conditions are diffeomorphic to Poincaré $AdS_3$, $H_R$ can act only by a boundary-metric-preserving diffeomorphism. In an asymptotically AdS spacetime, this must be a boundary conformal transformation. Our task is thus simply to identify the unique conformal transformation that acts on the right wedge of the boundary as a boost of magnitude $2\pi\lambda$ and of the appropriate sign.[5]

For each $\lambda$ we will describe this conformal transformation as a map $(u, v) \to (U(u), V(v))$ on the boundary spacetime and an associated Weyl rescaling. After acting with the transformation, our boundary conditions require the boundary metric to be

$$ds_\partial^2 = -dU dV, \tag{2.16}$$

so that the Weyl rescaling is determined by comparing (2.16) with $-dudv$.

In the left wedge we know that $H_R$ must act as the identity. And in order to undo the action of $\mathcal{K}[\gamma]$ on a Cauchy slice (shown in figure 2.1), our conformal transformation should boost the right wedge toward the future with rapidity $2\pi\lambda$. Since it must preserve continuity of each Cauchy slice, this uniquely singles out the transformation at each finite $\lambda$ to be

$$U = ue^{-2\pi\lambda\Theta(-u)}, \quad V = ve^{2\pi\lambda\Theta(v)}. \tag{2.17}$$

[5]While this conformal transformation is not smooth on the boundary spacetime, it nevertheless corresponds to a diffeomorphism that is smooth at every point in the bulk.

Since $u\delta(u) = 0 = v\delta(v)$, (2.17) yields

$$-dUdV = -e^{2\sigma(U)}e^{2\hat{\sigma}(V)}dudv \tag{2.18}$$

$$\text{with} \qquad e^{2\sigma(U)} = e^{-2\pi\lambda\Theta(-U)}, \quad e^{2\hat{\sigma}(V)} = e^{2\pi\lambda\Theta(V)}. \tag{2.19}$$

Thus we have $-dUdV = -dudv$ in both the left and right wedges. But this is not the case in either of the future or past wedges, so the $\sigma$ and $\hat{\sigma}$ define a non-trivial Weyl rescaling relating (2.19) to (2.16).

On any solution, $H_R$ will be the generator of the boundary conformal transformation (2.17). But since the kink transform acts trivially on Poincaré $AdS_3$, we can also take (2.17) to give the full finite-$\lambda$ action flow of this solution under $A_{HRT}/4G$. This in particular allows us to explicitly compute the action of this flow on both the boundary stress tensor and other HRT areas. We record these results below in sections 2.3.2 and 2.3.3 for later use in comparison with section 2.4.

### 2.3.2 HRT-area flow of $T_{ij}$

The action of a general finite conformal transformation on the stress energy tensor of a 1+1 dimensional conformal field theory is well known (see e.g. [127]) to give

$$T_{ab}dx^a dx^b = T^{\text{original}}_{ab}dx^a dx^b + \frac{c}{12\pi}\left[\partial_U^2\sigma + (\partial_U\sigma)^2\right]dU^2 + \frac{c}{12\pi}\left[\partial_V^2\hat{\sigma} + (\partial_V\hat{\sigma})^2\right]dV^2, \tag{2.20}$$

where $c$ is the central charge. For the boundary stress tensor of $AdS_3$, we have $c = 3/2G$. Since we are computing the effect on the planar vacuum, we have $T^{\text{original}}_{ab} = 0$. The

remaining terms in (2.20) then give

$$T_{UU} = \frac{1}{8G}\left(\lambda\delta'(U) + \pi\lambda^2[\delta(U)]^2\right), \text{ and} \tag{2.21}$$

$$T_{VV} = \frac{1}{8G}\left(\lambda\delta'(V) + \pi\lambda^2[\delta(V)]^2\right). \tag{2.22}$$

The final terms in (2.21) and (2.22) are sensible only in the presence of a UV regulator. This is consistent with comments in [113] on the singular nature of one-sided modular flow. Interestingly, however, there is no problem at linear order in $\lambda$. This makes clear that the infinitesimal action of HRT-area flow is well-defined on solutions that are sufficiently smooth, but that flowing a finite distance under this transformation creates UV divergences when the HRT surface $\gamma$ is anchored to an asymptotically AdS boundary. In all cases we nevertheless emphasize that the action of the flow on the bulk solution is nevertheless given in closed form.

### 2.3.3 The action of the flow on other HRT-areas

Despite the divergence it creates in the boundary stress tensor components (2.21) and (2.22), the finite flow generated by $A_{HRT}[R_0]/4G$ yields a well-defined action on other HRT areas. To write explicit formulae, recall that our $A_{HRT}$ denotes the *renormalized* HRT-area, which in $AdS_3$ with $\ell_{AdS} = 1$ may be written

$$A_{HRT} = L_{geodesic} + \sum_{anchors} L_{ct}, \tag{2.23}$$

where $L_{ct}$ is an appropriate $c$-number counterterm. In particular, in vacuum Poincaré $AdS_3$ we may introduce a regulated boundary at $z = \epsilon$ and write the renormalized area

as [128]

$$\begin{aligned} A^{vac}_{HRT} &= \lim_{\epsilon\to 0}[-2\ln\epsilon + \ln[(x_1-x_2)^2-(t_1-t_2)^2] + 2\ln(2\epsilon)] \\ &= \ln[(u_1-u_2)(v_2-v_1)] + 2\ln 2, \end{aligned} \tag{2.24}$$

where we have identified $L_{ct} = \ln(2\epsilon)$. Since the endpoints of the HRT surface must be spacelike separated on the boundary, without loss of generality we may take $u_1 > u_2$ and $v_1 < v_2$ (i.e., we number the endpoints left-to-right as opposed to past-to-future).

Furthermore, under a Weyl rescaling $ds^2_{\partial,new} = e^{2\sigma} ds^2_{\partial,old}$ we have

$$A^{new}_{HRT} = A^{old}_{HRT} + \sum_{anchors} \sigma. \tag{2.25}$$

We can now apply the conformal transformation (2.19) to the $A_{HRT}$ anchored at $(U_1, V_1)$ and $(U_2, V_2)$, which we write below as $A_{HRT}(U_1, V_1, U_2, V_2)$. First, however, it is useful to note that any $A_{HRT}$ evaluated in the Poincaré vacuum remains invariant under the conformal transformation defined by constant rescalings $U = e^{\alpha_u} u, V = e^{\alpha_v} v$ of the null coordinates. This is because the explicit expression (2.24) shifts by $-\alpha_u - \alpha_v$ under $(u, v) \to (U, V)$, but this is then cancelled by the conformal anomaly term in (2.25) since $\sigma = \frac{1}{2}(\alpha_u + \alpha_v)$ at each anchor point. This result is of course clear for the case $\alpha_u = -\alpha_v$ (which describes a boost), but it also holds for e.g. $\alpha_u = \alpha_v$ (which describes a dilation).

Since (2.19) is piecewise constant, the above observation makes it easy to apply the conformal transformation (2.17) to $A_{HRT}(U_1, V_1, U_2, V_2)$. Non-trivial effects can occur only when $U_1$ and $U_2$ have opposite signs or when $V_1, V_2$ have opposite signs so that the end points correspond to distinct values of $\hat{\sigma}$ and/or $\sigma$. When opposite signs do occur, we can evaluate the effect of (2.17) by computing (2.24) at the new endpoints and adding the anomalous term from (2.25). Again using spacelike separation of the anchor points

to take $U_1 > U_2$ and $V_1 < V_2$, we may write the transformed result in the form

$$A_{HRT,\lambda}(U_1, V_1, U_2, V_2) = A_U(U_1, U_2) + A_V(V_1, V_2) + 2\ln 2, \tag{2.26}$$

with

$$A_U = \begin{cases} \ln(U_1 - U_2), & U_1, U_2 < 0 \text{ or } U_1, U_2 > 0 \\ \ln(e^{-2\pi\lambda}U_1 - U_2), & U_2 < 0 < U_1 \end{cases} \tag{2.27}$$

and

$$A_V = \begin{cases} \ln(V_2 - V_1), & V_1, V_2 < 0 \text{ or } V_1, V_2 > 0 \\ \ln(V_2 - e^{2\pi\lambda}V_1), & V_1 < 0 < V_2. \end{cases} \tag{2.28}$$

As a result, we find

$$\left\{ \frac{1}{4G} A_{HRT}[R_0], A_{HRT}(U_1, V_1, U_2, V_2) \right\} \tag{2.29}$$

$$= \frac{d}{d\lambda} A_{HRT,\lambda}(U_1, V_1, U_2, V_2)\Big|_{\lambda=0} \tag{2.30}$$

$$= -2\pi \left( \frac{U_1 \Theta(-U_1 U_2)}{U_1 - U_2} + \frac{V_1 \Theta(-V_1 V_2)}{V_2 - V_1} \right). \tag{2.31}$$

## 2.4 Commutators from stress tensors

The previous section transformed the general arguments of section 2.2 into explicit results in $AdS_3$ for the particular choice of boundary region $R_0$ given by the half-line at $t = 0$ and when the area-flow acts on the Poincaré $AdS_3$ vacuum. We now present an independent calculation both to check the above results and as a means of generalizing them to allow arbitrary boundary regions $R$ and more general solutions of pure 2+1 Einstein-Hilbert gravity with negative cosmological constant and planar boundary. In particular, the generalization will allow planar black holes. The key ingredients in

this computation are (again) that all such solutions are related by boundary conformal transformations, and that any two spacetimes with the same boundary stress tensor are considered to be completely equivalent. Thus we may in principle express any observable in terms of the boundary stress tensor and use the well-known 2-dimensional stress tensor algebra to compute any commutators. This alternate technique may also be of interest in its own right as a means of studying commutators of general quantities for which an elegant geometric description of the flow is not known.

To follow this approach, one might like to proceed by finding an explicit expression in terms of the boundary stress tensor for the conformal transformation $(u, v) \to (U(u), V(v))$ that constructs an arbitrary solution in our class from the Poincaré $AdS_3$ vacuum, and in particular for the associated conformal factor $\sigma[T_{ij}]$. One could then use the relevant conformal anomaly to write any observable in terms of $\sigma$ and simply substitute $\sigma[T_{ij}]$ to write the observable as a functional of the stress tensor. However, it is not clear that a useful such closed-form solution $\sigma[T_{ij}]$ will exist. Luckily this work focusses on *semi-classical* commutators, for which such an explicit relation will not be needed. As in section 2.2, the key point is that the semiclassical commutator (aka the Poisson or Peierls bracket) is a derivation, meaning that for any observables $B$ and $C$ we may write the bracket in terms of the stress-tensor algebra using

$$\begin{aligned}
\{B, C\} &= \int d^2x_1 d^2x'_1 \frac{\delta B}{\delta T_{ij}(x_1)} \{T_{ij}(x_1), T_{i'j'}(x'_1)\} \frac{\delta C}{\delta T_{i'j'}(x'_1)} \\
&= \int d^2x_1 d^2x_2 d^2x'_2 d^2x'_1 \frac{\delta B}{\delta \sigma(x_2)} \frac{\delta \sigma(x_2)}{\delta T_{ij}(x_1)} \{T_{ij}(x_1), T_{i'j'}(x'_1)\} \frac{\delta \sigma(x'_2)}{\delta T_{i'j'}(x'_1)} \frac{\delta C}{\delta \sigma(x'_2)} \\
&= \int d^2x_2 d^2x'_2 \frac{\delta B}{\delta \sigma(x_2)} \{\sigma(x_2), \sigma(x'_2)\} \frac{\delta C}{\delta \sigma(x'_2)},
\end{aligned} \tag{2.32}$$

It is thus sufficient to know the functional derivatives of $B, C$ with respect to $\sigma$ and the functional derivatives of $\sigma$ with respect to the stress tensor, which in practice turns out to be a manageable task.

After computing such functional derivatives in section 2.4.1, we warm up with some relatively simple commutators involving $\sigma$ and $T_{ij}$ in sections 2.4.2 and 2.4.3 before finally studying commutators of HRT areas in section 2.4.4.

### 2.4.1 Functional derivatives of $\sigma$ with respect to $T_{ij}(x)$

Recall that our basic strategy will be to think of the boundary stress tensor $T_{ij}(U, V)$ as the fundamental observable in terms of which we will write all others. In particular, we will define an observable $\sigma$ as the conformal factor in (2.20) that generates $T_{ij}(U, V)$ from the vacuum (in which $T_{ij} = 0$), and which satisfies certain boundary conditions. In practice, we will then write general observables in terms of $\sigma$, which then implicitly expresses them in terms of $T_{ij}$.

To this end, let us thus consider the boundary metric

$$ds^2_\partial = -dUdV = -e^{2\sigma(u,v)}dudv, \tag{2.33}$$

with $\sigma(u, v) = \sigma(u) + \hat{\sigma}(v)$ and

$$\begin{aligned} dU &= e^{2\sigma(u)}du \\ dV &= e^{2\hat{\sigma}(v)}dv, \end{aligned} \tag{2.34}$$

and where $\sigma$ and $\hat{\sigma}$ are chosen so that $T_{ij}(U, V)$ can be written in the form (2.20) with $T^{original}_{uu}(u) = 0 = T^{original}_{vv}(v)$. Note that the coordinates $u, v$ defined by (2.34) are dynamical objects that will also be functions of the stress tensor $T_{ij(U,V)}$. In particular, we should think of the functions $u(U)$ and $v(V)$ as being defined by integrating the above equations subject to some boundary condition. These functions have range $u \in (-\infty, u_{max})$ and $v \in (-\infty, v_{max})$, where $u_{max} = v_{max} = \infty$ when solutions asymptote to

Poincaré $AdS_3$, and $u_{max} = v_{max} = 0$ when solutions instead asymptote to an $M > 0$ planar black hole.

When solutions asymptote to Poincaré $AdS_3$, it will be convenient to choose the boundary conditions to be simply

$$u(U = 0) = 0, \quad v(V = 0) = 0, \tag{2.35}$$

allowing us to define

$$u(U) = \int_0^U dU' e^{-2\sigma(U')} \tag{2.36}$$

$$v(V) = \int_0^V dV' e^{-2\hat{\sigma}(V')}. \tag{2.37}$$

We note in passing that $u = \pm\infty$ does not generally correspond to $U = \pm\infty$. In particular, at this stage the $SL(2, R) \times SL(2, R)$ isometries of the Poincaré vacuum allow us to introduce poles in the function $u(U)$. When solutions asymptote to an $M > 0$ planar black hole, we will instead choose our boundary conditions to be

$$u(U = \infty) = 0, \quad v(V = \infty) = 0, \tag{2.38}$$

allowing us to define

$$u(U) = \int_0^U dU' e^{-2\sigma(U')} - \int_0^\infty dU' e^{-2\sigma(U')} \tag{2.39}$$

$$v(V) = \int_0^V dV' e^{-2\hat{\sigma}(V')} - \int_0^\infty dV' e^{-2\hat{\sigma}(V')}. \tag{2.40}$$

Again we note in passing that $u = -\infty$ may not correspond to $U = -\infty$.

Since the trace of $T_{ij}$ vanishes, the only non-trivial stress tensor components are $T_{UU}(U)$ and $T_{VV}(V)$. For the moment, let us focus on $T_{UU}$ since corresponding results

for $V$ will satisfy analogous expressions.

The functional derivative $\frac{\delta\sigma(u(U))}{\delta T_{UU}(U')}$ can be computed by studying the variation of $T_{UU}$:

$$\begin{aligned}\delta T_{UU} =& \frac{c}{12\pi}(\partial_U^2\delta\sigma + 2\partial_U\sigma\partial_U\delta\sigma)\\ =& \frac{c}{12\pi}e^{-2\sigma}\partial_U(e^{2\sigma}\partial_U\delta\sigma).\end{aligned} \tag{2.41}$$

$$\begin{aligned}\delta\sigma(U) = \frac{12\pi}{c}\Bigg(\int_{U_0}^{U} e^{-2\sigma(U'')}\int_{U_0}^{U''} e^{2\sigma(U')}\delta T_{UU}(U')dU'dU''\\ + c_1\int_{U_0}^{U} e^{-2\sigma(U')}dU' + c_2\Bigg),\end{aligned} \tag{2.42}$$

for any finite $U_0$, and constants $c_1$ and $c_2$. This parametrization is somewhat redundant, as changes in $U_0$ can be absorbed into changes in $c_1$ and $c_2$.

The constants $c_1$ and $c_2$ are arbitrary and cannot influence the physics of our computation. But it will be convenient to fix them by recalling that, as previously noted, an overall scaling preserves the Poincaré vacuum. We are thus free to fix $\sigma(U)$ to be independent of the stress tensor for any one value $U$. We will choose this to be true at $U = U_0$, which imposes $\delta\sigma(U_0) = 0$. Additionally, the Poincaré vacuum is invariant under special conformal transformations, allowing us to fix $\partial_U\sigma(U)$ to be independent of the stress tensor for any one value $U$; we will again choose $U = U_0$, which imposes $\partial_U\delta\sigma(U_0) = 0$. Implementing these boundary conditions sets $c_1 = c_2 = 0$, and establishes that our definition of $\sigma$ depends on $U_0$. As a result, we now change notation to $\delta\sigma(U) = \delta\sigma_{U_0}(U)$, to make explicit the $U_0$ dependence. We similarly take $\sigma(U_0) = 0$ (and $\sigma(U) = \sigma_{U_0}(U)$).[6]

Rewriting (2.42) slightly, we have

[6]Additionally, $u(U)$ depends on $\sigma_{U_0}(U)$ through either Eq. (2.36) or (2.39), so we make explicit this $U_0$ dependence as $u(U) = u_{U_0}(U)$. Similarly with $v(V) = v_{V_0}(V)$.

$$\begin{aligned}\delta\sigma_{U_0}(U) =&\frac{12\pi}{c}\int_{-\infty}^{\infty} dU' e^{2\sigma_{U_0}(U')}\Theta(U-U')\Theta(U'-U_0)\delta T_{UU}(U')\int_{U'}^{U} dU'' e^{-2\sigma_{U_0}(U'')}\\ &+\frac{12\pi}{c}\int_{-\infty}^{\infty} dU' e^{2\sigma_{U_0}(U')}\Theta(U'-U)\Theta(U_0-U')\delta T_{UU}(U')\int_{U}^{U'} dU'' e^{-2\sigma_{U_0}(U'')},\end{aligned} \tag{2.43}$$

which yields

$$\frac{\delta\sigma_{U_0}(U)}{\delta T_{UU}(U')} = \frac{12\pi}{c}e^{2\sigma_{U_0}(U')}[u_{U_0}(U)-u_{U_0}(U')][\Theta(U-U')\Theta(U'-U_0)-\Theta(U'-U)\Theta(U_0-U')]. \tag{2.44}$$

We now use the above results to compute a series of semiclassical commutators below.

### 2.4.2 A first warm up: $\{\sigma, T_{ij}\}$

We begin by studying the semiclassical commutator

$$\{\sigma_{U_0}(U), T_{UU}(\tilde{U})\} = \int_{-\infty}^{\infty} dU' \frac{\delta\sigma_{U_0}(U)}{\delta T_{UU}(U')}\{T_{UU}(U'), T_{UU}(\tilde{U})\}. \tag{2.45}$$

Since our CFT is 2-dimensional, the stress tensor algebra can be determined from the familiar relations

$$\{L_m, L_n\} = i(n-m)L_{m+n} - \frac{ic}{12}m(m^2-1)\delta_{m+n,0}, \tag{2.46}$$

where $L_m$ and $T_{UU}$ are related by

$$\begin{aligned} L_m &= -\frac{1}{2\pi}\int_{S^1} dU e^{iUm}T_{UU}(U)\\ T_{UU}(U) &= \sum_{m=-\infty}^{\infty} e^{-iUm}L_m. \end{aligned} \tag{2.47}$$

These relations are well-known to yield

$$\{T_{UU}(U), T_{UU}(U')\} = 2T_{UU}(U')\delta'(U-U') - T'_{UU}(U')\delta(U-U') - \frac{c}{24\pi}\delta'''(U-U'). \quad (2.48)$$

We can now compute the right-hand side of (2.45) using (3.88). After some manipulation, (2.45) becomes

$$\begin{aligned}\{\sigma_{U_0}(U), T_{UU}(\tilde{U})\} = \Bigg[ & -2T_{UU}(\tilde{U})\partial_{U'}\left(\frac{\delta\sigma_{U_0}(U)}{\delta T_{UU}(U')}\right) - T'_{UU}(\tilde{U})\frac{\delta\sigma_{U_0}(U)}{\delta T_{UU}(U')} \\ & + \frac{c}{24\pi}\partial^3_{U'}\left(\frac{\delta\sigma_{U_0}(U)}{\delta T_{UU}(U')}\right)\Bigg]_{U'=\tilde{U}},\end{aligned} \quad (2.49)$$

where we have used (2.44) to integrate by parts and to show that the associated boundary terms vanish at $U = \pm\infty$. Using Eq. (2.44) then yields

$$\begin{aligned}\{\sigma_{U_0}(U), T_{UU}(\tilde{U})\} = & \sigma'_{U_0}(\tilde{U})\delta(U-\tilde{U}) - \frac{1}{2}\delta'(U-\tilde{U}) \\ & - \sigma''_{U_0}(U_0)[u_{U_0}(U) - u_{U_0}(U_0)]\delta(\tilde{U}-U_0) \\ & + \sigma'_{U_0}(U_0)[u_{U_0}(U) - u_{U_0}(U_0)]\delta'(\tilde{U}-U_0) \\ & - \sigma'_{U_0}(U_0)\delta(\tilde{U}-U_0) - \frac{1}{2}\delta'(\tilde{U}-U_0) \\ & + \frac{1}{2}[u_{U_0}(U) - u_{U_0}(U_0)]\delta''(\tilde{U}-U_0).\end{aligned} \quad (2.50)$$

We will use this result to calculate the commutator $\{\sigma(X), \sigma(X')\}$ in the next section, and we will use it again in Section 2.4.4 to calculate the commutator between an HRT-area and the stress-energy tensor.

### 2.4.3 The $\sigma$ commutator

Our next step will be to compute $\{\sigma(X), \sigma(X')\}$. By the Leibniz rule as expressed in Eq.(2.32), we have

$$\{\sigma_{U_0}(U), \sigma_{\tilde{U}_0}(\tilde{U})\} = \int_{-\infty}^{\infty} d\tilde{U}' \frac{\delta \sigma_{\tilde{U}_0}(\tilde{U})}{\delta T_{UU}(\tilde{U}')} \{\sigma_{U_0}(U), T_{UU}(\tilde{U}')\} \tag{2.51}$$

where $\tilde{U}_0$ is finite. Inserting (2.50) and manipulating the result yields

$$\begin{aligned} \{\sigma_{U_0}(U), \sigma_{\tilde{U}_0}(\tilde{U})\} =& \frac{6\pi}{c} \Big[ \Theta(\tilde{U} - U) \\ &+ 2(\sigma'_{U_0}(U) - \sigma'_{\tilde{U}_0}(U)) e^{2\sigma_{\tilde{U}_0}(U)} [u_{\tilde{U}_0}(\tilde{U}) - u_{\tilde{U}_0}(U)] \Theta(\tilde{U} - U) \\ &+ u_{\tilde{U}_0}(\tilde{U}) f_1(U) + f_2(U) + u_{U_0}(U) g_1(\tilde{U}) + g_2(\tilde{U}) \Big], \end{aligned} \tag{2.52}$$

with an analogous expression for $\{\hat{\sigma}_{V_0}(V), \hat{\sigma}_{\tilde{V}_0}(\tilde{V})\}$, and we also note that any $\sigma_{U_0}(U)$ commutes with any $\hat{\sigma}_{V_0}(V)$. The functions $f_{1,2}(U)$ and $g_{1,2}(\tilde{U})$ can depend on $U_0$ and $\tilde{U}_0$, and can be computed explicitly. However, we will not do so here, as we will show that their contribution can be ignored. This helpful, because the above expression (2.52) is rather cumbersome. At least some part of this is due to the dependence on the unphysical parameters $U_0, \tilde{U}_0$ associated with the boundary conditions that define $\sigma_{U_0}$ and $\sigma_{\tilde{U}_0}$. But physical observables cannot depend on these parameters, so the dependence on $U_0, \tilde{U}_0$ must cancel completely when computing (2.32). This suggests that for physical observables $B, C$ in (2.32), it should suffice to use a simplified version of (2.52) that is manifestly independent of $U_0, \tilde{U}_0$.

In particular, let us recall that, on the space of solutions we choose to study, any physical observable can be written as a functional of the boundary stress tensor. Comparing the three lines of (2.32) then shows that we will obtain the correct commutator $\{B, C\}$ so long as we include some subset of terms from (2.52) that gives the correct

expression for $\{T_{ij}(x_1), T_{i'j'}(x_1')\}$.

In the simple case where $\tilde{U}_0 = U_0$ and $\tilde{V}_0 = V_0$, it turns out that the following effective commutators suffice for this purpose:

$$\{\sigma_{U_0}(U), \sigma_{U_0}(\tilde{U})\}_{eff} = \frac{6\pi}{c}\Theta(\tilde{U} - U), \tag{2.53}$$

$$\{\hat{\sigma}_{V_0}(V), \hat{\sigma}_{V_0}(\tilde{V})\}_{eff} = -\frac{6\pi}{c}\Theta(V - \tilde{V}),. \tag{2.54}$$

This is straightforward to verify by simply taking appropriate derivatives of (2.53) and using (4.2) to compute

$$\begin{aligned}\{\sigma_{U_0}(U), T_{UU}(\tilde{U})\}_{eff} &= \frac{c}{12\pi}\frac{\partial^2}{\partial\tilde{U}^2}\{\sigma_{U_0}(U), \sigma_{U_0}(\tilde{U})\}_{eff} + \frac{c}{6\pi}\sigma'_{U_0}(\tilde{U})\frac{\partial}{\partial\tilde{U}}\{\sigma_{U_0}(U), \sigma_{U_0}(\tilde{U})\}_{eff} \\ &= \frac{1}{2}\delta'(\tilde{U} - U) + \sigma'_{U_0}(\tilde{U})\delta(\tilde{U} - U),\end{aligned} \tag{2.55}$$

and thus

$$\begin{aligned}\{T_{UU}(U), T_{UU}(\tilde{U})\}_{eff} &= \frac{c}{12\pi}\frac{\partial^2}{\partial U^2}\{\sigma_{U_0}(U), T_{UU}(\tilde{U})\}_{eff} + \frac{c}{6\pi}\sigma'_{U_0}(U)\frac{\partial}{\partial U}\{\sigma_{U_0}(U), T_{UU}(\tilde{U})\}_{eff} \\ &= \frac{c}{24\pi}\delta'''(\tilde{U} - U) + \frac{c}{12\pi}\sigma'_{U_0}(\tilde{U})\delta''(\tilde{U} - U) \\ &- \frac{c}{12\pi}\sigma'_{U_0}(U)\delta''(\tilde{U} - U) - \frac{c}{6\pi}\sigma'_{U_0}(U)\sigma'_{U_0}(\tilde{U})\delta'(\tilde{U} - U).\end{aligned} \tag{2.56}$$

Recall now the following easily verified identities that hold for any smooth functions $f_1(\tilde{U}, U)$ and $f_2(\tilde{U}, U)$ that vanish at $\tilde{U} = U$:

$$f_1\delta''(\tilde{U} - U) = -2\left(\partial_{\tilde{U}} f_1\right)\partial_{\tilde{U}}\delta(\tilde{U} - U) - \left(\partial^2_{\tilde{U}} f_1\right)\delta(\tilde{U} - U) \tag{2.57}$$

$$f_2\delta'(\tilde{U} - U) = -\left(\partial_{\tilde{U}} f_2\right)\delta(\tilde{U} - U). \tag{2.58}$$

Using (2.57) with $f_1 = \partial_{\tilde{U}}\sigma_{U_0}(\tilde{U}) - \partial_U \sigma_{U_0}(U)$ then yields

$$\begin{aligned}
\{T_{UU}(U), T_{UU}(\tilde{U})\}_{eff} = \quad & \frac{c}{24\pi}\delta'''(\tilde{U}-U) - \frac{c}{6\pi}\left(\sigma''_{U_0}(\tilde{U})\right)\partial_{\tilde{U}}\delta(\tilde{U}-U) \\
& -\frac{c}{12\pi}\left(\sigma'''_{U_0}(\tilde{U})\right)\delta(\tilde{U}-U) - \frac{c}{6\pi}\sigma'_{U_0}(U)\sigma'_{U_0}(\tilde{U})\delta'(\tilde{U}-U) \\
= \quad & \frac{c}{24\pi}\delta'''(\tilde{U}-U) - 2T_{UU}(\tilde{U})\partial_{\tilde{U}}\delta(\tilde{U}-U) \\
& -\frac{c}{12\pi}\left(\sigma'''_{U_0}(\tilde{U})\right)\delta(\tilde{U}-U) \\
& +\frac{c}{6\pi}\left([\sigma'_{U_0}(\tilde{U})]^2 - \sigma'_{U_0}(U)\sigma'_{U_0}(\tilde{U})\right)\delta'(\tilde{U}-U) \\
= \quad & \frac{c}{24\pi}\delta'''(\tilde{U}-U) - 2T_{UU}(\tilde{U})\partial_{\tilde{U}}\delta(\tilde{U}-U) \\
& -\frac{c}{12\pi}\left(\sigma'''_{U_0}(\tilde{U})\right)\delta(\tilde{U}-U) \\
& -\frac{c}{6\pi}\left(2\sigma'_{U_0}(\tilde{U})\sigma''_{U_0}(\tilde{U}) - \sigma''_{U_0}(U)\sigma'_{U_0}(\tilde{U})\right)\delta(\tilde{U}-U) \\
= \quad & \frac{c}{24\pi}\delta'''(\tilde{U}-U) - 2T_{UU}(\tilde{U})\partial_{\tilde{U}}\delta(\tilde{U}-U) \\
& -T'_{UU}(\tilde{U})\delta(\tilde{U}-U) \\
& -\frac{c}{6\pi}\left(\sigma'_{U_0}(\tilde{U})\sigma''_{U_0}(\tilde{U}) - \sigma''_{U_0}(U)\sigma'_{U_0}(\tilde{U})\right)\delta(\tilde{U}-U), \qquad (2.59)
\end{aligned}$$

where the third step used (2.58) with $f_2 = [\partial_{\tilde{U}}\sigma_{U_0}(\tilde{U})]^2 - \partial_U\sigma_{U_0}(U)\partial_{\tilde{U}}\sigma_{U_0}(\tilde{U})$. Since the final term in (2.59) vanishes, we see that (2.59) gives the standard stress tensor algebra as desired.

### 2.4.4 The HRT-area algebra

We now we turn to the commutator of HRT-areas. Using the results from Sections 2.4.2 and 2.4.3, we can compute the semiclassical commutator of an HRT-area operator with the boundary stress tensor, as well as that between two area operators $A_{HRT}(U_1, V_1, U_2, V_2)$ and $A_{HRT}(U'_1, V'_1, U'_2, V'_2)$. As in section 2.3.3, the arguments denote the coordinates of the two anchor points that define $\partial R$. We again use the renormalized area operator (2.23) whose dependence on $\sigma$ is given both by the explicit term in (2.25) and the dependence of (2.24) on $\sigma$ through $U(u)$ and $V(v)$. Using $\tilde{A}_{HRT}$ to denote the

renormalized area in the conformal frame where the stress tensor vanishes (and where the boundary metric is $-dudv$), the second of these takes the explicit form

$$\begin{aligned}\tilde{A}_{HRT}(U_1,V_1,U_2,V_2) &= \ln[4(u_1-u_2)(v_2-v_1)] \\ &= \ln\left[4\int_{U_2}^{U_1} dU e^{-2\sigma(U)}\int_{V_1}^{V_2} dV e^{-2\hat{\sigma}(V)}\right].\end{aligned} \tag{2.60}$$

Taking functional derivatives with respect to $\sigma$ yields

$$\begin{aligned}\frac{\delta A_{HRT}(U_1,V_1,U_2,V_2)}{\delta\sigma(U)} &= -\frac{2e^{-2\sigma(U)}}{\left|\int_{U_2}^{U_1} dU'' e^{-2\sigma(U'')}\right|}\Theta(\max(U_1,U_2)-U)\Theta(U-\min(U_1,U_2)) \\ &= -\frac{2e^{-2\sigma(U)}}{|u(U_1)-u(U_2)|}\Theta(\max(U_1,U_2)-U)\Theta(U-\min(U_1,U_2)),\end{aligned} \tag{2.61}$$

with an analogous expression for the functional derivative of the area with respect to $\hat{\sigma}$.

**The area operator and stress-energy tensor commutator**

We will now use the above results to understand the commutator of an HRT area operator with the boundary stress tensor. We introduce the notation $\tilde{A}_{HRT} \equiv \tilde{A}_{U_0,V_0}$, where $U_0$ and $V_0$ are the finite points at which $\sigma_{U_0}(U)$ and $\hat{\sigma}_{V_0}(V)$ are independent of the stress tensor. From Eq. (2.61), we find

$$\begin{aligned}\{\tilde{A}_{U_0,V_0}(U_1,V_1,U_2,V_2), T_{UU}(U)\} &= \int_{U_2}^{U_1} dU' \frac{\delta\tilde{A}_{U_0,V_0}(U_1,V_1,U_2,V_2)}{\delta\sigma_{U_0}(U')}\{\sigma_{U_0}(U'), T_{UU}(U)\} \\ &= -\frac{2}{u(U_1)-u(U_2)}\int_{U_2}^{U_1} dU' e^{-2\sigma_{U_0}(U')}\{\sigma_{U_0}(U'), T_{UU}(U)\}.\end{aligned} \tag{2.62}$$

Using Eq. (2.25), we see the full commutator is given by

$$\{A_{U_0,V_0}(U_1,V_1,U_2,V_2),T_{UU}(U)\}=\{\tilde{A}_{U_0,V_0},T_{UU}(U)\}+\{\sigma_{U_0}(U_1),T_{UU}(U)\}+\{\sigma_{U_0}(U_2),T_{UU}(U)\}. \tag{2.63}$$

Using the explicit form of $\{\sigma_{U_0}(U'),T_{UU}(U)\}$ as given in Eq. (2.50), most of the resulting terms cancel among themselves after insertion into (2.63). The result reduces to

$$\begin{aligned}\{A_{HRT}(U_1,V_1,U_2,V_2),T_{UU}(U)\}=&-\frac{2}{u(U_1)-u(U_2)}\int_{U_2}^{U_1}dU'e^{-2\sigma_{U_0}(U')}\{\sigma_{U_0}(U'),T_{UU}(U)\}_{phys}\\&+\{\sigma_{U_0}(U_1),T_{UU}(U)\}_{phys}+\{\sigma_{U_0}(U_2),T_{UU}(U)\}_{phys}.\end{aligned} \tag{2.64}$$

where

$$\{\sigma_{U_0}(U'),T_{UU}(U)\}_{phys}=\sigma'_{U_0}(U)\delta(U'-U)-\frac{1}{2}\delta'(U'-U). \tag{2.65}$$

Plugging Eq. (2.65) into Eq. (2.64) gives the final results

$$\begin{aligned}&\left\{\frac{A_{HRT}(U_1,V_1,U_2,V_2)}{4G},T_{UU}(U)\right\}=\\&\qquad\frac{1}{4G[u(U_1)-u(U_2)]}[e^{-2\sigma_{U_0}(U_1)}\delta(U_1-U)-e^{-2\sigma_{U_0}(U_2)}\delta(U_2-U)]\\&\qquad+\frac{\sigma'_{U_0}(U)}{4G}\delta(U_1-U)-\frac{1}{8G}\delta'(U_1-U)\\&\qquad+\frac{\sigma'_{U_0}(U)}{4G}\delta(U_2-U)-\frac{1}{8G}\delta'(U_2-U),\\&\left\{\frac{A_{HRT}(U_1,V_1,U_2,V_2)}{4G},T_{VV}(V)\right\}=\\&\qquad\frac{1}{4G[v(V_1)-v(V_2)]}[e^{-2\hat{\sigma}_{V_0}(V_1)}\delta(V_1-V)-e^{-2\hat{\sigma}_{V_0}(V_2)}\delta(V_2-V)]\\&\qquad+\frac{\hat{\sigma}'_{V_0}(V)}{4G}\delta(V_1-V)-\frac{1}{8G}\delta'(V_1-V)\\&\qquad+\frac{\hat{\sigma}'_{V_0}(V)}{4G}\delta(V_2-V)-\frac{1}{8G}\delta'(V_2-V).\end{aligned} \tag{2.66}$$

While the right-hand side appears to depend on $U_0$, the $U_0$ dependence of $\sigma_{U_0}$ (and thus of $u(U)$) is determined by (2.20) and the boundary conditions that both $\sigma_{U_0}(U)$ and its first $U$ derivative vanish at $U_0$. Using this result, a careful calculation shows the right-hand side to be independent of $U_0$.

Note that for the special case $U_1 = 0 = V_1$, $U_2 = -\infty$, $V_2 = \infty$ with $\sigma_{U_0}(U) = \hat{\sigma}_{V_0}(V) = 0$, our (2.66) reduces to the $\lambda$-derivatives of (2.21) and (2.22) evaluated at $\lambda = 0$. This establishes the consistency of the above with the results of sections 2.2 and 2.3.

**The commutator between two area operators**

Our final task will be to write the semiclassical commutator of two HRT area operators in a similar fashion. As in section 2.3.3, we write any $A_{HRT}(U_1, V_1, U_2, V_2)$ in the form

$$A_{HRT}(U_1, V_1, U_2, V_2) = A_U(U_1, U_2) + A_V(V_1, V_2) + 2\ln 2, \tag{2.67}$$

and similarly $\tilde{A}_{HRT} = \tilde{A}_U(U_1, U_2) + \tilde{A}_V(V_1, V_2) + 2\ln 2$. However, to make manifest the dependence of the renormalized HRT-area on $U_0$ and $V_0$ as functionals of the stress tensor, we will instead use the notation $\tilde{A}_U \equiv \tilde{A}_{U_0}$ and $\tilde{A}_V \equiv A_{V_0}$, where $U_0$ and $V_0$ are defined as above. Noting that the $U$ parts are functionals of the right-moving stress tensor while the $V$ parts are functionals of the left-moving stress tensor, we see that the $U$ and $V$ parts commute with each other. We may then focus on the commutator between two $U$ parts with the understanding that results for the $V$ commutators can be recovered using the symmetry $U \rightleftarrows V$.

For two HRT surfaces anchored respectively at $(U_1, U_2)$ and $(U_1', U_2')$, we have

$$\begin{aligned}\{A_U(U_1,U_2), A_U(U_1',U_2')\} =& \{\tilde{A}_{U_0}(U_1,U_2), \tilde{A}_{U_0'}(U_1',U_2')\} \\ &+ \{\tilde{A}_{U_0}(U_1,U_2), \sigma_{U_0'}(\tilde{U}_1)\} \\ &+ \{\tilde{A}_{U_0}(U_1,U_2), \sigma_{U_0'}(\tilde{U}_2)\} \\ &+ \{\sigma_{U_0}(U_1), \tilde{A}_{U_0'}(U_1',U_2')\} \\ &+ \{\sigma_{U_0}(U_2), \tilde{A}_{U_0'}(U_1',U_2')\} \\ &+ \{\sigma_{U_0}(U_1), \sigma_{U_0'}(U_1')\} + \{\sigma_{U_0}(U_1), \sigma_{U_0'}(U_2')\} \\ &+ \{\sigma_{U_0}(U_2), \sigma_{U_0'}(U_1')\} + \{\sigma_{U_0}(U_2), \sigma_{U_0'}(U_2')\}.\end{aligned} \tag{2.68}$$

The first term in the above expression is given by

$$\begin{aligned}&\{\tilde{A}_{U_0}(U_1,U_2), \tilde{A}_{U_0'}(U_1',U_2')\} = \\ &\qquad \int_{U_2}^{U_1} dU \int_{U_2'}^{U_1'} dU' \frac{\delta \tilde{A}_{U_0}(U_1,U_2)}{\delta \sigma_{U_0}(U)} \frac{\delta \tilde{A}_{U_0'}(U_1',U_2')}{\delta \sigma_{U_0'}(U')} \{\sigma_{U_0}(U), \sigma_{U_0'}(U')\},\end{aligned} \tag{2.69}$$

and the next four terms will have forms analogous to

$$\{\tilde{A}_{U_0}(U_1,U_2), \sigma_{U_0'}(U')\} = \int_{U_2}^{U_1} dU \frac{\delta \tilde{A}_{U_0}(U_1,U_2)}{\delta \sigma_{U_0}(U)} \{\sigma_{U_0}(U), \sigma_{U_0'}(U')\}. \tag{2.70}$$

We can evaluate (2.69) and (2.70) using the effective $\sigma$-commutators (2.53) and (2.54), as well as Eq. (2.61). We then use these results to solve for the full HRT are commutator (2.68). Due to the step functions in (2.53) and (2.54), it is convenient to divide the calculation into cases. Let us first consider the cases shown at left in figure 2.2, where the intervals $(U_1, U_2)$ and $(U_1', U_2')$ either have no intersection or where one interval is fully contained in the other. These two situations are equivalent due to the symmetry under interchange of $R$ with $\bar{R}$. For this case, one finds that the various terms cancel to

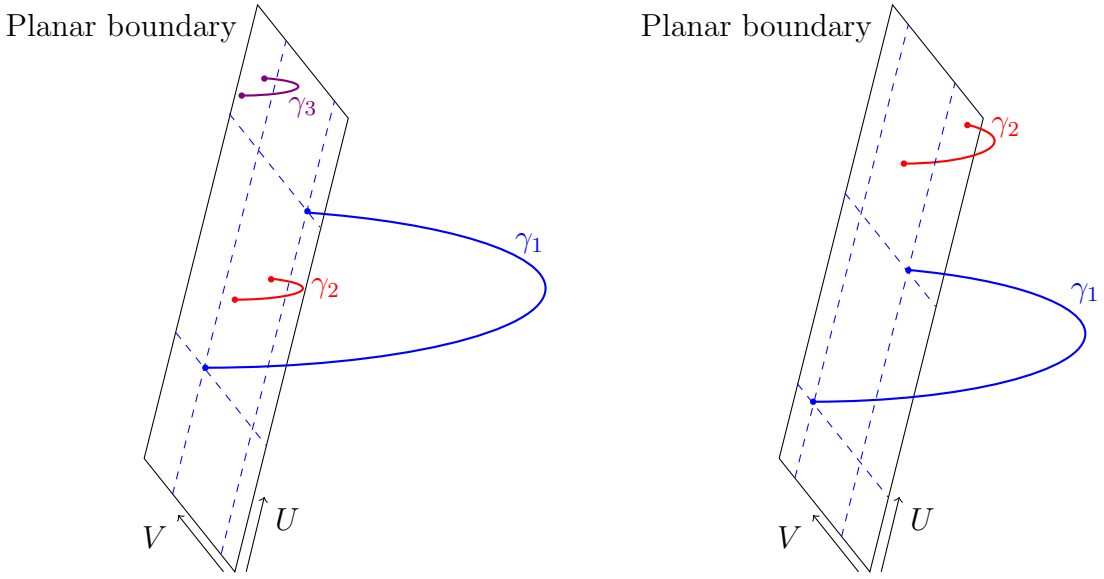


Figure 2.2: Various possible relative configurations for the anchor points of HRT surfaces. In the left panel, the $U$ coordinates of the anchors of $\gamma_2$ define an interval that is fully contained in the corresponding $U$ interval for $\gamma_1$, while the anchors of $\gamma_3$ define a $U$ interval that does not intersect that defined by $\gamma_1$. In such cases the $U$ parts of the HRT-areas commute. The same statements hold with $U$ replaced by $V$. In contrast, in the right panel the $U$ intervals defined by $\gamma_1$ and $\gamma_2$ intersect without one being fully contained in the other. In this case the commutator of the $U$ parts of the HRT-areas will not vanish.

give

$$\{A_U(U_1, U_2), A_U(U_1', U_2')\}_U = 0. \tag{2.71}$$

This should be no surprise as, depending on the $V$-values of the anchor points, this case allows the two HRT surfaces to be spacelike separated.

The remaining case occurs when the intervals $(U_1, U_2)$ and $(U_1', U_2')$ overlap without having one fully contained in the other; see right panel of figure 2.2. For notational simplicity we let $u_i = u(U_i), u_i' = u(U_i')$ and we take both $U_1 > U_2$ and $U_1' > U_2'$. In this

case we find

$$\{A_U(U_1,U_2),A_U(U_1',U_2')\}=\begin{cases}-\frac{6\pi}{c}\left(1-\frac{2(u_1-u_1')(u_2-u_2')}{(u_1-u_2)(u_1'-u_2')}\right), & U_2'<U_2<U_1'<U_1\\ \frac{6\pi}{c}\left(1-\frac{2(u_1-u_1')(u_2-u_2')}{(u_1-u_2)(u_1'-u_2')}\right), & U_2<U_2'<U_1<U_1',\end{cases} \tag{2.72}$$

again with analogous results for the $V$ parts. We see there is no remaining dependence on $U_0$ or $U_0'$,

Let us now further explore this result by studying special cases. We begin by noting that choosing $U_1 = 0$, $V_1 = 0$ and $U_2 = -\infty$, $V_2 = \infty$ sets $A_{HRT}(U_1, V_1, U_2, V_2) = A_{HRT}[R_0]$, which is the case studied previously[7] in section 2.3. Combining expression (2.72) with the corresponding result for $V$ then yields

$$\{A_{HRT}[R_0], A_{HRT}(U_1', V_1', U_2', V_2'))\} = -8\pi G\left(\frac{u_1'\Theta(-u_1'u_2')}{u_1'-u_2'}+\frac{v_1'\Theta(-v_1'v_2')}{v_2'-v_1'}\right). \tag{2.73}$$

To evaluate this on the $AdS_3$ vacuum we set $u_i' = U_i', v_i' = V_i'$. The result then agrees with (2.31). We thus conclude that (2.72) is the generalization of (2.29) to general intervals and to arbitrary solutions in our phase space.

Another interesting special case arises where we again evaluate the commutator on the $AdS_3$ vacuum (thus setting $u_i = U_i, u_i' = U_i'$), but where we take all of the anchor points to lie on a $t = constant$ slice of the boundary. Choosing this slice to be $t = 0$, this is equivalent to setting $u_i = U_i = -V_i = -v_i$, $u_i' = U_i' = -V_i' = -v_i'$. As a result, if the $U$ term gives the upper result on the right-hand-side of (2.72), then the $V$ term gives the analogue of the lower result and the two cancel; i.e., when $R_1, R_2$ are both subsets of the $t = 0$ slice on the boundary we find

[7]Section 2.3 in fact defined $R_0$ only in the Poincaré vacuum, but here we generalize the definition so that in any spacetime $R_0$ is the region between $(U, V) = (0, 0)$ and $(U, V) = (-\infty, \infty)$.

$$\{A_{HRT}[R_1], A_{HRT}[R_2]\} = 0. \tag{2.74}$$

This result is to be expected from the fact that commutators of real functions must change sign under time reversal (as indicated in the quantum mechanical context due to the required factor of $i$ in the commutator), while the specified configuration and background are manifestly invariant under time-reversal. Indeed, for this reason the leading semiclassical commutator of HRT-areas will always vanish on a background that enjoys a time-reversal symmetry that leaves invariant both $R_1$ and $R_2$.

## 2.5 Discussion

The goal of our work was to study the flow on phase space generated by HRT-areas $A_{HRT}[R]$ in Einstein-Hilbert gravity, filling in various gaps in the literature. In particular, we showed that the canonical commutation relations can be used to evaluate this flow on any bulk Cauchy surface $\Sigma$ passing through the HRT surface $\gamma_R$. On such surfaces, the flow leaves the induced metric invariant but shifts the extrinsic curvature by a delta-function as described by (2.13). As predicted in [115], this effectively boosts the entanglement wedge of $R$ relative to that of the complementary region $\bar{R}$. However, the effect on the region to the future or past of $\gamma_R$ must be determined by solving the bulk equations of motion in the presence of appropriate boundary conditions.

Such boundary conditions lead to a difference between HRT-area flow and the kink transformation of [115]. This difference was again predicted in [115]. For vacuum $AdS_3$ spacetimes one can compute this difference and use it to obtain explicit formulae for the action of our flow on both the boundary stress tensor and other HRT-areas. Results were presented in section 2.3 for quantities evaluated on the Poincaré $AdS_3$ vacuum.

Section 2.4 then used a different approach to evaluate the associated commutators on general vacuum solutions asymptotic to $AdS_3$. This latter approach was based on the fact that, since all such solutions can be generated from the Poincaré vacuum by acting with boundary conformal transformations, any observable in this context can in principle be written as a functional of the boundary stress tensor. This method may also be of interest in its own right for computing other commutators for which the action on initial data is more complicated than that of $A_{HRT}[R]$.

We note that [114] also studied the effect of applying the transformation (2.13) at *non*-extremal codimension-2 spacelike surfaces $\gamma$. Again, this corresponds to boosting the initial data in what one might call the right wedge relative to that in the complementary (left) wedge. It was noted in [114] that when $\gamma$ is non-extremal the resulting initial data fails to satisfy the constraint equations of Einstein-Hilbert gravity. From our perspective, this is no surprise. For extremal $\gamma$ our (2.13) is generated by a diffeomorphism invariant observable, which necessarily commutes with all constraints. But more generally we would expect this to fail. In particular, while the flow generated by any diffeomorphism-invariant $A[\gamma]$ must also preserve the constraints, for non-extremal $\gamma$ there will be a non-trivial contribution from the first term in (2.4), so that the flow would no longer be given simply by (2.13). In this case the contribution from the first term in (2.4) must precisely cancel the contribution from the constraint-violating part of (2.13).

Some of our results may have further implications for holography, especially in connection with tensor network models of quantum error correction [69, 71]. One such result is that the commutator of two HRT-areas vanishes at leading semiclassical order when evaluated on a background where both HRT-surfaces lie in a common surface of time-symmetry.[8] As a result, such HRT-areas may be specified simultaneously with high accuracy. This observation may be useful in constructing bulk analogues of the above

[8]This in fact follows directly from time symmetry and did not require detailed computation.

tensor networks (e.g. as in [78, 28]) which appears to require bulk states in which such areas are sharply peaked [129, 75].

Another result that deserves further investigation was the observation in section 2.3.2 that HRT-area flow produces states of infinite energy. As argued in [113, 44, 114], the development of a UV singularity should be no surprise. But note that any sharp quantum eigenstate of $A_{HRT}[R]$ will be invariant under the flow that this operator generates. In particular, the expectation value of the energy will not change under this flow. We thus conclude that the expected energy in such states must be divergent, or at least set by some UV regulator. This may again have implications for the use of tensor networks in holography. More generally, this feature may be relevant for understanding the sense in which holographic quantum error correcting codes decompose into superselection sectors defined by $A_{HRT}[R]$ [60]. The point here is that the relevant code subspace is often taken to be states of low energy in the dual gauge theory [58], while we now see explicitly that states in any given such superselection sector must have energies set by the UV cutoff. However, as we see from the 2+1 dimensional case, this need not cause large curvatures in the bulk.

With regard to future directions, we recall that our work focussed on Einstein-Hilbert gravity. But it is natural to expect similar results to hold in the presence of higher derivative corrections. This will be explored in the forthcoming work [124], which will also comment further on the relation of $A_{HRT}[R]$ to the modular Hamiltonians on $R$ and $\bar{R}$.

# Chapter 3

# The Action of Geometric Entropy in Topologically Massive Gravity

## 3.1 Introduction

The study of entanglement entropy has contributed crucially to progress across theoretical physics. For instance, entanglement entropy has played an integral part in understanding the nature of quantum field theories [130], as well as understanding topological order in quantum many-body systems [131, 132]. Additionally, in holography, a fundamental outcome of the Anti-de Sitter/Conformal Field Theory (AdS/CFT) correspondence is the relation between entanglement entropies in the CFT and geometric entropies $\sigma$ of codimension-2 extremal surfaces in the AdS bulk. This relation is described by the Ryu-Takayanagi (RT) correspondence [61, 62], or by its covariant generalization, the Hubeny-Rangamani-Takayanagi (HRT) correspondence [63]. In the limit where the bulk is described by Einstein-Hilbert gravity, the geometric entropy $\sigma$ is just $A/4G$ where $A$ is the area of the surface, though higher derivative terms in the action provide additional corrections to $\sigma$ [76].

Given an HRT surface defined by a boundary region $R$, the area $A_{HRT}[R]$ of this HRT surface is hence of great interest (even without reference to its CFT dual). In particular, one can think of $A_{HRT}[R]$ as a quantum operator in the bulk by promoting it from its classical role as a function on the gravitational phase space. The action of this operator in semiclassical gravity was studied directly in [3], which is reproduced in Section 2, where it was found to generate a boundary-condition-preserving kink transformation. As will be described in more detail in Section 3.2.1 below, this transformation acts as a relative boost between the entanglement wedges on either side of the HRT surface. Prior to the explicit study of the action of $A_{HRT}[R]$ in [3], there were many closely related results in various contexts [108, 109, 110, 111, 118, 119, 120], which suggested a similar form for the transformation. Most relevant to our work here are [112, 113, 44, 114, 115], which suggested that the HRT area action would generate this boost-like transformation based on comparison with modular Hamiltonians. These modular Hamiltonians are given by the expression $K = -\log \rho$ for some state $\rho$.

In Section 2 we determined the action of $A_{HRT}[R]$ in the gravitational phase space, working in $\mathrm{AdS}_D$ Einstein-Hilbert gravity and including arbitrary minimally coupled matter. To understand the action on the phase space, we calculated Poisson brackets between $A_{HRT}[R]$ and certain gravitational data. Semiclassically, these Poisson brackets correspond to commutators, up to a factor of $i$. We also computed explicit Poisson brackets between HRT areas defined by different boundary regions $R$ in the Poincaré AdS groundstate for $2+1$ Einstein-Hilbert gravity. This calculation proceeded by starting with the boundary stress tensor algebra, then extending it to an area commutator via the Leibniz rule. The goal of the current work is to extend the results of Section 2 to $2+1$-dimensional asymptotically AdS spacetimes with a chiral boundary CFT, by which we mean a CFT with unequal left and right central charges.

The present work is inspired by [104], where the authors find an explicit expression for

the modular commutator [133, 134] in $1+1$D chiral CFTs. This modular commutator is defined as $J(A,B,C)_\rho = \langle [K_{AB}, K_{BC}] \rangle$, where $K_{AB}$ and $K_{BC}$ are the boundary modular Hamiltonians associated with regions $AB$ and $BC$, respectively, $\rho = \rho_{ABC}$ is some state, and $\langle ... \rangle$ denotes expectation values in that state. For contiguous CFT intervals $A$, $B$, and $C$ on a Cauchy surface $\Sigma$, the authors of [104] find a modular commutator given by

$$J(A,B,C)_\Omega = \frac{\pi c_L}{6}(2\eta_v - 1) - \frac{\pi c_R}{6}(2\eta_u - 1) \tag{3.1}$$

where $c_L, c_R$ are the left and right central charge, respectively, $|\Omega\rangle$ is the vacuum state on $\Sigma$, and $u = t-x$ and $v = t+x$ are light cone coordinates. Additionally, $\eta_u = \frac{(u_1-u_2)(u_3-u_4)}{(u_1-u_3)(u_2-u_4)}$ and $\eta_v = \frac{(v_1-v_2)(v_3-v_4)}{(v_1-v_3)(v_2-v_4)}$, where $(u_1, v_1)$ and $(u_2, v_2)$ are the anchor points of region $A$, $(u_2, v_2)$ and $(u_3, v_3)$ are the anchor points of region $B$, and $(u_3, v_3)$ and $(u_4, v_4)$ are the anchor points of region $C$.

We would like to compare Eq. (3.1) to bulk area commutators for general pure states in the bulk. By the Jafferis-Lewkowycz-Maldacena-Suh (JLMS) relation [117], we have $K_R = \frac{A_{ext}}{4G} + K_{bulk} + S_{corrections}$, where $A_{ext}$ is the area of an extremal surface corresponding to the boundary region $R$, $K_{bulk}$ is the modular Hamiltonian of the bulk region enclosed by the extremal surface, and $S_{corrections}$ arise when computing quantum corrections. These include Wald-like terms and higher derivative corrections, allowing for terms built from extrinsic curvatures. In semiclassical gravity, we can safely ignore $K_{bulk}$, giving $\sigma[R] \approx K_R$, where $\sigma$ may include the higher derivative corrections found in $S_{corrections}$. However, this introduces a potential subtlety: $\sigma[R] \approx K_R$ is true in *any* state, whereas the modular commutator is given by a commutator of vacuum modular Hamiltonians.

We can remedy this issue by noting that, in the bulk semiclassical approximation,

$$e^{i\lambda\sigma} |\psi\rangle \approx e^{i\lambda K_\psi} |\psi\rangle \tag{3.2}$$

for a modular Hamiltonian $K_\psi$ defined by the holographic pure state $|\psi\rangle$, and some arbitrary parameter $\lambda$[1]. This is enough to compute expectation values of commutators. In particular, we find $\langle [K_{AB}, K_{BC}]\rangle_\Omega = \langle [\sigma[AB], \sigma[BC]]\rangle_\Omega$ for $K_{AB}$, $K_{BC}$ defined in the state $|\Omega\rangle$. In Einstein-Hilbert gravity, $\sigma$ is an HRT area. In this case, Eq. (3.1) reduces to $J(A, B, C)_\Omega = \frac{\pi c}{3}(\eta_v - \eta_u)$. This is exactly the area commutator computed in [3].

We now wish to extend the derivation of area commutators to find agreement with the full modular commutator in Eq. (3.1). To do this, we need to modify our bulk spacetime so that it is dual to a boundary CFT with $c_L \neq c_R$. This can be accomplished by adding to the Einstein-Hilbert action a gravitational Chern-Simons term, which is a higher-derivative term that preserves bulk diffeomorphism invariance, but which introduces a gravitational anomaly in the dual CFT. This anomaly manifests as either a non-conservation of the boundary stress tensor or, equivalently, as an anti-symmetric part of the boundary stress tensor, thus allowing for chiral behavior in our boundary CFT. This anomaly arises due to the theory's sensitivity to the choice of coordinate system at the boundary. In $2+1$ bulk dimensions, the resulting bulk theory is known as topologically massive gravity (TMG); see [135, 136, 137] for original references. Previous work studying TMG in a holographic context includes [138, 139, 140, 141].

In TMG, due to the presence of the bulk Chern-Simons term, the geometric entropy is no longer given by just the HRT area. Instead, the geometric entropy is given by the HRT area plus an extra term, as derived from the bulk perspective in [142] (using methods based on those in [65]). We will call this the TMG geometric entropy, and denote the corresponding quantum operator as $\sigma_{TMG}[R]$. We can gain more intuition about the TMG geometric entropy by comparing with Einstein-Hilbert gravity, where we can think of the HRT area as the action of a massive particle propagating in the bulk. In contrast, in TMG, the geometric entropy is given by the action of a massive

[1]This approximation will be explained in detail in the forthcoming work [125].

spinning particle in the bulk. See [143, 144] for other studies on entanglement entropy in the presence of gravitational anomalies.

Using the TMG geometric entropy computed in [142], we derive vacuum expectation values of commutators of $\sigma_{TMG}$, which indeed match the modular commutator in Eq. (3.1). We also derive the Hamiltonian flow generated by $\sigma_{TMG}$ in semiclassical gravity. This direct calculation is a first step in understanding the action of geometric entropies in general higher-derivative gravitational theories. References [115, 3] suggest that geometric entropy flow should remain a boundary-condition-preserving kink transformation, even with the inclusion of higher-derivative corrections to the Einstein-Hilbert action. This conjecture will be studied further in [124]. Our work here is an explicit verification of this hypothesis for TMG.

As a final comment before proceeding with an outline of the paper, we note that [145] showed that chiral CFTs admit no lattice regularization due to the gravitational anomaly. That reference also argued that this is an obstruction to defining and interpreting entanglement entropy of subregions in chiral CFTs. A potential resolution is that one can define entanglement entropy in another way, perhaps by topological-regulation (thinking of the chiral CFT as induced on some boundary by a higher-dimensional non-chiral CFT) or via a lattice-continuum correspondence (see, e.g., [146]). Or, it is possible entanglement entropy cannot be defined, but that derivatives of the entanglement entropy still make sense.[2] We will not attempt to resolve this issue in this paper. We simply note that it is subtle and remains an open question in the literature.

In Section 3.2.1, we reformulate the derivation of the phase space flow generated by HRT areas in the language of Peierls brackets [147], which are equivalent to the more familiar Poisson brackets but are more convenient for our purposes. We then use this same Peierls bracket method to compute TMG geometric entropy flow in Section 3.2.2.

[2]We thank Jon Sorce for his insight on the lattice regularization issue and its potential resolutions.

The result is a boundary-condition-preserving kink transformation, which is exactly the transformation found for HRT area flow [3]. This result holds in spacetimes without matter. More generally, it holds to first order in the flow parameter for spacetimes with matter fields whose action is algebraic in the metric. This includes the usual two-derivative scalar, Yang-Mills, and Proca fields.

In Section 3.3, we compute the algebra of TMG entropy operators. We use the bulk perspective throughout this calculation, taking special care to include the Chern-Simons contribution to the boundary stress tensor in Section 3.3.1, and computing $\sigma_{TMG}$ for general states in Poincaré $AdS_3$ in Section 3.3.2. In Section 3.3.3, we calculate the $\sigma_{TMG}$ algebra in the vacuum using TMG geometric entropy flow, and in Section 3.3.4 we calculate the $\sigma_{TMG}$ algebra in general states using the stress tensor algebra. We provide this calculation to make contact with [3], and as an independent check on our main result in Section 3.2.2. In Section 3.3.4, we extend the work of [104] by finding the TMG entropy algebra for disjoint boundary regions $A$, $B$, and $C$. Finally, in Section 5.6, we conclude with some comments and possible future directions.

## 3.2 Geometric entropy flow

This section derives the geometric flow induced by the TMG geometric entropy $\sigma_{TMG}$. The result applies to asymptotically $AdS_3$ spacetimes with negative cosmological constant $\Lambda$ and without matter. It also holds to first order in the flow parameter $\lambda$ in spacetimes with matter fields whose action is algebraic in the metric, i.e., "standard matter". In order to quantify the entropy flow, we compute Peierls brackets between the geometric entropy and data on a particular Cauchy slice. In the bulk semiclassical approximation, Peierls brackets describe commutatation relations between operators (up to the usual factor of $i$). Importantly, a Peierls brakcet $\{A, B\}$ is only well-defined if both $A$ and $B$

are gauge-invariant.

In the dual CFT, we consider the entanglement entropy of an achronal region $R$. In semiclassical Einstein-Hilbert gravity, the associated geometric entropy is given by $1/4G$ times the area of the corresponding HRT surface, which is the minimal codimension-2 extremal surface anchored to $\partial R$ that satisfies the homology constraint of [121]. As we will see, in TMG the geometric entropy is instead given by $1/4G$ times the area of some surface $\gamma$ (which lies in a Cauchy slice $\Sigma$), plus an additional term related to other data on $\Sigma$. The surface $\gamma$ is the one which extremizes the entropy functional $\sigma_{TMG}$. The surface $\gamma$ generally differs from the HRT surface one would find for $c_L = c_R$, but they are the same when matter is not present [142].

Our Peierls bracket analysis will focus on the effect of geometric entropy flow on Cauchy data on $\Sigma$. One can then solve the equations of motion to find the action on the rest of the spacetime. In particular, we compute the bracket between the geometric entropy $\sigma$ and $K^{ij}$, the extrinsic curvature of the codimension-1 surface $\Sigma$. Readers unfamiliar with the Peierls bracket may wish to consult [148] (and references therein) for background information.

The procedure to compute Peierls brackets starts by adding $\sigma$ as a source to the action. Then, we solve the new equations of motion to find the retarded and advanced solutions for the extrinsic curvature, denoted as $D^- K^{ij}_{tot}$ and $D^+ K^{ij}_{tot}$, respectively. The rest of the data on $\Sigma$ remains unchanged. Finally, the desired Peierls bracket is defined by

$$\left\{\sigma, K^{ij}(x)\right\} = D^- K^{ij}_{tot}(x) - D^+ K^{ij}_{tot}(x). \tag{3.3}$$

Section 3.2.1 computes $\{A_{HRT}[R]/4G, K^{ij}(x)\}$ in Einstein-Hilbert gravity to illustrate the Peierls bracket method. We then compute $\{\sigma_{TMG}[R], K^{ij}(x)\}$ in Section 3.2.2.

### 3.2.1 Revisiting HRT area flow in semiclassical Einstein-Hilbert gravity

In this section, we directly compute Peierls brackets in asymptotically $\mathrm{AdS}_D$ Einstein-Hilbert gravity with standard matter. This commutator was previously computed in Section 2.2 using the canonical commutation relations of Einstein-Hilbert gravity; here, we instead use the ADM formalism [149] and the Peierls bracket method. We perform this calculation as a simple illustration of this method, before applying it to the more complicated case of TMG. As we will show, our result here matches the previous result.

In the ADM formalism, we decompose the metric according to

$$ds^2 = (-N^2 + N_i N^i)dt^2 + 2N^i dx dt + h_{ij}dx^i dx^j, \tag{3.4}$$

where $x^i$ are coordinates in a Cauchy slice $\Sigma$ and $h_{ij}$ is the induced metric on $\Sigma$. Using this decomposition, up to boundary terms the action can be written as [150]

$$\begin{aligned} I &= \int_{\mathcal{M}} dt d^{D-1}x\sqrt{-g}\left[\frac{1}{16\pi G}(R - 2\Lambda) + \mathcal{L}_M\right] \\ &= \int_{\mathcal{M}} dt d^{D-1}x N\sqrt{h}\left[\frac{1}{16\pi G}(r - K^2 + K_{ij}K^{ij} - 2\Lambda) + \mathcal{L}_M\right], \end{aligned} \tag{3.5}$$

where $\mathcal{M}$ is the entire bulk manifold, $r$ is the Ricci scalar on $\Sigma$, $\mathcal{L}_M$ is the matter Lagrangian, and $K^{ij}$ is the extrinsic curvature on $\Sigma$. The extrinsic curvature is defined as

$$K_{ij} = \frac{1}{2N}(\dot{h}_{ij} - D_i N_j - D_j N_i), \tag{3.6}$$

with $D_i$ the covariant derivative on $\Sigma$. We write the trace of $K_{ij}$ as $K = h_{ij}K^{ij}$.

Following the Peierls bracket method, we now add the geometric entropy defined by a boundary region $R$ as a source to the action. For semiclassical Einstein-Hilbert gravity,

the geometric entropy is given by $1/4G$ times the area of the HRT surface $\gamma$ corresponding to the boundary region $R$. Additionally, we choose $\Sigma$ so that it contains $\gamma$. The HRT area is given by [3]

$$\begin{aligned}\frac{A_{HRT}[R]}{4G} =& \frac{1}{4G}\int_{\gamma} d^{D-2}w\sqrt{q(w)} \\ =& \frac{1}{4G}\int_{\mathcal{M}} dtd^{D-1}x\sqrt{q(x)}\delta_{\Sigma}(\gamma,x)\delta(t-t_{\Sigma}),\end{aligned} \tag{3.7}$$

where $q_{AB}$ is the metric on the HRT surface, $\delta_{\Sigma}(\gamma,x)$ is a one-dimensional Dirac delta-function on the Cauchy slice which localizes $x$ to $\gamma$, and $t_{\Sigma}$ is the time associated with the Cauchy slice. Adding this to the action in Eq. (3.5) with (infinitesimal) weight $\lambda$ gives the modified action

$$\begin{aligned}I' = \int_{\mathcal{M}} dtd^{D-1}x\Bigg(&\frac{N}{16\pi G}\sqrt{h(x,t)}[r(x,t)-K^2(x,t)+K_{ij}(x,t)K^{ij}(x,t)-2\Lambda] \\ &+N\sqrt{h(x,t)}\mathcal{L}_M(x,t)+\frac{\lambda}{4G}\sqrt{q(x)}\delta_{\Sigma}(\gamma,x)\delta(t-t_{\Sigma})\Bigg).\end{aligned} \tag{3.8}$$

Next, we set $\delta I' = 0$ and solve the resulting equations of motion. The modification of the action introduces a new term containing $\delta(t-t_{\Sigma})$, and so, to cancel this term in the equation of motion, we need another term proportional $\delta(t-t_{\Sigma})$. As we will show, this can be achieved with an ansatz in which advanced and retarded solutions of the induced metric remain continuous but in which advanced and retarded solutions for $K^{ij}$ involve terms proportional to a Heaviside-function $\Theta(t-t_{\Sigma})$. We will denote the retarded solution by $D^{-}K^{ij}_{tot}$ and the advanced solution by $D^{+}K^{ij}_{tot}$. Below, we will focus only on "relevant" terms in the equation of motion. This simply means we will only keep terms proportional to $\delta(t-t_{\Sigma})$ which, with the above ansatz, are simply those containing time-derivatives of $D^{\pm}K^{ij}_{tot}$.

To find $\delta I'$, we need to understand the functional derivatives of $h_{ij}$ and $q_{ij}$ with

respect to $h_{ij}$. These are given [3] by

$$\frac{\delta h_{kl}(x)}{\delta h_{ij}(y)} = \delta^i_k \delta^j_l \delta^{(D-1)}(x-y) \tag{3.9}$$

$$\frac{\delta q_{AB}(x)}{\delta h_{ij}(y)} = \frac{\partial y^i}{\partial \tilde{x}^A}\frac{\partial y^j}{\partial \tilde{x}^B}\delta^{(D-2)}_\gamma(x,\tilde{x}(y))\delta_\Sigma(\gamma,y). \tag{3.10}$$

We also need to understand the variation of $K_{ij}$ with respect to $h_{ij}$, which is

$$\frac{\delta K_{kl}(x)}{\delta h_{ij}(y)} = \frac{1}{2N}\partial_t\left(\frac{\delta h_{kl}(x)}{\delta h_{ij}(y)}\right), \tag{3.11}$$

and which can be evaluated fully using Eq. (3.9). Finally, we need the variation of $A_{HRT}[R]$ with respect to $h_{ij}$, which is given by

$$\frac{\delta A_{HRT}[R]}{\delta h_{ij}(y)} = \frac{1}{2}\int_{\mathcal{M}} dt d^{D-1}x \frac{\delta q_{AB}(x)}{\delta h_{ij}(y)} q^{AB}(x)\delta_\Sigma(\gamma,x)\delta(t-t_\Sigma), \tag{3.12}$$

where, when the metric and $K_{ij}$ are evaluated at $t_\Sigma$, we do not write their explicit $t$-dependence. We will evaluate this fully by inserting Eq. (3.10). This provides all of the pieces needed to evaluate the variation of the modified action.

Keeping only the relevant terms, we have

$$\begin{aligned}\delta I'_{rel} =& \frac{1}{16\pi G}\int dt\sqrt{h(t,y)}\delta h_{ij}(t,y)\Bigg(\partial_t[K(t,y)h^{ij}(t,y) - K^{ij}(t,y)] \\ &+ 2\pi\lambda\frac{\sqrt{q(\tilde{x}(y))}}{\sqrt{h(y)}}q^{AB}(\tilde{x}(y))\frac{\partial y^i}{\partial \tilde{x}^A}\frac{\partial y^j}{\partial \tilde{x}^B}\delta(t-t_\Sigma)\delta_\Sigma(\gamma,y)\Bigg).\end{aligned} \tag{3.13}$$

Notice that $\mathcal{L}_M$ does not factor into our calculation as long as it does not contain any extrinsic curvature components. This is true for standard matter, as defined above. We will now solve for the effect of the new source term at first order in $\lambda$ about a background solution of the $\lambda = 0$ theory. For source strength $\lambda$, we write the extrinsic curvature at

this order in the form

$$K^{ij}(t,y) = \tilde{K}^{ij}(t,y) + \lambda D^{\pm} K^{ij}_{tot}(t,y), \tag{3.14}$$

where $\tilde{K}^{ij}$ is the original extrinsic curvature of the $\lambda = 0$ background.[3] As discussed above, $D^{\pm}K^{ij}_{tot}$ must contain terms with $\Theta(t - t_\Sigma)$, but it can also contain continuous terms. Thus, we can write $D^{\pm}K^{ij}_{tot} = D^{\pm}K^{ij} + D^{\pm}K^{ij}_{cont}$, where $D^{\pm}K^{ij}$ contains all Heaviside-function terms and $D^{\pm}K^{ij}_{cont}$ contains all continuous terms. Since the continuous terms in the advanced and retarded solutions must agree on $\Sigma$, their difference vanishes in the Peierls bracket, and we can rewrite Eq. (3.3) as

$$\{A_{HRT}[R], K^{ij}(t_\Sigma, y)\} = D^{-}K^{ij}(t_\Sigma, y) - D^{+}K^{ij}(t_\Sigma, y). \tag{3.15}$$

We now wish to solve for the advanced and retarded solutions to evaluate this Peierls bracket.

Plugging Eq. (3.14) into Eq. (3.13) and setting $\delta I'_{rel} = 0$, we have

$$\begin{aligned} &\partial_t D^{\pm}K^{ij}(t,y) - h_{kl}(t,y)\partial_t D^{\pm}K^{kl}(t,y)h^{ij}(t,y) = \\ &\qquad 2\pi \frac{\sqrt{q(\tilde{x}(y))}}{\sqrt{h(y)}} q^{AB}(\tilde{x}(y)) \frac{\partial y^i}{\partial \tilde{x}^A} \frac{\partial y^j}{\partial \tilde{x}^B} \delta_\Sigma(\gamma, y)\delta(t - t_\Sigma). \end{aligned} \tag{3.16}$$

[3]The calculation of HRT area flow is unaffected by the smoothness of $\tilde{K}^{ij}$, which is important for including matter in the background spacetime. This is explained in more detail at the end of this section.

Integrating over time[4] and performing a trace reverse gives our two solutions

$$D^- K^{ij}(t,y) = \quad 2\pi \frac{\sqrt{q(\tilde{x}(y))}}{\sqrt{h(y)}} \delta_\Sigma(\gamma,y)\Theta(t-t_\Sigma)\left(q^{AB}(\tilde{x}(y))\frac{\partial y^i}{\partial \tilde{x}^A}\frac{\partial y^j}{\partial \tilde{x}^B} - h^{ij}(y)\right) \tag{3.17}$$

$$D^+ K^{ij}(t,y) = -2\pi \frac{\sqrt{q(\tilde{x}(y))}}{\sqrt{h(y)}} \delta_\Sigma(\gamma,y)\Theta(t_\Sigma-t)\left(q^{AB}(\tilde{x}(y))\frac{\partial y^i}{\partial \tilde{x}^A}\frac{\partial y^j}{\partial \tilde{x}^B} - h^{ij}(y)\right). \tag{3.18}$$

Finally, using the Peierls bracket definition in Eq.(3.3), we arrive at our result

$$\begin{aligned}\left\{\frac{A_{HRT}[R]}{4G}, K^{ij}(t_\Sigma,y)\right\} =& 2\pi \frac{\sqrt{q(\tilde{x}(y))}}{\sqrt{h(y)}} \delta_\Sigma(\gamma,y)\left(q^{AB}(\tilde{x}(y))\frac{\partial y^i}{\partial \tilde{x}^A}\frac{\partial y^j}{\partial \tilde{x}^B} - h^{ij}(y)\right) \\ =& -2\pi \hat{\delta}_\Sigma(\gamma,y)\ \perp^i \perp^j,\end{aligned} \tag{3.19}$$

where $\perp^i$ is the unit normal to $\gamma$ in $\Sigma$, and $\hat{\delta}_\Sigma(\gamma,y) = \frac{\sqrt{q(\tilde{x}(y))}}{\sqrt{h(y)}}\delta_\Sigma(\gamma,y)$ is a one-dimensional Dirac delta-function of the proper distance between $x$ and $\gamma$ measured along geodesics in $\Sigma$ orthogonal to $\gamma$. Since $h^{ij}$ remains unchanged under the addition of the source term $\sigma$, the Peierls bracket $\{A_{HRT}[R], h^{ij}(t_\Sigma,y)\}$ vanishes. The flow thus adds a $\delta$-function (times $-2\pi\lambda$) to $K^{\perp\perp}$, but leaves all other initial data on $\Sigma$ unchanged. This precisely matches our previous result for the HRT area flow in [3], which we arrived at using the standard Poisson brackets of phase space variables on the Cauchy slice.

How can we understand this result geometrically? We can integrate Eq. (3.19) to yield the effect of a finite flow by a parameter $\lambda$, and we see that the flow induced by the HRT area introduces a relative boost in $\Sigma$, on either side of $\gamma$. This "kinks" the data on the Cauchy slice in the bulk, as shown in Figure 3.1a, and the rest of the solution is determined by the equations of motion. However, we must take special care with boundary conditions. In particular, since $\Sigma$ represents a definite instant of time, the

[4]Because the induced metric $h_{ij}$ depends on time, our expressions for $D^\pm K^{ij}$ are not the exact results of these integrals. Instead, Eq. (3.17) and (3.18) give only the discontinuous terms. If we expand each metric as a power series in $t$, then our expressions for $D^\pm K^{ij}$ come from considering only the term proportional to $\theta(t-t_\Sigma)$; higher-order terms in the metric give continuous terms which do not contribute to the Peierls bracket.

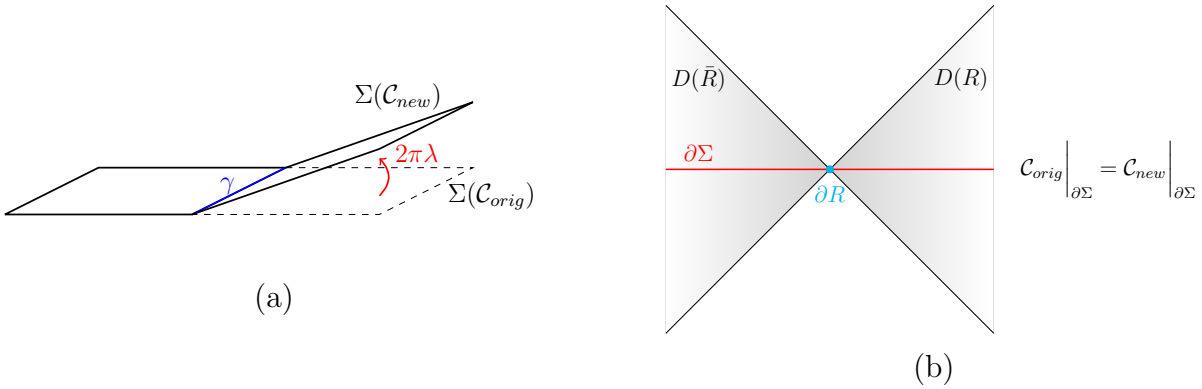


Figure 3.1: The geometry of the boundary-condition-preserving kink transformation. Figure 3.1a shows the transformation of the Cauchy data on $\Sigma$ in the bulk, from $\mathcal{C}_{orig}$ to $\mathcal{C}_{new}$. The flow induces a relative boost with parameter $2\pi\lambda$ between the left and right sides of $\Sigma$. Figure 3.1b depicts the transformation induced in the boundary, showing the domains of dependence $D(R)$ of $R$ and $D(\bar{R})$ of $\bar{R}$. $\partial R$ is the intersection between the boundary and $\gamma$, and $\partial\Sigma$ is the boundary of a smooth bulk Cauchy surface $\Sigma$ in the original spacetime. On the surface $\partial\Sigma$, $\mathcal{C}_{orig} = \mathcal{C}_{new}$. All boundary observables on that surface are preserved by the flow generated by $A_{HRT}[R]$.

boundary of $\Sigma$ ($\partial\Sigma$) must remain fixed due to the asymptotic AdS boundary conditions. This is shown in Figure 3.1b. Following [3], we refer to this transformation as a boundary-condition-preserving kink transformation.

The treatment of boundary conditions is in contrast to the original kink transformation introduced in [115]. Defining $\mathcal{K}[\gamma]$ as the generator of this original kink transformation by $\lambda$, then $\mathcal{K}[\gamma]$ has the same bulk action as $A_{HRT}[R]/4G$ but has different boundary conditions as $\mathcal{K}[\gamma]$ would instead introduce a relative boost on either side of $\partial R$, the boundary of $\gamma$. In particular, this $\mathcal{K}[\gamma]$ also acts as a relative boost at the boundary. Then, defining $H_R$ to be ($2\pi$ times) the generator of the boundary one-sided boost (taken to generate flow toward the future in the right wedge), the relation can be expressed in the form $\frac{A_{HRT}[R]}{4G} = H_R + \mathcal{K}[\gamma]$. This notation will be useful in Section 3.3.3.

As a final comment, we note that integrating the flow to finite $\lambda$ requires an understanding of the Peierls Bracket evaluated at certain background solutions that are non-smooth as well as at those that are smooth. This is because, if we take a smooth

background solution and apply HRT area flow, then the solution immediately becomes non-smooth due to the kink transformation. In the analysis above, we allowed for non-smooth $\tilde{K}^{ij}$, so there is no obstruction to integrating to finite $\lambda$. However, as we will see, integrating to finite $\lambda$ is more difficult for TMG entropy flow.

### 3.2.2 Entropy flow in TMG

We now apply the Peierls bracket method to TMG in spacetimes asymptotic to $AdS_3$ with standard matter. In this theory, the bulk action is

$$I = I_{EH} - \beta I_{CS}, \tag{3.20}$$

where $I_{EH}$ is the Einstein-Hilbert action and $I_{CS}$ is the Chern-Simons action, defined as

$$I_{CS} = \int_{\mathcal{M}} \mathrm{Tr}\left[\Gamma d\Gamma + \frac{2}{3}\Gamma^3\right]. \tag{3.21}$$

The constant $\beta$ measures the anomaly coefficient. It is defined as

$$\beta = \frac{c_L - c_R}{96\pi}, \tag{3.22}$$

and we can use this to write the left and right central charges as $c_L = c_0 + 48\pi\beta$ and $c_R = c_0 - 48\pi\beta$, where $c_0 = 3/2G$ is the central charge in the absence of the Chern-Simons term. For more information on the notation used above, we refer the reader to, e.g., [138].

Again, we have a boundary region $R$ and its corresponding HRT surface $\gamma$. We are interested in calculating the Peierls bracket between $\sigma_{TMG}[R]$, the geometric entropy determined by $R$, and $K^{ij}$, the extrinsic curvature of a Cauchy slice $\Sigma$ containing $\gamma$. To

do so, we add $\sigma_{TMG}$ as a source to the action, take the variation, and solve the equations of motion. Thus, we are interested in solutions to the equation

$$\delta I_{EH} - \beta \delta I_{CS} + \lambda \delta \sigma_{TMG}[R] = 0. \tag{3.23}$$

In Section 3.2.1, we calculated the relevant terms of $\delta I_{EH}$. As we will show, these terms will again be the only relevant terms in our TMG calculation. We are left with computing the relevant terms in $\delta I_{CS}$ and $\delta \sigma_{TMG}[R]$.

In what follows, we will fix our gauge so that $N = 1$ and $N^i = 0$. As we mentioned above, this gauge-fixing is allowed because a Peierls bracket $\{A, B\}$ must have gauge-invariant $A$ and $B$.

**Calculating $\delta \sigma_{TMG}[R]$**

In TMG, the geometric entropy is modified by an additional term, and so is no longer given by the HRT area. Instead, by Equation (3.26) of [142], the TMG geometric entropy defined by a boundary region $R$ is given by

$$\sigma_{TMG}[R] = \frac{1}{4G} \int_\gamma ds \left( \sqrt{g_{\mu\nu} \dot{X}^\mu \dot{X}^\nu} - 32\pi G \beta \tilde{\nu} \cdot \nabla \nu \right), \tag{3.24}$$

where $\gamma$ is the curve in spacetime that extremizes $\sigma_{TMG}$. The first term in the expression gives the area of $\gamma$. Without matter, $\gamma$ is the HRT surface one would find for $c_L = c_R$, and so the first term is the usual HRT area term. However, with matter present, $\gamma$ generally differs from the HRT surface. At each point of $\gamma$ the vectors $\nu^\mu$, $\tilde{\nu}^\mu$ define an orthonormal frame in the orthogonal plane. Now, the exact Poincaré $AdS_3$ solution has the metric

$$ds^2 = \frac{1}{z^2}(-dt^2 + dx^2 + dz^2), \tag{3.25}$$

where we set $l_{AdS} = 1$. Our spacetime is asymptotically $AdS_3$, so we can take our metric to asymptote to Eq. (3.25) and use the corresponding coordinates $(t, x)$ to specify vectors on the boundary. We define the normal frame at the boundary as $\nu_\partial = \partial_t$ and $\tilde{\nu}_\partial = \partial_x$. We choose a Cauchy slice $\Sigma$ so that it contains $\gamma$. The surface $\gamma$ has two endpoints, and, in general, they do not have the same $t$-coordinates but they do lie on the same spacelike line on the boundary. We are free to choose $\Sigma$ to asymptote to that line, which is a boost of the constant $t$ slice by some boost parameter $\alpha$. Then, we can define the boundary vectors,

$$n^\mu_\partial = \quad (\cosh\alpha, -\sinh\alpha, 0) \tag{3.26}$$

$$\perp^\mu_\partial = \quad (-\sinh\alpha, \cosh\alpha, 0) \tag{3.27}$$

where $n^\mu$ is the vector normal to $\Sigma$ and $\perp^\mu$ is the vector normal to $\gamma$ in $\Sigma$, and $n^\mu_\partial$ and $\perp^\mu_\partial$ are the boundary values of these vectors. Thus, in the bulk, we must have

$$\nu_\mu = \quad \cosh\alpha(n_\mu + \tanh\alpha \perp_\mu) \tag{3.28}$$

$$\tilde{\nu}^\mu = \quad \cosh\alpha(\tanh\alpha\, n^\mu + \perp^\mu). \tag{3.29}$$

Plugging into the last term in the action, we have

$$\begin{aligned} \tilde{\nu}^\mu \nabla \nu_\mu &= \perp^\mu v^\sigma K_{\mu\sigma} \\ &= \perp^i v^j K_{ij}, \end{aligned} \tag{3.30}$$

where, since $\perp^\mu$ and $v^\mu$ lie within $\Sigma$, we denote them with Latin indices.

Let us define the area of a surface $\xi$ as $A[\xi, g]$, where $g$ is the spacetime metric. Using

our above result in Eq. (3.24), we get

$$\begin{aligned}\sigma_{TMG}[R] =&\frac{A[\gamma,g]}{4G} - 8\pi\beta\int_\gamma ds\ \perp^k v^l K_{kl}(s)\\ =&\frac{A[\gamma,g]}{4G} - 8\pi\beta\int_\gamma dx\sqrt{q(x)}\ \perp^k v^l K_{kl}(x).\end{aligned} \tag{3.31}$$

We now wish to vary the geometric entropy. In general, there are two components to this variation: the variation with respect to the surface and the variation with respect to $g$. However, because $\gamma$ extremizes $\sigma_{TMG}$, the variation with respect to the surface vanishes when evaluated at $\gamma$. So, we need only consider variations with respect to the metric, and can treat $\gamma$ as fixed.[5] This yields

$$\begin{aligned}\delta\sigma_{TMG}[R] =&\frac{\tilde{\delta}A[\gamma,g]}{4G} - 8\pi\beta\int_\gamma dx\sqrt{q(x)}\Big[\ \perp^k v^l\delta K_{kl}(x) + \delta(\perp^k v^l)K_{kl}(x)\\ &+\frac{\delta\sqrt{q(x)}}{\sqrt{q(x)}}\ \perp^k v^l K_{kl}(x)\Big]\\ =&\frac{\tilde{\delta}A[\gamma,g]}{4G} - 8\pi\beta\int_{\mathcal{M}} dtd^2x\sqrt{q(x)}\Big[\ \perp^k v^l\delta K_{kl}(x) + \delta(\perp^k v^l)K_{kl}(x)\\ &+\frac{\delta\sqrt{q(x)}}{\sqrt{q(x)}}\ \perp^k v^l K_{kl}(x)\Big]\delta_\Sigma(\gamma,x)\delta(t-t_\Sigma),\end{aligned} \tag{3.32}$$

where $\tilde{\delta}A[\gamma,g]$ is the variation of the area at fixed $\gamma$, as given by Eq. (3.12).[6] As before, when the metric and $K_{ij}$ are evaluated at $t_\Sigma$, we do not write their explicit $t$-dependence. We also have expressions for $\delta K^{ij}$ and $\delta q_{ij}$, so all that is left to understand is the variation of $\perp^k v^l$. We have

$$0 = \delta(h_{ij}\ \perp^i\perp^j) =\perp^i\perp^j\ \delta h_{ij} + 2\ \perp_i\delta\ \perp^i, \tag{3.33}$$

[5]For a more detailed argument on why we treat $\gamma$ as fixed, we refer the reader to the discussion at the start of Section 2.1 in [3].

[6]While Eq. (3.12) was defined as the HRT area variation, it holds more generally as the variation of an area $A[\xi,g]$ with respect to the metric.

which gives

$$\delta \perp^i = -\frac{1}{2} \perp^i \perp^k \perp^l \delta h_{kl} + \zeta v^i, \tag{3.34}$$

where $\zeta$ is an unknown constant. Similarly, we can write

$$0 = \delta(h_{ij} v^i v^j) = v^i v^j \delta h_{ij} + 2 v_i \delta v^i, \tag{3.35}$$

which gives

$$\delta v^i = -\frac{1}{2} v^i v^k v^l \delta h_{kl} + \eta \perp^i, \tag{3.36}$$

where $\eta$ is a constant. Since we can treat $\gamma$ as a fixed surface, the only components of $\delta v^i$ we need are those which keep it normalized. Hence, $\eta = 0$, so

$$\delta v^i = -\frac{1}{2} v^i v^k v^l \delta h_{kl}. \tag{3.37}$$

To solve for $\zeta$, we now use

$$0 = \delta(h_{ij} \perp^i v^j) = \perp^i v^j \delta h_{ij} + \zeta, \tag{3.38}$$

yielding $\zeta = - \perp^i v^j \delta h_{ij}$. Thus, we have

$$\delta \perp^i = -\frac{1}{2} \perp^i \perp^k \perp^l \delta h_{kl} - v^i \perp^k v^l \delta h_{kl}. \tag{3.39}$$

We can now use Eq. (3.12) for the area variation, Eq. (3.37) for the variation of $v^i$,

and Eq. (3.39) for the variation of $\perp^i$ in Eq. (3.32). This gives

$$\begin{aligned}\delta\sigma_{TMG}[R] = \int dt\sqrt{q(\tilde{x}(y))}\Big( &- 4\pi\beta \perp^i v^j \delta'(t-t_\Sigma) \\ &+ \frac{1}{8G}q^{AB}(\tilde{x}(y))\frac{\partial y^i}{\partial \tilde{x}^A}\frac{\partial y^j}{\partial \tilde{x}^B}\delta(t-t_\Sigma) - 8\pi\beta v^k v^l K_{kl}(y) \perp^i v^j \delta(t-t_\Sigma) \\ &- 4\pi\beta \perp^k v^l K_{kl}(y) \perp^i \perp^j \delta(t-t_\Sigma) - 4\pi\beta \perp^k v^l K_{kl}(y) v^i v^j \delta(t-t_\Sigma) \\ &+ 4\pi\beta q^{AB}(\tilde{x}(y))\frac{\partial y^i}{\partial \tilde{x}^A}\frac{\partial y^j}{\partial \tilde{x}^B} \perp^k v^l K_{kl}(y)\delta(t-t_\Sigma)\Big)\delta_\Sigma(\gamma,y)\delta h_{ij}(y).\end{aligned} \tag{3.40}$$

As in Einstein-Hilbert gravity, the source variation includes terms proportional to a Dirac delta function, $\delta(t-t_\Sigma)$. However, unlike the previous case, the first term in Eq. (3.40) contains a time derivative of a delta function, denoted as $\delta'(t-t_\Sigma)$. We thus need other terms in the equation of motion to be proportional to $\delta$-functions and $\delta$-function derivatives, so they can cancel these new terms. As we will show in Section 3.2.2, there will be terms in the equation of motion containing $\partial_t^2 D^\pm K_{tot}^{ij}$, so we can use the same ansatz as before. Namely, we will choose the advanced and retarded solutions of the induced metric, $D^\pm h^{ij}$, to be continuous, but choose solutions of the extrinsic curvature, $D^\pm K_{tot}^{ij}$, to have discontinuous terms proportional to a Heaviside-function.

As before, we will focus below only on "relevant" terms in the equation of motion. In this case, the relevant terms are ones containing $\partial_t D^\pm K_{tot}^{ij}$ or $\partial_t^2 D^\pm K_{tot}^{ij}$; with our ansatz, these will give the necessary $\delta(t-t_\Sigma)$ and $\delta'(t-t_\Sigma)$ terms.

**Calculating $\delta I_{CS}$**

The variation of $I_{CS}$, as given in [139], is

$$\delta I_{CS} = -2\int_{\mathcal{M}} dt d^2x\sqrt{h}C^{\mu\nu}\delta g_{\mu\nu}, \tag{3.41}$$

where $C^{\mu\nu}$ is the Cotton tensor. In 3-dimensions, the Cotton tensor is

$$\begin{aligned} C^{\mu\nu} =& \epsilon^{\mu\alpha\sigma}\nabla_\alpha\left(R^\nu_\sigma - \frac{1}{4}\delta^\nu_\sigma R\right) \\ =& \epsilon^{\mu\alpha\sigma}\partial_\alpha R^\nu_\sigma + \epsilon^{\mu\alpha\sigma}\Gamma^\nu_{\alpha\lambda}R^\lambda_\sigma - \epsilon^{\mu\alpha\sigma}\Gamma^\lambda_{\alpha\sigma}R^\nu_\lambda - \frac{1}{4}\epsilon^{\mu\alpha\nu}\nabla_\alpha R. \end{aligned} \tag{3.42}$$

It is of course important that all equations of motion are satisfied. However, for the purposes of this calculation, we need only consider the equations involving the $\mu = i$, $\nu = j$ components of the Cotton tensor, where $i, j$ are spatial indices. This is because variations of $\sigma_{TMG}[R]$ depend only on the induced metric, and not on any other metric components. Thus, these are the parts of the equation of motion changed by the introduction of the source, and all the other equations are constraints. The Bianchi identities guarantee that if the constraints are satisfied on any surface (e.g., to the past in a retarded solution) and if the equations of motion studied in this section are satisfied, the constraints will continue to hold on any surface. As a result, we need not explicitly check that the constraints are satisfied, and we may focus our attention on the remaining equations of motion.

After some cancellations, the spatial components of the Cotton tensor are

$$C^{ij} = \frac{1}{2}\left(\epsilon^{i\alpha\sigma}\partial_\alpha R^j_\sigma + \epsilon^{i\alpha\sigma}\Gamma^j_{\alpha\lambda}R^\lambda_\sigma + \epsilon^{j\alpha\sigma}\partial_\alpha R^i_\sigma + \epsilon^{j\alpha\sigma}\Gamma^i_{\alpha\lambda}R^\lambda_\sigma\right), \tag{3.43}$$

where we made explicit the symmetry under exchange of $i$ and $j$. As above, we are only interested in contributions containing a time derivative of the extrinsic curvature. Evaluating Eq. (3.43) in the gauge $N = 1$ and $N^i = 0$, and keeping only relevant terms,

we arrive at

$$\begin{aligned} C^{ij}_{rel} =& \frac{1}{2}\epsilon^{itk}\Big(\partial_t^2 K^j_k - 4\partial_t(K_{lk}K^{lj}) + \partial_t(KK^j_k) + K^j_l\partial_t K^l_k - K^j_k\partial_t K\Big) \\ &+ \frac{1}{2}\epsilon^{jtk}\Big(\partial_t^2 K^i_k - 4\partial_t(K_{lk}K^{li}) + \partial_t(KK^i_k) + K^i_l\partial_t K^l_k - K^i_k\partial_t K\Big). \end{aligned} \tag{3.44}$$

Using Eq. (3.9) and the identity

$$\delta h_{ij}(x) = \frac{\delta h_{ij}(x)}{\delta h_{kl}(y)}\delta h_{kl}(y), \tag{3.45}$$

we plug into Eq. (3.41), yielding

$$\begin{aligned} \delta I_{CS,rel} =& -\int dt\sqrt{h(t,y)}\epsilon^{itk}\Big(\partial_t^2 K^j_k(t,y) - 4\partial_t(K_{lk}(t,y)K^{lj}(t,y)) \\ &+ \partial_t(K(t,y)K^j_k(t,y)) + K^j_l(t,y)\partial_t K^l_k(t,y) \\ &- K^j_k(t,y)\partial_t K(t,y)\Big)\delta h_{ij}(t,y) \\ &- \int dt\sqrt{h(t,y)}\epsilon^{jtk}\Big(\partial_t^2 K^i_k(t,y) - 4\partial_t(K_{lk}(t,y)K^{li}(t,y)) \\ &+ \partial_t(K(t,y)K^i_k(t,y)) + K^i_l(t,y)\partial_t K^l_k(t,y) \\ &- K^i_k(t,y)\partial_t K(t,y)\Big)\delta h_{ij}(t,y). \end{aligned} \tag{3.46}$$

We now have equations for the relevant terms in $\delta I_{CS}$, $\delta\sigma_{TMG}[R]$ from Eq. (3.40), and $\delta I_{EH}$ from Eq. (3.13). In the next section, we combine these equations together to solve the equation of motion.

### Solving the modified equations of motion

To find the Peierls bracket, we start by using our expressions for $\delta I_{EH}$, $\delta\sigma_{TMG}[R]$, and $\delta I_{CS}$ in Eq. (3.23). As in Section 3.2.1, we write $K^{ij} = \tilde{K}^{ij} + \lambda D^{\pm}K^{ij}_{tot}$, where $\tilde{K}^{ij}$

is the extrinsic curvature before introducing the source $\lambda\sigma_{TMG}[R]$. As stated above, the modified extrinsic curvature, $D^{\pm}K^{ij}_{tot}$, has terms proportional to a Heaviside-function. It can also have terms containing $(t-t_\Sigma)\Theta(t-t_\Sigma)$ (i.e., a sharp corner), which, under two time derivatives, becomes a $\delta$-function. We will thus write

$$D^{\pm}K^{ij}_{tot} = D^{\pm}K^{ij} + D^{\pm}\bar{K}^{ij} + D^{\pm}K^{ij}_{other}, \tag{3.47}$$

where $D^{\pm}K^{ij}$ contains all $\Theta$-function terms, $D^{\pm}\bar{K}^{ij}$ contains all corner terms, and $D^{\pm}K^{ij}_{other}$ contains any other continuous terms that come along for the ride (which, of course, will not contribute any $\delta$-functions, even under the action of second derivatives). To find the Peierls bracket we use Eq. (3.15), and hence we do not need to find the explicit expression for any continuous terms.

In contrast to the calculation of HRT area flow in Section 3.2.1, the flow calculation in this section *does* depend on the smoothness of $\tilde{K}^{ij}$. For the remainder of this section, we will take $\tilde{K}^{ij}$ to be smooth. This generally suffices to derive the flow only at first order in $\lambda$ around smooth solutions (see the comments at the end of Section 3.2.1). Without matter, the extension to all orders turns out to be trivial, since these spacetimes are always locally $AdS_3$, and the kink is just a coordinate artifact. While we expect our result to hold when matter is present, we save a proof of this for future work. At the moment, our results hold only at first order in $\lambda$ when matter is present.

Using our new expression for $K^{ij}$ in Eq. (3.48) and taking $\lambda$ small, we obtain an

equation relating the terms proportional to $\delta(t-t_\Sigma)$,

$$\begin{aligned}
0 =& -\frac{1}{16\pi G}\sqrt{h(t,y)}[\partial_t D^\pm K^{ij}(t,y) - \partial_t D^\pm K(t,y)h^{ij}(t,y)] \\
&+ \beta\sqrt{h(t,y)}\epsilon^{itk}\Big(\partial_t^2 D^\pm \bar{K}^j_k(t,y) - 4\tilde{K}^{lj}(t,y)\partial_t D^\pm K_{lk}(t,y) \\
&- 4\tilde{K}_{lk}(t,y)\partial_t D^\pm K^{lj}(t,y) + \tilde{K}^j_k(t,y)\partial_t D^\pm K(t,y) + \tilde{K}(t,y)\partial_t D^\pm K^j_k(t,y)) \\
&+ \tilde{K}^{lj}(t,y)\partial_t D^\pm K_{lk}(t,y) - \tilde{K}^j_k(t,y)\partial_t D^\pm K(t,y)\Big) \\
&+ \beta\sqrt{h(t,y)}\epsilon^{jtk}\Big(\partial_t^2 D^\pm \bar{K}^i_k(t,y) - 4\tilde{K}^{li}(t,y)\partial_t D^\pm K_{lk}(t,y) \\
&- 4\tilde{K}_{lk}(t,y)\partial_t D^\pm K^{li}(t,y) + \tilde{K}^i_k(t,y)\partial_t D^\pm K(t,y) + \tilde{K}(t,y)\partial_t D^\pm K^i_k(t,y)) \\
&+ \tilde{K}^{li}(t,y)\partial_t D^\pm K_{lk}(t,y) - \tilde{K}^i_k(t,y)\partial_t D^\pm K(t,y)\Big) \\
&+ \sqrt{q(\tilde{x}(y))}\delta_\Sigma(\gamma,y)\delta(t-t_\Sigma)\Big(\frac{1}{8G}q^{AB}(\tilde{x}(y))\frac{\partial y^i}{\partial \tilde{x}^A}\frac{\partial y^j}{\partial \tilde{x}^B} \\
&- 4\pi\beta \perp^k v^l K_{kl}(y) \perp^i \perp^j -4\pi\beta \perp^k v^l K_{kl}(y) v^i v^j \\
&- 8\pi\beta v^k v^l K_{kl}(y) \perp^{(i} v^{j)} + 4\pi\beta q^{AB}(\tilde{x}(y))\frac{\partial y^i}{\partial \tilde{x}^A}\frac{\partial y^j}{\partial \tilde{x}^B} \perp^k v^l K_{kl}(y)\Big),
\end{aligned} \tag{3.48}$$

and another equation relating terms proportional to $\delta'(t-t_\Sigma)$,

$$\partial_t^2(\epsilon^{itk}D^\pm K^j_k(t,y) + \epsilon^{jtk}D^\pm K^i_k(t,y)) = 4\pi\frac{\sqrt{q(\tilde{x}(y))}}{\sqrt{h(y)}}\delta_\Sigma(\gamma,y) \perp^{(i} v^{j)}\delta'(t-t_\Sigma). \tag{3.49}$$

Integrating the latter equation twice on both sides, we get an equation for the retarded and advanced solutions, respectively:

$$\epsilon^{itk}D^- K^j_k(t,y) + \epsilon^{jtk}D^- K^i_k(t,y) = \quad 4\pi\frac{\sqrt{q(\tilde{x}(y))}}{\sqrt{h(y)}}\delta_\Sigma(\gamma,y) \perp^{(i} v^{j)}\Theta(t-t_\Sigma), \tag{3.50}$$

$$\epsilon^{itk}D^+ K^j_k(t,y) + \epsilon^{jtk}D^+ K^i_k(t,y) = \quad -4\pi\frac{\sqrt{q(\tilde{x}(y))}}{\sqrt{h(y)}}\delta_\Sigma(\gamma,y) \perp^{(i} v^{j)}\Theta(t_\Sigma - t). \tag{3.51}$$

For now we will work with the retarded solution, saving the advanced solution for later.

Contracting Eq. (3.50) with $\perp_i \perp_j$ and $v_i v_j$, we find

$$\perp^k v_j D^- K^j_k(t,y) = 0 \quad \text{and} \quad v^k \perp_j D^- K^j_k(t,y) = 0. \tag{3.52}$$

To obtain the above equation, we used $\perp_i \epsilon^{itk} = v^k$ and $v_i \epsilon^{itk} = - \perp^k$. To derive these, we note that, due to the normalization and orthogonality constraints of $\perp^i$, $v^i$, and $n^a$, we have

$$\perp_i \epsilon^{i0k} = \pm v^k. \tag{3.53}$$

This then gives $\perp_i v_k \epsilon^{i0k} = \pm 1$, and so $\perp_k v_i \epsilon^{i0k} = \mp 1$. We then have

$$v_i \epsilon^{i0k} = \mp \perp^k . \tag{3.54}$$

In what follows, we choose the plus sign in Eq. (3.53) and so we have the minus sign in Eq. (3.54). We choose these signs so that our result in the limit $c_L = c_R$ matches what we find for Einstein-Hilbert gravity. This choice of sign appears to be consistent with standard conventions, e.g. in [151].

Now that we have derived these useful identities, let us contract Eq. (3.50) with $\perp_i v_j + v_i \perp_j$, yielding

$$(v_i v_j - \perp_i \perp_j) D^- K^{ij}(t,y) = 2\pi \frac{\sqrt{q(\tilde{x}(y))}}{\sqrt{h(y)}} \delta_\Sigma(\gamma, y) \Theta(t - t_\Sigma). \tag{3.55}$$

These are thus the only components of the solution that survive. We can therefore write the solution as

$$D^- K^{ij}(t,y) = 2\pi \frac{\sqrt{q(\tilde{x}(y))}}{\sqrt{h(y)}} \delta_\Sigma(\gamma, y) \Theta(t - t_\Sigma)(c_v v^i v^j + c_\perp \perp^i \perp^j), \tag{3.56}$$

with $c_v - c_\perp = 1$.

We now must solve for $c_v$ and $c_\perp$. We start by contracting Eq. (3.48) with $\perp_i\perp_j + v_i v_j$. Under this contraction, many terms will cancel out, and we are left with

$$\begin{aligned}0 =& -\frac{1}{16\pi G}\sqrt{h(t,y)}(\perp_i\perp_j + v_i v_j)\partial_t D^- K^{ij}(t,y) + \frac{1}{8\pi G}\sqrt{h(y)}\partial_t D^- K(t,y)\\ &+ \beta\sqrt{h(y)}(\perp_i\perp_j + v_i v_j)\epsilon^{itk}K^{lj}(t,y)\partial_t D^- K_{lk}(t,y)\\ &+ \beta\sqrt{h(t,y)}(\perp_i\perp_j + v_i v_j)\epsilon^{jtk}K^{li}(t,y)\partial_t D^- K_{lk}(t,y)\\ &+ \frac{1}{8G}\sqrt{q(\tilde{x}(y))}\delta_\Sigma(\gamma,y)\delta(t-t_\Sigma) - 4\pi\beta\sqrt{q(\tilde{x}(y))}\perp^k v^l K_{kl}(y)\delta_\Sigma(\gamma,y)\delta(t-t_\Sigma).\end{aligned} \tag{3.57}$$

Substituting the right-hand side of Eq. (3.56) into the equation above, we find

$$\frac{1}{8G}(c_\perp + c_v) + 4\pi\beta(c_v - c_\perp)\perp^k v^k K_{kl}(y) = -\frac{1}{8G} + 4\pi\beta\perp^k v^l K_{kl}(y). \tag{3.58}$$

Since $c_v - c_\perp = 1$, the equation above reduces to $c_\perp + c_v = -1$. Then we have $c_\perp = -1$ and $c_v = 0$. Using Eq.(3.56), we obtain the retarded solution

$$\begin{aligned}D^- K^{ij}(t,y) =& -2\pi\frac{\sqrt{q(\tilde{x}(y))}}{\sqrt{h(y)}}\delta_\Sigma(\gamma,y)\Theta(t-t_\Sigma)\perp^i\perp^j\\ =& -2\pi\hat{\delta}_\Sigma(\gamma,y)\Theta(t-t_\Sigma)\perp^i\perp^j .\end{aligned} \tag{3.59}$$

To solve for the advanced solution, $D^+K^{ij}$, we start from Eq. (3.51) and follow the same steps as for the retarded solution. We thus obtain

$$D^+ K^{ij}(t,y) = 2\pi\hat{\delta}_\Sigma(\gamma,y)\Theta(t_\Sigma - t)\perp^i\perp^j . \tag{3.60}$$

Combining Equations (3.59) and (3.60) yields the Peierls bracket

$$\left\{\sigma_{TMG}[R], K^{ij}(t_\Sigma,y)\right\} = -2\pi\hat{\delta}_\Sigma(\gamma,y)\perp^i\perp^j . \tag{3.61}$$

This is our main result, and it agrees exactly with Eq. (3.19), the result for Einstein-Hilbert gravity. The action of $\sigma_{TMG}[R]$ is thus the same as the HRT area action, generating a boundary-condition-preserving kink transformation as shown in Figure 3.1. In particular, we can write the relation $\sigma_{TMG}[R] = H_R + \mathcal{K}[\gamma]$ as before, where $H_R$ is the generator of the boundary one-sided boost and $\mathcal{K}[\gamma]$ is the kink transform.

## 3.3 Geometric entropy commutators

In this section, we aim to reproduce the modular commutator result of [104], but from the bulk perspective. We do this in two ways: by using the results above, and by using the boundary stress tensor algebra. We indeed find agreement between our results and [104]. In addition, the nature of our calculation allows us to easily extend the results of [104] to disjoint boundary regions. This is difficult in their setting as the modular commutator is defined only for three contiguous boundary regions.

We work in topologically massive gravity with negative cosmological constant and without matter, for spacetimes asymptotic to Poincaré $AdS_3$. Spacetimes of this form are always diffeomorphic to TMG in Poincaré $AdS_3$. Thus, if we start in TMG in vacuum Poincaré $AdS_3$, we can obtain any other spacetime of this form via a boundary conformal transformation. Defining $u = t - x$ and $v = t + x$, the Poincaré $AdS_3$ metric of Eq. (3.25) becomes

$$ds^2 = \frac{1}{z^2}(-dudv + dz^2). \tag{3.62}$$

Then a boundary conformal transformation will be a map $(u, v) \to (U(u), V(v))$, such that the boundary metric becomes

$$ds^2_\partial = -dUdV = -e^{2\sigma_-(U)}e^{2\sigma_+(V)}dudv. \tag{3.63}$$

We see the flat boundary metric is rescaled by some conformal factor $e^{2\sigma_-(U)}e^{2\sigma_+(V)}$.

We start in Section 3.3.1 by deriving the change of the boundary stress energy tensor due to this conformal transformation. Then, in Section 3.3.2, we write the renormalized geometric entropy in this theory. In Section 3.3.3 we calculate the effect of TMG entropy flow on the stress energy tensor. We then use the geometric flow given by Eq. (3.61) to calculate, in vacuum Poincaré $AdS_3$ and with a specific choice of boundary region $R$, commutators between TMG entropies defined by different boundary regions. In Section 3.3.4 we generalize these results to include general $R$ and all spacetimes diffeomorphic to vacuum Poincaré $AdS_3$ (which, in particular, include planar black holes). Finally, in Section 3.3.4, we use our results to understand the entropy algebra with disjoint boundary regions.

### 3.3.1 The boundary stress energy tensor

We write the full boundary stress energy tensor in TMG as $\tilde{T}_{ij} = T_{ij} - T^{CS}_{ij}$, where $T_{ij}$ is the stress tensor in Einstein-Hilbert gravity and $T^{CS}_{ij}$ represents the contribution from the Chern-Simons term to the stress tensor. If we know the variation for the Chern-Simons term in the action, then $T^{ij}_{CS}$ can be found by evaluating

$$\begin{aligned} \delta I_{CS} =& \frac{1}{2}\int_{\partial\mathcal{M}} T^{ij}_{CS}\delta g_{ij}\sqrt{g}d^2x \\ =& -\frac{1}{2}\int_{\partial\mathcal{M}} T^{CS}_{ij}\delta g^{ij}\sqrt{g}d^2x. \end{aligned} \tag{3.64}$$

We know $\delta I_{CS}$ from Eq. (3.41), however we will instead use the form of the variation found in [138]. Hence, the variation takes the form

$$\begin{aligned}\delta I_{CS} =& 2\beta \int_{\partial\mathcal{M}} d^2x\sqrt{g}R^{\eta j}_{\ \ \eta k}\delta g_{ij}\epsilon^{i\eta k} + \beta\int_{\partial\mathcal{M}} d^2x\sqrt{g}[2K^k_i\delta K_{kj} - \Gamma^k_{li}\delta\Gamma^l_{kj}]\epsilon^{ij} \\ &- \beta\int_{\mathcal{M}} d^3x\sqrt{g}\nabla_\beta(R^{\beta\rho}_{\ \ \mu\nu})\epsilon^{\gamma\mu\nu}\delta g_{\gamma\beta}.\end{aligned} \tag{3.65}$$

In our work below we will use a Fefferman-Graham expansion, writing the metric as

$$ds^2 = d\eta^2 + g_{ij}dx^i dx^j, \tag{3.66}$$

where we define $g_{ij}$ as an expansion about the boundary metric $g^{(0)}_{ij}$: $g_{ij} = e^{2\eta}g^{(0)}_{ij} + g^{(2)}_{ij} + ....$ For Poincaré AdS in $2+1$-dimensions, we have the Minkowski metric on the boundary, and

$$g^{(2)}_{ij} = \kappa T_{ij}. \tag{3.67}$$

In vacuum Poincaré $AdS_3$ all terms in Eq. (3.65) independently vanish, and so $\delta I_{CS} = 0$. The first term vanishes since $R^{\eta j}_{\ \ \eta k} \propto \delta^j_k$ for large $\eta$, and the last term vanishes since the curvature is covariantly constant. The vanishing of the second term is not as obvious, but it is due to that fact that $g^{(0)}_{ij} = \eta_{ij}$, and $T_{ij} = 0$. We thus see that the original $T_{CS}$ (i.e., before the conformal transformation) is zero.

We will now apply a conformal transformation to Eq. (3.65), then extract the stress energy tensor. Since we are perturbing about a flat boundary metric, all terms vanish except the extrinsic curvature term (we refer the reader to [138] for more details):

$$\begin{aligned}K^k_i\delta K_{kj}\epsilon^{ij} =& -g^{kl}_{(2)}g^{(0)}_{li}\delta g^{(0)}_{kj}\epsilon^{ij} + ... \\ =& \kappa T_{ki}g^{(0)}_{jl}\delta g^{kl}_{(0)}\epsilon^{ij} + ....\end{aligned} \tag{3.68}$$

Using Eq. (3.64), we can extract $T_{ki}^{CS}$, yielding

$$T_{kl}^{CS} = -4\kappa\beta T_{ki} g_{jl}^{(0)} \epsilon^{ij}. \tag{3.69}$$

(This verifies that $T_{kl}^{CS} = 0$ when $T_{ki} = 0$ in the vacuum.) Now, under the conformal transformation in Eq. (3.63), the stress tensor will transform as [152]

$$T_{ab}dx^a dx^b \to T_{ab}^{original} dx^a dx^b + \frac{c_0}{12\pi}[\partial_u^2\sigma - (\partial_u\sigma)^2]du^2 + \frac{c_0}{12\pi}[\partial_v^2\sigma - (\partial_v\sigma)^2]dv^2. \tag{3.70}$$

Hence, applying this transformation to $T_{ki}$ in Eq. (3.69), we get

$$\begin{aligned} T_{ab}^{CS}dx^a dx^b \to & -4\kappa\beta\bigg(\frac{c_0}{12\pi} g_{uv}^{(0)}\epsilon^{uv}[\partial_u^2\sigma - (\partial_u\sigma)^2]du^2 \\ & \qquad - \frac{c_0}{12\pi} g_{uv}^{(0)}\epsilon^{uv}[\partial_v^2\sigma - (\partial_v\sigma)^2]dv^2\bigg) \\ \to & 4\beta([\partial_u^2\sigma - (\partial_u\sigma)^2]du^2 - [\partial_v^2\sigma - (\partial_v\sigma)^2]dv^2) \\ \to & 4\beta([\partial_U^2\sigma + (\partial_U\sigma)^2]dU^2 - [\partial_V^2\sigma + (\partial_V\sigma)^2]dV^2). \end{aligned} \tag{3.71}$$

where we used the fact that the original stress tensor is zero. To obtain the second line of the equation, we use the convention $\epsilon^{tx} = -1$ to get

$$\epsilon^{uv} = \frac{\partial u}{\partial t}\frac{\partial v}{\partial x}\epsilon^{tx} + \frac{\partial u}{\partial x}\frac{\partial v}{\partial t}\epsilon^{xt} = -2. \tag{3.72}$$

Finally, under a conformal transformation from the vacuum, the full stress tensor in

this theory becomes

$$\begin{aligned}\tilde{T}_{ij}dx^i dx^j \rightarrow & \frac{1}{12\pi}(c_0 - 48\pi\beta)[\partial_U^2\sigma + (\partial_U\sigma)^2]dU^2 \\ & + \frac{1}{12\pi}(c_0 + 48\pi\beta)[\partial_V^2\sigma + (\partial_V\sigma)^2]dV^2 \\ \rightarrow & \frac{c_R}{12\pi}[\partial_U^2\sigma + (\partial_U\sigma)^2]dU^2 + \frac{c_L}{12\pi}[\partial_V^2\sigma + (\partial_V\sigma)^2]dV^2.\end{aligned} \tag{3.73}$$

We define the TMG stress tensor components as $\tilde{T}_{UU}(U) = \frac{c_L}{12\pi}[\partial_U^2\sigma + (\partial_U\sigma)^2]$ and $\tilde{T}_{VV}(V) = \frac{c_L}{12\pi}[\partial_V^2\sigma + (\partial_V\sigma)^2]$. By comparison with Eq. (3.70), we see that $\tilde{T}_{UU}(U) = \frac{c_L}{c_0}T_{UU}(U)$ and $\tilde{T}_{VV}(V) = \frac{c_R}{c_0}T_{VV}(V)$. We note that these relations are more obvious from the CFT perspective, where, under Wick rotation, we can relate the $u$ and $v$ terms of the stress tensor to holomorphic and anti-holomorphic parts $T(z)$ and $T(\bar{z})$, respectively. Then we replace $c_0$ with $c_R$ in $T(z)$ and with $c_L$ in $T(\bar{z})$. Here, however, we wished to understand the stress tensor transformation from the bulk perspective.

### 3.3.2 Geometric entropy in TMG asymptotic to Poincaré $AdS_3$

The geometric entropy of TMG is given by Eq. (3.24), as proven by [142] using the replica trick. Now suppose we have a $1+1$D chiral CFT region $R$ anchored at $(u_1, v_1)$ and $(u_2, v_2)$. We take $R$ to be the straight line segment between the anchor points. In vacuum Poincaré $AdS_3$, the non-renormalized TMG entropy can be written as [144]

$$\tilde{\sigma}_{TMG}^{vac}[R] = \frac{c_L}{12}\ln\left(\frac{(v_1 - v_2)^2}{\epsilon_{v_1}\epsilon_{v_2}}\right) + \frac{c_R}{12}\ln\left(\frac{(u_1 - u_2)^2}{\epsilon_{u_1}\epsilon_{u_2}}\right) \tag{3.74}$$

where $\epsilon_{u_i}$ and $\epsilon_{v_i}$ for $i = 1, 2$ are the cut-offs in the $u$ and $v$ directions for each anchor point. To maintain translation invariance we can choose $\epsilon_{u_1} = \epsilon_{u_2} = \epsilon_u$ and $\epsilon_{v_1} = \epsilon_{v_2} = \epsilon_v$. Then, to renormalize the TMG entropy, we follow the standard approach of adding counterterms

and taking the limit $\epsilon \to 0$:

$$\begin{aligned}\sigma^{vac}_{TMG}[R] =& \lim_{\epsilon\to 0}\left(\tilde{\sigma}^{vac}_{TMG}[R] + \frac{c_L}{6}\ln\epsilon_v + \frac{c_R}{6}\ln\epsilon_u\right)\\ =& \frac{c_L}{6}\ln|v_1 - v_2| + \frac{c_R}{6}\ln|u_1 - u_2|.\end{aligned} \tag{3.75}$$

The renormalized entropy is not invariant under the conformal transformation $(u, v) \to (U(u), V(v))$ given in Eq. (3.63). This conformal transformation consists of two parts: a diffeomorphism taking $u \to U(u)$ and $v \to V(v)$, and a Weyl rescaling of the metric. The metric is invariant under such a transformation, but Eq. (3.74) is not, because the cut-offs transform as

$$\epsilon_{v_i} \to e^{2\sigma_+(V_i)}\epsilon_{v_i}, \tag{3.76}$$

$$\epsilon_{u_i} \to e^{2\sigma_-(U_i)}\epsilon_{u_i}. \tag{3.77}$$

If one wishes to use the same cut-offs before and after the conformal transformation, then the renormalized entropy is defined via the same subtraction, and so transforms by adding $\sigma_\pm$:

$$\begin{aligned}\sigma_{TMG}[R] =& \sigma^{vac}_{TMG}[R] + \frac{c_L}{6}[\sigma_+(V_1) + \sigma_+(V_2)] + \frac{c_R}{6}[\sigma_+(U_1) + \sigma_+(U_2)].\\ =& \frac{c_L}{6}\ln|v_2 - v_1| + \frac{c_L}{6}\ln|u_1 - u_2|\\ &+ \frac{c_L}{6}[\sigma_+(V_1) + \sigma_+(V_2)] + \frac{c_R}{6}[\sigma_+(U_1) + \sigma_+(U_2)].\end{aligned} \tag{3.78}$$

This is the renormalized TMG entropy, which is of course similar to the result for the renormalized HRT area under a conformal transformation, except with $c_0$ replaced by $c_L$ in anti-holomorphic terms and by $c_R$ in holomorphic terms.

In particular, in Poincaré $AdS_3$ in Einstein-Hilbert gravity, we instead have

$$\frac{A_{HRT}[R]}{4G} = \frac{c_0}{6}(A_V(V_1, V_2) + A_U(U_1, U_2)) \tag{3.79}$$

up to a possible constant term which will not factor into our analysis, with

$$A_V(V_1, V_2) = \ln|v(V_2) - v(V_1)| + \sigma_+(V_1) + \sigma_+(V_2), \tag{3.80}$$

$$A_U(U_1, U_2) = \ln|u(U_1) - u(U_2)| + \sigma_-(U_1) + \sigma_-(U_2). \tag{3.81}$$

Hence, we can write the TMG entanglement entropy in terms of the $U$ and $V$ pieces of the HRT-area as as simple rescaling:

$$\sigma_{TMG}[R] = \frac{c_L}{6}A_V(V_1, V_2) + \frac{c_R}{6}A_U(U_1, U_2). \tag{3.82}$$

In what follows, we will use this expression to rewrite the entropy commutators in [3].

### 3.3.3 Entropy algebra from geometric flow

We will now use the geometric picture of TMG entropy flow to compute the action of $\sigma_{TMG}[R]$ on the stress tensor, and the commutator between the TMG entropies of two different boundary regions. As discussed above, this entropy flow kinks $\Sigma$ in the bulk, but preserves $\partial\Sigma$. In this section, we work in asymptotically Poincaré $AdS_3$ TMG without matter and without black holes, although we will later generalize to spacetimes allowing planar black holes. We follow the same approach as in Section 3 of [3], and refer the reader to the discussion there for more details. Our goal here is to review the essential parts of that calculation, and to note any differences (or lack thereof) between TMG and Einstein-Hilbert gravity.

Our result for the geometric action of the $\sigma_{TMG}$ flow agrees precisely with that for ($1/4G$ times the) HRT-area flow in Einstein-Hilbert gravity. In particular, $\{\sigma[R]/4G, K^{ij}(y)\}$ has not changed with the addition of the Chern-Simons term, and we still have $\sigma[R] = H_R + \mathcal{K}[\gamma]$. The kink transform $\mathcal{K}[\gamma]$ introduces a relative boost between the two sides of $\gamma$, and so leaves $\gamma$ invariant. In asymptotically Poincaré $AdS_3$ TMG, the action of $\mathcal{K}[\gamma]$ on the boundary introduces a gravitational anomaly, but this anomaly does not change the equations of motion: the equations of motion change by the addition of the Cotton tensor, which vanishes in Poincaré $AdS_D$. Nor does $\mathcal{K}[\gamma]$ change the boundary metric in the boosted wedge. Hence, the action of $\mathcal{K}[\gamma]$ leaves TMG invariant, and we need only consider the action of $H_R$, which must be a boundary conformal transformation. This is the transformation which "undoes" the boundary action of the kink transformation, and so is a boost with a rapidity we will denote as $2\pi\lambda$.

As in [3], we take the action of $H_R$ to be a map $(u, v) \to (U(u), V(v))$ defined by (3.63).[7] We can specify the conformal factor explicitly by taking a boundary region $R_0$, which is the half-line $x \in [0, \infty)$ at $t = 0$ on the boundary at $z = 0$, and considering the extremal surface corresponding to $R_0$. Without matter, this extremal surface is the HRT surface $\gamma_{R_0}$, and it is the bulk geodesic at $x = t = 0$ for all $z$. Then

$$U = ue^{-2\pi\lambda\Theta(-U)}, \quad V = Ve^{2\pi\lambda\Theta(V)}, \tag{3.83}$$

giving

$$\sigma_-(U) = -\pi\lambda\Theta(-U), \quad \sigma_+(V) = \pi\lambda\Theta(V). \tag{3.84}$$

[7]Note, however, that the purpose of this conformal transformation is different than the purpose of the transformation introduced in Eq. (3.63)

Plugging into Eq. (3.73), the stress tensor under the action of $\sigma_{TMG}[R_0]$ is

$$T_{VV} = \frac{c_L}{12\pi}(\lambda\delta'(V) + \pi\lambda^2[\delta(V)]^2) \tag{3.85}$$

$$T_{UU} = \frac{c_R}{12\pi}(\lambda\delta'(U) + \pi\lambda^2[\delta(U)]^2). \tag{3.86}$$

We can also calculate the effect of $\sigma_{TMG}[R_0]$ on another TMG entropy defined by a different boundary region $R$. This is the same calculation as in Einstein-Hilbert gravity: we write $\sigma_{TMG}[R]$ under the conformal transformation defined in Eq. (3.83), thus giving it explicit $\lambda$ dependence. We write this transformed entropy as $\sigma_{TMG,\lambda}[R]$. Then

$$\begin{aligned}\{\sigma_{TMG}[R_0], \sigma_{TMG}[R]\} =& \frac{d}{d\lambda}\sigma_{TMG,\lambda}[R]\Big|_{\lambda=0} \\ =& -\frac{\pi c_L}{3}\frac{V_1\Theta(-V_1V_2)}{V_2 - V_1} - \frac{\pi c_R}{3}\frac{U_1\Theta(-U_1U_2)}{U_1 - U_2}.\end{aligned} \tag{3.87}$$

In the next section, we generalize this result to spacetimes diffeomorphic to subregions of vacuum Poincaré $AdS_3$; in particular, we will now be able to include planar black holes. We also generalize to commutators between TMG entropies defined by arbitrary boundary regions.

### 3.3.4 Entropy algebra from stress tensors

Now, we consider spacetimes diffeomorphic to subregions of vacuum Poincaré $AdS_3$. By allowing for certain singular conformal transformations from the vacuum, i.e. ones where we specify the boundary conditions $v(V = \infty) = 0$ and $u(U = \infty) = 0$, our solutions asymptote to $M > 0$ planar black holes. Otherwise, for solutions that asymptote to Poincaré $AdS_3$, we choose $v(V = 0) = 0$ and $u(U = 0) = 0$. Let us now proceed with a calculation of the commutator between the geometric entropies of two different boundary regions. We do this by starting from the stress tensor algebra (i.e, the Virasoro algebra

with the appropriate chiral central charge), then use the Leibniz rule to get the TMG entropy algebra. We mainly include this section as an independent check on our TMG entropy flow calculation in Section 3.2.2. We also include it to make contact with [3]: in [3], we calculated the geometric entropy commutator in Einstein-Hilbert gravity following this same method of starting from the stress tensor algebra.

The boundary stress tensor algebra in Einstein-Hilbert gravity is [127]

$$\{T_{VV}(V), T_{VV}(V')\} = 2T_{VV}(V')\delta'(V-V') - T'_{VV}(V')\delta(V-V') - \frac{c_0}{24\pi}\delta'''(V-V'), \quad (3.88)$$

and similarly for the algebra of $T_{UU}$. Suppose we have the boundary region $R$ anchored at $(U_1, V_1)$ and $(U_2, V_2)$, and the boundary region $R'$ anchored at $(U'_1, V'_1)$ and $(U'_2, V'_2)$. Without loss of generality, we take $U_1 > U_2$, $V_1 < V_2$, $U'_1 > U'_2$, and $V'_1 < V'_2$. Then, the Leibniz rule is used to obtain the HRT area algebra from the Virasoro algebra:

$$\begin{aligned}\left\{\frac{A_{HRT}[R]}{4G}, \frac{A_{HRT}[R']}{4G}\right\} = \\ \int dV dV' d\bar{V} d\bar{V}' \frac{1}{4G}\frac{\partial A_{HRT}[R]}{\partial \sigma_+(V)}\frac{\partial \sigma_+(V)}{\partial T_{VV}(V')}\{T_{VV}(V'), T_{VV}(\bar{V}')\} \\ \times \frac{\partial \sigma_+(\bar{V})}{\partial T_{VV}(\bar{V}')}\frac{1}{4G}\frac{\partial A_{HRT}[R']}{\partial \sigma_+(\bar{V})} \\ + \int dU dU' d\bar{U} d\bar{U}' \frac{1}{4G}\frac{\partial A_{HRT}[R]}{\partial \sigma_-(U)}\frac{\partial \sigma_-(U)}{\partial T_{UU}(U')}\{T_{UU}(U'), T_{UU}(\bar{U}')\} \\ \times \frac{\partial \sigma_-(\bar{U})}{\partial T_{UU}(\bar{U}')}\frac{1}{4G}\frac{\partial A_{HRT}[R']}{\partial \sigma_-(\bar{U})}.\end{aligned} \quad (3.89)$$

In TMG, using the stress tensor components defined after Eq. (3.73), the Virasoro algebra becomes

$$\{\tilde{T}_{VV}(V), \tilde{T}_{VV}(V')\} = \frac{c_L}{c_0}\{T_{VV}(V), T_{VV}(V')\}_{E-H} \quad (3.90)$$

$$\{\tilde{T}_{UU}(U), \tilde{T}_{UU}(U')\} = \frac{c_R}{c_0}\{T_{UU}(U), T_{UU}(U')\}_{E-H}. \quad (3.91)$$

where the E-H subscript stands for Einstein-Hilbert. The other terms in the integrals are related to their Einstein-Hilbert counterparts as

$$\frac{\partial\sigma_{TMG}[R]}{\partial\sigma_+(V)} = \frac{c_L}{4Gc_0}\frac{\partial A_{HRT}[R]}{\partial\sigma_+(V)} \quad \text{and} \quad \frac{\partial\sigma_{TMG}[R]}{\partial\sigma_-(U)} = \frac{c_R}{4Gc_0}\frac{\partial A_{HRT}[R]}{\partial\sigma_-(U)}, \tag{3.92}$$

and

$$\frac{\partial\sigma_+(V)}{\partial\tilde{T}_{VV}(V')} = \frac{c_0}{c_L}\frac{\partial\sigma_+(V)}{\partial T_{VV}(V')} \quad \text{and} \quad \frac{\partial\sigma_-(U)}{\partial\tilde{T}_{UU}(U')} = \frac{c_0}{c_R}\frac{\partial\sigma_-(U)}{\partial T_{UU}(U')}. \tag{3.93}$$

Putting this all together, Eq. (3.89) becomes

$$\begin{aligned}\{\sigma_{TMG}[R],\sigma_{TMG}[R']\} =& \frac{c_L}{c_0}\left\{\frac{1}{4G}A_V(V_1,V_2),\frac{1}{4G}A_V(V_1',V_2')\right\} \\ &+ \frac{c_R}{c_0}\left\{\frac{1}{4G}A_U(U_1,U_2),\frac{1}{4G}A_U(U_1',U_2')\right\}.\end{aligned} \tag{3.94}$$

In Einstein-Hilbert gravity, we had

$$\left\{\frac{1}{4G}A_V(V_1,V_2),\frac{1}{4G}A_V(V_1',V_2')\right\} = \frac{\pi c_0}{6}\begin{cases}2\eta_v-1, & V_1'<V_1<V_2'<V_2\\ 1-2\eta_v, & V_1<V_1'<V_2<V_2'\\ 0, & \text{otherwise}\end{cases} \tag{3.95}$$

$$\left\{\frac{1}{4G}A_U(U_1,U_2),\frac{1}{4G}A_U(U_1',U_2')\right\} = \frac{\pi c_0}{6}\begin{cases}2\eta_u-1, & U_2'<U_2<U_1'<U_1\\ 1-2\eta_u, & U_2<U_2'<U_1<U_1'\\ 0, & \text{otherwise,}\end{cases} \tag{3.96}$$

where we define the cross ratios $\eta_u = \frac{(u_1-u_1')(u_2-u_2')}{(u_1-u_2)(u_1'-u_2')}$ and $\eta_v = \frac{(v_1-v_1')(v_2-v_2')}{(v_1-v_2)(v_1'-v_2')}$. So, plugging

these into Eq. (3.94), the entanglement entropy algebra in TMG is given by

$$\{\sigma_{TMG}[R], \sigma_{TMG}[R']\} = \frac{\pi c_L}{6}\begin{cases} 2\eta_v - 1, & V_1' < V_1 < V_2' < V_2 \\ 1 - 2\eta_v, & V_1 < V_1' < V_2 < V_2' \\ 0, & \text{otherwise} \end{cases} + \frac{\pi c_R}{6}\begin{cases} 2\eta_u - 1, & U_2' < U_2 < U_1' < U_1 \\ 1 - 2\eta_u, & U_2 < U_2' < U_1 < U_1' \\ 0, & \text{otherwise.} \end{cases} \tag{3.97}$$

This agrees with the result of [104], given in Eq. (3.1). In vacuum Einstein-Hilbert gravity, the entropy commutator vanishes when we restrict all anchor points to lie on a constant time slice on the boundary. However, in TMG, this configuration instead gives a non-vanishing result. For $x_1' < x_1 < x_2' < x_2$,

$$\{\sigma_{TMG}[R], \sigma_{TMG}[R']\} = \frac{\pi c_-}{6}(2\eta - 1), \tag{3.98}$$

with $c_- = c_L - c_R$ and $\eta = \frac{(x_1 - x_1')(x_2 - x_2')}{(x_1 - x_2)(x_1' - x_2')}$. This again agrees with [104].

**Disjoint intervals**

We can also apply our results to slightly more general situations than those considered in [104]. In particular, in the semiclassical approximation, their result calculates the commutator between $\sigma_{TMG}[AB]$ and $\sigma_{TMG}[BC]$, the geometric entropies of boundary regions $AB$ and $BC$, respectively, where $A$, $B$ and $C$ are contiguous. See Figure 3.2 for an illustration. By contrast, the commutators calculated in this work can be defined for disjoint intervals $A$, $B$ and $C$. This is because, in Eq. (3.24), the TMG entropy is defined as an integral over the extremal surface. Hence, if we have a disconnected surface, the integral splits into two, and the contributions from each piece are additive.

For instance, take $B$ and $C$ to be disjoint. We take the anchor points of $A$ to be

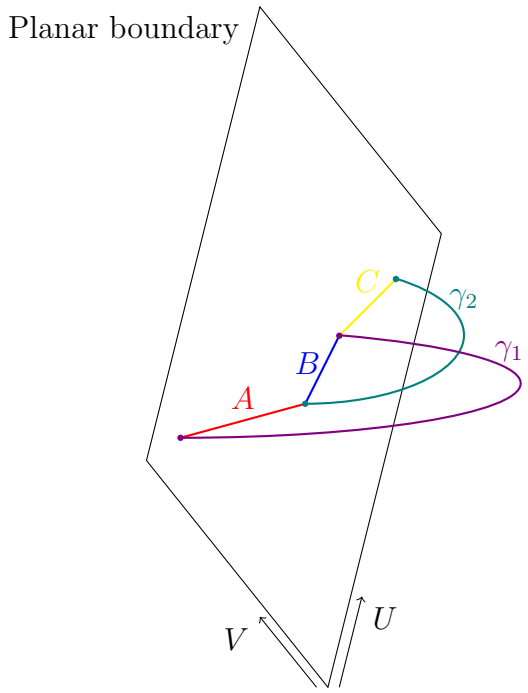


Figure 3.2: For contiguous CFT regions $A$, $B$, and $C$, we can draw $\gamma_1$, the extremal surface corresponding to region $AB$, and $\gamma_2$, the extremal surface corresponding to region $BC$. This is the configuration studied in [104], where the authors find the modular commutator $J(A, B, C)_\Omega$, equivalent to the commutator between the TMG entropies of $AB$ and $BC$.

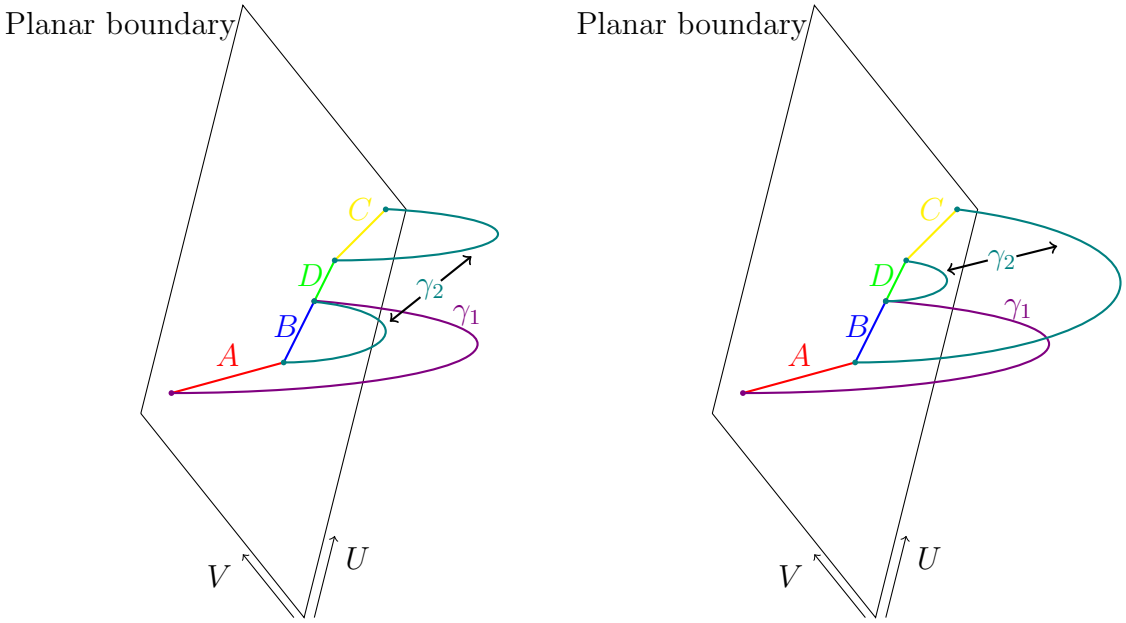


Figure 3.3: For contiguous CFT regions $A$ and $B$, and disconnected region $C$, we can draw $\gamma_1$, the extremal surface corresponding to region $AB$, and $\gamma_2$, the extremal surface corresponding to region $BC$. We label the region between $B$ and $C$ as region $D$. As opposed to the contiguous case, $\gamma_2$ splits into two surfaces. In the left figure, $\gamma_2$ is the HRT surface corresponding to region $B$ combined with the HRT surface corresponding to $C$. In the right figure, $\gamma_2$ is the HRT surface corresponding to region $BDC$ combined with the HRT surface corresponding to $D$. This is a configuration we can now study using Eq. (3.97).

$(U_1, V_1)$ and $(U_2, V_2)$, the anchor points of $B$ to be $(U_2, V_2)$ and $(U_3, V_3)$, and the anchor points of $C$ to be $(U_4, V_4)$ and $(U_5, V_5)$. Additionally, we will define a new region $D$ between $B$ and $C$, that is anchored at $(U_3, V_3)$ and $(U_4, V_4)$. Then the bulk extremal surfaces corresponding to boundary region $BC$ have two possible configurations, as shown in Figure 3.3. Thus, $\sigma_{TMG}[BC]$ is given by the configuration with minimal entropy:

$$\sigma_{TMG}[BC] = \min\Big[\sigma_{TMG}[B] + \sigma_{TMG}[C], \sigma_{TMG}[BDC] + \sigma_{TMG}[D]\Big]. \tag{3.99}$$

We can hence define $\sigma_{TMG}[BC]$ in terms of TMG entropies defined by contiguous boundary regions, and thus compute $\sigma_{TMG}$ commutators.

In particular, in the disconnected phase (the left diagram in Fig. 3.3), both $\sigma_{TMG}[B]$ and $\sigma_{TMG}[C]$ commute separately with the $\sigma_{TMG}[AB]$. Then,

$$\{\sigma_{TMG}[AB], \sigma_{TMG}[BC]\}_{disconnected} = 0. \tag{3.100}$$

In the connected phase (the right diagram of Fig. 3.3), we see that $\sigma_{TMG}[D]$ commutes with $\sigma_{TMG}[AB]$, but $\sigma_{TMG}[BCD]$ and $\sigma_{TMG}[AB]$ do not commute. Without loss of generality, we choose $U_1 > U_3$, $V_1 < V_3$, $U_2 > U_5$, and $V_2 < V_5$. This yields

$$\begin{aligned}&\{\sigma_{TMG}[AB], \sigma_{TMG}[BC]\}_{connected} = \\ &\frac{\pi c_L}{6}\begin{cases} 2\eta_v - 1, & V_2 < V_1 < V_5 < V_3 \\ 1 - 2\eta_v, & V_1 < V_2 < V_3 < V_5 \\ 0, & \text{otherwise} \end{cases} + \frac{\pi c_R}{6}\begin{cases} 2\eta_u - 1, & U_5 < U_3 < U_2 < U_1 \\ 1 - 2\eta_u, & U_3 < U_5 < U_1 < U_2 \\ 0, & \text{otherwise.} \end{cases}\end{aligned} \tag{3.101}$$

Thus, we have a generalization of Eq. (3.1) to disjoint boundary intervals.

## 3.4 Discussion

This work began by studying the flow on the covariant phase space induced by geometric entropy in topologically massive gravity, computed in spacetimes asymptotic to $AdS_3$ with standard matter. In terms of Cauchy data on a Cauchy slice $\Sigma$ containing the HRT surface, we found exactly the same result as in [3] for HRT area flow in Einstein-Hilbert gravity. In particular, the flow leaves the induced metric invariant but shifts the extrinsic curvature by a $\delta$-function as described by Eq. (3.61), essentially boosting the entanglement wedge of $R$ relative to that of the complementary region. Without matter, this result holds to all orders in the flow parameter $\lambda$; with matter, our result holds only to first order in $\lambda$. We save the generalization to finite $\lambda$ for future work.

After deriving the geometric entropy flow, we used it to explicitly compute the commutator between TMG entropies defined by different boundary CFT regions. We also derived this commutator by extrapolating from the stress tensor algebra. Our commutators agree with the modular commutator found in [104], the original motivation for this work. We concluded with a short discussion about applying our results to disjoint boundary regions, which is difficult to do with the modular commutator.

It is perhaps surprising that geometric entropy flow in TMG is precisely the same as HRT area flow in Einstein-Hilbert gravity. Arriving at this result through the Peierls bracket method was rather complicated, and required many cancellations between terms. This suggests there may be a more elegant way to approach this calculation, which would make the physical mechanisms behind these cancellations more obvious. Understanding this result more fully could allow generalizations to higher dimensional theories with boundary chiral CFTs, and potentially to theories with other types of higher derivative terms. Geometric entropy flow in higher derivative theories of gravity will be explored in [124]. Our work here is an important first step to understanding geometric entropy flow

more generally.

In the same vein, our Peierls bracket calculation could be extended to higher dimensional theories with boundary chiral CFTs. Explicit formulas for the corresponding geometric entropies have been computed in, for example, $3+1$, $4+1$, and $6+1$ bulk dimensions [143, 153]. The Peierls bracket calculation for geometric entropy flow in higher dimensions would then follow the same steps as in our work here (expect would be considerably more complicated). As already mentioned, it would thus be helpful to have a more elegant understanding of our result instead of resorting to an explicit calculation.

It would also be interesting to compute explicit TMG entropy commutators in more general configurations, e.g. with matter present or in higher dimensions. Indeed, this has not yet been done for HRT area commutators in Einstein-Hilbert gravity. Additionally, area commutators may have further implications tensor network models, as will be explored in Section 4 and in the forthcoming work [154]. We would also like to understand the implications of our TMG entropy commutator on tensor network constructions, especially since TMG is an example of a higher derivative theory.

# Chapter 4

# Link-Area Commutators in $AdS_3$ Area Networks

## 4.1 Introduction

Over the last decade, tensor networks have played a key role in developing our understanding of the AdS/CFT correspondence [52]. They were first proposed as toy models of AdS/CFT in [73, 74], based in part on the observation that the entanglement entropy of a boundary subregion is bounded by an area law that agrees with the Ryu-Takayanagi (RT) formula [61, 62]. It was then shown that certain tensor network constructions saturate this bound [69, 71]. Tensor networks can also model other important aspects of AdS/CFT, including quantum error correction properties [58] of the holographic dictionary; see e.g. models in [69, 70, 72].

The random tensor networks of [71] have been of particular interest. However, their qualitative properties differ from those of familiar semiclassical bulk states of AdS/CFT as the entanglement spectrum is flat for any boundary region $R$. By this we mean that the Renyi entropies $S_n$ are approximately independent of $n$. The same feature arises in

the HaPPY code [69].

In the AdS/CFT context, for a given boundary region $R$, and as described in [129, 75], producing a state with flat entanglement spectrum requires suppressing fluctuations in the area of the associated Hubeny-Rangamani-Takayanagi (HRT) surface[1] [63] relative to those in standard semiclassical states. Bulk states with such suppressed fluctuations are known as *fixed-area states*.

For a given HRT-surface (associated with a given boundary region $R$), fixed-area states can be produced by projecting more general states onto appropriately-sized windows of HRT-area eigenvalues, perhaps with the window width scaling as $G^{1/2+\epsilon}$ for some small $\epsilon > 0$ in terms of the bulk Newton constant $G$. However, given a set of regions $R_i$, the corresponding collection of entanglement spectra can be rendered flat only if we simultaneously suppress area fluctuations for all of the relevant HRT-surfaces $\gamma_i$. This in turn requires the associated HRT-area operators to approximately commute.

Unfortunately, as emphasized in [78], commutators of HRT-areas can be large even when all regions $R_i$ lie in a single Cauchy surface of the asymptotically-AdS boundary. This is in part because the HRT-surfaces $\gamma_i$ generally fail to lie in a single Cauchy surface of the bulk; i.e., points on $\gamma_i$ can be causally separated from points on $\gamma_j$. The mixing of operators under time-evolution then makes it difficult to avoid sizeable commutators[2].

One way to address this issue is to modify the notion of a tensor network model following e.g. [155, 33]. However, it is also natural to ask whether the issue can be ameliorated by using the collection of regions $R_i$ to construct a network of HRT-like surfaces that do in fact always lie in a single bulk Cauchy surface, and which thus might potentially have area operators that commute. Here the use of the term 'network' reminds

[1] I.e., for the covariant generaliztaion of the RT surface.

[2] In a time-symmetric context, the *expectation values* of HRT-area commutators generally vanish. But the commutators still do not vanish as operators, even if their properties are non-trivial to compute in the semiclassical approximation.

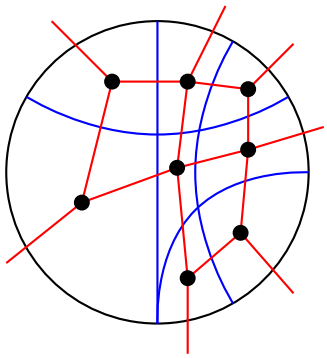

Figure 4.1: An example area network and its corresponding tensor network, modelled off of the networks in [78]. The area network is shown in blue. The tensors are black nodes, and tensor index contractions are shown as red edges. See [78] for explanations.

us that a collection of codimension-2 surfaces lying in a (codimension-1) Cauchy surface will generally intersect. One might in particular hope such a network to be related to the tensor network constructions of [78, 28]; see e.g. figure 4.1 below. We emphasize that both the precise notion of what is meant by an HRT-like surface and the extent to which they are useful in producing flat entanglement spectra or the networks of [78, 28] remain to be investigated.

The present work addresses the first of these steps by considering various constructions of such networks in semiclassical bulk geometries and computing commutators of the areas of the HRT-like surfaces comprising these networks. We will require our "HRT-like surfaces" to be extremal away from points where they intersect other surfaces in the network. The work below is exploratory, and our goal is merely to investigate a few such networks and collect results that may inform future constructions.

We will analyze the area-operators associated with our network in the semiclassical approximation. In this context, the operators are described by observables on the classical phase space and their commutators become $i$ times Poisson brackets. It is then interesting to study the flow generated by such an operator on the classical phase space. Throughout this work we will use the terms "operator" and "observable" interchangeably. For HRT-

area operators, studies in this direction include [112, 113, 44, 114, 115, 3]. Much of this work made use of the JLMS formula [117] relating the HRT area to the boundary modular Hamiltonian, though see [3] for a self-contained bulk analysis. The phase space flow generated by an HRT-area in Einstein-Hilbert gravity turns out to take a simple geometric form that acts as a boundary-condition-preserving kink transformation (see [3] for refinements of the discussion in [114, 115]). Extensions to topologically-massive gravity in $AdS_3$ were studied in [2]. While studies of geometric flow can be of great use, the present work will simply focus on computing commutators associated with our networks and will save analysis of geometric features for future work[3].

We focus on pure Einstein-Hilbert gravity in $AdS_3$ when the boundary metric is 1+1 Minkowski space. In this context we expect that all operators can be expressed in terms of the boundary stress tensor. An explicit such expression would then allow us to use the boundary stress tensor algebra to compute arbitrary commutators. While such explicit expressions are difficult to obtain, at the semiclassical level it suffices to work with *implicit* expressions as described in [3]. The point here is that since the Poisson Bracket $\{A, B\}$ of observables $A, B$ is defined in terms of derivatives of $A, B$ on the phase space, using the chain rule one can use the stress-tensor algebra to compute $\{A, B\}$ even if one knows only the derivatives of $A, B$ with respect to each component of the stress tensor. Following [3], expressions for such derivatives turn out to be straightforward to construct in the sector of our theory given by acting on Poincaré $AdS_3$ or a planar black hole with boundary conformal transformations.

We will consider only this sector below. We will also refer to these Poisson bracket calculations as "semiclassical commutators" despite the lack of a factor of $i$. Our main results are as follows:

[3]Since we consider areas of surfaces with boundaries, the flow generated by these areas may have a non-trivial effect extending to the boundary, similar to what is found in [148].

- It is generally difficult to construct arbitrarily fine discretizations of the bulk with commuting areas.
- We do, however, find a simple 4-link network (analogous to the extremal surface configuration building the four-tensor network of [78]) for which the link-areas all commute.

The outline of our paper is as follows. Section 4.2 reviews the formalism of [3] for computing Poisson brackets of observables in the above sector of vacuum $AdS_3$. In Section 4.3, we analyze a 4-link *constrained geodesic* network defined by choosing a single HRT surface and two additional boundary-anchor points. We then follow [105] in adding a second surface defined by extremizing the length of a curve connecting the additional two anchors with the constraint that the curve intersects the above-chosen HRT surface. This is the constrained geodesic. The resulting network is an analogue of the four-tensor network of [78], and we find that all of its areas commute. Appendix B then analyzes an extension of this simple network, though we find non-vanishing area commutators.

Since the entanglement wedge cross section (EWCS) has been of particular interest in the recent literature [156, 157, 158, 159, 160], we turn to the study of an associated network in section 4.4. Again, this network has non-vanishing area-commutators. In particular, the EWCS area fails to commute with other areas in the configuration. We conclude with a brief summary and discussion in section 5.6.

## 4.2 Commutators from the boundary stress-energy tensor

The work below will consider pure 2+1 Einstein-Hilbert gravity with negative cosmological constant, and we will restrict attention to solutions that can be obtained from

Poincaré AdS$_3$ or an $M > 0$ planar black hole by acting with boundary conformal transformations[4]. Furthermore, since solutions in the above classes are equivalent when their boundary stress tensors agree, we may express all observables in our theory in terms of the boundary stress tensor. This section is a brief review of the commutator framework considered in Section 2.4.

In Poincaré AdS$_3$, the metric is given by Eq. 2.15. All of the solutions we consider can be generated from (2.15) by acting with boundary conformal transformations. In particular, any such transformation can be described by two functions, $U(u)$ and $V(v)$, such that the boundary metric in the solution of interest takes the form (2.33), with $\sigma(u,v) = \sigma(u) + \hat{\sigma}(v)$ so that $dU$ and $dV$ are given by Eq. (2.34), i.e.

$$\begin{aligned} dU &= e^{2\sigma(u)} du \\ dV &= e^{2\hat{\sigma}(v)} dv. \end{aligned} \tag{4.1}$$

The action of a general finite conformal transformation on the stress-energy tensor of a 1+1 dimensional conformal field theory is well known, and is given by Eq. (2.20). We will choose $U(u), V(v)$ so that the transformation (4.1) maps the (vanishing) boundary stress tensor $T_{ab}^{\text{original}} = 0$ of (2.15) to the boundary stress tensor $T_{ab}$ of the desired solution. We then have

$$T_{UU} = \frac{c}{12\pi} \left[ \partial_U^2 \sigma_U + (\partial_U \sigma_U)^2 \right] \tag{4.2}$$

$$T_{VV} = \frac{c}{12\pi} \left[ \partial_V^2 \hat{\sigma}_V + (\partial_V \hat{\sigma}_V)^2 \right] \tag{4.3}$$

We also define the functions $u(U)$ and $v(V)$ to be the solutions of (2.34) subject to

[4]As described in e.g. [161], the full theory consists of a direct sum of disjoint (superselected) phase spaces, each of which can be generated by acting with boundary conformal transformations on any point in the phase space. The methods used here should thus also be applicable to more general sectors, where one expects them to yield similar results.

certain boundary conditions. And, for a given $T_{ab}$, $\sigma_U$ and $\hat{\sigma}_V$ are solutions of (4.2) and (4.3), respectively. We will specify the boundary conditions for (4.1) and for (4.2) and (4.3) at different locations. All boundary conditions will be the same as those chosen in Section 2.4, and we remind the reader now of those choices. To define boundary conditions for (4.2) and (4.3) we choose some $U_0, V_0$ and define $\sigma_{U_0}(U), \hat{\sigma}_{V_0}(V)$ to be the solutions of (4.1) that satisfy

$$\begin{aligned} \sigma_{U_0}(U)|_{U=U_0} &= \partial_U \sigma_{U_0}(U)|_{U=U_0} = 0 \\ \hat{\sigma}_{V_0}(V)|_{V=V_0} &= \partial_V \hat{\sigma}_{V_0}(V)|_{V=V_0} = 0. \end{aligned} \tag{4.4}$$

In contrast, to define boundary conditions for (4.1) we simply note that $U(u), V(v)$ will be defined on intervals $u \in (-\infty, u_{max})$ and $v \in (-\infty, v_{max})$. We will take $u_{max} = v_{max} = \infty$ for solutions asymptoting to Poincaré AdS$_3$ and $u_{max} = v_{max} = 0$ for solutions asymptoting to an $M > 0$ planar black hole. We choose our boundary conditions to be $u(U = 0) = 0$, $v(V = 0) = 0$ for solutions asymptoting to Poincaré AdS$_3$, and $u(U = \infty) = 0$, $v(V = \infty) = 0$ for solutions asymptoting to an $M > 0$ planar black hole. In either case, $u_{U_0}(U)$ and $v_{\hat{V}_0}(V)$ can be written in the form

$$u_{U_0}(U) = \int_0^U dU' e^{-2\sigma_{U_0}(U')} + c_u \tag{4.5}$$

$$v_{\hat{V}_0}(V) = \int_0^V dV' e^{-2\hat{\sigma}_{V_0}(V')} + c_v, \tag{4.6}$$

where, as a consequence of our choice above, $c_u = c_v = 0$ when solutions asymptote to Poincaré AdS$_3$, while for solutions asymptoting to an $M > 0$ black hole we have

$$c_u = -\int_0^\infty dU' e^{-2\sigma_{U_0}(U')}, \;\; c_v = -\int_0^\infty dV' e^{-2\hat{\sigma}_{V_0}(V')}. \tag{4.7}$$

As described above, the objects $\sigma_{U_0}$, $\hat{\sigma}_{V_0}$ are functionals of $T_{ab}$ determined by solving

(4.2) and (4.3). While a closed form solution is not available, we can differentiate (4.2) with respect to $\sigma_{U_0}(U)$ to obtain a *linear* differential equation for $\frac{\delta\sigma_{U_0}(U)}{\delta T_{UU}(U')}$. That linear equation can then be solved to find $\frac{\delta\sigma_{U_0}(U)}{\delta T_{UU}(U')}$ and $\frac{\delta\hat{\sigma}_{V_0}(V)}{\delta T_{VV}(V')}$, as given in Eq. (2.44). Since commutators between boundary stress tensors are given by the Virasoro algebra, the result (2.44) can be used to compute the Poisson Bracket algebra of conformal factors $\sigma(U,V)$. Doing so yields a commutator of the form ((2.52)), which can be reduced to the effective commutator in Equations (2.53) and (2.54), reproduced here for convenience:

$$\{\sigma_{U_0}(U), \sigma_{U_0}(\tilde{U})\}_{eff} = \quad \tfrac{6\pi}{c}\Theta(\tilde{U}-U), \tag{4.8}$$

$$\{\hat{\sigma}_{V_0}(V), \hat{\sigma}_{V_0}(\tilde{V})\}_{eff} = \quad -\tfrac{6\pi}{c}\Theta(V-\tilde{V}). \tag{4.9}$$

Now, for any two observables $B$ and $C$, we can compute their semiclassical commutator using Eq. (2.52):

$$\{B,C\} = \int d^2x_2 d^2x_2' \frac{\delta B}{\delta\sigma(x_2)}\{\sigma(x_2),\sigma(x_2')\}\frac{\delta C}{\delta\sigma(x_2')}, \tag{4.10}$$

in terms of the functional derivatives of $B$ and $C$ with respect to $\sigma(U,V)$. Using the effective commutators (2.53), (2.54), we may thus write the commutator between areas $A_1$ and $A_2$ in the form

$$\begin{aligned}\{A_1,A_2\} =& \frac{6\pi}{c}\int_{-\infty}^{\infty} d\tilde{U}\frac{\delta A_2}{\delta\sigma_{\tilde{U}_0}(\tilde{U})}\int_{-\infty}^{\infty} dU\frac{\delta A_1}{\delta\sigma_{\tilde{U}_0}(U)}\Theta(\tilde{U}-U)\\ &- \frac{6\pi}{c}\int_{-\infty}^{\infty} d\tilde{V}\frac{\delta A_2}{\delta\hat{\sigma}_{\tilde{V}_0}(\tilde{V})}\int_{-\infty}^{\infty} dU\frac{\delta A_1}{\delta\hat{\sigma}_{\tilde{V}_0}(V)}\Theta(V-\tilde{V}).\end{aligned} \tag{4.11}$$

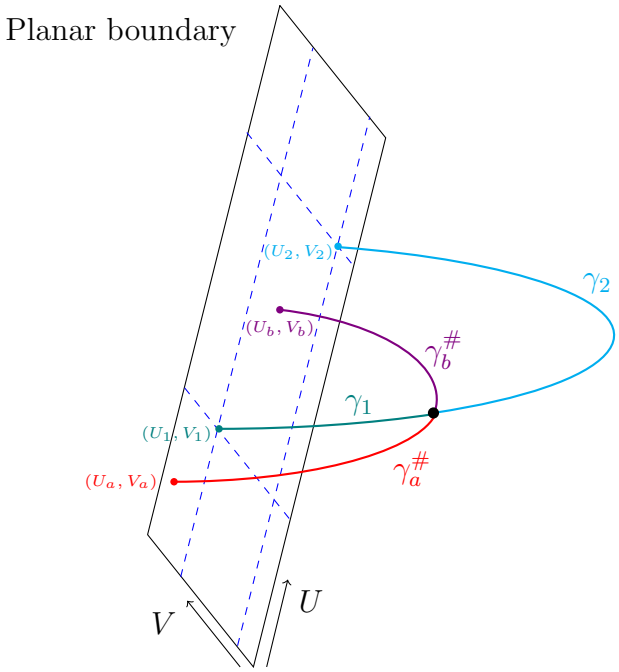


Figure 4.2: A constrained geodesic network, with HRT surface $\gamma = \gamma_1 \cup \gamma_2$, and two additional links $\gamma_a^{\#}$ and $\gamma_b^{\#}$ that together form a constrained HRT surface $\gamma^{\#} = \gamma_a^{\#} \cup \gamma_b^{\#}$. The anchor points of $\gamma$ are $(U_1, V_1)$ and $(U_2, V_2)$, while $\gamma_a^{\#}$ is anchored at $(U_a, V_a)$ and $\gamma_b^{\#}$ at $(U_b, V_b)$.

## 4.3 A simple constrained-surface network with vanishing commutators

As mentioned in the introduction, we will construct networks of surfaces by extremizing areas subject to constraints that require them to intersect in various ways. The first such networks will be based on the constrained HRT-surfaces of [105]. Such codimension-2 surfaces $\gamma^{\#}$ are defined by first choosing an HRT surface $\gamma$ and choosing an anchor set for $\gamma^{\#}$ on the AdS boundary. The constrained HRT-surface $\gamma^{\#}$ is then defined by extremizing its area subject to the usual requirements that its anchors remain fixed and that it satisfy the homology constraint [121], but where we also impose the additional constraint that $\gamma^{\#}$ must intersect $\gamma$; see figure 4.2.

The locus of the intersection is then determined by the extremization. In $AdS_3$, extremal codimension-2 surfaces are geodesics and the intersection occurs at a single point. In any dimension, the intersection divides $\gamma$ into two half-infinite links $\gamma_1, \gamma_2$, and it also divides $\gamma^\#$ into $\gamma_a^\#$, $\gamma_b^\#$. This configuration thus defines a network with a single vertex (at the intersection) and 4 links $\gamma_1, \gamma_2, \gamma_a^\#, \gamma_b^\#$.

Section 4.3.1 below computes the renormalized areas of $\gamma_a^\#, \gamma_b^\#$. Commutators between the renormalized areas of $\gamma_1, \gamma_2, \gamma_a^\#, \gamma_b^\#$ are then computed in section 4.3.2, where they are shown to vanish.

### 4.3.1 Area-operators for half-infinite links

Our task in this section is to compute the areas of $\gamma_a^\#, \gamma_b^\#, \gamma_1, \gamma_2$ for given boundary anchors. We first focus on $\gamma_a^\#, \gamma_b^\#$. We take the anchor points of $\gamma$ to be $(U_1, V_1)$ and $(U_2, V_2)$, while $\gamma_a^\#$ is anchored at $(U_a, V_a)$ and $\gamma_b^\#$ at $(U_b, V_b)$.

It will be convenient to begin with a simple case in Poincaré $AdS_3$ where $\gamma$ is in fact defined by the boundary region $R_0$ given by the half-line $x \in [x_1, \infty)$ at some $t = t_1$ on the boundary at $z = 0$. Since we are Poincaré $AdS_3$, we use the coordinates of (2.15) given by lower-case roman letters. The associated HRT surface $\gamma_{R_0}$ is then just the line of constant $u, v$ with $u = u_1 = t_1 - x_1$ and $v = v_1 = t_1 + x_1$ for all $z$. We then define an associated constrained geodesic $\bar{\gamma}^\#$ by choosing two boundary points $(u_a, v_a)$ and $(u_b, v_b)$, where without loss of generality we assume $u_a < u_1 < u_b$ and $v_a > v_1 > v_b$. The intersection point then breaks $\bar{\gamma}^\#$ into two half-infinite links $\bar{\gamma}_a^\#, \bar{\gamma}_b^\#$.

Since the intersection point lies on $\gamma_{R_0}$, it must be of the form $(u_1, v_1, z)$. But for any half-infinite link $\gamma_{half}$ anchored to $(u_i, v_i)$ on the boundary and the point $(u_1, v_1, z)$ in the bulk, the renormalized area in planar BTZ coordinates with horizon at $z = z_H$ was

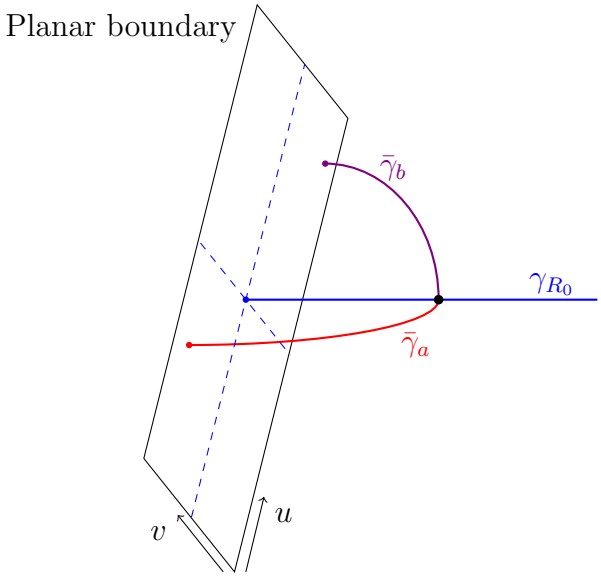


Figure 4.3: A simple HRT surface $\gamma_{R_0}$ in the vacuum (Poincaré AdS$_3$), along with two additional links $\bar{\gamma}_a^{\#}$ and $\bar{\gamma}_b^{\#}$ defined by extremizing the area of $\bar{\gamma}_a^{\#} \cup \bar{\gamma}_b^{\#}$.

found in [128] to be

$$A^{vac}_{\gamma_{half}} = \ln\left( -\frac{2z_H}{z}\left[\sqrt{z_H^2 - z^2}\cosh\left(\frac{t_1 - t_i}{z_H}\right) - z_H \cosh\left(\frac{x_1 - x_i}{z_H}\right)\right]\right). \tag{4.12}$$

In the limit $z_H \to \infty$, the BTZ metric becomes Poincaré AdS. Taking this limit, we find the geodesic length

$$A^{vac}_{\gamma_{half}} = \ln\left(2z + \frac{2(u_1 - u_i)(v_i - v_1)}{z}\right). \tag{4.13}$$

We now take $\bar{\gamma}_a^{\#}$ to be the half-infinite link with boundary anchor $(u_a, v_a)$, and $\bar{\gamma}_b^{\#}$ to be the half-infinite link with boundary anchor $(u_b, v_b)$. We wish to extremize the total length $A^{vac}_{\bar{\gamma}_a^{\#}} + A^{vac}_{\bar{\gamma}_b^{\#}}$ of $\bar{\gamma}^{\#}$ over possible intersection points on $\gamma_{R_0}$. Since the points on $\gamma_{R_0}$ are labelled by the value of $z$ in (4.13), a short computation yields:

$$z_{ext} = [(u_1 - u_a)(v_a - v_1)(u_b - u_1)(v_1 - v_b)]^{1/4}. \tag{4.14}$$

Inserting this result into (4.13) gives

$$A^{vac}_{\bar{\gamma}^{\#}_a} = \ln\left[2\left(\frac{(u_1-u_a)(v_a-v_1)}{(u_b-u_1)(v_1-v_b)}\right)^{1/4}(\sqrt{(u_1-u_a)(v_a-v_1)}+\sqrt{(u_b-u_1)(v_1-v_b)})\right] \quad (4.15)$$

$$A^{vac}_{\bar{\gamma}^{\#}_b} = \ln\left[2\left(\frac{(u_b-u_1)(v_1-v_b)}{(u_1-u_a)(v_a-v_1)}\right)^{1/4}(\sqrt{(u_1-u_a)(v_a-v_1)}+\sqrt{(u_b-u_1)(v_1-v_b)})\right]. \quad (4.16)$$

We will now use the above above results to compute similar areas for the general configuration shown in figure 4.2. As usual, the idea is to apply an appropriate boundary conformal transformation as in (3.25). This transformation generates a non-trivial boundary stress tensor, and in that sense takes us out of the vacuum state. For any half-infinite link area it yields

$$A_{\gamma_{half}} = A^{vac}_{\gamma_{half}} + \sigma_{U_0}(U_i) + \hat{\sigma}_{V_0}(V_i), \quad (4.17)$$

where $U_i = U(u_i)$ and $V_i = V(v_i)$.

Note that $A^{vac}_{\gamma_{half}}$ depends on the vacuum coordinates $u_i, v_i$ of all three anchor points. Since we wish to fix the physical coordinates $U_i, V_i$ of the anchors, we should regard $u_i, v_i$ as functions of $U_i, V_i$ that depend on some $\sigma_{U_0}, \hat{\sigma}_{V_0}$ via (4.5) and (4.6). Thus, all three terms in Eq. (4.17) can contribute to our commutators.

The last generalization we will need is to transform $\gamma_{R_0}$ into a general HRT-surface $\gamma$ anchored at arbitrary spacelike-separated boundary points $(U_1, V_1)$ and $(U_2, V_2)$. This will also move the other links, transforming our $\bar{\gamma}^{\#}_a$ to some $\gamma^{\#}_a$ and taking our $\bar{\gamma}^{\#}_b$ to some $\gamma^{\#}_b$. See Figure 4.2, which shows the result of this transformation. Without loss of generality, we take $U_a < U_1 < U_b < U_2$ and $V_a > V_1 > V_b > V_2$. We perform this generalization by taking a fractional linear transformation which brings the second anchor point of $\gamma_{R_0}$ back from infinity, i.e. we take $u \to \frac{1}{u_2-u}$ and $v \to \frac{1}{v_2-v}$. Under this

transformation one finds

$$\sigma_{U_0}(U(u_i)) \to \sigma_{U_0}(U(u_i)) + \ln(u_2 - u_i), \tag{4.18}$$

with analogous results for $\hat{\sigma}_{V_0}(V)$. As a result, in the general configuration given in Figure 4.2 the link areas take the form

$$\begin{aligned} A_{\gamma_a^\#} =& \ln\left[\sqrt{\frac{(u_1-u_a)(v_a-v_1)}{(u_2-u_a)(v_a-v_2)}} + \sqrt{\frac{(u_b-u_1)(v_1-v_b)}{(u_2-u_b)(v_b-v_2)}}\right] \\ &+ \frac{1}{4}\ln\left[\frac{(u_1-u_a)(v_a-v_1)(u_2-u_b)(v_b-v_2)(u_2-u_a)^3(v_a-v_2)^3}{(u_2-u_1)^2(v_1-v_2)^2(u_b-u_1)(v_1-v_b)}\right] \\ &+ \sigma_{U_0}(U_a) + \hat{\sigma}_{V_0}(V_a) + \ln 2, \end{aligned} \tag{4.19}$$

and

$$\begin{aligned} A_{\gamma_b^\#} =& \ln\left[\sqrt{\frac{(u_1-u_a)(v_a-v_1)}{(u_2-u_a)(v_a-v_2)}} + \sqrt{\frac{(u_b-u_1)(v_1-v_b)}{(u_2-u_b)(v_b-v_2)}}\right] \\ &+ \frac{1}{4}\ln\left[\frac{(u_b-u_1)(v_1-v_b)(u_2-u_b)^3(v_b-v_2)^3(u_2-u_a)(v_a-v_2)}{(u_2-u_1)^2(v_1-v_2)^2(u_1-u_a)(v_a-v_1)}\right] \\ &+ \sigma_{U_0}(U_b) + \hat{\sigma}_{V_0}(V_b) + \ln 2. \end{aligned} \tag{4.20}$$

Our ultimate goal in this calculation is to understand commutators between the areas of the four links $\gamma_a^\#$, $\gamma_b^\#$, $\gamma_1$, and $\gamma_2$. Here $\gamma_1$ runs from $(U_1, V_1)$ on the boundary to the intersection point in the bulk, and $\gamma_2$ runs from $(U_2, V_2)$ on the boundary to the intersection point in the bulk. It thus remains to compute the areas of $\gamma_1$ and $\gamma_2$ by first calculating the renormalized areas of each piece of $\gamma_{R_0}$, performing the fractional linear transformation $u \to \frac{1}{u_2-u}$ and $v \to \frac{1}{v_2-v}$ to find $A_{\gamma_1}$ and $A_{\gamma_2}$, and finally applying the

above conformal transformation. Doing so yields the renormalized areas

$$\begin{aligned} A_{\gamma_1} =& \frac{1}{4}\ln\left(\frac{(u_1-u_a)(v_a-v_1)(u_b-u_1)(v_1-v_b)(u_2-u_1)^2(v_1-v_2)^2}{(u_2-u_a)(v_a-v_2)(u_2-u_b)(v_b-v_2)}\right) \\ &+\sigma_{U_0}(U_1)+\hat{\sigma}_{V_0}(V_1)+\ln 2, \end{aligned} \tag{4.21}$$

and

$$\begin{aligned} A_{\gamma_2} =& \frac{1}{4}\ln\left(\frac{(u_2-u_a)(v_a-v_2)(u_2-u_b)(v_b-v_2)(u_2-u_1)^2(v_1-v_2)^2}{(u_1-u_a)(v_a-v_1)(u_b-u_1)(v_1-v_b)}\right) \\ &+\sigma_{U_0}(U_2)+\hat{\sigma}_{V_0}(V_2)+2\ln 2. \end{aligned} \tag{4.22}$$

As a check, adding the above two results one finds the renormalized area of the full geodesic $\gamma = \gamma_1 \cup \gamma_2$ to be

$$A_\gamma = \ln[2(u_1-u_a)(v_a-v_1)] + \sigma_{U_0}(U_1)+\hat{\sigma}_{V_0}(V_1)+\sigma_{U_0}(U_2)+\hat{\sigma}_{V_0}(V_2)+2\ln 2, \tag{4.23}$$

which agrees with [3]. As another check, although the above area expressions are written in terms of $\sigma_{U_0}(U)$ and $\hat{\sigma}_{V_0}(V)$, a short computation shows that derivatives of these areas with respect to both $U_0$ or $V_0$ give zero. This is the correct result since $A_{\gamma_a^\#}$, $A_{\gamma_b^\#}$, $A_{\gamma_1}$ and $A_{\gamma_2}$ are physical observables whose definitions do not depend on our arbitrary choice of $U_0$, $V_0$.

In order to calculate commutators, one must take care to express $u, v$ as $\sigma$-dependent functions of $U, V$. After doing so, one may compute the relevant functional derivatives

for use in (2.32):

$$\begin{aligned}\frac{\delta A_{\gamma_a^\#}}{\delta\sigma_{U_0}(U)} =&\delta(U-U_a)+e^{-2\sigma_{U_0}(U)}\bigg[-\frac{1+2C}{2(u_1-u_a)}\Theta(U_1-U)\Theta(U-U_a)\\ &-\frac{3-2C}{2(u_2-u_a)}\Theta(U_2-U)\Theta(U-U_a)-\frac{1-2C}{2(u_b-u_1)}\Theta(U_b-U)\Theta(U-U_1)\\ &+\frac{1-2C}{2(u_2-u_b)}\Theta(U_2-U)\Theta(U-U_b)+\frac{1}{u_2-u_1}\Theta(U_2-U)\Theta(U-U_1)\bigg],\end{aligned} \tag{4.24}$$

$$\begin{aligned}\frac{\delta A_{\gamma_b^\#}}{\delta\sigma_{U_0}(U)} =&\delta(U-U_b)+e^{-2\sigma_{U_0}(U)}\bigg[\frac{1-2C}{2(u_1-u_a)}\Theta(U_1-U)\Theta(U-U_a)\\ &-\frac{1-2C}{2(u_2-u_a)}\Theta(U_2-U)\Theta(U-U_a)-\frac{3-2C}{2(u_b-u_1)}\Theta(U_b-U)\Theta(U-U_1)\\ &-\frac{1+2C}{2(u_2-u_b)}\Theta(U_2-U)\Theta(U-U_b)+\frac{1}{u_2-u_1}\Theta(U_2-U)\Theta(U-U_1)\bigg]\end{aligned} \tag{4.25}$$

$$\begin{aligned}\frac{\delta A_{\gamma_1}}{\delta\sigma_{U_0}(U)} =&\delta(U-U_1)+e^{-2\sigma_{U_0}(U)}\bigg[-\frac{1}{2(u_1-u_a)}\Theta(U_1-U)\Theta(U-U_a)\\ &+\frac{1}{2(u_2-u_a)}\Theta(U_2-U)\Theta(U-U_a)-\frac{1}{2(u_b-u_1)}\Theta(U_b-U)\Theta(U-U_1)\\ &+\frac{1}{2(u_2-u_b)}\Theta(U_2-U)\Theta(U-U_b)-\frac{1}{u_2-u_1}\Theta(U_2-U)\Theta(U-U_1)\bigg],\end{aligned} \tag{4.26}$$

$$\begin{aligned}\frac{\delta A_{\gamma_2}}{\delta\sigma_{U_0}(U)} =&\delta(U-U_2)+e^{2\sigma_{U_0}(U)}\bigg[-\frac{1}{2(u_1-u_a)}\Theta(U_1-U)\Theta(U-U_a)\\ &-\frac{1}{2(u_2-u_a)}\Theta(U_2-U)\Theta(U-U_a)+\frac{1}{2(u_b-u_1)}\Theta(U_b-U)\Theta(U-U_1)\\ &-\frac{1}{2(u_2-u_b)}\Theta(U_2-U)\Theta(U-U_b)-\frac{1}{u_2-u_1}\Theta(U_2-U)\Theta(U-U_1)\bigg],\end{aligned} \tag{4.27}$$

with analogous expressions for functional derivatives with respect to $\hat{\sigma}_{V_0}(V)$. In the above we have defined the quantity

$$C=\frac{\sqrt{\frac{(u_1-u_a)(v_a-v_1)}{(u_2-u_a)(v_a-v_2)}}}{\sqrt{\frac{(u_1-u_a)(v_a-v_1)}{(u_2-u_a)(v_a-v_2)}}+\sqrt{\frac{(u_b-u_1)(v_1-v_b)}{(u_2-u_b)(v_b-v_2)}}}. \tag{4.28}$$

### 4.3.2 Vanishing commutators for the 4-link constrained HRT-surface network

We now use the above results and (4.11) to compute the desired commutators. First, as a check on our results above, let us compute $\{A_{\gamma_a^\#}, A_\gamma\}$ and $\{A_{\gamma_b^\#}, A_\gamma\}$. Each of these must vanish since the flow generated by $A_\gamma$ is known to introduce a relative boost between the entanglement wedges on either side of $\gamma$ but to preserve the geometry of each wedge separately; see e.g. [3] which builds on [114, 115]. Since $\gamma_a^\#$ and $\gamma_b^\#$ each lie entirely in one of these wedges, the relative boost has no effect on their areas. Thus their area operators must commute with $A_\gamma$. Combining the above equations does indeed yield this result.

We next examine commutators between any two of $\gamma_a^\#$, $\gamma_b^\#$, $\gamma_1$, and $\gamma_2$. A priori, we have no argument for the form that these should take. However, direct calculation shows that all terms cancel. In particular, the $U$-parts alone give a result of the form

$$c_1 + c_2 C, \tag{4.29}$$

with constants $c_1$ and $c_2$. For example, $\{A_{\gamma_a^\#}, A_{\gamma_1}\}_{U-component} = \frac{1}{2}(1-C)$. The calculation of the $V$-components then follows immediately: The functional derivatives with respect to $V$ are direct analogues of those with respect to $U$, but with the ordering of the anchor points reversed. However, we must also take into account the various signs that arise in comparing the $U$- and $V$-dependent pieces in (4.11). The changes inside the step-function are just those associated with the above reversal in the order of the anchor points, but there nevertheless remains an overall difference in sign. The result of the computation of the $V$-parts is thus identical to that for the $U$-parts up to this overall sign. Since $C$ is invariant under $u \to v$, this means the $V$-parts of the commutator take the form

$-c_1 - c_2 C$ so that they precisely cancel the contributions from the $U$-parts. We thus find that the areas of $\gamma_a^{\#}$, $\gamma_b^{\#}$, $\gamma_1$, and $\gamma_2$ mutually commute.

This is an intriguing result. One may then wonder whether similar results hold for other simple networks. We explore a 6-link example in Appendix B obtained by adding a further constrained HRT-surface to the network above. However, in that case we find link-area commutators that fail to vanish.

## 4.4 Link-area algebras for the cross section network

It is interesting that the link-area commutators vanished for the constrained HRT-surface network of figure 4.2. However, following our original motivations requires us to ask whether the same result can hold in a more complicated network. While there are clearly many options that one can consider, we focus here on a network associated with the entanglement wedge cross section (see figure 4.4a), for which the resulting link-area operators may be of interest in their own right. As before, we begin by finding expressions for the areas of the entanglement wedge cross section and the four half-infinite HRT-surfaces in section 4.4.1. We then compute the various area commutators in Section 4.4.2. In contrast to the previous section, we find that some of these commutators do not vanish.

### 4.4.1 Area operators

Our goal in this section is to find expressions for the areas of all of the links in the network shown in Figure 4.4a, but in the context of a general spacetime in our phase space (i.e., with a general $T_{ab}$ in the allowed class) and with general positions of the anchor points. We consider in detail only cases where the cross section $\gamma_{CS}$ is spacelike (though we briefly comment on the case when the cross section is timelike in Appendix D).

The network is defined by first choosing two HRT surfaces, $\bar{\gamma}'_a$ and $\bar{\gamma}_b$, and constructing the associated cross-section $\gamma_{CS}$, defined as the codimension-2 surface whose boundaries lie on the above HRT-surfaces and which has extremal length[5]. In particular, this extremization condition fixes the locations of the cross-section boundaries on the original HRT-surfaces. When the region between the HRT-surfaces is an entanglement wedge, this construction defines an entanglement-wedge cross section (though our computation holds more generally).

As before, we will generate general configurations by acting on simple ones with boundary conformal transformations. We start in the Poincaré AdS$_3$ vacuum and choose two boundary subregions, $R_a$ and $R_b$. Both regions are to be defined by straight line segments on the boundary, though they need not lie in any $t = constant$ slice. However, we can simplify the configuration by acting with boundary conformal transformations that act on the boundary as fractional linear transformations in either $u$ or $v$, as such boundary conformal transformations preserve the vanishing of the boundary stress tensor. The resulting 6-parameter group can generally[6] be used to move both $R_a$ and $R_b$ to line segments that are symmetric about the origin $(u, v) = (0, 0)$ of the boundary Minkowski space; see figure 4.4b.

These conditions fix a 4-parameter subgroup of the above symmetries, but they still allow further action by both boosts and dilations. It is convenient to use the boosts to place the segment $R_b$ in the surface $t = 0$.

[5]As usual, if there is more than one such surface we would choose the minimal one. We should also enforce a homology constraint. However, neither of these details are relevant in the simple context studied here.

[6]The only exceptions correspond to cases where $R_a$ and $R_b$ define a common Lorentz frame but fail to share a common time-slice. Such exceptions can be treated as degenerate limits of the more general case studied explicitly.

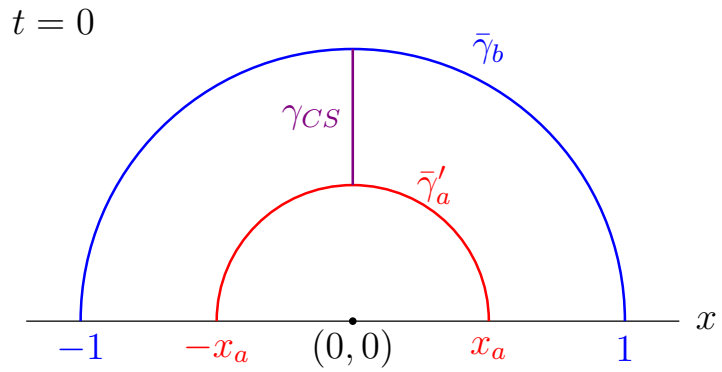


(a)

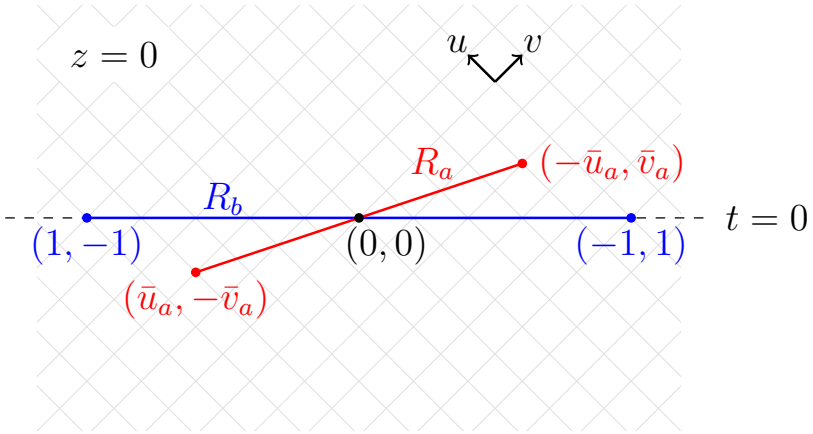


(b)

Figure 4.4: A simple example of a cross-section network. Panel (a) shows the $t = 0$ slice, which we take to contain two HRT surfaces $\bar{\gamma}'_a$ and $\bar{\gamma}_b$. Although the figure shows $x_a$ less than 1, any value $x_a > 0$ is allowed. Panel (b) shows the $z = 0$ boundary for a more general configuration in which $R_a$ and $R_b$ are boundary regions respectively homologous to $\bar{\gamma}_a$ and $\bar{\gamma}_b$, but with $R_a$ (and thus also $\bar{\gamma}_a$) now boosted relative to $R_b$ and $\bar{\gamma}_b$ (which continue to lie in the $t = 0$ slice).

Indeed, it will be useful to begin with an even simpler class of configurations in which all anchor points lie in a constant time slice as shown in Figure 4.4a. We emphasize that this configuration is no longer related by symmetries to the most general ones, but we will see that it is nevertheless useful starting point for our analysis. We choose the anchor points of the first HRT surface, $\bar{\gamma}'_a$, to lie at $x = \pm x_a$, with $x_a > 0$. The anchor

points of the second HRT surface, $\bar{\gamma}_b$, are fixed at $x = \pm 1$. Given any 4 values of $x$ one can define a useful cross-ratio (see also (4.39) below) which for these anchor points takes the value

$$\chi = \frac{4x_a}{(x_a+1)^2}. \tag{4.30}$$

From this we can compute the area of the cross section, either directly or by using results from [162, 158]. We find

$$A_{CS} = \ln\left(\frac{1+\sqrt{1-\chi}}{\sqrt{\chi}}\right) = \frac{1}{2}|\ln x_a|. \tag{4.31}$$

Notice that, since the cross-section $\gamma_{CS}$ does not extend to the AdS boundary, its renormalized area is just its (finite) area. As a result, for any solution in our phase space (with general $T_{ab}$) the cross-section area $A_{CS}$ continues to be given by (4.31) so long as $u, v$ are expressed in terms of the physical coordinates $U, V$.

We would now like to generalize the configuration in Figure 4.4a by boosting $R_a$, the boundary region that defines $\bar{\gamma}'_a$, relative to $R_b$ as shown in Figure 4.4b. We will denote the resulting HRT surface by $\bar{\gamma}_a$, with anchor points at $(\bar{u}_a, -\bar{v}_a)$ and $(-\bar{u}_a, \bar{v}_a)$. We take $\bar{u}_a > 0$ and $\bar{v}_a > 0$.

Note that the cross-section itself is invariant under this boost. Since the result of any boost satisfies

$$x_a^2 = \bar{u}_a \bar{v}_a, \tag{4.32}$$

we can write (4.31) in terms of the anchor points in this new configuration to find

$$A_{CS} = \frac{1}{4}|\ln \bar{u}_a \bar{v}_a|. \tag{4.33}$$

We can also write down the vacuum values of the areas of the four half-infinite links in

our network. For any HRT surface with anchor points $(\bar{u}, -\bar{v})$ and $(-\bar{u}, \bar{v})$, the vacuum area of each half-infinite link is given by Eq. (4.13) with $(u_2, v_2) = (0, 0)$ and $z = \sqrt{\bar{u}\bar{v}}$. This yields

$$A^{vac}_{\gamma_{half}} = \frac{1}{2} \ln[4(\bar{u} - (-\bar{u}))(\bar{v} - (-\bar{v}))], \tag{4.34}$$

where we have made manifest the contributions from each anchor point. Thus, the vacuum areas of the links cut from $\bar{\gamma}_a$ and $\bar{\gamma}_b$ are

$$A^{vac}_{\bar{\gamma}_{a,half}} = \frac{1}{2} \ln[4(\bar{u}_a - (-\bar{u}_a))(\bar{v}_a - (-\bar{v}_a))], \tag{4.35}$$

$$A^{vac}_{\bar{\gamma}_{b,half}} = \frac{1}{2} \ln[4(\bar{u}_b - (-\bar{u}_b))(\bar{v}_b - (-\bar{v}_b))], \tag{4.36}$$

where we have $\bar{u}_b = 1$ and $\bar{v}_b = 1$. Writing $A^{vac}_{\bar{\gamma}_{b,half}}$ in the somewhat awkward form above will turn out to clarify later calculations. We can now apply the conformal transformation (3.25), under which the vacuum areas above transform as in (4.17). This gives the area of the half-infinite links cut from $\bar{\gamma}_a$ and $\bar{\gamma}_b$ in any solution.

We can now move our anchor points into an almost fully general configuration in the Poincaré AdS$_3$ vacuum by acting with an SL(2,$\mathbb{R}$) $\times$ SL(2,$\mathbb{R}$) transformation. We wish to find the transformation that takes two general HRT surfaces, $\gamma_a$ and $\gamma_b$, into the previous configuration, transforming $\gamma_a$ into $\bar{\gamma}_a$ and $\gamma_b$ into $\bar{\gamma}_b$. If $\gamma_a$ has anchor points $(u_{a1}, v_{a1})$ and $(u_{a2}, v_{a2})$, then we have the constraints

$$\frac{a_u u_{a1} + b_u}{c_u u_{a1} + d_u} = \bar{u}_a, \;\; \frac{a_u u_{a2} + b_u}{c_u u_{a2} + d_u} = -\bar{u}_a, \;\; \frac{a_v v_{a1} + b_v}{c_v v_{a1} + d_v} = -\bar{v}_a, \;\; \frac{a_v v_{a2} + b_v}{c_v v_{a2} + d_v} = \bar{v}_a. \tag{4.37}$$

Additionally, if $\gamma_b$ has anchor points $(u_{b1}, v_{b1})$ and $(u_{b2}, v_{b2})$, then we have

$$\begin{aligned} \frac{a_u u_{b1} + b_u}{c_u u_{b1} + d_u} &= \bar{u}_b = 1, \quad \frac{a_u u_{b2} + b_u}{c_u u_{b2} + d_u} = -\bar{u}_b = -1, \\ \frac{a_v v_{b1} + b_v}{c_v v_{b1} + d_v} &= -\bar{v}_b = -1, \quad \frac{a_v v_{b2} + b_v}{c_v v_{b2} + d_v} = \bar{v}_b = 1. \end{aligned} \tag{4.38}$$

We are also free to impose the additional constraints $a_u = a_v = 1$. We can then solve for $\bar{u}_a$ and $\bar{v}_a$ in terms of the four anchor points of our general HRT surfaces. In terms of the cross ratios

$$\chi_u = \frac{(u_{a2} - u_{a1})(u_{b2} - u_{b1})}{(u_{a1} - u_{b2})(u_{b1} - u_{a2})}, \quad \chi_v = \frac{(v_{a2} - v_{a1})(v_{b2} - v_{b1})}{(v_{a1} - v_{b2})(v_{b1} - v_{a2})}, \tag{4.39}$$

we find[7]

$$\bar{u}_a = \left( \frac{1 + \sqrt{1 - \chi_u}}{\sqrt{\chi_u}} \right)^2, \quad \bar{v}_a = \left( \frac{1 + \sqrt{1 - \chi_v}}{\sqrt{\chi_v}} \right)^2. \tag{4.40}$$

Since $\chi_u, \chi_v < 1$, the expressions for $\bar{u}_a$, $\bar{v}_a$ are real[8]. Using these definitions in (4.33) then yields

$$A_{CS} = \frac{1}{2} \left( \ln \left[ \frac{1 + \sqrt{1 - \chi_u}}{\sqrt{\chi_u}} \right] + \ln \left[ \frac{1 + \sqrt{1 - \chi_v}}{\sqrt{\chi_v}} \right] \right), \tag{4.41}$$

where we have dropped the absolute value sign since the expression is manifestly positive (the arguments in the logarithms are greater than one since $\chi_u, \chi_v < 1$). Note that this reduces to the result (4.33) when all anchor points lie on a slice with time-reversal symmetry, since in that case $\chi_u = \chi_v$.

The four half-infinite links are now $\gamma_{a1}$ anchored to $(u_{a1}, v_{a1})$, $\gamma_{a2}$ anchored to $(u_{a2}, v_{a2})$, $\gamma_{b1}$ anchored to $(u_{b1}, v_{b1})$, and $\gamma_{b2}$ anchored to $(u_{b2}, v_{b2})$. Writing the constraints with parameters $b_{u,v}$, $c_{u,v}$, and $d_{u,v}$ expressed in terms of the anchor points, and using the

[7] The constraints (4.37) and (4.38) admit two solutions, differing by a sign in front of the square root term in the numerator. We choose the sign consistent with the case where both intervals lie in the $t = 0$ surface.

[8] The cross-ratios can be written as $\chi_u = \frac{4\bar{u}_a}{(\bar{u}_a+1)^2}$ and $\chi_v = \frac{4\bar{v}_a}{(\bar{v}_a+1)^2}$, which are less than 1 for any $\bar{u}_a \neq 1$ and $\bar{v}_a \neq 1$, respectively. This can also be argued directly from the form of $\chi_{u,v}$ in Eq. (4.39).

conformally transformed versions of Equations (4.35) and (4.36), we obtain the final expressions for the areas of the half-infinite links

$$\begin{aligned} A_{a1} =& \frac{1}{4}\ln\left|\frac{(u_{a1}-u_{b1})(u_{a1}-u_{b2})(v_{a1}-v_{b1})(v_{a1}-v_{b2})}{(u_{b1}-u_{a2})(u_{b2}-u_{a2})(v_{b1}-v_{a2})(v_{b2}-v_{a2})}\right| \\ &+ \frac{1}{2}\ln|4(u_{a1}-u_{a2})(v_{a2}-v_{a1})| + \sigma_{U_0}(U_{a1}) + \sigma_{V_0}(V_{a1}), \end{aligned} \tag{4.42}$$

$$\begin{aligned} A_{a2} =& \frac{1}{4}\ln\left|\frac{(u_{b1}-u_{a2})(u_{b2}-u_{a2})(v_{b1}-v_{a2})(v_{b2}-v_{a2})}{(u_{a1}-u_{b1})(u_{a1}-u_{b2})(v_{a1}-v_{b1})(v_{a1}-v_{b2})}\right| \\ &+ \frac{1}{2}\ln|4(u_{a1}-u_{a2})(v_{a2}-v_{a1})| + \sigma_{U_0}(U_{a2}) + \sigma_{V_0}(V_{a2}), \end{aligned} \tag{4.43}$$

$$\begin{aligned} A_{b1} =& \frac{1}{4}\ln\left|\frac{(u_{a1}-u_{b1})(v_{a1}-v_{b1})(u_{b1}-u_{a2})(v_{b1}-v_{a2})}{(u_{a1}-u_{b2})(v_{a1}-v_{b2})(u_{b2}-u_{a2})(v_{b2}-v_{a2})}\right| \\ &+ \frac{1}{2}\ln|4(u_{b1}-u_{b2})(v_{b2}-v_{b1})| + \sigma_{U_0}(U_{b1}) + \sigma_{V_0}(V_{b1}), \end{aligned} \tag{4.44}$$

$$\begin{aligned} A_{b2} =& \frac{1}{4}\ln\left|\frac{(u_{a1}-u_{b2})(v_{a1}-v_{b2})(u_{b2}-u_{a2})(v_{b2}-v_{a2})}{(u_{a1}-u_{b1})(v_{a1}-v_{b1})(u_{b1}-u_{a2})(v_{b1}-v_{a2})}\right| \\ &+ \frac{1}{2}\ln|4(u_{b1}-u_{b2})(v_{b2}-v_{b1})| + \sigma_{U_0}(U_{b2}) + \sigma_{V_0}(V_{b2}). \end{aligned} \tag{4.45}$$

Having found these results, it is also useful to note that, if we had been satisfied with less detailed knowledge of the above functions, we could have obtained certain information about these areas by following a much simpler route. In particular, since each half-infinite HRT-surface has a single anchor point, it is manifest that each such area transforms covariantly under boundary conformal transformations, and that it transforms as the logarithm of a local operator that has conformal weight 1 at its anchor point.

In particular, these areas must transform in this way under the SL(2,$\mathbb{R}$) $\times$ SL(2,$\mathbb{R}$) group of fractional linear transformations. Since any SL(2,$\mathbb{R}$) $\times$ SL(2,$\mathbb{R}$)-invariant function of four anchor points is a function of the cross-ratios $\chi_u, \chi_v$, for e.g. $\gamma_{b1}$ we must

have

$$\begin{aligned} A_{b1} =& \frac{1}{2}\ln\left(\frac{(u_{a1}-u_{b1})(v_{b1}-v_{a1})(u_{a2}-u_{b1})(v_{b1}-v_{a2})}{(u_{a2}-u_{a1})(v_{a1}-v_{a2})}\right) \\ &+ f_{b1}(\chi_u,\chi_v) + \sigma_{U_0}(U_{b1}) + \sigma_{V_0}(V_{b1}), \end{aligned} \tag{4.46}$$

where $f_{b1}(\chi_u,\chi_v)$ is some (separable) function of the cross ratios that can be found by comparing with (4.42). The areas of the other three half-infinite links take similar forms. This form turns out to be useful in simplifying some of the commutator calculations since all functions of $u$-coordinates commute with all functions of $v$-coordinates so that we also have $\{\chi_u, f_{b1}(\chi_u,\chi_v)\} = 0$.

It is now a straightforward exercise to compute functional derivatives of link areas with respect to $\sigma(U,V)$, after first expressing the area operators in terms of coordinates $U,V$ using (4.5) and (4.6). We can do this for the half-infinite link areas as well as for the cross-section area. We save detailed expressions for Appendix C, but note here that for the area $A_{CS}$ of the cross-section $\gamma_{CS}$, we can write

$$\begin{aligned} \frac{\delta A_{CS}}{\delta\sigma_U(U)} =& \frac{\partial A_{CS}}{\partial\chi_u}\frac{\delta\chi_u}{\delta\sigma_U(U)} \\ =& -\frac{1}{4\chi_u\sqrt{1-\chi_u}}\frac{\delta\chi_u}{\delta\sigma_U(U)}, \end{aligned} \tag{4.47}$$

and similarly for $\frac{\delta A_{CS}}{\delta\hat{\sigma}_{V_0}(V)}$. As in section 4.3, such formulae can be combined with (2.32) to compute the desired semiclassical commutators. We discuss the results in section 4.4.2 below.

### 4.4.2 Results

We now compute commutators between (i) any two half-infinite link areas and (ii) the cross-section area and any of the half-infinite link areas. In general, commutators of

type (i) vanish, but those of type (ii) are non-zero.

Let us start by computing commutators of type (i). Commutators between half-infinite links on the same HRT surface must vanish since these are equivalent to commutators between a half-infinite link and the HRT surface containing it. HRT area flow leaves the HRT surface invariant, and so it should leave the link area unaffected. However, to understand commutators between half-infinite links on *different* HRT surfaces, we must perform a calculation. We do this by first taking the link-area functional derivatives given in Equations (C.4)-(C.7), then using them in Eq. (4.11). We find that all such commutators vanish. And, unlike the link-area algebra of Section 4.3.2, the $U$- and $V$-components of these commutators vanish individually.

The commutators between $A_{CS}$ and the half-infinite link areas are more interesting. We will focus on $\{A_{CS}, A_{b1}\}$. Since $A_{CS}$ depends only on $\chi_u$ and $\chi_v$, we can use Eq. (4.46) for $A_{b1}$ and ignore the $\chi$-dependent piece $f_{b1}(\chi_u, \chi_v)$, since this commutes with all functions of $\chi_u$ and $\chi_v$. We choose the ordering $U_{b1} < U_{a1} < U_{a2} < U_{b2}$ and $V_{b1} > V_{a1} > V_{a2} > V_{b2}$. Using the functional derivative of $A_{b1}$ in Eq. (C.8), and the functional derivative of $A_{CS}$ in Eq. (C.3) (and their $V$-dependent counterparts), we find

$$\{A_{CS}, A_{b1}\} = \frac{3\pi}{2c}\sqrt{1-\chi_u} - \frac{3\pi}{2c}\sqrt{1-\chi_v}. \tag{4.48}$$

A similar non-vanishing result is of course obtained when $b1$ is replaced with any other half-infinite links (the result will be the same up to an overall sign). The relative sign difference between $U$-components and $V$-components appears for the same reason as described in Section 4.3.2. We will hence always have a difference in overall sign between commutators with $\chi_u$ and $\chi_v$; otherwise, they will be the same up to a replacement of all instances of $\chi_u$ with $\chi_v$.

Furthermore, one may check that indeed

$$\{A_{CS}, A_{\gamma_{b1}\cup\gamma_{b2}}\} = \{A_{CS}, A_{\gamma_{b1}}\} + \{A_{CS}, A_{\gamma_{b2}}\} = 0, \tag{4.49}$$

as is required by the fact that $\gamma_{b1} \cup \gamma_{b2}$ is an HRT surface relative to which $\gamma_{CS}$ lies entirely in one of the associated entanglement wedges. In particular, since the action of the HRT area is just to introduce a relative boost between the two entanglement wedges, the area $A_{CS}$ is unaffected. The same result holds for $\gamma_{a1} \cup \gamma_{a2}$. As an aside, we note that these HRT areas will fail to commute with $A_{CS}$ if we allow the cross section to be timelike. We elaborate on this result in Appendix D.

## 4.5 Discussion

Motivated by a desire to improve the understanding of tensor-network models of holography, our work above probed the feasibility of simultaneously fixing the areas of all surface segments in an area-network. We studied several such area-networks in the context of pure $AdS_3$ Einstein-Hilbert gravity (where the areas are in fact lengths and extremal codimension-2 surfaces are geodesics) and computed the relevant commutators at leading order in the semiclassical approximation.

Our first network contained precisely 4 links and was defined by a single HRT surface and a single constrainted HRT-surface. All link-area commutators in this network were found to vanish at leading semiclassical order. While higher-order effects remain to be considered, they would necessarily be small. We thus conclude that, at least in the pure-$AdS_3$ context, this network is one for which fluctuations of all areas can be simultaneously suppressed relative to the $O(\sqrt{G})$ fluctuations found in typical semiclassical states.

However, such results are not generic. In particular, Appendix B analyzed a 6-link

generalization of the above model defined by adding an additional constrained geodesic. For this network we found non-vanishing commutators.

We then moved on to study a network with two HRT surfaces and their cross-section $\gamma_{CS}$. When the region between the two HRT surfaces is an entanglement wedge, this $\gamma_{CS}$ in the associated entanglement-wedge cross-section. Here we again found non-vanishing area commutators.

The present work was exploratory and did not seek deeper understanding of the results. It is thus far from clear that we have exhausted the space of interesting constructions, though it is also unclear which additional area-networks would be of significant interest for further study. On the other hand, it *would* clearly be of interest to understand whether the area-link algebra found for the 4-link constrained-HRT network of section 4.3 remains Abelian in theories with matter and/or in higher dimensions. If it does, the result would then call out for an explanation or interpretation in terms of a dual CFT.

Another issue to which we expect to return is the question of obtaining a more geometric understanding of the commutators described above and the flows generated by them. The fact that HRT areas are known to generate flows on phase space described by geometric operations [114, 115, 3] that something similar may be true of the HRT area-links studied in the present work. And since such links have boundaries, it is natural to expect the flow generated by these areas may have a non-trivial effect extending to the boundary, as in [148] for similar operators associated with codimension-1 surfaces. Such an understanding might be particularly useful in the context of entanglement-wedge cross-sections, where the cross-section area is associated with reflected entropy [158] and has been related to entanglement of purification [156, 157]. These issues will be addressed in forthcoming work.

# Chapter 5

# De Sitter quantum gravity and the emergence of local algebras

## 5.1 Introduction

It has long been recognized that the physics of quantum gravity will involve at least some degree of non-locality, with familiar local physics emerging in the perturbative limit $G \to 0$. While some such effects may stem from topology-changing processes in the gravitational path integral, we will focus here a form of non-locality that is directly associated with diffeomorphism-invariance (see e.g. discussions in [163, 164, 165, 166, 167, 168, 169, 170, 101, 171]), and which are expected to be arise even when topology-change is absent.

In addition, recent progress on understanding gravitational entropy in this limit [37, 39, 38, 40, 172, 46, 45] has emphasized the importance of the emergence of an *algebra* of local fields. Our goal here is to perform the next steps in investigating just how such algebras appear as $G \to 0$ by exploring a construction advocated in [102] for the interesting-but-tractable context of perturbative gravity around global de Sitter ($\mathrm{dS}_D$)

space, with metric

$$ds^2 = -dt^2 + \ell^2 \cosh^2(t/\ell) d\Omega_d^2, \tag{5.1}$$

where $d = D - 1$, $\ell$ is the de Sitter scale, and $d\Omega_d^2$ is the round metric on the unit sphere $S^d$.

As emphasized in [171], perturbative quantum gravity is manifestly local when formulated around a background that completely breaks diffeomorphism-invariance. In particular, in that context it can be described by gauge-invariant operators that satisfy exact microcausality. But this is not the case when the background leaves a subgroup of gauge diffeomorphisms unbroken; i.e., when the Cauchy surfaces of the background are compact (so that all diffeomorphisms are gauge) and when there is an isometry that also leaves invariant any matter fields that may be present. In this more subtle context, even at the perturbative level any gauge invariant observable must be invariant under the unbroken isometries.[1] As a result, a gauge-invariant observable in perturbative gravity can be supported in a small region of spacetime localized near a single point $p$ only if $p$ is a fixed point of every unbroken isometry.

When expanding around global de Sitter, such observables must be invariant under the full de Sitter group and are thus maximally delocalized. Nevertheless, we expect to recover a notion of local physics by making use of relational constructions; see e.g. [163, 164, 165, 166, 167, 168, 169, 170, 101, 102]. Indeed, in an appropriate limit we should obtain the usual local algebra of quantum fields on a fixed spacetime background.

[1] This is, of course, just the gravitational version of a general fact about gauge symmetries and perturbation expansions. Given a gauge transformation $g$ that acts on fields $\phi$ via $\phi \mapsto \phi_g$, we may choose a classical background $\bar{\phi}$ and define the perturbative field $\delta\phi := \phi - \bar{\phi}$ and the perturbative gauge transformation $(\delta\phi)_g := \phi_g - \bar{\phi}$. When $\bar{\phi}_g \neq \bar{\phi}$, the space of small perturbations is preserved only when $g - 1$ is of order $\delta\phi$, so that dropping terms of order $(\delta\phi)^2$ yields $\phi_g \approx \delta\phi + \bar{\phi}_g$ and thus $\delta\phi_g \approx \delta\phi + (\bar{\phi}_g - \bar{\phi})$. On the other hand, for a family of transformations with $\bar{\phi}_g = \bar{\phi}$, we may take $g$ arbitrarily large. Furthermore, the action of $g$ on $\delta\phi$ is then essentially the same as the action of $g$ on $\phi$. In particular, in the gravitational case the unbroken diffeomorphisms act as finite diffeomorphisms on the perturbative fields $\delta\phi$.

Related issues were recently addressed in [45], which explored how a rolling inflaton field could replace the clock used for the construction described in [39] of a type II von Neumann algebra for the static patch of dS. However, our treatment differs from that of [45] in three important ways. The first is that [45] assumed that a definition of a preferred static patch $P$ of their de Sitter space had already been given in a gauge-invariant manner. This then left only the isometry associated with time translations within $P$ to be treated explicitly. One might thus say that they took locality in space as a given and focussed instead on issues associated with the emergence of locality in time. In contrast, we treat all de Sitter isometries on an equal footing and explicitly study the emergence of locality in both space and time. A second difference is that, in addition to understanding the limiting algebra, we will also characterize the departures from the $G = 0$ limit that arise at small-but-finite values of $G$. Finally, a third difference is that we consider perturbations around a *stable* de Sitter space, and in particular one in which all matter fields (including any field that might be called an 'inflaton') has a stable vacuum. We expect this to be a good starting point for discussion of more interesting scenarios that involve eternal inflation with a small probability of ending inflation in each Hubble volume; see e.g. [93, 96] for progress on embedding such constructions in string theory.

Our focus on stable (or nearly-stable) $\mathrm{dS}_{d+1}$ vacuua has important implications for our construction of gauge-invariant observables. To explain the details, it will be useful to refer to the theory at order $G^0$ as quantum field theory on a fixed de Sitter background (dS QFT), where we take this to include the theory of linearlized gravitons. In constructing perturbative observables, it may then seem natural to follow [164] and consider observables of the form

$$\mathcal{O} = \int \sqrt{-g} A(x) \tag{5.2}$$

for some local scalar field $A(x)$ in our dS QFT. This approach has been shown to be

successful in certain simple models of quantum gravity [173, 174, 170, 101]. The analogous construction was also used in [45] (where the integral was only over static patch time translations since, as noted above, that work assumed that a preferred notion of a static patch had already been given), and in [39, 40, 46] (though with an ad hoc observer clock instead of just local quantum fields). However, since local correlators in any state[2] $\big|\Psi\big]$ are well-approximated by correlators in the vacuum $\big|0\big]$ at late times, the integral in (5.2) will diverge when acting on *any* state $\big|\Psi\big]$ in the dS QFT Hilbert space $\mathcal{H}_{QFT}$ [101, 102].

In particular, for any $\big|\Psi\big]$ and for $\mathcal{O}$ as in (5.2), in a computation of the norm-squared

$$\Big|\mathcal{O}\big|\Psi\big]\Big|^2 = \big[\Psi\big|\mathcal{O}\mathcal{O}\big|\Psi\big] = \int dxdy\sqrt{-g(x)}\sqrt{-g(y)}\big[\Psi\big|A(x)A(y)\big|\Psi\big], \tag{5.3}$$

the leading term at large separations between $x$ and $y$ is given by the norm-squared of the state

$$\int \sqrt{-g}A(x)\big|0\big]. \tag{5.4}$$

But by dividing the integral over $\mathrm{dS}_{d+1}$ in (5.4) into an infinite number of large-but-finite regions, and using the decay of dS correlators at large separations, we may write (5.4) as an infinite sum over approximately-orthogonal states. This representation thus makes manifest the divergent nature of its norm. An equivalent observation was also mentioned in [39, 45] using the static patch language that every state in dS will thermalize at late times. As noted in [102], the issue may be considered to be an operator-realization of the so-called 'Boltzman brain' problem since, no matter how complicated we make the operator $A(x)$ (perhaps in an attempt to make the operator respond only to large and complicated excitations of $\big|0\big]$), our $A(x)$ will still fail to annihilate the vacuum $\big|0\big]$ and will thus respond to virtual (or, in the thermal static patch description, Boltzman)

[2]Due to our introduction of the group averaging inner product in section 5.2.1, we use square brackets to denote bra states $\big[\Psi\big|$ and ket states $\big|\Psi\big]$ of dS QFT.

versions of such excitations with at least some small probability $p$ per unit spacetime volume. For any $p > 0$, integrating over the infinite volume of $\mathrm{dS}_{d+1}$ then gives the divergence described above.

The success of the use of (5.2) in [45] was thus directly tied to the assumption in of a rapidly decaying inflaton field made in that work. Since we take all matter fields to be stable, we will require a different approach. In particular, we choose to follow [102] in replacing the local observable $A(x)$ with a distinctly *non-local* operator $A$ that does in fact annihilate the dS vacuum (though the actual form of the operators we will use is rather different from that described in [102]). Since $A$ is not a local field, there is then no meaning to $A(x)$, and thus no direct analogue of (5.2). However, we can still apply a de Sitter transformation $g$ to the operator $A$ by computing $U(g)AU(g^{-1})$, where $U(g)$ is the unitary representation of $g$ on the Hilbert space of the associated quantum field theory on a fixed de Sitter background (dS QFT). We may then again follow [102] in constructing de Sitter-invariant observables by writing

$$\mathcal{O} = \int_{g \in \mathrm{SO}_0(D,1)} dg U(g) A U(g^{-1}). \tag{5.5}$$

The expression (5.5) uses the Haar measure $dg$ to integrate over all elements $g$ of the subggroup $\mathrm{SO}_0(D,1) \subset \mathrm{SO}(D,1)$ of isometries of $\mathrm{dS}_D = dS_{d+1}$ that are connected to the identity (i.e., over the orthochronous Lorentz group).

In the main text below we will consider a context with two independent fields, $\phi$ and $\psi$, so that our dS QFT Hilbert space takes the form $\mathcal{H}_{QFT} = \mathcal{H}^{\phi}_{QFT} \otimes H^{\psi}_{QFT}$. Here $\phi$ and $\psi$ need not be scalars and, in particular, we can include linearized gravitons in our dS QFT by taking them to be part of the field $\phi$. We then choose a local operator $\tilde{A}(x)$ on $\mathcal{H}^{\phi}_{QFT}$ and a vaccum-orthogonal state $\big|\psi_0\big] \in \mathcal{H}^{\psi}_{QFT}$ (so that $[0|\psi_0] = 0$). Taking $A := \tilde{A}(x) \otimes \big|\psi_0\big]\big[\psi_0\big|$ for any fixed $x$ will then define a finite $\mathcal{O}$ with the desired properties

for appropriate choices of $\big|\psi_0\big]$. In effect, as will be made manifest in section 5.2.2, we will use the state $\big|\psi_0\big]$ to define a quantum version of a reference frame with respect to which positions and directions in de Sitter space can then be specified[3] . In particular, despite the integral over de Sitter transformations in (5.5), we will see explicitly below that the definition of the observable $\mathcal{O}$ depends on the choice of the point $x$. Note that what is really needed is just an origin for this reference frame, together with a way to specify directions emanating from that origin, as one can then use the background de Sitter metric to construct e.g. a set of Riemann normal coordinates (or any other coordinate system on $dS_D$) with respect to which the point $x$ can be specified. Below, we will thus refer to $\big|\psi_0\big]$ as a *reference state*. We emphasize that the associated reference field $\psi$ is a part of the dS QFT and, in particular, that it will backreact on the geometry at higher orders in perturbation theory.

For the above non-local operators $A$, we will see explicitly in section 5.2.2 that the operators (5.5) act like local quantum fields in any limit where $\big[\psi_0\big|U(g)\big|\psi_0\big]$ becomes $\delta(g)$, the Haar-measure delta-function on the de Sitter group supported at the identify. Such limits are straightforward to construct when we take $G \to 0$ so that $\big|\psi_0\big]$ may contain arbitrarily large energies and momenta without inducing a large gravitational backreaction.

In contrast, if we want to approximate QFT on empty de Sitter space, at finite $G$ the backreaction effects from the state $\big|\psi_0\big]$ prevent us from taking a strict delta-function limit. As a result, the integration over $g$ in (5.5) causes our gauge-invariant observables to be somewhat-smeared versions of local quantum $\phi$-fields, so that the desired local algebra is recovered only approximately.

[3]There is a vast literature on so-called quantum reference frames; see e.g. [175, 176] for foundational works, [177, 178] for recent works including broad reviews, and [179, 180] for relations to [39, 40, 45, 46]. This literature addresses themes that strongly overlap with our current discussion, though often with a slightly different emphasis and formalism.

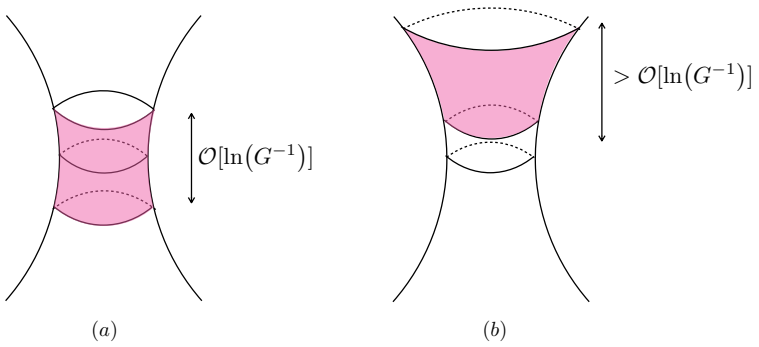


Figure 5.1: A sketch of global $dS_{d+1}$ indicating regions (shaded pink) where we construct good approximations to dS QFT at non-zero $G$. **(a):** Regions that contain a minimal $S^d$ can span only global time intervals $\Delta t \lesssim \mathcal{O}[\ln(G^{-1})]$. **(b):** Regions far to the future (or past) of a minimal $S^d$ can span arbitrarily large global time intervals.

As we will see, the accuracy of this approximation is far from uniform across the de Sitter background. Instead, it is typically best in a region near where the reference objects in the state $\left|\psi_0\right]$ are well-localized. The approximation then degrades as one moves to more distant regions of the spacetime. Our results also indicate that it is difficult (and likely impossible) to engineer settings where the dS QFT approximation holds to high accuracy over regions that span a global time interval of more than $O(\ell \ln G^{-1})$ that is symmetric with respect to the past and future of global de Sitter or, more generally, which contains a minimal $S^d$ that we may call $t = 0$ ; see figure 5.1 (a). On the other hand, because such minimal spheres describe the most fragile regions of global dS, we find that we can nevertheless obtain a good approximation to dS QFT over arbitrary spans of global time, so long as we take the associated regions to be far to the future (or far to the past) of the associated minimal $S^d$; see figure 5.1 (b).

It will be useful to begin by describing the Hilbert space of gauge-invariant states on which the operators (5.5) will act. We review this construction in section 5.2.1, using the group-averaging construction of [181, 182]. We then apply this formalism to $dS_{1+1}$ in Section 5.3. While Einstein-Hilbert gravity is trivial in two-dimensions, it is

nevertheless useful to analyze $dS_{1+1}$ as a toy model of the higher dimensional cases[4]. We first consider a reference state $\left|\psi_0\right]$ for which the classical limit describes having a single particle in each of two complementary static patches. We identify the regions of spacetime in which the dS QFT approximation breaks down, and we estimate the size of the region in which the dS QFT approximation holds. We then introduce additional reference particles, localizing at additional events, such that these events all lie on a single pair of antipodally-related timelike geodesics. However, we find that the size of the allowed region remains the same (or becomes slightly smaller). We then demonstrate analogous results for higher dimensions in section 5.4, before finally arguing in section 5.5 that dropping the requirement of time-symmetry *does* in fact allow us to approximate dS QFT well over arbitrary intervals of global time (so long as they are sufficiently far to the future or past). We then conclude in Section 5.6 with comments on cosmological interpretations of our results and outlook for the future.

## 5.2 Group averaging and perturbative dS gravity

In a perturbative analysis of any quantum theory, one expands both the operators and the quantum states in powers of a small parameter $\epsilon$. The expansion is typically performed about a background classical solution $s_0$, in which case the leading term in any quantum state $|\Psi\rangle$ is generally expected to be a state $|\Psi_1\rangle$ of the linearized theory around $s_0$. However, subtleties arise when the background $s_0$ leaves some of the gauge symmetries unbroken.

The issue can be explained simply by using the Hamiltonian formalism of the classical theory. In this formalism, the phase space is subject to constraints $C$ which generate

[4]While one can also study $dS_{1+1}$ in Jackiw-Teitelboim (JT) gravity, the JT dilaton always breaks the de Sitter isometry group to a smaller (one-dimensional) group. However, constructions analogous to those below could be studied for the case where the remaining gauge group is noncompact.

gauge transformations by taking Poisson Brackets. When $s_0$ leaves a gauge symmetry unbroken, there will be a corresponding constraint $C$ such that all Poisson Brackets $\{C, A\}$ vanish at $s_0$ (regardless of whether $A$ is gauge invariant). This is of course equivalent to requiring all first order variations $\delta C$ to vanish at $s_0$; i.e., $s_0$ is a stationary point of $C$.

As a result, the leading term in the equation of motion $C = 0$ is of *second* (quadratic) order at $s_0$. In particular, when passing from linear to quadratic order in perturbation theory, one encounters this new equation of motion even though it has no analogue in the linear theory. Such new quadratic equations of motion are called *linearization stability constraints*. This terminology refers to the fact that solutions to the linearized theory can be perturbatively corrected at higher orders of perturbation theory *only* if they satisfy such constraints. Solutions of the linearized theory that fail to satisfy such constraints are simply spurious and do not represent linearizations of solutions to the full theory. See e.g. [183, 184, 185, 186, 187] for discussion of such issues in classical general relativity.

A classic example of this phenomenon occurs in Maxwell theory coupled to charged fields on $S^d \times \mathbb{R}$ (where the $\mathbb{R}$ factor is the time direction). The linearized theory will admit general linearized solutions for the charged fields. But since the charge-density is typically quadratic in the charged fields, at quadratic order the charged fields will source the Maxwell field. And since $S^d$ has no boundary, there is no way for electric flux to leave the sphere. As a result, the Maxwell Gauss law requires the total electric charge to vanish; see figure 5.2. It is thus only linearized solutions with vanishing net electric charge that can be linearizations of solutions to the full theory.

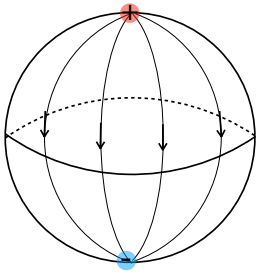

Figure 5.2: A positive charge (red) sources a flux of electric field (arrows) as shown. However, if the charge lives on a sphere (say, at the north pole), the resulting field lines are forced to cross again at least at one other point (at the south pole in the example shown here). The Gauss law then requires the resulting convergence to coincide with the location of a negative charge (blue). As a result, only configurations of charges with zero net charge can consistently source electric fields on $S^d$.

In the Maxwell example above, it is straightforward to impose the linearization stability constraints at the quantum level as well. After constructing the states of the linearized theory, one need only truncate that Hilbert space to the sector with vanishing total charge. Charge conservation then prohibits such states from mixing with the states that have been discarded. Since no new constraints arise at higher orders, we can then proceed to arbitrary orders in perturbation theory without further obstacles.

The gravitational case is qualitatively similar in many ways. Consider in particular gravitational perturbation theory around global $\mathrm{dS}_D$. The $\mathrm{SO}(D,1)$ isometries are unbroken diffeomorphisms and, since the Cauchy surfaces of global dS are compact, all diffeomorphisms are gauge symmetries. The associated $\mathrm{SO}(D,1)$ generators must therefore vanish and, at quadratic order, this simply sets to zero all de Sitter charges of the linearized theory. At the classical level it is then straightforward to select linearized solutions with vanishing charges and to correct them at higher orders.

However, a subtlety arises in the quantum theory. Since $\mathrm{SO}(D,1)$ is non-compact, the spectra of its generators are generally continuous. As a result, in the linearized theory, the only normalizable state with vanishing $\mathrm{SO}(D,1)$ charges is the de Sitter-invariant

vacuum $|0\rangle$. Restricting to this state would then forbid the study of any excitations at all.

Nevertheless, a so-called group-averaging approach to constructing a larger Hilbert space for the perturbative theory was described by Higuchi in [181, 182]. In essence, the idea is to first note that the linearized theory *does* contain states with vanishing charges, though they are non-normalizable[5]. Since states that are annihilated by the de Sitter charges must be invariant under the de Sitter group, we will henceforth refer to these as de Sitter-invariant states. It turns out that one may then usefully renormalize the inner product of the linearized theory to yield a well-defined Hilbert space $\mathcal{H}_{LPG}$ of de Sitter-invariant states satisfying the linearized stability constraints. We will refer to this $\mathcal{H}_{LPG}$ as the Hilbert space of linearized perturbative gravity in the expectation that each state in $\mathcal{H}_{LPG}$ is indeed the linearized description of a state in the full quantum gravity theory.

In particular, we will see that operators of the form (5.5) are densely defined on $\mathcal{H}_{LPG}$. The general theory of the Hilbert space $H_{LPG}$ has been discussed in [173, 188, 189, 190, 191] under a variety of names. It will be reviewed briefly in sections 5.2.1 and 5.2.2 below, after which we analyze special observables of the form (5.5) in section 5.2.3. It is useful to mention that the group averaging construction has also been called the method of coinvariants in [39, 45]. See also [103] for a recent discussion of such constructions in the context of the gravitational path integral.

### 5.2.1 Review of group averaging

It is natural to expand perturbative quantum gravity in powers of $G$. As a result, the first-order theory will consist of linearized gravitons together with a matter quantum

[5] As described in [45], these non-normalizable states may be better thought of as well-defined weights on an appropriate algebra.

field theory on a fixed de Sitter background. As mentioned above, we refer to the Hilbert space of this matter-plus-graviton theory as $\mathcal{H}_{QFT}$. The matter quantum field theory can in principle be strongly coupled, though we will restrict to free theories below for simplicity.

The group averaging construction of [181, 182] can then be described as follows. For a state $\big|\Psi\big] \in \mathcal{H}_{QFT}$, consider the formal integral

$$|\Psi\rangle = \int_{g\in G} dg U(g)\big|\Psi\big], \tag{5.6}$$

where $G$ is the orthochronous de Sitter group $\mathrm{SO}_0(D,1)$, $U(g)$ gives the unitary representation of $G$, and $dg$ is the Haar measure on $G$. Since $G$ is non-compact, the states $|\Psi\rangle$ are not normalizable using the standard inner product on $\mathcal{H}_{QFT}$. Let us therfore introduce a new group-averaged inner product,

$$\langle\Psi_1|\Psi_2\rangle := [\Psi_1|\cdot|\Psi_2\rangle = \int_{g\in G} dg\big[\Psi\big|U(g)\big|\Psi\big], \tag{5.7}$$

which removes one integration over $g$. The inner product (5.7) thus effectively divides the old inner product by the (infinite) volume of the de Sitter group. The Hilbert space $\mathcal{H}_{LPG}$ of de Sitter invariant states (which provide the linearized (L) description of valid perturbative gravity (PG) states) is then defined by choosing a useful linear space of states $V \subset \mathcal{H}_{QFT}$ with finite group-averaged inner products (5.7) and completing the space spanned by their linear combinations (modulo null states).

We note that the expression (5.6) plays only a formal role in this construction and that one may alternately consider (5.7) as a new inner product on the original states $\big|\Psi\big]$. With respect to this new inner product, states of the form $(U(g)-1)\big|\Psi\big]$ are null states for all $g, \big|\Psi\big]$. Using this description of the group-averaging inner product, the above

construction was called the method of coinvariants in [39, 45].

The group-averaging construction is useful when $V \subset \mathcal{H}_{QFT}$ results in a finite and positive semi-definite inner product (5.7). Since (5.7) clearly diverges for a de Sitter-invariant vacuum $\big|0\big]$, our $V$ can only contain states orthogonal to $\big|0\big]$. This is not to say that there can be no well-defined state of quantum gravity associated with $\big|0\big]$, but merely that the inner product on $\big|0\big]$ should not be renormalized. Furthermore, since $\big|0\big]$ is the unique normalizable de Sitter-invariant state in $\mathcal{H}_{QFT}$, any well-defined de Sitter-invariant operator whose domain includes $\big|0\big]$ can only map $\big|0\big]$ to a multiple of itself. Thus such observables cannot mix the state $\big|0\big]$ with states defined from the above domain $V$. As a result, unless one has good reason to introduce additional de Sitter invariant observables, it suffices to treat $\big|0\big]$ separately from all other states; see [192] for general discussion of this issue.

In a theory with well-defined particle number (say, in the sense of being positive frequency with respect to global time), one might thus like to find that (5.7) is both finite and positive definite for a natural space $V$ that is dense in the space of states with $N \geq 1$ particles. As explained in appendix E, the full story is more complicated, and there remain holes in the existing literature associated with light scalar fields and fields with spin. However, at least for gravitons on $dS_{3+1}$ and for scalar fields in any dimension with mass $M > (D-1)/2\ell$, there is strong evidence that the above is essentially correct, though there are three subtleties.

The first subtlety is that, as written, (5.7) is in fact ill-defined for $N = 1$ particle states but, as explained in E, one should nevertheless define it to be zero for such states. This result is natural quantum analogue of the observation that single point-particles in dS always have at least one non-vanishing dS charge and, as a result, that a single particle never satisfies the linearization stability constraints described in the introduction. It would be interesting to understand whether this feature might be related to complications

described in [39] when they attempted to introduce an observer in only one static patch.

The second subtlety is that two-particle states again have divergent group-averaging norm. As described in appendix E, this appears to be associated with the fact that all classical 2-particle configurations with vanishing dS charges continue to leave a non-compact subgroup of $\mathrm{SO}(D,1)$ unbroken and, as a result, well-defined de Sitter-invariant operators again cannot cause 2-particle states to mix with standard Fock states having $N \geq 3$ particles.

Finally, the third subtlety is that, while positivity for $3+1$-dimensional linearized gravitons was checked explicitly in [182], there is not yet a complete proof that the group averaging inner product is positive semi-definite for all states of $N \geq 3$ particles of scalar fields with the masses indicated above. See appendix E for discussion of the current status of this issue.

### 5.2.2 Group averaging with a Reference

Let us now divide our de Sitter QFT into a target system and a reference system. For simplicity we will assume that $\mathcal{H}_{QFT}$ takes the form of a tensor product,

$$\mathcal{H}_{QFT} = \mathcal{H}^{\phi}_{QFT} \otimes \mathcal{H}^{\psi}_{QFT}, \tag{5.8}$$

where $\mathcal{H}^{\psi}_{QFT}$ describes a system to be used as a reference and $\mathcal{H}^{\phi}_{QFT}$ describes the target system whose physics we wish to more actively probe. We will imagine that, before imposing de Sitter invariance, the system induces a definite pure state $\big|\psi_0\big] \in \mathcal{H}^{\psi}_{QFT}$, so that we need only consider states of the full system of the form $\big|\alpha\big] \otimes \big|\psi_0\big] \in \mathcal{H}_{QFT}$ for some $\big|\alpha\big] \in \mathcal{H}^{\phi}_{QFT}$. Group averaging such states produces de Sitter-invariant states of

the form

$$|\alpha; LPG\rangle := \int dg U(g)\big|\alpha\big] \otimes \big|\psi_0\big], \tag{5.9}$$

which then live in the space of allowed states for perturbative gravity (PG) at order $G^0$ (at which the gravitational theory is linear (L)). We will use $\mathcal{H}_{LPG,\psi_0}$ to refer to the Hilbert space defined by states of the form (5.9) using the group-averaging inner product.

We expect to be able to take a limit in which $\big|\psi_0\big]$ serves as a sharp reference within our de Sitter space, and with respect to which at least certain observables can be well-localized. For example, for the right fields, and in the correct limit, $\big|\psi_0\big]$ could describe a very classical planet Earth equipped with all manner of laboratories and marked reference points with respect to which one could classically construct relational gauge-invariant observables (e.g., the average value of the Higgs field in the city of Paris during the opening ceremonies of the 2024 Olympics). We therefore expect that, under the right conditions, we can also construct relational quantum observables which are well-described by local quantum field theory on a fixed de Sitter spacetime.

Before turning to the observables themselves, it is useful to further investigate the Hilbert space structure associated with the states (5.9). The group-averaging inner product of two such states takes the form

$$\langle \beta; LPG| \, |\alpha; LPG\rangle = \int dg \big[\psi_0\big|U(g)\big|\psi_0\big] \big[\beta\big|U(g)\big|\alpha\big]. \tag{5.10}$$

The expression (5.10) is a convolution over the group of a state-dependent factor $\big[\beta\big|U(g)\big|\alpha\big]$ and a factor $\big[\psi_0\big|U(g)\big|\psi_0\big]$ that will remain fixed so long as our reference system is undisturbed. We will refer to the fixed factor $\big[\psi_0\big|U(g)\big|\psi_0\big]$ as the *group averaging kernel*.

If there were a normalizable state $\big|\psi_0\big]$ for which this kernel was a Dirac delta-function, $\big[\psi_0\big|U(g)\big|\psi_0\big] = \delta(g)$, then the inner product (5.10) would reduce precisely to the inner

product on $\mathcal{H}_\phi$, i.e. we would have $\langle \beta, \psi_0 | \, | \alpha, \psi_0 \rangle = \big[\beta \big| \alpha\big]$. While this seems unlikely to be the case for any normalizable state, it is nevertheless true that for *any* state $\big|\psi_0\big]$ with absolutely-convergent group-averaging norm

$$\langle \psi_0 | \psi_0 \rangle := \int dg \big[\psi_0 \big| U(g) \big| \psi_0\big], \tag{5.11}$$

the appearance of this group-averaging kernel in (5.10) will tend to localize the integral over $g$ to a region surrounding the identity. This follows from the fact that, since $U(g)$ is unitary, we must have $\big[\psi_0\big|U(g)\big|\psi_0\big] \leq 1$ with equality only for $U(g) = 1$. Furthermore, if (5.11) converges absolutely, then the kernel will suppress contributions far from the identity.

Of course, this region may be very large for a general state $\big|\psi_0\big]$. But we will study limits in which $\big[\psi_0\big|U(g)\big|\psi_0\big]$ becomes sharply peaked, so that the associated region is small. The inner product (5.10) will then be given by the usual dS QFT inner product on $\mathcal{H}^\phi_{QFT}$ with small corrections associated with the finite width of the peak of $\big[\psi_0\big|U(g)\big|\psi_0\big]$.

We will characterize these corrections more precisely in sections 5.3 and 5.4 for particular choices of reference state $\big|\psi_0\big]$. In particular, we will see there that the associated corrections to correlation functions are not uniformly small across the entire de Sitter space, but that their size depends on the location of the arguments of such correlators in relation to structures defined by $\big|\psi_0\big]$.

Let us now consider the case where $\phi$ and $\psi$ describe independent local quantum fields with no mutual interactions. For the moment, we will still allow both $\phi$ and $\psi$ to have self-interactions. Furthermore, we can in fact allow $\phi$ to denote a collection of mutually-interacting quantum fields, and similarly for $\psi$, so long as the fields of $\phi$ and the fields of $\psi$ do not interact with each other[6].

[6]We expect the inclusion of perturbative interactions between $\phi$ and $\psi$ will be straightforward, but we will not pursue it here. We thus see no obstacle to including linearized gravitons in either $\phi$ or $\psi$.

### 5.2.3 Relational Observables for perturbative dS gravity

Since operators can be built from bra- and ket-states, and since limits where $\big[\psi_0\big|U(g)\big|\psi_0\big]$ is sharply peaked make $\mathcal{H}_{LPG,\psi_0}$ canonically isomorphic to $\mathcal{H}^{\phi}_{QFT}$, we should also expect there to be an algebra of gauge-invariant (i.e., de Sitter-invariant) observables that reduces in this limit to the algebra of local $\phi$-fields. The construction we will use is a direct analogue of our construction (5.9) of quantum states. Given a local field $\hat{\phi}_{QFT}$ that acts on $\mathcal{H}^{\phi}_{QFT}$, for any point $x$ in global dS we simply define the operators

$$\begin{aligned}\hat{\phi}_{LPG}(x) &:= \int \mathrm{d}g\, U(g)\Big(\hat{\phi}_{QFT}(x)\otimes\big|\psi_0\big]\big[\psi_0\big|\Big)U(g^{-1}) \\ &= \int \mathrm{d}g\,\Big(\hat{\phi}_{QFT}(gx)\otimes U(g)\big|\psi_0\big]\big[\psi_0\big|U(g^{-1})\Big)\,, \end{aligned} \tag{5.12}$$

where $gx$ denotes the image of the point $x$ under the de Sitter isometry $g$. Note that, even for a fixed value of $x$, we can use the fact that the Haar measure is invariant under $g\to g_0 g$ to write $U(g_0)\hat{\phi}_{LPG}(x) = \hat{\phi}_{LPG}(x)U(g_0)$. The operators (5.12) are thus de Sitter-invariant and represent observables of the linearized perturbative gravity (LPG) theory for each fixed value of $x$.

As forshadowed in the introduction, this construction makes use of non-local elements both in the integral over the group of de Sitter isometries and also through the explicit use of the global quantum state $\big|\psi_0\big]$. This feature will play a critical role in ensuring that the operators (5.12) are well-defined and, in particular, that they have finite matrix elements between states of the form (5.9). Such matrix elements take the form:

$$\begin{aligned}&\langle\beta; LPG|\,\hat{\phi}_{LPG}(x_1)\hat{\phi}_{LPG}(x_2)\ldots\hat{\phi}_{LPG}(x_n)\,|\alpha; LPG\rangle \\ &= \int \mathrm{d}g_1\,\mathrm{d}g_2\ldots\mathrm{d}g_{n+1}\Big(\big[\psi_0\big|U(g_1)\big|\psi_0\big]\prod_{k=1}^{n}\big[\psi_0\big|U(g_k g_{k+1}^{-1})\big|\psi_0\big]\Big) \\ &\quad\times\big[\beta\big|\hat{\phi}_{QFT}(g_1x_1)\ldots\hat{\phi}_{QFT}(g_nx_n)U(g_{n+1})\big|\alpha\big], \end{aligned} \tag{5.13}$$

where we have used the fact that $dg_{n+1}$ is invariant under $g_{n+1} \to g_{n+1}^{-1}$. Convergence of the integrals in (5.13) is guaranteed by the absolute convergence of (5.11). Again, it is manifest that (5.13) reduces to the $\phi$ correlators of dS QFT in limits where our group-averaging kernel $\big[\psi_0\big|U(g)\big|\psi_0\big]$ approaches $\delta(g)$.

In the particular case where either $\big|\alpha\big]$ or $\big|\beta\big]$ is the de Sitter-invariant $\phi$-vacuum $\big|0;\phi\big]$, the factor of $U(g_{n+1})$ can be dropped from the final line. Since it will be natural to focus on this case below, we define the notation

$$|0\rangle_{LPG} := \int \mathrm{d}g\, U(g)\big(\big|0;\phi\big] \otimes \big|\psi_0\big]\big). \tag{5.14}$$

Thus we may also define

$$\begin{aligned}\hat{\phi}_{LPG}(x_1)\ldots\hat{\phi}_{LPG}(x_n) &:= \langle 0;LPG|\,\hat{\phi}_{LPG}(x_1)\ldots\hat{\phi}_{LPG}(x_n)\,|0;LPG\rangle \\ &= \int \mathrm{d}g_1\,\mathrm{d}g_2\ldots\mathrm{d}g_{n+1}\left(\big[\psi_0\big|U(g_1)\big|\psi_0\big]\prod_{k=1}^{n}\big[\psi_0\big|U(g_k g_{k+1}^{-1})\big|\psi_0\big]\right) \\ &\quad\times\big[0;\phi\big|\hat{\phi}_{QFT}(g_1x_1)\ldots\hat{\phi}_{QFT}(g_nx_n)\big|0;\phi\big].\end{aligned} \tag{5.15}$$

However, we emphasize that the state (5.14) is only vacuum with respect to $\phi$, and that the $\psi$ field is in a group-averaged version of the state $\big|\psi_0\big]$. In particular, the state $|0\rangle_{LPG}$ defined above still contains our reference and is thus *not* the vacuum of the full perturbative gravity theory. It will thus induce non-trivial backreaction at higher orders in $G$.

Since states $\big|\psi_0\big]$ with absolutely-convergent group-averaging norm will define group averaging kernels $\big[\psi_0\big|U(g)\big|\psi_0\big]$ with finite width, choosing some of the points $x_i$ to lie on each other's light-cones will cause (5.15) to differ infinitely from the corresponding correlator in dS QFT. However, this strong difference is clearly associated with very high

energies. It is thus useful to describe the manner in which (5.15) approximates correlators of dS QFT by studying smeared correlators (which are sensitive only to the physics below an energy scale set by the smearing function). For example, in a free theory it suffices to study smeared two-point functions of the form

$$\int dx_1 dx_2 F_1(x_1) F_2(x_2) \hat{\phi}_{LPG}(x_1) \hat{\phi}_{LPG}(x_2) \tag{5.16}$$

for appropriate smearing functions $F_1, F_2$. We will focus below on the case where $F_1, F_2$ are members of a family of functions $F_y(x)$ that are well-approximated by Gaussian functions of both the global time $t$ and of the location on the sphere $S^d$ at fixed $t$ that are peaked at the point $y$ in global dS. We will take the width of these Gaussians in both global time $t$ and in location on the sphere to be identical as measured in terms of proper time and distance. For example, when $y$ lies at the north pole of the sphere $S^d$ at some time $t_y$, and for an appropriate normalization factor $N$ we may take

$$F_y(x) = N e^{-\frac{(t-t_y)^2}{2\sigma^2}} e^{\frac{[\cos(\theta)-1]}{\cosh^2(t/\ell)\,\sigma^2}} \approx N e^{-\frac{1}{2\sigma^2}\left[(t-t_y)^2 + \frac{\ell^2\theta^2}{\cosh^2(t/\ell)}\right]}, \tag{5.17}$$

where $t, \theta$ are the global coordinates of the point $x$ with $\theta$ being the polar angle on $S^d$, and where the final approximation holds for $\theta \ll 1$. We note for future reference that the final exponent on the right-hand-side defines an effective flat Euclidean-signature metric with line element

$$ds_E^2 := dt^2 + \frac{d\theta^2}{\cosh^2(t/\ell)} + \frac{\ell^2\theta^2}{\cosh^2(t/\ell)} d\Omega_{d-1}, \tag{5.18}$$

so that

$$F_y(x) \approx e^{-\frac{|x-y|_E^2}{2\sigma^2}}, \tag{5.19}$$

where $|x-y|_E$ is the Euclidean distance between $x$ and $y$ defined by[7] (5.18).

[7]The astute reader will not that, if we wish to define $F_y$ for general $y$ away from the north pole by

We also note that the effect of convolving smeared dS QFT correlators with our group averaging kernel will depend on the extent to which $F_y(x)$ differs from $F_y(gx)$, and thus the extent to which the exponent on the right-hand-side of (5.17) differs between $x$ and $gx$. Since the triangle inequality bounds the change in $|x-y|_E$ in terms of $|gx-x|_E$, we see that for $|x-y|_E \lesssim \sigma$ the change in the smearing function $F_y$ is small when $|gx-x|_E \ll \sigma$. The question of whether this small change in the smearing function can cause a significant change in smeared correlators can be studied by using a standard partition of unity to divide the domain of integration into subregions based on whether subsets of the $x_i$ are close together or far apart. For example, when studying the smeared two-point function (5.16), we divide the domain of integration into a region with (Lorentz-signature de Sitter distance) $|x_1 - x_2| \lesssim \epsilon$ and a region with $|x_1 - x_2| \gtrsim \epsilon$. In the former region, the integral is well-approximated by a smeared Minkowski-space correlator. Since the Wightman axioms require Minkowski-space correlators to be tempered distributions [193], and since tempered distributions are continuous linear functionals on the space of test functions, the integral over this region will change by only a small amount under a small change in the smearing functions $F_y$. Here it is important to that we consider Wightman correlators rather than their time-ordered counterparts. Similar continuity follows for the integral over the region $|x_1 - x_2| \gtrsim \epsilon$ since the correlator is bounded in that region and the smearing function changes by a function of integrable norm; (i.e., by a function in $L^1(dS)$)[8]. As a result, when $|gx-x|_E \ll \sigma$ for all $g$ within the peak of the group-averaging kernel, a given set of smeared dS QFT correlators will be

rotating (5.17), then the analogue of (5.18) in fact depends on the location of $y$ on the sphere $S^d$. While this fact is not explicitly indicated by the notation $|x-y|_E$, it will not play an important role in our analysis.

[8]For free fields on dS, one may alternatively proceed by writing the field operator as an expansion in global dS mode functions that solve the equation of motion. Integrating any given mode against a smooth function of time yields a result that must vanish faster than any polynomial as the angular momentum of the mode becomes large. It thus follows that the relevant mode sums converge absolutely. The desired result then follows from the fact that the above convolution makes negligible change in the high-frequency components of $F_y$.

well-approximated by the correspondingly smeared versions of the perturbative gravity correlators (5.15).

## 5.3 Reference states in $dS_{1+1}$

The above section described our general framework for using perturbative gravity to approximate the algebra of local observables in dS QFT. There we saw that a central role is played by the group averaging kernel $\big[\psi_0\big|U(g)\big|\psi_0\big]$, and that comparison of the perturbative gravity and dS QFT correlators is controlled by i) the width of the peak of $\big[\psi_0\big|U(g)\big|\psi_0\big]$ about the identity and ii) by the effect of those isometries $g$ that lie within the above peak on the points $x$ at which we wish to evaluate such correlators.

We thus now turn to a detailed investigation of this kernel for interesting classes of states. In this section we consider the simple-but-illustrative case of $1+1$ global de Sitter, taking the field $\psi$ to be a collection of free scalar fields with mass $M > 1/2\ell$ (so that the one-particle states lie in principal series representations of $\mathrm{SO}(2,1)$ [194, 195]). Thinking of $\psi$ as a *collection* of fields allows us to choose each particle to be associated with a distinct scalar field. We may thus treat the $\psi$-particles as distinguishable, which provides a slight simplification of the calculations. While Einstein-Hilbert gravity is trivial for the case $D = 2$, our goal is to use $D = 2$ as a toy model of higher dimensional physics. We thus simply analytically continue certain formulae from higher dimensions to $D = 2$ in order to discuss versions of $D = 2$ linerization stability constraints (which are again solved by group averaging), $D = 2$ perturbative gravity operators, and a (dimensionless) $D = 2$ Newton constant $G$. However, we will postpone any more involved discussions of back-reaction to section 5.4 (where the higher-dimensional case will be addressed).

### 5.3.1 Preliminaries

Studying our kernel requires an understanding of how the de Sitter isometries act on our states. It is useful to begin by recalling that, in global coordinates, the metric on $\mathrm{dS}_{1+1}$ takes the form

$$ds^2 = -dt^2 + \ell^2 \cosh^2 t d\theta^2, \tag{5.20}$$

where $\ell$ is the de Sitter scale. It will sometimes also be useful to write the metric in conformal coordinates $T, \theta$, where $\cosh(t/\ell) = \sec T$ with $T \in [-\pi/2, \pi/2]$, so that the line element becomes

$$ds^2 = \frac{\ell^2}{\cos^2 T}(-dT^2 + d\theta^2). \tag{5.21}$$

In these coordinates, the generators of the isometry group are

$$B_1 \equiv \xi_2 \equiv \cos T \cos\theta \partial_T - \sin T \sin\theta \partial_\theta, \tag{5.22}$$

$$B_2 \equiv \xi_1 \equiv \cos T \sin\theta \partial_T + \sin T \cos\theta \partial_\theta, \tag{5.23}$$

$$R \equiv \xi_\theta \equiv \theta, \tag{5.24}$$

where the notation $B_1$, $B_2$, $R$ classifies the generators of $\mathrm{SO}(2,1)$ according to their action as either boosts or rotations when one thinks of $\mathrm{SO}(2,1)$ as Lorentz transformations on 2+1 Minkowski space. The actions of these Killing fields on de Sitter space is shown in Figure 5.3 below.

The action of the generators on our states can be understood by defining

$$B_\pm \equiv B_2 \pm iB_1. \quad \text{Hence } B_1 = \frac{1}{2i}(B_+ - B_-), \text{ and } B_2 = \frac{1}{2}(B_+ + B_-). \tag{5.25}$$

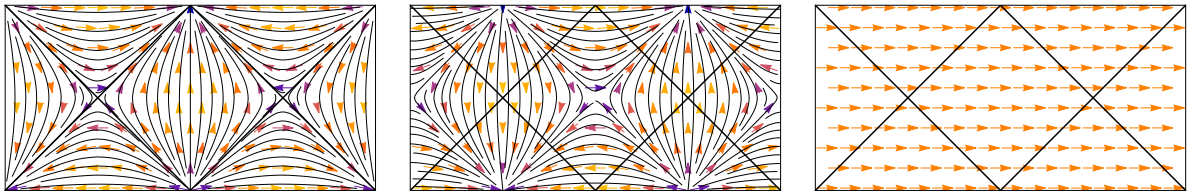

Figure 5.3: The Killing vector fields $B_1$ (left), $B_2$ (center), and $R$ (right), in $\mathrm{dS}_{1+1}$. The figures are drawn using conformal coordinates $T, \theta$ with $-\pi < \theta < \pi$, $-\pi/2 < T < \pi/2$.

We then have the commutation relations [196].

$$[R, B_+] = B_+, \quad [R, B_-] = -B_-, \quad [B_-, B_+] = 2R. \tag{5.26}$$

The Casimir operator $\mathcal{C}_2$ is given by

$$\mathcal{C}_2 = B_+B_- + R(1-R) = B_1^2 + B_2^2 - R^2. \tag{5.27}$$

We now let $|m]$ be the 1-particle eigenstate of the $R$ operator with $R|m] = m|m]$. In particular, we may take it to be the state created from the $\psi$-vacuum by acting with the creation operator associated with the usual mode of the scalar field $\psi$ having angular quantum number $m$. For one-particle states, the Klein-Gordon equation gives $\mathcal{C}_2|m] = M^2\ell^2|m]$, where $M$ is the mass of the scalar field and where we consider only the case $M > 1/2\ell$. It will be useful to introduce the parameter $\Delta$ through

$$\Delta(1-\Delta) = M^2\ell^2. \tag{5.28}$$

By convention, we take the imaginary part of $\Delta$ to be positive for $M > 1/2\ell$, so that we

have $\Delta = \frac{1}{2} + i\sqrt{M^2\ell^2 - 1/4}$. We may thus choose the phases of the states $|m]$ to satisfy

$$B_-|m] = (m-\Delta)|m-1], \quad B_+|m] = (m+\Delta)|m+1], \tag{5.29}$$

$$B_1|m] = \frac{1}{2i}\Big[(m+\Delta)|m+1] - (m-\Delta)|m-1]\Big], \tag{5.30}$$

$$B_2|m] = \frac{1}{2}\Big[(m+\Delta)|m+1] + (m-\Delta)|m-1]\Big]. \tag{5.31}$$

Below, we will also use the notation

$$\mu = \mathrm{Im}\Delta = \sqrt{M^2\ell^2 - 1/4}. \tag{5.32}$$

Let us now conclude our discussion of preliminaries by reviewing the results of [197] describing the asymptotics of the kernel $\big[\psi_0\big|U(g)\big|\psi_0\big]$ at large $g$. For this purpose we will in fact consider scalar fields of any mass $M > 0$, where we take $\Delta$ to be defined by (5.28) with the convention that $\Delta < 1/2$ for $M < 1/2\ell$. We will take $\big|\psi_0\big]$ to be an $N$-particle state and, for each particle, we take the state to be a finite linear combination of the above states $|m]$.

The results of [197] were expressed by writing a general $g \in \mathrm{SO}_0(2,1)$ in the form $g = e^{i\theta_1 R}e^{i\lambda B_1}e^{i\theta_2 R}$. Since $\theta_1, \theta_2$ range over a compact space, and since the resulting rotations simply map any given angular momentum mode to a superposition of other such modes, the large $g$ behavior is controlled by the behavior of $e^{i\lambda B_1}$ at large $\lambda$. And since de Sitter isometries act diagonally on multi-particle states, our group averaging kernel will contain factors of $[m|e^{i\lambda B_1}|n]$ for each particle, where $n$ again denotes an angular quantum number. At large $\lambda$, the asymptotic behavior of this 1-particle matrix element was shown to be

$$\Big|[m|e^{i\lambda B_1}|\vec{n}]\Big| \sim e^{-\lambda \mathrm{Re}\,\Delta} \tag{5.33}$$

so that the group averaging kernel decays exponentially with large boost parameter. Since the relevant integration measure for $\mathrm{dS}_{1+1}$ is $\sinh\lambda\, d\lambda$ (see again [197]), we see that (5.11) converges absolutely for $N\mathrm{Re}\,\Delta > 1$. In particular, for $M > 1/2\ell$ we require $N \geq 3$. As discussed in [197], this is also the case for scalar fields of mass $M > d/2\ell$ in $dS_{d+1}$ for any $d \in \mathbb{Z}^+$.

### 5.3.2 A pair of reference particles on opposite sides of dS

Having seen that our kernel strongly suppresses contributions from large $g$ for $N \geq 3$ particles with $M > 1/2\ell$, we can now turn our attention to the region near the identity ($g \sim 1$) at which the group-averaging kernel is peaked. Though one can certainly engineer special cases where there are also important contributions from outside this peak, having a second peak of height near 1 clearly requires fine tuning. Furthermore, if the height of another peak is not near 1, a different form of fine tuning is required if its contributions are to be comparable to or greater than those of the unit-height central peak. Since we do not expect this to occur for generic $\left|\psi_0\right]$, we will defer consideration of this possibility until introducing the particular states we wish to study. At that point, we will display numerical results supporting the above expectations.

For the moment, however, we will simply compute the width of the central peak for interesting classes of states by writing $U(g) = e^{i(\lambda_1 B_1 + \lambda_2 B_2 + \theta R)}$ and expanding to second order in $\lambda_1, \lambda_2, \theta$. We will in fact focus on the simple case of 2-particle states (with $M > 1/2\ell$). As noted above, to control contributions from large $g$ the full state $\left|\psi_0\right]$ must contain a third particle. But we are free to choose the state of the third particle to have a much broader peak near the identity (perhaps engineered by smearing an arbitrary state over a large-but-finite range of de Sitter transformations), so that the width of the kernel is set by just the first two particles.

At the classical level, a pair of identical-mass particles can satisfy the linearization stability constraints in $dS_{1+1}$ only if their de Sitter charges cancel exactly. This requires the geodesics followed by the two particles to be related by a rotation through an angle $\pi$ for some rotation generator. We will take this to be the rotation $e^{i\pi R}$. We will thus choose a quantum state $\big|\psi_+\big]$ for the first particle and then simply take the state of the second particle to be $\big|\psi_-\big] = e^{i\pi R}\big|\psi_+\big]$, with the full 2-particle reference state being the tensor product

$$\big|\psi_0\big] = \big|\psi_+\big] \otimes \big|\psi_-\big]. \tag{5.34}$$

Rather than attempt a general classification of the possible such states $\big|\psi_+\big]$, we will confine our investigation to a simple choice that facilitates explicit calculations. We take the first particle to be localized around $(T, \theta) = (0, 0)$, so that the other is then localized around $(0, \pi)$. In particular, we take $\big|\psi_\pm\big]$ to be of the form

$$\big|\psi_\pm\big] = \frac{1}{\sqrt{2j_\# + 1}} \sum_{m=-j_\#}^{j_\#} (\pm 1)^m |m] \tag{5.35}$$

for some cutoff $j_\#$, where the coefficients $(\pm 1)^m$ are found by expanding Dirac delta-functions $\delta(\theta)$ and $\delta(\theta - \pi)$ in terms of rotational harmonics $Y_m(\theta) = \frac{1}{\sqrt{2\pi}} e^{-im\theta}$. This is a convenient choice, since Equations (5.29)-(5.31) give the action of all generators on these eigenstates. As $j_\# \to \infty$, the particles become perfectly localized at the points $\theta = 0, \pi$ at time $t = 0$.

Since the magnitude of our kernel is greatest at the identity, we can study the width of the peak by expanding $U(g)$ to quadratic order in $\lambda_1, \lambda_2$ and $\theta$. To this order, the kernel $\big[\psi_0\big|U(g)\big|\psi_0\big]$ is then determined by the expectation values of $B_1, B_2, R$ and the expectation value of symmetrized products of pairs of generators. However, many of these moments vanish even in the state $\big|\psi_+\big]$ since $\big|\psi_+\big]$ is invariant under $\theta \to -\theta$ (which as

shown in figure 5.3 maps $B_1, B_2, R$ to $B_1, -B_2, -R$). Using $[X]$ to denote the expectation value of an observable $X$ in the state $\big|\psi_+\big]$ we thus find

$$[B_2] = [R] = [B_1B_2 + B_2B_1] = [RB_1 + B_1R] = 0, \tag{5.36}$$

so that the only non-vanishing moments in $\big|\psi_+\big]$ at this order are $[B_1]$, $[R^2]$, $[B_2^2]$, $[RB_2 + B_2R]$, and $[B_1^2]$. Furthermore, since $\big|\psi_0\big]$ is invariant under the rotation $\theta \to \theta + \pi$ (which as shown in figure 5.3 maps $B_1, B_2, R$ to $-B_1, -B_2, R$), the contributions to $\big[\psi_0\big|RB_2 + B_2R\big|\psi_0\big]$ and $\big[\psi_0\big|B_1\big|\psi_0\big]$ from $\big|\psi_\pm\big]$ must cancel against each other. Direct computation of the remaining moments at this order then yields

$$\begin{aligned}\big[\psi_0\big|U(g)\big|\psi_0\big] =& \big[\psi_+\big|U(g)\big|\psi_+\big]\big[\psi_-\big|U(g)\big|\psi_-\big] \\ =& 1 - \lambda_1^2\left([B_1^2] - [B_1]^2\right) - \lambda_2^2[B_2^2] - \theta^2[R^2] + O([g-1]^3) \\ =& 1 - \frac{1}{2}\lambda_1^2 j_\# \left(1 + \frac{4\mu^2}{(2j_\#+1)^2}\right) - \lambda_2^2 \frac{8{j_\#}^3 + 4j_\# + 3 + 12\mu^2}{12(2j_\#+1)} \\ & - \frac{1}{3}\theta^2 j_\#(j_\#+1) + O([g-1]^3),\end{aligned} \tag{5.37}$$

where $\mu$ was defined in (5.32). Let us therefore introduce the parameters

$$\chi_1 = j_\# \left(1 + \frac{4\mu^2}{(2j_\#+1)^2}\right), \quad \chi_2 = \frac{8{j_\#}^3 + 4j_\# + 3 + 12\mu^2}{6(2j_\#+1)}, \quad \chi_\theta = \frac{2}{3}j_\#(j_\#+1), \tag{5.38}$$

in order to write the group averaging kernel as an approximate Gaussian

$$\big[\psi_0\big|U(g)\big|\psi_0\big] \approx e^{-\chi_1\lambda_1^2/2} e^{-\chi_2\lambda_2^2/2} e^{-\chi_\theta\theta^2/2}, \tag{5.39}$$

where we emphasize that $\chi_i \geq 0$ for all $i \in \{1, 2, \theta\}$. The widths of the peak in the various directions are then proportional to $\chi_i^{-1/2}$ and, in the $\chi_i \to \infty$ limit, the Gaussians

become proportional[9] to a delta-function that sets $\lambda_i = 0$ for all $i$. In this limit, the inner product between two physical states reduces to the standard QFT inner product without additional smearing.

However, the large $\chi_i$ limit requires $j_\#$ and/or $\mu$ to become large. In the presence of dynamical gravity, either option would induce a large gravitational backreaction. Hence the $\chi_i$ must remain bounded if we wish to keep such backreaction is small. We will characterize this backreaction more precisely in section 5.3.2 below.

### Characterizing backreaction

In order to estimate the bounds imposed on the $\chi_i$ associated with the restriction to small backreaction, we will need to say more about how this backreaction will be measured. Gravitational backreaction on $(d+1)$-dimensional de Sitter space is generally highly non-uniform, so that for any classical perturbation of dS one can find *some* sense in which the backreaction is large. This is perhaps most simply illustrated by making use of the Gao-Wald theorem [198], showing that any perturbation satisfying the null energy condition forces the past (or future) of any timelike geodesic to contain a complete Cauchy surface. There is thus a sense in which applying a large boost to any spherical cross-section of the perturbed de Sitter space must give a Cauchy surface of vanishingly small total volume. This is in sharp contrast to the case of unperturbed dS, where applying any dS isometry to the $S^d$ at $t = 0$ of course exactly preserves its finite volume.

We will choose to measure the backreaction near the round $S^d$ that passes through the spacetime points at which our $\psi$ particles are well-localized; i.e., the $S^d$ at $t = 0$ with the coordinates and states defined as above. As discussed in [102], a reasonable measure

[9]Since we have chosen $\big|\psi_0\big]$ to be normalized, we will always find $\big[\psi_0\big|U(1)\big|\psi_0\big] = 1$. So, as written, the limit $\chi_i \to \infty$ gives a delta-function with a vanishing coefficient. However, for the same reason, the norm $\langle \alpha; LPG|\alpha; LPG\rangle$ also vanishes in this limit for any normalized $\big|\alpha\big] \in \mathcal{H}^\phi_{QFT}$. Obtaining normalized states $|\alpha; LPG\rangle$ thus requires taking $\big[\alpha\big|\alpha\big]$ to scale as $\sqrt{\chi_1\chi_2\chi_\theta}$. Combining this factor with the Gaussian (5.39) yields the desired delta-function.

of the backreaction in this region is the total flux $F$ of energy through this $S^d$, where

$$F = \int_{t=0} \sqrt{h} T_{ab} n^a n^b \tag{5.40}$$

in terms of the QFT stress tensor $T_{ab}$, the unit normal $n^a$ to the surface $t = 0$, and the volume element $h$ of the induced metric on this surface. If we wish to keep the level of backreaction on the geometry below some fixed cut-off, then in terms of the bulk Newton constant $G$, the maximal allowed value of $F$ will of course scale as $1/G$ in the limit $G \to 0$. While Einstein-Hilbert gravity is not dynamical in 1+1 dimensions, we can nevertheless use our investigation of $\mathrm{dS}_{1+1}$ as a toy model of the higher-dimensional case by introducing a (dimensionless) parameter $G$ and imposing the restriction $F \lesssim 1/G\ell$.

To understand the constraint this imposes on our $\chi_i$, we will need to estimate the contributions to $F$ arising from the mass and angular momentum of our $\psi$-particles. This is straightforward due to the fact that the time derivative of the metric vanishes at $t = 0$. As a result, the local notion of positive-frequency mode near $t = 0$ associated with the standard definition of particles in global de Sitter coincides with the notion of positive frequency for the static cylinder metric

$$ds^2 = -dt^2 + \ell^2 d\theta^2. \tag{5.41}$$

Our $F$ thus coincides with what one would call the energy $E$ on the static cylinder (5.41) when computed in terms of the angular momentum $m$. It is thus clear that, If both particles were in modes having angular momentum precisely $m$, we would find

$$F = 2\sqrt{M^2 + m^2/\ell^2}. \tag{5.42}$$

In order to limit backreaction, we must thus take the mass parameter $\mu$ and the maximum

angular momentum $j_\#$ to satisfy $M\ell \ll 1/G$ and $j_\# \ll 1/G$ as $G \to 0$.

Let us first we examine the ultrarelativistic limit ($j_\# \gg \mu$, though with $1/G \gg j_\#$). The results (5.38) then simplify significantly to yield

$$\chi_1 = j_\# + \mathcal{O}(1), \quad \chi_2 = \frac{2}{3}{j_\#}^2 + \mathcal{O}(j_\#), \quad \chi_\theta = \frac{2}{3}{j_\#}^2 + \mathcal{O}(j_\#). \tag{5.43}$$

We see that the dependence on $\mu$ disappears at leading order in $j_\#/\mu$.

As described in section 5.2.3 the effect of group averaging on correlation functions smeared with the global coordinate near-Gaussians $F_y$ of (5.17) will be small when the smearing is confined to de Sitter isometries $g$ such that

$$|gx - x|_E \ll \sigma, \tag{5.44}$$

where $|x_1 - x_2|_E$ is the flat Euclidean distance defined by (5.18) and we consider all $x$ located within the peak of each near-Gaussian $F_y$. Since the Gaussian (5.39) gives significant weight only to group elements with $\lambda_i \lesssim \chi_i^{-1/2}$, for large-but-finite $\chi_i$ the condition (5.44) is equivalent to

$$\chi_i^{-1/2}|\xi_i|_E \ll \sigma, \tag{5.45}$$

where $|\xi_i|_E$ is the Euclidean norm of the appropriate vector field from (5.22)-(5.24). In particular, we have

$$|\xi_1|_E^2/\ell^2 = \cos^2\theta + \sinh^2(t/\ell)\sin^2\theta \tag{5.46}$$

$$|\xi_2|_E^2/\ell^2 = \sin^2\theta + \sinh^2(t/\ell)\cos^2\theta \tag{5.47}$$

$$|\xi_\theta|_E^2/\ell^2 = \cosh^2(t/\ell). \tag{5.48}$$

In regions of spacetime where any of the bounds (5.45) are exceeded, the spacetime resolution of the observables $\hat{\phi}_{LPG}$ is low, and the dS QFT approximation to perturbative gravity breaks down even for correlators smeared with the functions (5.17). The corresponding cutoff contours (at which $|\xi_i|_E^2 \sim \chi_i \sigma^2$) are shown in Figure 5.4 for specific values of $\sigma$ and $j_\#$. At sufficient depth within the region between these contours, dS QFT correlators smeared with the function (5.17) will be well-approximated by correspondingly-smeared perturbative gravity correlators.

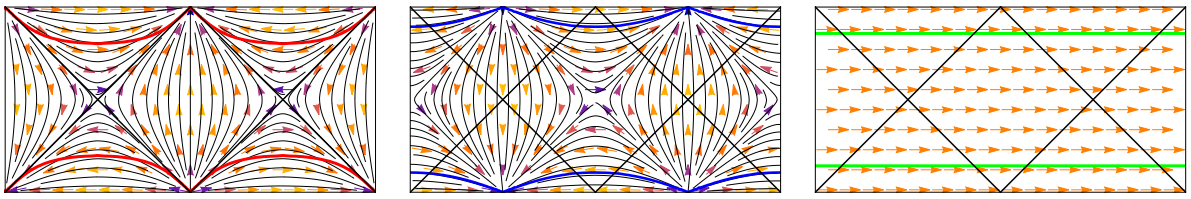

(a) The KVFs and cutoff contours for $B_1$ (left), $B_2$ (center), and $R$ (right) are drawn using conformal coordinates $(T, \theta)$ for $dS_{1+1}$.

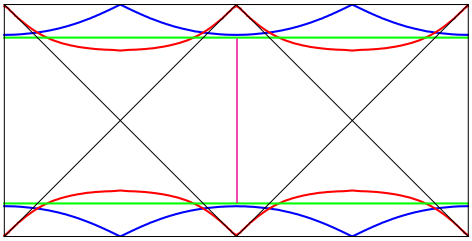

(b) The above cutoff contours are displayed on together on a single conformal diagram. We also show the part of the timelike geodesic at $\theta = 0$ (pink vertical line) that is consistent with all cutoffs.

Figure 5.4: Cutoff surfaces $|\xi_i| = \chi_i \sigma^2$ are shown for the ultrarelativistic limit of the reference state given by (5.34) and (5.35). For illustration purposes we have used the values $2\sigma^2 = 1$ and $j_\# = 4$. At sufficient depth within these cutoffs, our perturbative gravity correlators provide good approximations to corresponding dS QFT correlators.

Note that at large $j_\#$ we have $\chi_1 \ll \chi_2, \chi_\theta$. As a result, consulting (5.46) and taking $t$ large as well, we see that over most of the spacetime the large $j_\#$ cutoff will be set by

$$|t/\ell| \sim \frac{1}{2} \ln j_\# + \ln \frac{\sigma}{\ell \sin \theta}. \tag{5.49}$$

However, inside the static patch around either $\theta = 0$ or $\theta = \pi$, the Euclidean norm of $\xi_1$ always satisfies $|\xi_1|_E^2 \leq 2$. Thus, inside such static patches, the cutoff is instead set by $B_2$ or $R$, both of which give

$$|t/\ell| \sim \ln j_\# + \ln \frac{\sigma}{\ell}. \tag{5.50}$$

So, for $j_\# \sim 1/G$, we have a good approximation to dS QFT only for global times $|t/\ell| \lesssim \ln G^{-1} + \mathcal{O}(1)$, with the actual cutoff being twice as large inside our static patches as it is at generic points outside. In particular, the spacetime volume of the region where our approximation is good is of order $(1/G)$.

We can now return to (5.38) and consider other cases with $\mu\, j_\# \lesssim 1/G$. So long as $\mu$ and $j_\#$ are both in fact of order $1/G$, we see that the leading behavior of both $\chi_2$ and $R$ is always independent of $\mu$ in the limit $G \to 0$, and that it thus agrees with our ultrarelativistic analysis above. It is only $\chi_1$ that depends on the ratio $\mu/j_\#$ at this order. We see that $\chi_1$ is in fact largest in the non-relativistic limit $\mu \gg j_\#$. However, if we wish to make $\mu/j_\#$ parametrically large as a power of $1/G$, then we must take $j_\#$ to scale as a power $1/G^\alpha$ with $\alpha < 1$, so that $\chi_\theta$ is no longer of order $1/G^2$. In fact, analyzing (5.38) shows that if we wish to make all $\chi_i$ scale with the same power of $1/G$, we should take $\mu \sim 1/G$ and $j_\# \sim 1/G^{2/3}$ so that $\chi_i \sim 1/G^{4/3}$. In any such case, however, the cutoffs on global time will be logarithmic in $G$. Adjusting the scalings of $\mu$ and $j_\#$ serves only to alter the coefficient of $\ln G^{-1}$, though we see that it does so differently inside the static patch than it does outside.

### 5.3.3 Adding more reference particles

For the above reference state, we found that smeared dS QFT correlators are well-approximated by our smeared perturbative gravity correlators only in a region of de Sitter space spanning global times of order $\ln G^{-1}$. It is thus interesting to explore whether

this region can be enlarged by considering a more complicated reference state. We are particularly motivated by a desire to understand whether the region can be enlarged within a natural static patch of dS, perhaps at the expense of shrinking the allowed region outside. In this section, we investigate the effect of adding additional reference particles localized at points along the $\theta = 0$ and $\theta = \pi$ geodesics.

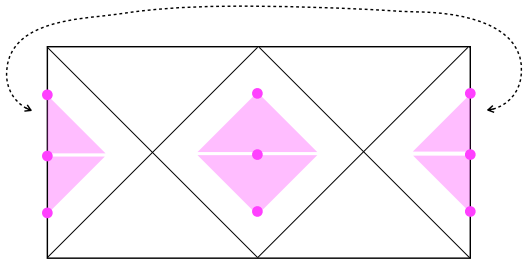

Figure 5.5: Events at which each particle localizes (dots) are shown together with the light cones of these points.

As before, it will be useful to keep the full reference state $\big|\psi_0\big]$ properly 'balanced' in the sense that it has vanishing expectation values of $B_1, B_2, R$ to avoid giving $\big|\psi_0\big]$ de Sitter charges that are parametrically larger than those of the $\phi$-system (as that would then require group averaging to nearly annihilate the resulting state in order to extract a state in which the total de Sitter charges vanish).

We will consider states of the form $\big|\psi_0\big] = |\psi_+^3] \otimes |\psi_-^3]$ with $|\psi_-^3] = e^{i\pi R}|\psi_+^3]$, but where $|\psi_+^3]$ now contains three particles that become well localized along the geodesic $\theta = 0$ at times $-t_\#$, 0, and $t_\#$. In particular, we take

$$|\psi_\pm^3] = \left(e^{-it_\# B_1/\ell}\big|\psi_\pm\big]\right) \otimes \big|\psi_\pm\big] \otimes \left(e^{it_\# B_1/\ell}\big|\psi_\pm\big]\right), \tag{5.51}$$

where $\big|\psi_+\big]$ is again given by (5.35). Thinking of $B_1$ as the static patch Hamiltonian, we see that moments of $B_1, B_2, R$ in the various one-particle states will be given by moments of static-patch time-translations of $B_1, B_2, R$ in $\big|\psi_\pm\big]$. It will thus be useful to compute

expectation values like

$$\big[\psi_\pm\big|e^{iB_1 t_\#} A e^{-iB_1 t_\#}\big|\psi_\pm\big], \tag{5.52}$$

where $A$ is a linear or quadratic expression in $B_1, B_2, R$. For $A = B_1$ or $A = B_1^2$, the time translation has no effect and (5.52) reduces to matrix elements calculated previously. For $B_2$ and $R$, it is useful to define operators $L_\pm = R \pm B_2$ corresponding to lightlike (null) rotations which have commutation relations

$$[L_\pm, B_1] = \mp i L_\pm, \quad [L_+, L_-] = -2iB_1. \tag{5.53}$$

As a result, under a time translation, these operators satisfy $e^{iB_1 t_\#/\ell} L_\pm e^{-iB_1 t_\#/\ell} = L_\pm e^{\mp t_\#/\ell}$, from which we obtain the time translations of $R$ and $B_2$:

$$e^{iB_1 t_\#/\ell} R e^{-iB_1 t_\#/\ell} = R\cosh(t_\#/\ell) - B_2 \sinh(t_\#/\ell), \tag{5.54}$$

$$e^{iB_1 t_\#/\ell} B_2 e^{-iB_1 t_\#/\ell} = B_2\cosh(t_\#/\ell) - R \sinh(t_\#/\ell). \tag{5.55}$$

We can now use the above results to compute the group averaging kernel. Since our new $\big|\psi_0\big]$ still enjoys the symmetries discussed near (5.36), the moments listed in (5.36) once again vanish. It thus remains only to compute $[B_1^2]$, $[B_2^2]$, and $[R^2]$. These moments receive contributions from the corresponding moments of each 1-particle state. The moment $[B_1^2]$ also receives contributions from cross terms between various pairs of particles, associated with the fact that $\big[\psi_+\big|B_1\big|\psi_+\big]$ is non-zero in all one-particle states. Other cross terms vanish since $\big[\psi_+\big|B_2\big|\psi_+\big] = \big[\psi_+\big|R\big|\psi_+\big] = 0$. The final result for our

kernel is thus

$$\begin{aligned}[\psi_0^3|U(g)|\psi_0^3] =& 1 + 3\lambda_1^2([B_1]^2 - [B_1^2]) - \lambda_2^2\bigg([B_2^2](1 + 2\cosh^2(t_\#/\ell)) + 2[R^2]\sinh^2(t_\#/\ell)\bigg) \\ &- \theta^2\bigg([R^2](1 + 2\cosh^2(t_\#/\ell)) + 2[B_2^2]\sinh^2(t_\#/\ell)\bigg) + O([g-1]^3) \\ =& 1 - \lambda_1^2\tilde{\chi}_1/2 - \lambda_2^2\tilde{\chi}_2/2 - \theta^2\tilde{\chi}_\theta^2/2 + O([g-1]^3),\end{aligned} \tag{5.56}$$

where the coefficients $\tilde{\chi}$ are

$$\tilde{\chi}_1 = 3j_\#\left(1 + \frac{4\mu^2}{(2j_\#+1)^2}\right), \tag{5.57}$$

$$\tilde{\chi}_2 = \frac{8{j_\#}^3 + 4j_\# + 3 + 12\mu^2}{6(2j_\#+1)}(1 + 2\cosh^2(t_\#/\ell)) + \frac{4}{3}j_\#(j_\#+1)\sinh^2(t_\#/\ell), \tag{5.58}$$

$$\tilde{\chi}_\theta = \frac{2}{3}j_\#(j_\#+1)(1 + 2\cosh^2(t_\#/\ell)) + \frac{8{j_\#}^3 + 4j_\# + 3 + 12\mu^2}{3(2j_\#+1)}\sinh^2(t_\#/\ell). \tag{5.59}$$

As in the two particle case, the QFT approximation holds exactly in the limit $\tilde{\chi} \to \infty$. The coefficients $\tilde{\chi}$ still grow with increasing $j_\#$ and $\mu$, but now they also grow with increasing $t_\#$.

Let us thus investigate how large we can take $t_\#$ while keeping the backreaction small as measured by (5.40); i.e., for $F \lesssim 1/G$. Recall that $F$ gives the total energy $E$ that the state would have if it were placed in a static cylinder spacetime of radius $\ell$ (keeping the state unchanged in the Fock basis defined by angular momentum modes). The particles at $t = 0$ will contribute to $F$ according to (5.40) as they did before. However, the contributions of the time translated particles are easiest to study by evolving the particles from $t = \pm t_\#$ to $t = 0$.

For the particles that localize at $\theta = 0$, it is convenient to perform this evolution using the description provided by the static patch centered at $\theta = 0$. The time translation from

$t = 0$ to $t = \pm t_\#$ is then trivial but, as we evolve them back to $t = 0$, the particles move to higher energies as they fall away from $\theta = 0$ toward the static patch horizon.

Let us first consider the limit $j_\# \gg \mu$ so that the particles are relativistic, and so travel along null rays. Such particles rapidly approach the de Sitter horizon and then blueshift exponentially with respect to the vector field $n^a$ in (5.42). We thus find that the total flux of energy through $t = 0$ is

$$F = (2 + 4\cosh(t_\#/\ell))\sqrt{{j_\#}^2 + \mu^2} \sim 2 j_\# e^{t_\#/\ell}, \tag{5.60}$$

where the final right-hand-side gives the leading behavior at large $j_\#$ and $t_\#$.

At leading order in $1/j_\#$ and $1/t_\#$ we also find

$$\tilde{\chi}_1 \sim \frac{3}{2} j_\#, \quad \tilde{\chi}_2 \sim \frac{1}{3} {j_\#}^2 e^{2t_\#/\ell}, \quad \tilde{\chi}_\theta \sim \frac{1}{3} {j_\#}^2 e^{2t_\#/\ell}. \tag{5.61}$$

The cutoff contours will look very similar to the ones we found before, except that there is now an extra parameter to vary. Outside the static patch, we expect the cutoffs to again be set by $\chi_1$ since it remains of order $j_\#$ (since particles related by static-patch time-translations must contribute equally to $\chi_1$). Inside the static patch, estimating the cutoff time $t_c$ using either $\chi_2$ or $\chi_\theta$ leads to

$$\cosh^2(t_c/\ell) = \frac{1}{3} {j_\#}^2 e^{2t_\#/\ell} \sim \frac{1}{G^2}, \tag{5.62}$$

so that we again find $t_c \lesssim \ell \ln(1/G)$ for any allowed choice of $j_\#, t_\#$. We thus see that, with a given finite energy budget measured by $F$, adding localized particles along the geodesics $\theta = 0, \pi$ fails to increase the size of the allowed region. In fact, a careful check of the coefficients shows that the region in which we find a good approximation to dS QFT has actually shrunk by a small amount.

While we have not investigated other choices of reference states in detail, the exponential increase of kinetic energies with static patch time is typical of any particles falling toward a de Sitter horizon. This suggests that the above behavior is generic when we require backreaction to be small at $t = 0$ for our global time $t$; i.e., at a minimal $S^d$. For example, the same exponential factors arise in the nonrelativistic limit $\mu \gg j_{\#}$. However, in section 5.5 we will explore the possibility of allowing backreaction at such minimal spheres to be large, and thus allowing $F$ to be large, while requiring backreaction to be small in other regions of de Sitter space. Due to that fact that it will require a slightly more involved discussion of backreaction in Einstein-Hilbert gravity, and since our discussion of 'backreaction' for $D = 2$ was simply a convenient fiction designed to provide a toy model of well-known results for Einstein-Hilbert gravity in the higher dimensional case, we postpone that discussion to section 5.5 and, in particular, until after treating group averaging in higher dimensions in section 5.4.

## 5.4 Reference states in $\mathbf{dS}_{d+1}$

We will now see that essentially the same results found above for $dS_{1+1}$ also hold for $\mathrm{dS}_D$ for all $D > 1$. We begin with a discussion of particle states and the associated action of $\mathrm{SO}(D, 1)$ generators following [197]. To this end, we consider a sphere $S^d$, with metric

$$ds^2 = d\theta_1^2 + \sin^2\theta_1^2 d\Omega_{d-1}^2, \tag{5.63}$$

where $\theta_1$ is the polar angle and we use coordinates $\Omega_{d-1} = (\theta_1, ..., \theta_d)$. In global dS we use the corresponding global coordinates (with global time $t$) in which the metric takes the form

$$ds^2 = -dt^2 + \cosh^2 t(d\theta_1^2 + \sin^2\theta_1 d\Omega_{d-1}^2). \tag{5.64}$$

One-particle wavefunctions on $S^d$ can be written in terms of spherical harmonics labelled by angular momentum vectors $\vec{j} = (j_d, \ldots, j_1)$ with $j_k \geq 0$ for $k \geq 2$. For $k \geq 1$, we take $j_k$ to be the total angular momentum quantum number for the $\mathrm{SO}(k+1)$ subgroup of $\mathrm{SO}(D,1)$ associated with the $S^k$ sphere at constant $\theta_n$ for $n \leq d-k+1$. The above quantum numbers thus satisfy

$$j_d \geq j_{d-1} \geq ... \geq j_2 \geq |j_1|. \tag{5.65}$$

In analogy with the construction in section 5.3.2, we begin by considering a reference state $\big|\psi_1\big] = \big|\psi_+\big] \otimes \big|\psi_-\big]$ where each state describes a particle that is well-localized at $t = 0$ at one of the poles of the $S^d$. For simplicity, we take each particle to be invariant under the $\mathrm{SO}(d)$ rotations that preserve the poles. As a result, two particles will not suffice to break all of the dS isometries, so we will need to add more particles later. Indeed, we will soon define $\big|\psi_0\big] = \big|\psi_1\big] \otimes \big|\psi_2\big] \otimes \ldots \big|\psi_D\big]$, where the $\big|\psi_i\big]$ for $i \geq 2$ are constructed from $\big|\psi_1\big]$ by applying rotations by $\pi/2$ in $d = D-1$ orthogonal directions; see the discussion below.

In the state $\big|\psi_1\big] = \big|\psi_+\big] \otimes \big|\psi_-\big]$, the only non-zero angular momentum will be $j_d$, for which we henceforth use the simplified notation $j = j_d$. We will again consider a free scalar field with 1-particle states in the principle series, with $\Delta = d/2 + i\mu$. We take the state of each particle to be of the form

$$\big|\psi_\pm\big] = N \sum_{j=0}^{j_\#} c_j^\pm |\Delta, j, \vec{0}], \tag{5.66}$$

where $+$ denotes a particle at the north pole and $-$ denotes a particle at the south pole, and where $N$ is a normalization constant.

The coefficients $c_j^\pm$ will be given by the spherical harmonic expansion of an $S^d$ Dirac

$\delta$-function localized at the relevant pole. It is natural to write this delta function $\tilde{\delta}(\theta_1)$ in the form

$$\tilde{\delta}(\theta_1) = \frac{\delta(\theta_1)}{V_{d-1}\sin^{d-1}\theta_1}, \tag{5.67}$$

where $\delta(\theta_1)$ is the standard Dirac delta-function associated with the measure $d\theta_1$ and $V_{d-1} = \int_{\Omega_{d-1}} d\Omega_{d-1}$ is the volume of the unit $d-1$ sphere. There is an analogous result for the $\delta$-function at the south pole. The $d$-dimensional spherical harmonics for $j_{d-1} = j_{d-2} = ... = j_1 = 0$ are given (see e.g.[197]) by

$$^{(d)}Y_{\vec{j}}(\Omega_d) = \frac{1}{\sqrt{2\pi}}\,{}^{(d)}\mathcal{Y}_{j0}(\theta_1)\prod_{n=2}^{d-1}{}^{(n)}\mathcal{Y}_{00}(\theta_{d+1-n}), \tag{5.68}$$

where there is no $\theta_d$ dependence, since the associated harmonic simplifies to $1/\sqrt{2\pi}$. The other harmonics are given by

$$\begin{aligned}{}^{(d)}\mathcal{Y}_{j0}(\theta_1) =& \frac{1}{2^{(d-2)/2}\Gamma(\frac{d}{2})}\left[\left(j+\frac{d-1}{2}\right)\frac{\Gamma(j+d-1)}{\Gamma(j+1)}\right]^{1/2}\cos^j\theta_1 \\ &\times_2 F_1(-\frac{j}{2},\frac{1-j}{2};\frac{d}{2};-\tan^2\theta_1),\end{aligned} \tag{5.69}$$

and by

$${}^{(n)}\mathcal{Y}_{00}(\theta_{d+1-n}) = \frac{\left[(n-1)\Gamma(n-1)\right]^{1/2}}{2^{(n-1)/2}\Gamma(\frac{n}{2})}, \tag{5.70}$$

where we see the ${}^{(n)}\mathcal{Y}_{00}(\theta_{d+1-n})$ above are independent of $\theta_{d+1-n}$. Thus the relevant spherical harmonics depend only on $\theta_1$. We can now determine the coefficients $c_j^{\pm}$ in the expansion of $\tilde{\delta}(\theta_1)$ and $\tilde{\delta}(\theta_1-\pi)$ in terms of the spherical harmonics $^{(d)}Y_{\vec{j}}(\theta_1)$ noting that, since we will normalize the answer afterwards, we care only about the $j$-dependent factors. We find

$$c_j^{\pm} = (\pm 1)^j\left[\left(j+\frac{d-1}{2}\right)\frac{\Gamma(j+d-1)}{\Gamma(j+1)}\right]^{1/2}. \tag{5.71}$$

With these coefficients, the normalizations $N$ for the $\big|\psi_\pm\big]$ states are

$$N = \sqrt{\frac{2d\Gamma(j_\# + 1)}{(2j_\# + d)\Gamma(j_\# + d)}}. \tag{5.72}$$

The generators of the de Sitter group $U(g)$ consist of the $\frac{D(D-1)}{2}$ rotations $J_{ij}$ about each spatial direction (with $i < j$ and $i, j = 1, ..., D$), and $D$ boosts $B_k$. It is convenient to use the embedding space formalism to find the expressions for the corresponding Killing vector fields in terms of global coordinates. In this formalism, we represent our de Sitter space as the hypersurface $X_\mu X^\mu = 1$ in a $(D+1)$-dimensional Minkowski space with metric $ds^2 = -dX_0^2 + dX_1^2 + ... + dX_D^2$. On the hyperboloid, the Minkowski coordinates are then related to global coordinates through $X_0 = \sinh t$, $X_i = z_i \cosh t$, where the $z_i$ are functions of the angles on $S^d$ that define the standard embedding of $S^{D-1}$ in $\mathbb{R}^D$; e.g. $z_1 = \cos\theta_1$, $z_2 = \sin\theta_1 \cos\theta_2$, etc. The Killing fields are thus

$$B_k = z_k \partial_t + \sum_{l=1}^{k} \frac{z_k}{z_l^2} \tanh t \cot\theta_l (\cos^2\theta_l - \delta_{lk}) \partial_{\theta_l}, \quad \text{and} \tag{5.73}$$

$$J_{ij} = \sum_{l=i}^{j} \frac{z_i z_j}{z_l^2} \cot\theta_l (\cos^2\theta_l + \sin^2\theta_i \delta_{li} - \delta_{lj}) \partial_{\theta_l}. \tag{5.74}$$

Note that the action of $B_1$ is the same as in $\mathrm{dS}_{1+1}$ given by Eq. (5.23), but with $\theta$ replaced by $\theta_1$ and with (5.23) rewritten in terms of global coordinates.

As in Section 5.3, we use the above description of $U(g)$ to compute the group averaging kernel to order $(g-1)^2$ in order to determine its width around the identity. The calculation of the kernel is greatly simplified by the symmetries of our reference state. First, $J_{ij}\big|\psi_\pm\big]$ vanishes for $i, j \neq 1$, since these rotations have no effect on scalar particles at the poles. Second, the expectation values of all rotation generators $J_{ij}$ also vanish, and so too will the expectation values of all $B_l$ for $l = 2, ..., D$ due to the invariance of our states under

reflections. In particular, the states $\big|\psi_\pm\big]$ are each individually invariant under reflections defined by choosing some $i \geq 2$ and mapping $X_i \to -X_i$ while holding fixed all $X_j$ with $j \neq i$. Additionally, under the reflection $X_1 \to -X_1$, the $B_1$ generator transforms as $B_1 \to -B_1$. This leads to a cancellation between the remaining terms of order $(g-1)$ (since the only such terms were those associated with the expectation value of $B_1$).

Finally, we consider the cross terms $[J_{1i}J_{1j}]$, $[B_1B_i]$, $[B_iB_j]$, and $[B_kJ_{1i}]$, for $i,j \neq 1$, and where the expectation values $[...]$ are taken in either the $+$ or $-$ state. That these all vanish can be seen by applying the reflection symmetries $X_i \to -X_i$, under which each of the above combinations of generators picks up a sign, but under which the states $\big|\psi_\pm\big]$ are individually invariant. Due to the above vanishing moments and cancellations, the group averaging kernel defined by $\big|\psi_1\big]$ becomes just

$$\begin{aligned}\big[\psi_1\big|U(g)\big|\psi_1\big] =& \big[\psi_+\big|U(g)\big|\psi_+\big]\big[\psi_-\big|U(g)\big|\psi_-\big] \\ =& 1 - \frac{\lambda_1^2}{2}\left([B_1^2] - [B_1]^2\right) - \sum_{\ell=2}^{D}\frac{(\lambda_\perp^l)^2}{2}[B_l^2] - \sum_{1\leq i<j\leq D}\frac{(\theta^{ij})^2}{2}[J_{ij}^2] + \mathcal{O}([g-1]^3).\end{aligned} \tag{5.75}$$

The analysis of the above coefficients is somewhat tedious. We therefore relegate the details to appendix F and merely quote the leading results at large $j_\#$ from (F.21)

$$\begin{aligned}\left([B_1^2] - [B_1]^2\right) &= \left[\frac{d}{d+2} - \frac{d^2}{(d+1)^2}\right]{j_\#}^2, \quad [B_l^2] = \frac{1}{2(d+1))}j_\#, \\ [J_{ij}^2] &= \frac{1}{d+2}{j_\#}^2\delta_{i,1} \quad \text{for } j > i.\end{aligned} \tag{5.76}$$

For $k = 2,\ldots,D$, we now define $\big|\psi_k\big] = e^{i\frac{\pi}{2}J_{k1}}\big|\psi_1\big]$, and we use these states to

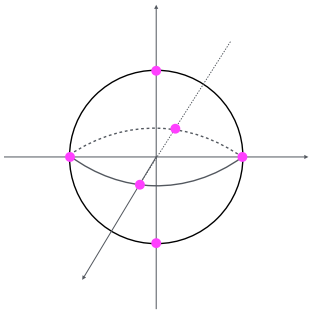

Figure 5.6: The state (5.77) contains $2D$ particles, each of which localizes at a point (pink dot) on the $S^d$ at global time $t^\#$ along one of the coordinate axes of $\mathbb{R}^D$.

construct

$$\big|\psi_0\big] = \prod_{k=1}^{D} \big|\psi_k\big]; \tag{5.77}$$

see figure 5.6. For the state (5.77) we find

$$\big[\psi_0\big|U(g)\big|\psi_0\big] = 1 - \frac{1}{2}\sum_{i=1}^{D} \lambda_i^2 \chi_i - \frac{1}{2}\sum_{1\le i<j\le D} \lambda_{ij}^2 \chi_{ij} + O([g-1]^3), \tag{5.78}$$

with

$$\begin{aligned} \chi_i &= \big([B_1^2] - [B_1]^2\big) + \sum_{k=2}^{D} [B_k^2] \approx \left[\frac{d}{d+2} - \frac{d^2}{(d+1)^2}\right] {j_\#}^2, \quad \text{and} \\ \chi_{ij} &= [J_{1j}^2] \approx \frac{1}{d+2} {j_\#}^2 \quad \text{for } j > i. \end{aligned} \tag{5.79}$$

Here $[X]$ still denotes the expectation value of $X$ in the original state $\big|\psi_+\big]$ and the approximation is valid at leading order in $j_\#$.

We see that all $\chi_i, \chi_{ij}$ are positive for all $d$. By the same argument as in $\mathrm{dS}_{1+1}$, our dS QFT correlators will be well-approximated by our perturbative gravity correlators in regions where the Euclidean norms (see (5.18)) of the killing vectors are much smaller than the $\chi_i^{1/2}$, $\chi_{ij}^{1/2}$. To find the relevant $|B_k|_E^2$, we use (5.73). To find the magnitude of the $|J_{ij}|^2$ in Euclidean signature, we can use (5.74), or we can make direct use of the

embedding space coordinates. The results are

$$|B_k|_E^2/\ell^2 = z_k^2 + (1 - z_k^2)\sinh^2(t/\ell), \quad \text{and} \tag{5.80}$$

$$|J_{ij}|_E^2/\ell^2 = (z_i^2 + z_j^2)\cosh^2(t/\ell). \tag{5.81}$$

In order to describe the region in which our dS QFT correlators are well-approximated by our perturbative gravity correlators, let us note that since $\chi_i$ is independent of $i$, and since $\chi_{ij}$ is independent of $i, j$, the region in which our dS QFT approximation holds to any fixed accuracy $\epsilon$ will be invariant under the full $\mathrm{SO}(D)$ group of rotations that preserve the global time $t$. It therefore suffices to test the conditions $|gx - x|_E \ll \sigma$ only at the pole where $\theta_1 = 0$. Furthermore, we may focus on the generators $B_2$ and $J_{12}$ since, for large $t_\#/\ell$, we see from (5.80) that all other boosts and rotations have equal or smaller Euclidean norm at $\theta = 0$. Using either $B_2$ or $J_{12}$ leads to the condition

$$e^{t/\ell} \ll \chi^{1/2}\sigma \sim j_\#\sigma. \tag{5.82}$$

So, as in our 1+1 toy model, for $j_\# \lesssim 1/G$, we find that our dS QFT approximation can hold only in a region spanning a global time interval of size $\Delta t \sim \ln G^{-1}$.

## 5.5 Reference particles in future dS

In section 5.3.3 we found that, with a fixed energy budget measured by the flux $F$ through a minimal $S^1$ in $\mathrm{dS}_{1+1}$, adding boosted particles in states $e^{\pm i t_\# B_2}\big|\psi_\pm\big]$ did not improve our approximation of the local algebra dS QFT in any region of $\mathrm{dS}_{1+1}$. Since the results in section 5.4 for particles localized at $t = 0$ in $dS_{d+1}$ are quite similar to those in section 5.3.2, it is again clear that with fixed total energy-flux $F$ through a

minimal $S^d$, adding more particles localized at other times will again fail to improve our approximation of local algebras in $(d+1)$-dimensional dS QFT.

However, the key limitation in section 5.3.3 arose from fixing $F$. Furthermore, as discussed in section 5.3.2, there is generally no sense in which backreaction can remain small across *all* of dS, so one must make a choice of both where, and in what sense, one wishes perturbation theory to hold. Finally, since global de Sitter space is exponentially large in both the far future and the far past, the energy carried by perturbations tends to become extremely diluted in such regions and backreaction tends to be much smaller than at a minimal $S^d$.

Let us therefore investigate what we can do if we decide to allow large backreaction near the minimal $S^d$ at $t = 0$ (thus dropping the constraint on $F$), though we will still require backreaction to be small to the future of some global time slice $t = t_\# > 0$. We will do so using the reference state

$$\big|\psi_0\big] = \prod_{k=1}^{D} \big|\psi_k\big], \tag{5.83}$$

$$\big|\psi_1\big] := e^{it_\# B_1}\big|\psi_+\big] \otimes e^{-it_\# B_1}\big|\psi_-\big], \tag{5.84}$$

$$\big|\psi_k\big] := e^{i\frac{\pi}{2}J_{k1}}\big|\psi_+\big], \quad \text{for } 2 \le k \le D, \tag{5.85}$$

where $\big|\psi_\pm\big]$ are again given by (5.66); i.e., we use *only* particles that become localized at global time $t = t_\# > 0$ and we again impose $j_\# \ll 1/G$ in (5.66). At time $t = t_\#$, each particle thus gives only a small perturbation, and the perturbation toward the future should be even smaller. We will investigate later the extent to which the resulting perturbations can remain small at times $t < t_\#$.

Since each state $\big|\psi_k\big]$ is invariant under the same set of (spatial) reflection and rotation symmetries as the similarly-labeled state in section 5.3.3, the non-vanishing moments that contribute to the group-averaging kernel are again just the expectation values of $B_k^2$

and $J_{ij}^2$, for which will again define squared-widths $\chi_k$ and $\chi_{ij}$. Furthermore, while it is straightforward to compute these expectation values from the results in section 5.3.3, the analyses of the previous sections show that we do not in fact need the detailed forms of the results. Instead, the important point is that, due to the boost transformations of $B_k, J_{ij}$ (analogous to those in (5.54)), for the particles in state $\left|\psi_k\right]$ and for $i \neq k$ we will find $\chi_i$ and $\chi_{kj}$ to be proportional to $e^{2t_\#/\ell}$ for large $t_\#$, though $\chi_k$ and $\chi_{ij}$ for $i, j \neq k$ will be unchanged by the boost.

As a result, in the full state $\left|\psi_0\right]$ we will find all $\chi_i, \chi_{ij}$ to be proportional to $e^{2t_\#/\ell}$ for large $t_\#$. This will then compensate for the fact that the Euclidean norms $|B_i|_E^2$ and $|J_{ij}|_E^2$ are exponentially large at $t = t_\#$, and it will similarly allow these vector fields to satisfy our criterion for a good approximation to dS QFT for a global time interval of order $\ln G^{-1}$ to the future of $t = t_\#$. This condition is also satisfied whenever $|t| < t_\#$, so long as we consider a region of dS in which backreaction is small.

It thus remains only to estimate the backreaction from our state. There are several pieces to this discussion. First, we may note that at time $t = t_\#$ we have only $2D$ particles on a sphere $S^d$ of volume $\cosh^d(t_\#/\ell)\, V_d \ell^d$, where $V_d$ is the volume of the unit sphere. Furthermore, by construction each particle alone has small backreaction, meaning that it can be modeled as a Schwarzschild black hole of radius much less than $\ell$. As a result, for all $t \gg \ell$ the particles are exponentially far apart, and – in some reference frame[10] – the region near each particle can be modeled as a Schwarzschild de Sitter solution (again with Schwarzschild radius much less than $\ell$). In this sense the backreaction is small at

[10]For $t_\# - t \gg \ell$, the particle will be highly relativistic in the reference frame associated with slices of constant global time $t$. It should then be described as a de Sitter version of the Aichelberg-Sexl solution [199]. In 2+1 dimensions there is no curvature away from the particle, and for $d \geq 4$ the Aichelberg-Sexl solution decays at long distance. But in 3+1 dimensions the Aichelburg-Sexl metric grows logarithmically. Of course, curvatures still decay and, more importantly, the gravitational field is entirely confined to a shock wave in a null plane. As a result, for $t \gg \ell$ the vast majority of de Sitter space remains exponentially far from such shock waves and, indeed, the total probability for an object in dS to encounter such a shock wave between global time $t$ and global time $t = \infty$ is exponentially small.

$t = t_{\#}$ unless one probes the small region very close to one of the particles. Recalling that metric perturbations can in principle be included in the field we call $\phi$, such comments can be promoted to statements about gauge-invariant operators of the form (5.12) if desired.

It is important to realize, however, that there are small perturbations to de Sitter at $t = t_{\#}$ even far away from the expected locations of the particles. Some of this effect is due to the fact that, since we cut off the mode sum defining each particle's state at some $j_{\#}$, the particles are not perfectly localized and their wavefunctions have long tails that extend across all of de Sitter space. That, however, is a minor issue as, at large $j_{\#}$, those long tails correspond to only a tiny net probability for the particles to be far from their expected location. Furthermore, one could remove the long tails by replacing each particle by the coherent state obtained by making a unitary transformation of the $\psi$-vacuum using $e^{i \int \psi(x) f(x)}$ for some compactly-supported $f(x)$.

While $e^{i \int \psi(x) f(x)}$ is invariant under linearized gauge-transformations, it will not be gauge-invariant at the higher orders in perturbation theory used to compute backreaction. Instead, as usual, it must be 'gravitationally dressed'. In the present context, the only structure to which such operators can be dressed is the background itself. This is simply a set of words which means that the backreaction need not vanish in regions that are causally separated from the support of $f$, and that one must instead solve the gravitational constraints to analyze what happens in such regions.

It is reasonable to expect that the overall effect on the expansion/contraction of the spheres $S^d$ will be well-approximated by smearing the particles over the sphere. By this we mean that we will simply solve the Friedman equations for homogeneous isotropic cosmologies using the homogeneous energy density $\rho$ that gives a flux $F_t = \int_t \sqrt{h} T_a b n^a n^b = \rho \cosh^d(t_{\#}/\ell)\, V_d \ell^d$ of energy through the given sphere $S^d$ that agrees with the flux $F_t$ computed perturbatively for our $2D$ particles. Since angular momentum

is conserved, assuming that $\mu$ and $j_\#$ are of the same order in $1/G$, once $t$ is signifcantly less than $t_\#$ the particles will be relativistic and we will have

$$F_t \sim \frac{2Dj_\#}{\ell} e^{\frac{t^*-t}{\ell}}. \tag{5.86}$$

Replacing our particles with a uniform energy density

$$\rho(t) \sim F_t e^{-dt/\ell} \ell^{-(d+1)} \sim j_\# e^{\frac{t^*-t}{\ell}}, \tag{5.87}$$

and comparing this with the energy density $\rho_\Lambda = \frac{d(d-1)}{16\pi G\ell^2}$ associated with the de Sitter cosmological constant, we find that $\rho(t) \ll \rho_\Lambda$ for

$$e^{(d+1)\frac{t}{\ell}} \gg \frac{Gj_\#}{\ell^{d-1}} e^{t_\#/\ell}; \tag{5.88}$$

i.e., the backreaction from our homogeneous $\rho$ will be small whenever $t$ exceeds $\frac{t_\#}{d+1} - \frac{\ell}{d+1} \ln\left(\frac{\ell^{d-1}}{Gj_\#}\right)$ by at least a few e-folding times.

Now, since the state $\big|\psi_0\big]$ contains only a smll number $(2D)$ of particles, it is clear that the actual energy density is far from homogeneous. Some of the issues involving the inhomogeneous part of $\rho$ were discussed above and relate to probing the local spacetime near each particle. However, additional effects arise when, e.g. by random chance, some subset of the particles finds themselves closer together than other subsets. It is then natural to model such circumstances by a $\rho$ that is again smooth, but where the local energy density in that region is larger than in other regions. Comparing with our analysis above, we see that this will then increase the backreaction in such regions, though this can only be the case in small regions of spacetime. Qualitatively, then, this is similar to the comments above about probing small regions near each particle. In this sense, then, we expect backreaction to be small over the vast majority of the region of our de Sitter

space at global times

$$t > \frac{t_\#}{d+1} - \frac{\ell}{d+1} \ln \left( \frac{\ell^{d-1}}{G j_\#} \right). \tag{5.89}$$

As a result, our perturbative gravity correlators will be a good approximation to our dS QFT correlators over the vast majority of the region satisfying

$$t_\# + \ln \left( \frac{j_\# \sigma}{\ell} \right) > t > \frac{t_\#}{d+1} - \frac{\ell}{d+1} \ln \left( \frac{\ell^{d-1}}{G j_\#} \right). \tag{5.90}$$

Taking $\sigma = \epsilon_1 \ell$, $j_\# = \epsilon_2 \ell^{d-1}/G$ then yields

$$t_\# + \ln \left( \epsilon_1 \epsilon_2 \frac{\ell^{d-1}}{G} \right) > t > \frac{t_\#}{d+1} + \frac{\ell}{d+1} \ln \epsilon_2. \tag{5.91}$$

Taking $t_\#$ large (say, with $\epsilon_1$ and $\epsilon_2$ small but with $\epsilon_1 \epsilon_2 \frac{\ell^{d-1}}{G}$ large) then allows us to make our approximation highly accurate over a region with arbitrarily large spacetime volume and which spans an arbitrarily large interval of global time.

## 5.6 Discussion

Our work above studied the use of the perturbative gravity observables (5.12) in approximating algebras of local quantum fields on a fixed de Sitter spacetime $dS_{d+1}$. In the limit $G \to 0$, one can approximate such local fields well over arbitrarily large regions of dS. However, if the region of interest includes a minimal $S^d$, we found this approximation to fail at small $G$ when the region spanned a global time interval significantly larger than $\ln(\ell^{d-1}/G)$ (plus subleading corrections). On the other hand, we argued that the approximation could hold to high precision in regions spanning arbitrarily large global time intervals so long as they are located far to the future (or far to the past) of the associated minimal $S^d$. This in particular includes arbitrarily large regions of any static

patch of the de Sitter space.

Although our analysis of the possible constructions was far from exhaustive, and although our detailed computations were performed only for free scalar fields with masses $M > 2/d\ell$, we saw that the main results depended only on the presence of certain exponential behaviors that follow from basic de Sitter kinematics. We therefore expect our conclusions to be quite robust. It would nevertheless be useful to make the analysis more complete with respect to possible choices of reference $\left|\psi_0\right]$, and to incorporate perturbative interactions, gravitational or otherwise. Similarly, for simplicity we treated our $\psi$-particles as distinguishable but, since no two $\psi$-particles occupy the same mode, it is clear that symmetrizing/antisymmetrizing over particles in $\left|\psi_0\right]$ will not affect our results.

We emphasize that our interest here concerned *algebras* of local fields. In particular, we may consider arbitrary products of the perturbative gravity observables $\hat{\phi}_{PG}(x)$ defined in (5.12). While there are subtleties related to the fact that our $\hat{\phi}_{PG}(x)$ are unbounded, this is easily remedied by replacing the operators $\hat{\phi}_{QFT}(x)$ in the integrand of (5.12) with bounded functionals of $\hat{\phi}_{QFT}(x)$.

Of course, our dS QFT approximation does not hold uniformly for all elements of the resulting algebra, nor does it hold uniformly in all states. In particular, at any fixed value of $G$, operators formed by taking sufficiently large products will create states with large back-reaction. Nevertheless, it is clear that as $G \to 0$ one can choose parameters such that the approximation holds for a larger and larger subset of elements of the algebra, and such that it holds well over a larger and larger set of states. Thus as $G \to 0$ one should recover the entire algebra of local quantum $\phi$-fields, though filling in the technical details and characterizing the various rates of convergence remains a project for future investigation.

In contrast, had we been interested only in computing vacuum correlation functions

(without first constructing an algebra), we could have approximated the results of dS QFT to much higher precision. At the physical level, this relates to the point often made by cosmologists that, since the vacuum is de Sitter invariant, if one wishes to compute the vacuum two-point function $\big[0\big|\phi(x)\phi(y)\big|0\big]$, then there is no need to sharply define the location of both points $x$ and $y$ so long as the geodesic distance between the two is sharply defined. Mathematically, we may note that we can construct a de Sitter-invariant perturbative-gravity observable

$$\mathcal{O}(x,y) := \int dg \phi(gx)\phi(gy) \otimes U(g)\big|\psi_0\big]\big[\psi_0\big|U(g^{-1}) \tag{5.92}$$

whose expectation value in our $\phi$-vacuum state $|0; LPG\rangle$ is

$$\langle 0; LPG|\mathcal{O}(x,y)|0; LPG\rangle = \big[0\big|\phi(x)\phi(y)\big|0\big] \left(\int dg \Big|\big[\psi_0\big| \otimes U(g)\big|\psi_0\big]\Big|^2\right), \tag{5.93}$$

so that it *exactly* reproduces the two-point function of dS QFT at all $x, y$ for any value of $G$. However, since (5.92) is not the product of two perturbative gravity observables (5.12), the result (5.93) says nothing about the accuracy of approximating the *algebra* of local fields.

Our interest in local algebras was in part motivated by recent works constructing type II von Neumann algebras of local fields [39, 38, 172, 40, 45, 46]. Specifically, we wished to investigate the way in which the static patch algebra of [39] could emerge from perturbative gravity observables. In this regard, there are several aspects of our approach on which we wish to remark.

The first of these is that the algebra of perturbative-gravity observables generated by $\hat{\phi}_{PG}(x)$ does not directly reproduce the *full* algebra of dS QFT, but only the algebra of $\phi$-fields. In particular, it does not include the algebra of $\psi$-fields which can change

our reference state $\big|\psi_0\big]$. Nevertheless, this precisely matches the structure of the Hilbert space used in [39] in the sense that that work assumed the existence of a so-called observer, and that the operator algebra was not allowed to either create or destroy such observers. Furthermore, while the observer's clock operator was used at an intermediate point of the construction, the observables constructed in [39] can be described as what we would call $\phi$-observables defined at times relative to the observer's clock. This is clearly in direct parallel with our perturbative-gravity observables, which describe $\phi$-fields relative to our reference state $\big|\psi_0\big]$.

However, there should be no problem with including additional operators that allow the creation/annihilation of $\psi$-quanta which are *not* to be considered part of our reference state; e.g. which act on modes with much smaller angular momentum on each $S^d$. Indeed, to the extent that we can treat $\psi$-particles as distinguishable, one may simply consider a space of states that is the tensor product of a high-angular-momentum $\big|\psi_0\big]$ state with arbitrary low-angular-momentum states of the $\psi$-field, and one may then define perturbative-gravity observables that act on this space in direct analogy with (5.12). Taking into account that $\psi$-particles are identical then involves a formal symmetrization/antisymmetrization depending on the bosonic/fermionic nature of the $\psi$-particles but, as usual, this has little effect when the relevant two sets of particles occupy very different modes.

A more interesting point is that, while they clearly reproduce a local algebra in the limit $G \to 0$, from the perspective of the dS quantum field theory that acts on the Hilbert space $\mathcal{H}_{QFT} = \mathcal{H}^{\phi}_{QFT} \otimes \mathcal{H}^{\psi}_{QFT}$ the operators $\hat{\phi}_{PG}$ are highly non-local even before they are group-averaged. This is due to the fact that, in contrast to the constructions used in [163, 170, 101, 171, 45], the integrand in (5.12) contains a factor of $\big|\psi_0\big]\big[\psi_0\big|$, which is an operator not contained in the local algebra of quantum $\psi$-fields for any subregion of dS which cannot describe a complete Cauchy surface. As discussed in the

introduction (following [102]), this property is absolutely essential if the group averaging integral in (5.12) is to converge in the presence of a long-lived de Sitter vacuum state. While it naturally viewed as a surprise, and perhaps in fact a distasteful one from the perspective of local quantum field theory, we emphasize that perturbative gravity about a background that fails to break all diffeomorphism gauge symmetries is *not* a local quantum field theory. In particular, since observables in perturbative gravity about dS must be invariant under the entire de Sitter group (see again the discussion at the beginning of section 5.2), they are in some sense necessarily as far from local operators as one can get. In any case, whatever the philosophical issues may be regarding our construction, we see that it does in fact reproduce local quantum field theory in the limit $G \to 0$.

The idea of using highly non-local ingredients like quantum states to define observables which, in some limit, nevertheless reproduce local physics seems likely to be extremely useful in in quantum gravity more generally, and especially in attempts to go beyond perturbation theory. The point here is that the path integral is naturally taken to define an inner product on quantum states that projects onto gauge-invariant states, and which can then be used to build a gauge-invariant Hilbert space; see e.g. the discussions in [200, 192, 201]. As a result, this path integral inner product automatically implements group averaging when expanded perturbatively (see e.g. the recent discussion in [103]). Thus, to the extent that we understand how to compute gravitational path integrals, we already have the desired Hilbert space of states at hand. We may thus use such states $|\Psi_1\rangle, |\Psi_2\rangle$ to directly construct gauge-invariant operators $|\Psi_1\rangle\langle\Psi_2|$ rather than take on the technical challenge of attempting to perform an integral over the diffeomorphism group of some more local operator expression (and then needing to worry further if e.g. topology-changing processes further enlarge the gauge group in the non-perturbative quantum theory; see e.g. the discussion in [202]).

Our work also reported some technical progress regarding the de Sitter group-averaging inner product that underlies our analysis. Appendix A proposed a potential alternate formulation of this inner product that, based on the uniqueness theorem of [190] and the freedom to tune a parameter ($\alpha$) to make the result finite and non-zero, we expect (for some value of $\alpha$) to be equivalent to group averaging. However, the alternate inner product is manifestly positive semi-definite. We also argued that any inner product for perturbative gravity on dS must map one-particle states of our $\mathcal{H}_{QFT}$ to null states. The argument was a direct quantum analogue of the fact that classical one-particle states cannot satisfy the linearization stability constraints. Finally, we argued that the divergence of group averaging for Fock-basis 2-particle states of massive scalar fields is related to the fact that all classical 2-particle solutions preserve a notion of static-patch time-translation symmetry and thus, like the de Sitter-invariant vacuum $\big|0\big]$, leave a non-compact gauge group unbroken. The fact that the unbroken gauge group is now only $\mathbb{R}$ is then naturally associated with the fact that group-averaging diverges only linearly for such 2-particle states, while it diverges exponentially for $\big|0\big]$. While it would be useful to sharpen this last argument, and also to rigorously prove equivalence of group-averaging with our alternate inner product, for heavy fields in dS (e.g., for scalars with $M > d/2\ell$), this gives a rather complete understanding of the group averaging inner product.

This technical progress again has implications for the construction of local algebras and the connection between our work and that of [39, 40, 45, 46]. In particular, the two-particle states with linearly-divergent divergent group-averaging norm naturally play the role of a clock-less version the observer assumed in [39, 40, 45, 46]. Indeed, without a clock, group-averaging would again diverge linearly in the context studied in those works. Adding an appropriate clock degree of freedom, whether realized as the relative motion of a 3rd particle or as the addition of infinitely many internal states that mix under time evolution, will thus cause group averaging to converge. The resulting states can then be

used as a reference $\left|\psi_0\right]$ in precisely the manner described here.

Finally, some readers may be surprised that we have focused so heavily on the study of *global* de Sitter space. In contrast, many treatments of de Sitter or inflation discuss only the inflating patch of de Sitter. Since the inflating patch has *noncompact* Cauchy surfaces, its Killing fields are not normally treated as generating gauge symmetries. In effect, one typically assumes (perhaps implicitly) that boundary conditions are imposed at the upper corner of the inflating patch such that the associated diffeomorphisms are non-trivial asymptotic symmetries rather than gauge. However, we are not aware of a complete technical specification and treatment of such boundary conditions and, perhaps as a result, many longstanding questions and confusions remain regarding the detailed relationship between analyses of global dS and analyses in the inflating patch. Nevertheless, it seems likely that, as discussed briefly in [203], the physics of global dS linearization stability constraints is directly related to large logarithms that arise when studying gravitational perturbation theory in the inflating patch; see, e.g., [204] and reference therein, [205, 206]. It would thus be very interesting to better understand the implications of constructions described here for physics in the inflating patch and, in particular, to understand if (despite the seemingly different time-dependence involved) the above-mentioned large logarithms might be related to the fact that our perturbative gravity correlators become highly smeared versions of dS QFT correlators at late times.

We thank Xi Dong, Gary Horowitz, and Geoff Penington for useful discussions. This research was supported by NSF grants PHY-2107939 and PHY-2408110, and by funds from the University of California. Y.Z. was supported in part by the National Science Foundation under Grant No. NSF PHY-1748958, by a grant from the Simons Foundation (815727, LB), by Heising-Simons Foundation award-6950153, and by David and Lucile Packard Foundation Fellowship-2749255.

# Chapter 6

# Concluding Remarks

Through the work in this thesis, we have gained a better understanding of operators in quantum gravity in both AdS and dS spacetimes.

In Chapters 2-4, we considered geometric entropy operators in semiclassical AdS (or AdS with an added Chern-Simons term), which are of great importance as the bulk dual to boundary subregion entanglement entropy. First, we studied the flow generated by the HRT area operator in Einstein-Hilbert gravity, as well as the algebra of these operators. We then showed in Chapter 3 that this flow is preserved for geometric entropy in 3D gravity with a gravitational anomaly, a first test at understanding the action of geometric entropy in higher-derivative theories of gravity. In Chapter 4, motivated by the connection between networks of intersecting bulk surfaces and random holographic tensor networks, we computed commutators between areas of these bulk surfaces. We were successful in constructing a four-link area network where all area commutators vanish, but showed it is generally hard to construct larger commuting networks.

In Chapter 5, we considered quantum observables in global de Sitter. Since the only dS-invariant state is the vacuum, we used a group averaging procedure to find a usable basis of dS-invariant states, and these states included both an observable degree

of freedom and the reference state wavefunction. For a reference state localized near a minimal $S^d$ of $\mathrm{dS}_{d+1}$, we showed that the observables become smeared once they are far enough in the future or past from the chosen reference system (in particular, the observables are unsmeared only within the region where the global time coordinate spans an interval of order $\Delta t \lesssim \ln G^{-1}$). This means these observables can only be modeled by the physics of QFT in curved spacetime in a rather limited region of global dS. However, if we do not restrict to reference states near a minimal $S^d$, observables can be modelled accurately by QFT in arbitrarily large regions of $\mathrm{dS}_{d+1}$.

There is much that remains to be understood about operators in quantum gravity. For instance, what is the action of geometric entropy operators in general higher-dimensional theories, and can this be derived in a simple way using the boundary modular Hamiltonian? And what about the action of areas of other surfaces in the AdS bulk, like the links of the entanglement wedge cross section? Are there ways to construct arbitrarily fine discretizations of the bulk where every link-area commutator vanishes, or is it better to consider tensor network constructions that do not rely on suppressing fluctuations of all areas simultaneously? And finally, for quantum observables in global de Sitter, what is the cosmological interpretation of the "allowed" region where these observables experience minimal smearing? What significance does this effect have for quantum gravity in our own universe?

# Appendix A

# Normalizations and the One-Sided Boost

As discussed in section 2.2.3, both the flow generated by $A_{HRT}$ and the kink transformation can be described as a sort of one-sided boost. This appendix verifies the details of this relationship, and shows in particular that such a transformation leads precisely to (2.13) with the stated normalizations. We perform an explicit computation below for spacetimes that admit a bulk Killing field $\xi^a$ which acts locally like a boost near $\gamma$. We also study the effect on initial data defined for particularly convenient Cauchy surfaces. But since the flow clearly does not affect initial data within either wedge, the delta-function terms in (2.13) can depend only on the local structure near $\gamma$. It will thus be clear that the same normalizations continue to hold for the more general transformation described in section 2.2.3 (and originally defined in [115]), where we allow arbitrary Cauchy surfaces through $\gamma$ and where the boost operator is defined only in the local approximation where one replaces each plane orthogonal to $\gamma$ with flat Minkowski space.

We will call our one-sided boost $\eta_\alpha$. Before proceeding, recall that $\gamma$ defines two entanglement wedges, one on each side of the surface, and that $\xi^a$ is past-directed in one

(which we call the left wedge) and is future directed in the other (which we call the right wedge). In the left entanglement we take $\eta_\alpha$ to be the identity. In the right wedge we instead take $\eta_\alpha$ to be the diffeomorphism generated by moving points along the orbits of the KVF $\xi^a$ by a Killing parameter $\alpha/\kappa$, where $\kappa$ is the surface gravity of $\xi^a$. Thus $\eta_\alpha$ is a diffeomorphism in each entanglement wedge, though it is not smooth at $\gamma$ and we have not defined its action at points that lie inside[1] the chronological future or past of $\gamma$.

We thus examine the action of $\eta_\alpha$ on Cauchy surfaces that contain $\gamma$. Note that $\eta_\alpha$ will map any such Cauchy surface $\Sigma$ to another such surface $\tilde{\Sigma}$. To simplify our discussion, we will make a special choice for the Cauchy surface $\Sigma$, or at least for the part of that Cauchy surface near $\gamma$. We begin by choosing a unit spacelike vector field $m^a$ normal to $\gamma$ and defined smoothly everywhere on $\gamma$. We then extend $m^a$ to some region near $\gamma$ by taking $m^a$ to be the unit affinely-parameterized tangent to a congruence of geodesics. At least near $\gamma$, these geodesics will generate a hypersurface. We take this to coincide with the part of $\Sigma$ near our HRT surface.[2] The normal $n^a$ to $\Sigma$ then satisfies $m^a n_a = 0$ in the region near $\gamma$. We then further extend both $m^a$ and $n^a$ off of the original slice $\Sigma$ in an arbitrary smooth manner that preserves the conditions $n^a m_a = 0$ and $n_a n^a = -1$. Thus we have the useful relations

$$m^a \nabla_a m^b = 0 \tag{A.1}$$

$$m^a n_b \nabla_a n^b = \frac{1}{2} m^a \nabla_a (-1) = 0 \tag{A.2}$$

$$m^a m_b \nabla_a n^b = m^a \nabla_a (m^b n_b) = 0. \tag{A.3}$$

We also use $s$ to denote proper distance along geodesics in the original congruence, with

[1] On the boundary of the future or past of $\gamma$ the action of $\eta_\alpha$ can be defined by continuity.

[2] Had we started with a generic hypersurface, we could consider the family of spacetime geodesics which happen to be tangent to the hypersurface at $\gamma$. The analysis would then be identical to leading order near $\gamma$, and in particular would give precisely the same delta-function terms in (2.13).

$s = 0$ at $\gamma$.

Let us now construct a second Cauchy surface $\tilde{\Sigma}$ by applying a map $\eta_\alpha$ to $\Sigma$. The map $\eta_\alpha$ is almost a diffeomorphism, except that it is not smooth at $\gamma$. Before proceeding, note that $\gamma$ defines two entanglement wedges, one on each side of the surface, and that $\xi^a$ is past-directed in one (which we call the left wedge and in which we take $s < 0$) and is future directed in the other (which we call the right wedge and in which we take $s > 0$). In the left entanglement we take $\eta_\alpha$ to be the identity. In the right wedge we instead take $\eta_\alpha$ to be the diffeomorphism generated by moving points along the orbits of the KVF $\xi^a$ by a Killing parameter $\alpha/\kappa$, where $\kappa$ is the surface gravity of $\xi^a$. As a result, the normal $\tilde{n}^a$ to $\tilde{\Sigma}$ satisfies

$$\tilde{n}^a = \cosh(\alpha\Theta(s))n^a + \sinh(\alpha\Theta(s))m^a \ldots, \tag{A.4}$$

where $\ldots$ denotes terms that are smooth but which depend on the way that our vector fields were extended off of the original Cauchy surface $\Sigma$. Similarly, the normal $\tilde{m}$ to $\gamma$ in $\tilde{\Sigma}$ satisfies

$$\tilde{m}^a = \cosh(\alpha\Theta(\tilde{s}))m^a + \sinh(\alpha\Theta(\tilde{s}))n^a \ldots, \tag{A.5}$$

where we have used the fact that $\tilde{\Sigma}$ is isometric to $\Sigma$ to introduce a coordinate $\tilde{s}$ that measures proper distance from $\gamma$ along $\tilde{\Sigma}$ in the same way that $s$ does along $\Sigma$. Note that the conditions $m_a m^a = -n_a n^a = 1$ and $n_a m^a = 0$ give

$$\begin{aligned} \tilde{m}_b \nabla_a n^b &= 0 \\ \tilde{m}_b \nabla_a m^b &= 0. \end{aligned} \tag{A.6}$$

Let us now recall that the extrinsic curvature of $\Sigma$ can be described by a degenerate tensor $K_{ab} = -h_a^c \nabla_c n_b$ whose indices range over all coordinates of our spacetime (and not just those on $\Sigma$). Although it is not manifest from the definition, this tensor is

symmetric. From (A.4), we thus see that the extrinsic curvatures $K_{ab}$ and $\tilde{K}_{ab}$ of $\Sigma$ and $\tilde{\Sigma}$ are related everywhere by the action of $\eta_\alpha$ except for the component $\tilde{m}^a\tilde{m}^b\tilde{K}_{ab}$ which will be sensitive to derivatives of the theta-functions in (A.4):

$$\tilde{m}^a\tilde{m}^b\tilde{K}_{ab} = \tilde{m}^a\tilde{m}^b\nabla_a\tilde{n}_b. \tag{A.7}$$

Such derivatives introduce $\delta$-function terms in $\tilde{K}_{ab}$ that are not present in the image[3] $\eta_\alpha^* K_{ab}$ of $K_{ab}$ under the flow $\eta_\alpha$.

Furthermore, since when acting on scalars we have $\tilde{m}^a\nabla_a = \partial_{\tilde{s}}$, we may write

$$\tilde{m}^a\nabla_a\tilde{n}_b = \alpha\delta(\tilde{s})\tilde{m}_b + \big(\sinh(\alpha\Theta(\tilde{s}))\tilde{m}^a\tilde{m}^b\nabla_a n_b + \cosh(\alpha\Theta(\tilde{s}))\tilde{m}^a\tilde{m}^b\nabla_a m_b + \dots\big)\,, \tag{A.8}$$

where the final step uses (A.6). Since the final $\dots$ terms in (A.8) are smooth, they are determined by their values in the left and right wedges and must thus be a part of $\eta_\alpha^* K_{ab}$. We therefore conclude that the extrinsic curvatures of $\Sigma$ and $\tilde{\Sigma}$ are related by

$$\tilde{K}_{ab} = \eta_\alpha^* K_{ab} + \alpha\delta(\tilde{s})\ \tilde{m}^a\tilde{m}^b, \tag{A.9}$$

which agrees with (2.13) if we set $\alpha = -2\pi$ and take the bracket with $A_{HRT}/4G$ to give $d/d\lambda$.

As mentioned in footnote 1, the form of the normalization factor in (A.9) differs from that presented in [115]. This difference arises from the fact that the results of [115] were expressed using coordinates that are not smooth on $\tilde{\Sigma}$, and thus which introduce significant dependence on regulators. In contrast, even though it is not smoothly embedded

[3]Since $\tilde{K}_{ab}$ is defined only on $\tilde{\Sigma}$, there is no need to define this flow in the causal past or future of $\gamma$. Furthermore, since the extrinsic curvature $K_{ab}$ of $\Sigma$ is smooth at $\gamma$, we can define $\eta_\alpha^* K_{ab}$ at $\gamma$ by requiring it to be a smooth tensor on $\tilde{\Sigma}$ when expressed in terms of coordinates on $\tilde{\Sigma}$ obtained by acting with $\eta_\alpha$ on smooth coordinates for $\Sigma$. We emphasize that $\tilde{\Sigma}$ can be regarded as an intrinsically-smooth manifold whose embedding in the bulk happens not to be smooth.

in the bulk, we emphasize that $\tilde{\Sigma}$ has the intrinsic structure of a smooth manifold, so that the corresponding proper distance coordinate $\tilde{s}$ is smooth on $\tilde{\Sigma}$. This turns out to remove detailed dependence on regulators found in [115] and leads to the elegant result (A.9).

# Appendix B

# Adding Additional Constrained HRT Surfaces

We now generalize the network of Figure 4.2 by adding an additional constrained HRT surface as shown in figure B.1, and which is associated with the links $\gamma_c, \gamma_d$. We again start with an HRT surface $\gamma$, which is now taken to be anchored to the boundary at $(U_1, V_1)$ and $(U_2, V_2)$. We then add two constrained geodesics: one anchored to $(U_a, V_a)$ and $(U_b, V_b)$, and the other anchored to $(U_c, V_c)$ and $(U_d, V_d)$. See Figure B.1. The two intersection points divide the original HRT-surface $\gamma$ into the three segments: $\gamma_1$, $\gamma_3$, and $\gamma_2$.

Since the network of figure B.1 contains the network of figure 4.2 as a sub-network, the results of section 4.3.2 yield

$$\{A_{\gamma_a}, A_{\gamma_b}\} = \{A_{\gamma_{a,b}}, A_{\gamma_1}\} = \{A_{\gamma_{a,b}}, A_{\gamma_2 \cup \gamma_3}\} = \{A_{\gamma_1}, A_{\gamma_2 \cup \gamma_3}\} = 0, \tag{B.1}$$

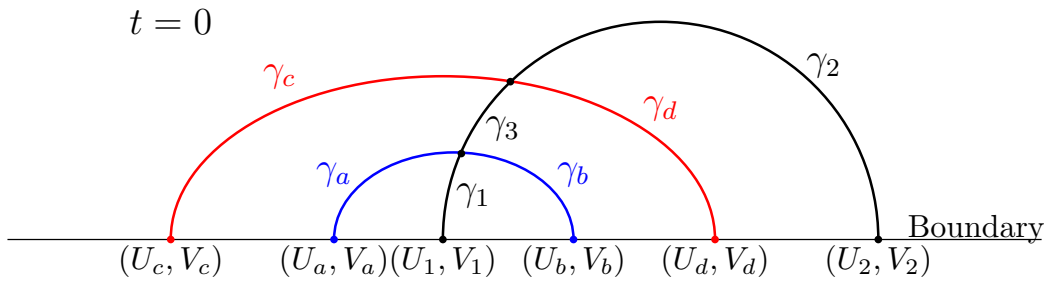


Figure B.1: For visual simplicity, we show the configuration projected into a time slice. We start with an HRT surface, shown in black and given by $\gamma = \gamma_1 + \gamma_2 + \gamma_3$. We then add two constrained geodesics, one in blue ($\gamma_a + \gamma_b$) and one in red ($\gamma_c + \gamma_d$), which each intersect the HRT surface.

and, analogously,

$$\{A_{\gamma_c}, A_{\gamma_d}\} = \{A_{\gamma_{c,d}}, A_{\gamma_2}\} = \{A_{\gamma_{c,d}}, A_{\gamma_1 \cup \gamma_3}\} = \{A_{\gamma_2}, A_{\gamma_1 \cup \gamma_3}\} = 0. \tag{B.2}$$

As a result, only three classes of commutators remain for direct computation:

$$\{A_{\gamma_{a,b,c,d}}, A_{\gamma_3}\}, \{A_{\gamma_{a,b}}, A_{\gamma_{c,d}}\}, \text{ and } \{A_{\gamma_{1,2}}, A_{\gamma_3}\}. \tag{B.3}$$

Note that we can also obtain $\{A_{\gamma_1}, A_{\gamma_2}\}$ from $\{A_{\gamma_{1,2}}, A_{\gamma_3}\}$ using the final commutator in (B.1).

Our present goal is not to obtain a full analysis of this network, but rather only to find a case where commutators fail to vanish. As a result, we will focus on the first class of commutators, where we will indeed find a non-vanishing example.

Without loss of generality, we take $U_c < U_a < U_1 < U_b < U_d < U_2$, and hence $V_c > V_a > V_1 > V_b > V_d > V_2$ to ensure spacelike separation of the anchor points. We will calculate $\{A_{\gamma_a}, A_{\gamma_3}\}$. For simplicity, we rewrite the commutator as

$$\{A_{\gamma_a}, A_{\gamma_3}\} = \{A_{\gamma_a}, A_{\gamma_1 \cup \gamma_3} - A_{\gamma_1}\} = \{A_{\gamma_a}, A_{\gamma_1 \cup \gamma_3}\}, \tag{B.4}$$

where we used $\{A_{\gamma_a}, A_{\gamma_1}\} = 0$ from (B.1). The functional derivatives of $A_{\gamma_a}$ and $A_{\gamma_1 \cup \gamma_3}$ with respect to $\sigma_{U_0}(U)$ are given in Eq. (4.24), respectively. One can also find the analogous expressions for functional derivatives with respect to $\sigma_{V_0}(V)$.

Combining these results with the effective $\sigma$-commutators in (2.53) and (2.54), we find

$$\begin{aligned}\{A_{\gamma_a}, A_{\gamma_3}\} =& \frac{3}{8}\chi^{(U)}_{21ac} + \frac{1}{8}\chi^{(U)}_{bd21} - \frac{1}{4}C\left(\chi^{(U)}_{21ac} + \chi^{(U)}_{bd21}\right) \\ & - \frac{3}{8}\chi^{(V)}_{21ac} - \frac{1}{8}\chi^{(V)}_{bd21} + \frac{1}{4}C\left(\chi^{(V)}_{21ac} + \chi^{(V)}_{bd21}\right),\end{aligned} \tag{B.5}$$

where we define the cross ratios

$$\chi^{(U)}_{ijkl} = \frac{(u_i - u_j)(u_k - u_l)}{(u_i - u_k)(u_j - u_l)} \quad \text{and} \quad \chi^{(V)}_{ijkl} = \frac{(v_i - v_j)(v_k - v_l)}{(v_i - v_k)(v_j - v_l)}. \tag{B.6}$$

In (B.5), $C$ is given in Eq. (4.28). Clearly, this result does not vanish in general, though it does vanish in the limit where $(U_c, V_c)$ and $(U_d, V_d)$ approach $(U_2, V_2)$ so that $\gamma_c, \gamma_d$ recede to infinity and our current network reduces to the one studied previously in section 4.3.2. Similar calculations show that other link-area commutators also generally fail to vanish, including commutators between links on different constrained geodesics (e.g. $\gamma_a$ and $\gamma_c$).

# Appendix C

# Link-Area Functional Derivatives for the Cross Section Network

In this section we record the functional derivatives for the link areas in the (entanglement wedge) cross section network. First, we find the functional derivatives of the cross ratios $\chi_u$ and $\chi_v$; $\chi_u$ and $\chi_v$ are given in Eq. (4.39). Their functional derivatives are hence

$$\begin{aligned}\frac{\delta\chi_u}{\sigma_{U_0}(U)} =&\chi_u e^{-2\sigma_{U_0}(U)}\bigg[\frac{2}{u_{b2}-u_{a1}}\Theta(U_{b2}-U)\Theta(U-U_{a1})\\ &+\frac{2}{u_{a2}-u_{b1}}\Theta(U_{a2}-U)\Theta(U-U_{b1})-\frac{2}{u_{a2}-u_{a1}}\Theta(U_{a2}-U)\Theta(U-U_{a1})\\ &-\frac{2}{u_{b2}-u_{b1}}\Theta(U_{b2}-U)\Theta(U-U_{b1})\bigg],\end{aligned} \tag{C.1}$$

$$\begin{aligned}\frac{\delta\chi_v}{\sigma_{V_0}(V)} =&\chi_v e^{-2\sigma_{V_0}(V)}\bigg[\frac{2}{v_{b2}-v_{a1}}\Theta(V_{b2}-V)\Theta(V-V_{a1})\\ &+\frac{2}{v_{a2}-v_{b1}}\Theta(V_{a2}-V)\Theta(V-V_{b1})-\frac{2}{v_{a2}-v_{a1}}\Theta(V_{a2}-V)\Theta(V-V_{a1})\\ &-\frac{2}{v_{b2}-v_{b1}}\Theta(V_{b2}-V)\Theta(V-V_{b1})\bigg],\end{aligned} \tag{C.2}$$

and using these and Eq. (4.47), the functional derivative of the cross section area $A_{CS}$ immediately follows

$$\begin{aligned}\frac{\delta A_{CS}}{\sigma_{U_0}(U)} =& -\frac{1}{4\sqrt{1-\chi_u}}e^{-2\sigma_{U_0}(U)}\Bigg[\frac{2}{u_{b2}-u_{a1}}\Theta(U_{b2}-U)\Theta(U-U_{a1}) \\ &+\frac{2}{u_{a2}-u_{b1}}\Theta(U_{a2}-U)\Theta(U-U_{b1})-\frac{2}{u_{a2}-u_{a1}}\Theta(U_{a2}-U)\Theta(U-U_{a1}) \\ &-\frac{2}{u_{b2}-u_{b1}}\Theta(U_{b2}-U)\Theta(U-U_{b1})\Bigg],\end{aligned} \tag{C.3}$$

and similarly for the functional derivative with respect to $\hat{\sigma}_{V_0}(V)$. Next, we wish to find the functional derivatives of the half-infinite link areas, as given in Equations (4.42)-(4.45), with respect to $\sigma_{U_0}(U)$:

$$\begin{aligned}\frac{\delta A_{a1}}{\delta\sigma_{U_0}(U)} =&\delta(U-U_{a1})+e^{-2\sigma_{U_0}(U)}\Bigg[\frac{1}{2(u_{a2}-u_{b1})}\Theta(U_{a2}-U)\Theta(U-U_{b1}) \\ &+\frac{1}{2(u_{b2}-u_{a2})}\Theta(U_{b2}-U)\Theta(U-U_{a2}) \\ &-\frac{1}{2(u_{a1}-u_{b1})}\Theta(U_{a1}-U)\Theta(U-U_{b1}) \\ &-\frac{1}{2(u_{b2}-u_{a1})}\Theta(U_{b2}-U)\Theta(U-U_{a1}) \\ &-\frac{1}{u_{a2}-u_{a1}}\Theta(U_{a2}-U)\Theta(U-U_{a1})\Bigg],\end{aligned} \tag{C.4}$$

$$\begin{aligned}\frac{\delta A_{a2}}{\delta \sigma_{U_0}(U)} =&\delta(U-U_{a2}) + e^{-2\sigma_{U_0}(U)}\Bigg[\frac{1}{2(u_{a1}-u_{b1})}\Theta(U_{a1}-U)\Theta(U-U_{b1}) \\ &+\frac{1}{2(u_{b2}-u_{a1})}\Theta(U_{b2}-U)\Theta(U-U_{a1}) \\ &-\frac{1}{2(u_{a2}-u_{b1})}\Theta(U_{a2}-U)\Theta(U-U_{b1}) \\ &-\frac{1}{2(u_{b2}-u_{a2})}\Theta(U_{b2}-U)\Theta(U-U_{a2}) \\ &-\frac{1}{u_{a2}-u_{a1}}\Theta(U_{a2}-U)\Theta(U-U_{a1})\Bigg],\end{aligned} \tag{C.5}$$

$$\begin{aligned}\frac{\delta A_{b1}}{\delta \sigma_{U_0}(U)} =&\delta(U-U_{b1}) + e^{-2\sigma_{U_0}(U)}\Bigg[\frac{1}{2(u_{b2}-u_{a1})}\Theta(U_{b2}-U)\Theta(U-U_{a1}) \\ &+\frac{1}{2(u_{b2}-u_{a2})}\Theta(U_{b2}-U)\Theta(U-U_{a2}) \\ &-\frac{1}{2(u_{a1}-u_{b1})}\Theta(U_{a1}-U)\Theta(U-U_{b1}) \\ &-\frac{1}{2(u_{a2}-u_{b1})}\Theta(U_{a2}-U)\Theta(U-U_{b1}) \\ &-\frac{1}{u_{b2}-u_{b1}}\Theta(U_{b2}-U)\Theta(U-U_{b1})\Bigg],\end{aligned} \tag{C.6}$$

$$\begin{aligned}\frac{\delta A_{b2}}{\delta \sigma_{U_0}(U)} =&\delta(U-U_{b2}) + e^{-2\sigma_{U_0}(U)}\Bigg[\frac{1}{2(u_{a1}-u_{b1})}\Theta(U_{a1}-U)\Theta(U-U_{b1}) \\ &+\frac{1}{2(u_{a2}-u_{b1})}\Theta(U_{a2}-U)\Theta(U-U_{b1}) \\ &-\frac{1}{2(u_{b2}-u_{a1})}\Theta(U_{b2}-U)\Theta(U-U_{a1}) \\ &-\frac{1}{2(u_{b2}-u_{a2})}\Theta(U_{b2}-U)\Theta(U-U_{a2}) \\ &-\frac{1}{u_{b2}-u_{b1}}\Theta(U_{b2}-U)\Theta(U-U_{b1})\Bigg],\end{aligned} \tag{C.7}$$

and analogously for functional derivatives with respect to $\hat{\sigma}_{V_0}(V)$. Also useful are the functional derivatives for the half-infinite link areas as expressed in the simpler form given by Eq. (4.46) for $A_{b1}$, with analogous expressions for the other link areas. We thus have

$$\begin{aligned}\frac{\delta A_{b1}}{\delta\sigma_{U_0}(U)} =&\delta(U-U_{b1})+\frac{\delta f_{b1}(\chi_u,\chi_v)}{\sigma_{U_0}(U)}\\ &+e^{-2\sigma_{U_0}(U)}\Bigg[\frac{1}{u_{a2}-u_{a1}}\Theta(U_{a2}-U)\Theta(U-U_{a1})\\ &-\frac{1}{u_{a1}-u_{b1}}\Theta(U_{a1}-U)\Theta(U-U_{b1})\\ &-\frac{1}{u_{a2}-u_{b1}}\Theta(U_{a2}-U)\Theta(U-U_{b1})\Bigg]\end{aligned} \tag{C.8}$$

and similarly for the functional derivative with respect to $\hat{\sigma}_{V_0}(V)$.

# Appendix D

# Failure of HRT Area Commutation for a Timelike Cross Section

In considering the cross section network of Section 4.4, we restricted to the case where the cross section $\gamma_{CS}$ is spacelike. We now briefly discuss the case when $\gamma_{CS}$ is timelike. This can be achieved if we take, for instance, the anchor point ordering $U_{b1} < U_{a1} < U_{b2} < U_{a2}$ and $V_{b1} > V_{a1} > V_{b2} > V_{a2}$. We will consider in detail the commutator between $A_{\gamma_{b1} \cup \gamma_{b2}}$, i.e. the area of HRT surface $\gamma_{b1} \cup \gamma_{b2}$, and the cross section area $A_{CS}$. A similar result will hold for the commutator between $A_{\gamma_{a1} \cup \gamma_{a2}}$ and $A_{CS}$. In the case where $\gamma_{CS}$ is spacelike, we expected this commutator to vanish because the flow induced by the HRT area leaves $\gamma_{CS}$ unaffected. We indeed showed this was true via an explicit calculation. However, when $\gamma_{CS}$ is timelike, we do expect it to be affected by the flow induced by the HRT areas in the network. We show this explicitly below.

We begin with a calculation of $\{\chi_u, A_{\gamma_{b1} \cup \gamma_{b2}}\}$. As in all previous calculations, we perform this calculation by integrating over the functional derivatives of the area operators and the effective $\sigma$-commutators in Equations (2.53) and (2.54). The $\chi_u$ functional derivative is given by Eq. (C.1), and the HRT area functional derivative can be found

either directly (by differentiating the HRT area) or by adding $\frac{\delta A_{b1}}{\sigma_{U_0}(U)}$ and $\frac{\delta A_{b2}}{\sigma_{U_0}(U)}$ as given in Equations (C.6) and (C.7), respectively. We find

$$\{\chi_u, A_{\gamma_{b1}\cup\gamma_{b2}}\} = \frac{12\pi}{c}(1-\chi_u). \tag{D.1}$$

As explained in Section 4.4.2, commutators with $\chi_v$ will be the same up to a sign and replacement of $\chi_u$ with $\chi_v$, yielding

$$\{\chi_v, A_{\gamma_{b1}\cup\gamma_{b2}}\} = -\frac{12\pi}{c}(1-\chi_v). \tag{D.2}$$

We can now use Eq. (4.47) to calculate the commutator with $A_{CS}$. We find

$$\{A_{CS}, A_{\gamma_{b1}\cup\gamma_{b2}}\} = -\frac{3\pi}{c}\frac{\sqrt{1-\chi_u}}{\chi_u} + \frac{3\pi}{c}\frac{\sqrt{1-\chi_v}}{\chi_v}. \tag{D.3}$$

A similar result holds for $\{A_{CS}, A_{\gamma_{a1}\cup\gamma_{a2}}\}$. As expected, this does not vanish.

# Appendix E

# Group averaging and its extensions

This appendix addresses the finiteness and positivity properties of the group averaging inner product. We begin in section E.0.1 with a summary of results in the existing literature. We then propose a family (labeled by a single parameter $\alpha$) of potential alternative inner products in section E.0.2. The uniqueness theorem of [207] to argue that, if there is a value of $\alpha$ such that this alternate inner product is well-defined on the space $V \subset \mathcal{H}_{QFT}$ of states on which group-averaging converges absolutely, then the two inner products must coincide on $V$, so that the alternate inner product is in fact an extension of the group-averaging inner product. The extended definition is manifestly positive semi-definite and, as discussed in section E.0.3, it assigns vanishing norm to all 1-particle states. One may also independently show that any allowed extension must assign vanishing norms to these states. For scalar fields with masses $M > d/2\ell$, this would thus suffice to show that the extended inner product is finite and positive semi-definite for seed states in a dense subspace of the space that is both orthogonal to the dS-invariant vacuum $\left|0\right]$ and orthogonal to all 2-particle states. Finally, the case of 2-particle states is discussed in section E.0.4, where we suggest that their divergent group-averaging norm is related to the fact that the corresponding classical solutions leave unbroken a non-

compact subgroup of $\mathrm{SO}(D,1)$.

### E.0.1 Summary of previous results

The case of linearized gravitons on $\mathrm{dS}_4$ turns out to be exactly solvable, and (5.7) was shown in [182] to be finite and positive semi-definite when $V$ is the space spanned by Fock basis-states with $N \geq 2$ particles associated with the standard linearized graviton modes on global $\mathrm{dS}_4$. While it was not obviously finite for $N = 1$ particle states, we will return to that case in section E.0.3 below.

For general massive free minimally-coupled scalar fields, the group averaging integral (5.7) was shown to be finite in [208] for standard Fock states that contain a sufficient number of particles. For scalar fields in the so-called principal series of $\mathrm{SO}(D,1)$ representations (having $M^2 > (D-1)^2/4\ell^2$ where $\ell$ is the de Sitter length scale), this result holds for $N > 2$ particles. The threshold particle number for scalar fields is higher than for the free gravitons studied in [182] because convergence is aided by adding angular momentum and because there are no gravitons with angular momentum quantum number $j_{d-1}$ (as defined in section 5.4) satisfying $j_{d-1} < 2$. The reader may think of this result as a generalization of Birkhoff's theorem (which immediately excludes gravitons with $j_{d-1} = 0$).

Larger numbers of particles are required for fields with smaller masses. The required number $N$ diverges as $m \to 0$ due to the fact that massless fields on dS have a zero mode, though sufficient excitations of this zero-mode also provide convergence; see [209] for discussion of the $\mathrm{dS}_{1+1}$ case. For smaller numbers of particles the integral (5.7) fails to converge absolutely, though for the $N = 1$ particle case this can be dealt with as described in section E.0.3 below.

### E.0.2 An alternate definition?

An important part of justifying the group-averaging inner product (5.7) is that it satisfies a certain uniqueness result [207]. We will now use this uniqueness to outline an argument that (5.7) is positive semi-definite when it converges absolutely. The argument involves the introduction of an alternate inner product which, if it is finite and non-zero on *any* state in the space $V$ on which group-averaging converges absolutely (and for which the group-averaging norm is non-zero), must agree with group-averaging on all of $V$ by the argument of [207]. We in fact introduce a one-parameter family of potential alternate inner products in the expectation that there will be a value of this parameter which gives a finite no-zero result on $V$. Unfortunately, however, the alternate inner products are difficult to compute. We thus leave detailed investigation of this expectation for future work.

Translating to the language of the current paper, the uniqueness theorem of [207] shows that if $V \subset \mathcal{H}_{QFT}$ is a space of states on which (5.7) converges absolutely, then there is an associated algebra $\mathcal{A}_V$ of de Sitter-invariant linear operators defined by

$$a_{\psi_1,\psi_2} := \int dg U(g) \big|\psi_1\big] \big[\psi_2\big| U(g^{-1}) \tag{E.1}$$

for $\psi_1, \psi_2 \in V$. Since the Haar measure $dg$ is invariant under $g \to g^{-1}$, these operators map $V$ to itself and also satisfy

$$\big[\phi_1\big| a_{\psi_1,\psi_2}\phi_2\big] = \big[a_{\psi_2,\psi_1}\phi_1\big|\phi_2\big] \tag{E.2}$$

for all $\phi_1, \phi_2 \in V$. Here as usual we have defined $|a\phi_1] := a\big|\phi_1\big]$. The theorem then shows that, up to an overall normalization, (5.7) is the unique product on $V$ that satisfies

linearity with respect to the 2nd argument, the complex conjugation condition

$$\langle \phi_1 | \phi_2 \rangle^* = \langle \phi_2 | \phi_1 \rangle, \tag{E.3}$$

the $*$-representation condition[1]

$$\langle \phi_1 | a_{\psi_1,\psi_2} \phi_2 \rangle = \langle a_{\psi_2,\psi_1} \phi_1 | \phi_2 \rangle, \tag{E.4}$$

and with respect to which $(U(g) - 1)|\phi]$ is a null vector for all $g \in \mathrm{SO}_0(D,1)$ and all $|\phi] \in V$.

As a result, if we can find another inner product satisfying the above properties on the same domain $V$, it must be equivalent to (5.7) up to an overall normalization (though we must then check that this normalization constant is finite and non-zero). Let us therefore think of $\mathrm{dS}_D$ as embedded in $D+1$ Minkowski space so that, choosing a standard set of inertial coordinates $X^0, \ldots, X^D$ on that Minkowski space (with Minkowski metric $\eta_{\mu\nu} = \mathrm{diag}(-1, 1, \ldots, 1)$), we can write the generators of the de Sitter group as the generators $J_{\mu\nu} = -J_{\nu\mu}$ of Lorentz transformations on Minkowski space and define the operators

$$J^2 := \sum_{i,j=1}^{D-1} J_{ij}^2, \quad B^2 := \sum_{i=1}^{D-1} J_{0i}^2. \tag{E.5}$$

For any real parameter $\alpha$ we may then consider the inner product

$$(\phi_1|\phi_2) = \big[\phi_1\big| \, |B|^\alpha \delta(B^2) \Pi_{J^2=0} \big|\phi_2\big] := \frac{1}{2\pi} \int_{\lambda \in \mathbb{R}} d\lambda \big[\phi_1\big| \, |B|^\alpha e^{i\lambda B^2} \Pi_{J^2=0} \big|\phi_2\big], \tag{E.6}$$

where $|B|^\alpha := (B^2)^{\alpha/2}$ and where $\Pi_{J^2=0}$ is the projection onto states with $J^2 = 0$;

[1]The theorem of [207] is stated in terms of so-called rigging maps which are analogues of (5.6). In that language, the main result is that the rigging map commutes with all $a \in \mathcal{A}_V$. But the reality property of rigging maps together with (E.2) makes this equivalent to (E.4).

i.e., onto states that are invariant under the rotational subgroup $\mathrm{SO}_0(D) \subset \mathrm{SO}_0(D,1)$. This inner product is written with round brackets to distinguish it from the other inner products used in this work. Expression (E.6) satisfies the complex conjugation condition (E.3) since

$$\begin{aligned}(\phi_1|\phi_2)^* &= \frac{1}{2\pi}\int_{\lambda\in\mathbb{R}} d\lambda \left(\big[\phi_1\big|\,|B|^\alpha e^{i\lambda B^2}\Pi_{J^2=0}\big|\phi_2\big]\right)^* \\ &= \frac{1}{2\pi}\int_{\lambda\in\mathbb{R}} d\lambda \left(\big[\phi_2\big|\,|B|^\alpha e^{-i\lambda B^2}\Pi_{J^2=0}\big|\phi_1\big]\right) = (\phi_2|\phi_1). \end{aligned} \tag{E.7}$$

Furthermore, since $B^2$ commutes with all rotations, and since $\Pi_{J^2=0} = \int_{r\in\mathrm{SO}_0(D)} U(r)dr$ (where $dr$ is the normalized Haar measure on $\mathrm{SO}_0(D)$), we see that the factors $|B|^\alpha$, $e^{i\lambda B^2}$, and $\Pi_{J^2=0}$ (or equivalently $|B|^\alpha$, $\delta(B^2)$, and $\Pi_{J^2=0}$) all commute with each other. In the same way we see that if the integral in (E.6) converges, then we have

$$(\phi_1|J_{\mu\nu}\phi_2) = 0 \tag{E.8}$$

for all $\mathrm{SO}(D,1)$ generators $J_{\mu\nu}$. For rotations this follows immediately from $\Pi_{J^2=0}J_{ij} = 0$, while for boosts it follows from the fact that $\delta(B^2) = \frac{1}{2\pi}\int_{\lambda\in\mathbb{R}} d\lambda e^{i\lambda B^2}$ is the $\epsilon \to 0$ limit of projectors onto the part of the spectrum of $B^2$ in the range $[0,\epsilon]$. Since $B^2$ is a positive-definite quadratic combination of the $J_{0i}$ (see (E.5)), this implies that at finite $\epsilon$ it also restricts the spectrum of any $J_{0i}$ to the interval $[0,\sqrt{\epsilon}]$. For $(\mu,\nu) = (0,i)$, expressions like (E.8) then contain an extra factor of $\sqrt{\epsilon}$ and thus vanish as $\epsilon \to 0$. As a result, for $\big|\phi_1\big], \big|\phi_2\big] \in V$ and any $g \in \mathrm{SO}_0(D,1)$ we have

$$(\phi_1|[U(g)-1]\phi_2) = 0. \tag{E.9}$$

We can also show that the alternative inner product (E.6) satisfies the $*$-representation

condition (E.4). To do so, we simply note that $a_{\psi_1,\psi_2}$ commutes with all $U(g)$, and that it thus commutes with $\Pi_{J^2=0}$, $|B|^\alpha$, and $e^{i\lambda B^2}$. We may then use (E.2) to write

$$(a_{\psi_2,\psi_1}\phi_1|\phi_2) = \big[\phi_1\big|a_{\psi_1,\psi_2}\int d\lambda |B|^\alpha e^{i\lambda B^2}\Pi_{J^2=0}\big|\phi_2\big] = (\phi_1|a_{\psi_1,\psi_2}\phi_2), \tag{E.10}$$

as desired.

As a result, if we can find a value of $\alpha$ for which (E.6) is finite on the domain $V$ spanned by global dS Fock basis states which contain enough particles for group averaging to converge absolutely, and if (E.6) is finite non-zero for that $\alpha$ and any choice of $\big|\phi_1\big], \big|\phi_2\big] \in V$ then, up to an overall normalization, for that $\alpha$ and all $\big|\psi_1\big], \big|\psi_2\big] \in V$ the alternative inner product $(\psi_1, \psi_2)$ must agree with the group averaging inner product (5.7). Moreover, since $\delta(B^2)$ can be expressed as a limit of spectral projections, the alternative inner product (E.6) is manifestly poistive-definite. Finding the above $\alpha$ would then also establish positive semi-definiteness of group averaging on $V$.

The existence of such an $\alpha$ is certainly plausible, but the inner product (E.6) appears difficult to compute. We thus leave further investigation of this issue for future work.

### E.0.3 One-particle states for free fields

In section E.0.2, we suggested that the inner product (E.6) (for some $\alpha$) provides an alternative way of writing the group-averaging inner product (5.7) on the original domain $V$. However, it can happen that expression (5.7) is well-defined for states where (5.7) is not. If the alternate and group-averaging inner products do in fact agree on $V$ for some $\alpha$, this would then suggest that (E.6) is well-defined on a domain $V_{alt}$ that is strictly larger than the original domain $V$. It would then be tempting to define the desired de Sitter invariant Hilbert space $\mathcal{H}_{LPG}$ using (E.6) on the full domain $V_{alt}$. In this context, we could refer to (E.6) as an extended group-averaging inner product.

Of course, doing so immediately raises the question of the extent to which this supposed extension would be unique. We now will answer this question for the case of $N = 1$ particle states for *any* free field. This is an interesting case since, when combined with the results reviewed in section E.0.1 and with the discussion of section E.0.4 below, it provides a rather complete picture of group-averaging for both 3+1 gravitons and free scalar fields with $M > d/2\ell$.

The alternate inner product (E.6) is well-defined for 1-particle states of any free field and, in fact, defines any 1-particle state to be a null state. To see this, note that the factor $\Pi_{J^2=0}$ in (E.6) means that the only 1-particle state that could possibly have non-zero norm is the state $|\vec{j} = 0\rangle$ associated with the zero angular-momentum mode of the field. Yang-Mills fields and gravitons have no such modes, so this completes the analysis for such cases. Similarly, for minimally-coupled massless scalars the zero angular-momentum mode is also a zero-frequency mode and so does not have particle excitations. While it would be interesting to return to states of that zero mode in the future (in order to extend the 1+1 analysis of [209]), this again completes the analysis of 1-particle states for such fields.

It thus remains only to consider fields with minimally-coupled masses $M^2 > 0$. The 1-particle states of such fields are irreducible representations of $\mathrm{SO}(D, 1)$ with values of the quadratic Casimir $B^2 - J^2 = \mu^2$ for $\mu^2 > 0$. As a result, the rotationally-invariant one-particle state $\big|\vec{j} = 0\big]$ is an eigenstate of $B^2$ with eigenvalue $\mu^2 > 0$. Thus $\delta(B^2)$ must annihilate $\big|\vec{j} = 0\big]$, so that $\big|\vec{j}\big]$ is a null state under the inner product (E.6).

Furthermore, the above argument also shows these definitions to be unique. Indeed, let us consider a basis of one-particle states that are eigenstates of $J^2$. If $J^2\big|\phi\big] = \lambda\big|\phi\big]$ then, unless $\big|\phi\big]$ is proportional to the rotationally invariant state $\big|\vec{j} = 0\big]$, the fact that

$J^2$ is a sum of squares requires $\lambda > 0$. We may thuswrite

$$\big|\phi\big] = \frac{J^2}{\lambda}\big|\phi\big] = \sum_{i,j=1}^{D-1} J_{ij}\left(\frac{J_{ij}}{\lambda}\big|\phi\big]\right). \tag{E.11}$$

But since $(U(g)-1)\big|\Psi\big]$ must be a null state for all $\psi$, the same must be true of $J_{ij}\big|\Psi\big]$. Thus (E.11) must be null as well. It then remains only to discuss the rotationally-invariant one-particle state $\big|\vec{j}=0\big]$. But it was shown above that this state is an eigenvector of $B^2$ with eigenvalue $\mu^2 > 0$. It is thus of the form

$$\frac{B^2}{\mu^2}\big|\vec{j}=0\big] = \sum_{i,j=1}^{D-1} J_{0i}\left(\frac{J_{0i}}{\mu^2}\big|\vec{j}=0\big]\right). \tag{E.12}$$

The same argument used above then shows that $\big|\vec{j}=0\big]$ must be null in $\mathcal{H}_{LPG}$.

The statement that one-particle states map to null states in $\mathcal{H}_{LPG}$ is a direct analogue of the classical statement that any single particle in dS has at least one non-vanishing de Sitter charge. In particular, for free particles with mass $M > 0$, if one considers the static patch associated with the particle's geodesic, then the corresponding static-patch energy takes the value $M$. There are thus no classical single-particle states for which all de Sitter charges vanish.

### E.0.4 The divergent group-averaging norm of 2-scalar-particle states

We now briefly address the case of 2-particle states of scalar fields. The asymptotic expansions of [209] show that the group averaging norms of such states fail to converge absolutely and, in fact, that they in fact diverge linearly. This is a slower divergence than the exponential divergence one finds for the group-averaging norm of the de Sitter-

invariant vacuum $\big|0\big]$, but it is a divergence nonetheless. In fact, it is precisely the degree of divergence one would expect if such states left unbroken a 1-dimensional subgroup of $\mathrm{SO}(D,1)$ generated by some boost transformation.

While the 2-particle states $\big|\Psi\big]$ do not appear to leave such a group unbroken, the corresponding classical solutions *do* exhibit an unbroken such symmetry. Indeed, setting the de Sitter charges to zero forces a pair of classical particles to travel along antipodally-related geodesics (as in the particle approximation to the Schwarzschild-de Sitter solution). Such solutions clearly leave one boost symmetry intact. Some quantum version of this residual symmetry thus appears to be associated with the above divergence, though it would be useful to understand the relationship in more detail. In particular, following similar discussions in [188], one might expect to be able to use an improved such understanding to argue that no well-defined de Sitter-invariant operator can cause such 2-particle states to mix with states having $N \geq 3$ particles.

# Appendix F

# Generator moments in general dimensions.

We now compute and analyze the coefficients in (5.75) associated with the expectation values of $B_1, B_k^2, J_{ij}^2$ in the state $\big|\psi_+\big]$ for all $D$. Our goal is to extract useful expressions for these moments at leading order in large $j_\#$.

Let us start by computing the expectation value $[B_1] = \big[\psi_+\big|B_1\big|\psi_+\big]$. On the states $\big|\psi_\pm\big]$, the action of $B_1$ is

$$B_1\big|\psi_\pm\big] = N\sum_{j=0}^{j_\#} c_j^\pm b_j^+ \big|\Delta, j+1, \vec{0}\big] + N\sum_{j=1}^{j_\#} b_j^- \big|\Delta, j-1, \vec{0}\big], \tag{F.1}$$

with

$$b_j^+ = \left[\frac{(j+d-1)(j+1)(j+d-\Delta)(j+\Delta)}{(2j+d-1)(2j+d+1)}\right]^{1/2}, \quad \text{and} \tag{F.2}$$

$$b_j^- = \left[\frac{(j+d-2)j(j-1+d-\Delta)(j-1+\Delta)}{(2j+d-3)(2j+d-1)}\right]^{1/2}. \tag{F.3}$$

$$\tag{F.4}$$

Utilizing $b_j^- = b_{j-1}^+$, this yields

$$\big[\psi_\pm\big|B_1\big|\psi_\pm\big] = \pm 2N^2 \sum_{j=0}^{j_\#-1} c_j^+ c_{j+1}^+ b_j^+. \tag{F.5}$$

As we will find with most of our other moments, a simple closed-form expression for this sum is not readily available. However, we are mostly interested in the asymptotic behavior at large $j_\#$, since in this limit the group averaging kernel will approximate a Gaussian with shrinking width. In particular, given our results in $\mathrm{dS}_{1+1}$, it is natural to take the ultrarelativistic limit $j_\# \gg \mu$. However, for now we will proceed with computing the remaining expectation values; we will then return later to the question of asymptotic behavior.

For $[B_1^2]$, we find the result

$$\big[\psi_\pm\big|B_1^2\big|\psi_\pm\big] = N^2 \sum_{j=1}^{j_\#} (c_j^+)^2 (b_{j-1}^+)^2 + N^2 \sum_{j=0}^{j_\#} (c_j^+)^2 (b_j^+)^2 + 2N^2 \sum_{j=0}^{j_\#-2} c_j^+ c_{j+2}^+ b_j^+ b_{j+1}^+. \tag{F.6}$$

Similarly, calculating $[J^2]$ gives

$$\big[\psi_\pm\big|J^2\big|\psi_\pm\big] = N^2 \sum_{j=0}^{j_\#} j(j+d-1) c_j^2 = \frac{d}{d+2} j_\#^2 + \frac{d^2}{d+2} j_\# \tag{F.7}$$

Finally, to find the expectation value of $B_k^2$ for $k > 1$, we use the Casimir equation

$$\mathcal{C}_2 = B_1^2 + B_\perp^2 - J^2, \tag{F.8}$$

where we have used the notation $B_\perp^2 := \sum_{n=2}^d B_n^2$. Since we have

$$\big[\psi_\pm\big|\mathcal{C}_2\big|\psi_\pm\big] = \Delta(d-\Delta), \tag{F.9}$$

we can easily compute $[B_\perp^2]$.

We now return to the question of asymptotic behavior. For $[B_1]$ and $[B_1^2]$, it is natural to assume that keeping only the leading terms in the summands will give the correct large $j_\#$ behavior at leading order in $1/j_\#$. We will then check this assumption. The leading order behavior of the normalization constant is, using Stirling's approximation, $N^2 = d{j_\#}^{-d}[1 + \mathcal{O}(1/j_\#)]$. And, in the limit $j >> d$ and $j >> \Delta$, we have

$$b_j^+ = \frac{j}{2}[1 + \mathcal{O}(1/j)], \tag{F.10}$$

$$c_j^+ = j^{(d-1)/2}[1 + \mathcal{O}(1/j)], \tag{F.11}$$

(which have the same leading order asymptotic behavior for $j \to j+1$ or $j \to j+2$). While this large $j$ limit will not hold for the terms in the sum where $j$ is small, we will shortly show that the terms where it fails do not contribute significantly in the limit of large $j_\#$. For convenience, we consider only $[\psi_+|B_1\big|\psi_+]$, which differs from $[\psi_-|B_1\big|\psi_-]$ only by an overall sign. For $\big[\psi_+\big|B_1\big|\psi_+\big]$, we have

$$\big[\psi_+\big|B_1\big|\psi_+\big] = \frac{d}{d+1} j_\# + \mathcal{O}(1), \tag{F.12}$$

where we have used Faulhaber's formula for the sum: $\sum_{n=0}^{j_\#-x} j^{d+y} = \frac{1}{d+y+1}{j_\#}^{d+y+1} + \mathcal{O}({j_\#}^{d+y})$ for the cases $x = 0, 1, 2$ and $y = 0, 1$. Similarly, for $[B_1^2]$ we find

$$\big[\psi_\pm\big|B_1^2\big|\psi_\pm\big] = \frac{d}{d+2}{j_\#}^2 + \mathcal{O}(j_\#). \tag{F.13}$$

Applying the Casimir equation (F.8), we find $\big[\psi_\pm\big|B_\perp^2\big|\psi_\pm\big]$ is zero at order $j_\#^2$. At next to leading order, there are contributions from $c_j$, $b_j^+$, $N^2$, and Faulhaber's formula, the

latter of which becomes

$$\sum_{n=0}^{j_\#-x} j^{d+y} = \frac{1}{d+y+1} {j_\#}^{d+y+1} + (1/2-x){j_\#}^{d+y} + \mathcal{O}({j_\#}^{d-1}). \tag{F.14}$$

Taking these contributions at next to leading order into account, we find

$$\left[\psi_\pm\middle|B_1^2\middle|\psi_\pm\right] = \frac{d}{d+2}{j_\#}^2 + \frac{d(2d^2+d-2)}{2(d+1)(d+2)} j_\# + \mathcal{O}({j_\#}^0), \tag{F.15}$$

and so by the Casimir equation

$$\left[\psi_\pm\middle|B_\perp^2\middle|\psi_\pm\right] = \frac{d}{2(d+1)} j_\# + \mathcal{O}({j_\#}^0). \tag{F.16}$$

We may now verify that the above guess indeed gives the correct large $j_\#$ behavior of the desired moments (despite the fact that we used Equations (F.10) and (F.11) in regimes where they were not fully applicable). For our summands $f(j)$, we have

$$\int_{a-1}^{b} f(x)dx \leq \sum_{j=a}^{b} f(j) \leq \int_{a}^{b+1} f(x)dx, \tag{F.17}$$

since $f(j)$ is increasing with $j$. In particular, for $[B_1]$ we find

$$\lim_{j_\#\to\infty} \frac{2N^2 \int_{-1}^{j_\#-1} f(x)dx}{\frac{d}{d+1} j_\#} \leq \lim_{j_\#\to\infty} \frac{\left[\psi_+\middle|B_1\middle|\psi_+\right]}{\frac{d}{d+1} j_\#} \leq \lim_{j_\#\to\infty} \frac{2N^2 \int_{0}^{j_\#} f(x)dx}{\frac{d}{d+1} j_\#}. \tag{F.18}$$

The lower bound evaluates to

$$\lim_{j_\#\to\infty} \frac{2\int_{-1}^{j_\#-1} f(x)dx}{\frac{1}{d+1}{j_\#}^{d+1}} = \lim_{j_\#\to\infty} \frac{2f(j_\#-1)}{{j_\#}^d} = 1. \tag{F.19}$$

We can see that the upper bound will also evaluate to 1. Thus, we must have

$$\lim_{j_\# \to \infty} \frac{\left[\psi_\pm \middle| B_1 \middle| \psi_\pm\right]}{\pm \frac{d}{d+1} j_\#} = 1. \tag{F.20}$$

The same argument holds for $[B_1^2]$, proving we have the correct asymptotic behavior of our sums.

We will also need to find $[B_l^2]$ for $l \geq 2$ and $[J_{ij}^2]$. The symmetry of $\left|\psi_+\right]$ requires all $[B_l^2]$ to be equal for $l \geq 2$. Additionally, all $[J_{ij}^2]$ with $i = 1$ (or $j = 1$) must be equal, while all others must vanish. At leading order in the $1/j_\#$ expansion, we thus find,

$$\begin{aligned} \left([B_1^2] - [B_1]^2\right) &= \left[\frac{d}{d+2} - \frac{d^2}{(d+1)^2}\right] {j_\#}^2, \quad [B_l^2] = \frac{1}{2(d+1)} j_\#, \\ [J_{ij}^2] &= \frac{1}{d+2} {j_\#}^2 \delta_{i,1} \quad \text{for } j > i. \end{aligned} \tag{F.21}$$

# Appendix G

# The Art of Science

Art, in many forms, has always played an important role in my life. Though my scientific and artistic interests are often distinct—but never completely separate—there have been a handful of times where they have become entwined. For instance, in 2022 and 2023, I created two projects for entry into UCSB's Art of Science Competition, held by the Center for Science and Engineering Partnerships (CSEP). As I believe these projects to be a valuable part of my graduate school experience, I describe them briefly below.

## G.1 A Wormhole Lullaby

As discussed in Chapter 1, the black hole information problem saw important developments in the last five years. Inspired by this new research, and in particular by the calculations in [9], I created *A Wormhole Lullaby*. In [9], the authors consider a black hole in a simple 2D model of gravity, with an asymptotic boundary. This black hole has a so-called "end-of-the-world" (EOW) brane behind the horizon. The authors compute the entropy of the Hawking radiation produced by this black hole; in particular, they compute the Renyi entropy, which is given by $\frac{1}{n-1}\mathrm{Tr}(\rho^n)$ for integer $n$ and where $\rho$ is the

Figure G.1: A spacetime configuration that contributes to the Renyi six-entropy.

density matrix of the radiation. To compute this quantity, one can use the replica trick, where one takes $n$ copies of the asymptotic boundary conditions, then sums over the partition functions for all possible configurations of the interior. Many of these configurations will include connections between different boundaries, creating wormholes. Then, taking the limit of $n \to 1$ gives the von Neumann entropy of the radiation.

The painting in Figure G.1 shows an example configuration with a three-sided wormhole, a two-sided wormhole, and a disconnected black hole. The EOW branes follow the white lines (though for the 3D black holes and wormholes depicted they should instead be 2D sheets). Of course, one should not take this rendering too seriously. The musical por-

tion of the project can be found at `https://www.youtube.com/watch?v=5P_Zagp-jZg`. It follows the calculation of the Renyi entropy with $n = 6$, starting with no wormholes between the boundaries (and one EOW brane) and ending with one wormhole connecting all six asymptotic boundaries (and six different EOW branes). The calculation includes a normalization constant, which is represented by the background piano chords. Each piano melody on top of that represents a wormhole configuration connecting a particular number of boundaries, with a string harmonizing for every copy of that type of wormhole. And, for each new EOW brane, a new instrument is added. For example, the configuration in Figure G.1 has three different melodies, no string harmonies, and four extra instruments.

I am especially interested in this type of music, that transcribes equations into pieces of a song. The music in this next project also falls in this category, though now using lyrics to represent quantum states.

## G.2 The Dance of the Qutrits

This work is based on a toy model of a quantum error correcting code, called the three qutrit code [106]. A qutrit, as opposed to a qubit, is realized by a three-level system. The three qutrit code has two parts: first is the encoding, where the quantum state of one qutrit (the "message") is copied into the state of three qutrits. Next is the decoding, where one can act on the three qutrit state in a clever way to get back the original message. The original state is $|\psi\rangle = c_0 |0\rangle + c_1 |1\rangle + c_2 |2\rangle$. This get encoded as

Figure G.2: The Elwood bluffs in Goleta, CA, affected by the quantum information exchange between three qutrits.

the state $|\tilde{\psi}\rangle = c_0 |\tilde{0}\rangle + c_1 |\tilde{1}\rangle + c_2 |\tilde{2}\rangle$, where

$$|\tilde{0}\rangle = \frac{1}{\sqrt{3}}(|000\rangle + |111\rangle + |222\rangle) \tag{G.1}$$

$$|\tilde{1}\rangle = \frac{1}{\sqrt{3}}(|012\rangle + |120\rangle + |201\rangle) \tag{G.2}$$

$$|\tilde{2}\rangle = \frac{1}{\sqrt{3}}(|021\rangle + |102\rangle + |210\rangle). \tag{G.3}$$

To get back the original state $|\psi\rangle$ from $|\tilde{\psi}\rangle$, we can use an operator that only acts on two of the three qutrits in $|\tilde{\psi}\rangle$. Say this map is $U_{12}^{\dagger}$, acting only on the first two qutrits. Then we have

$$U_{12}^{\dagger} |\tilde{\psi}\rangle = |\psi\rangle_1 \otimes \frac{1}{\sqrt{3}}(|00\rangle_{23} + |11\rangle_{23} + |22\rangle_{23}). \tag{G.4}$$

and we can extract the original state from the state of the first qutrit. Notice that, since the decoding map only acts on the first two qutrits, it is immune to any errors that may have occurred in the third qutrit.

The musical component of this project can be found at https://www.youtube.com/watch?v=LK5LvfkE__U. The lyrics are shown below, and we see they follow the three-qutrit code in detail, with the words "tangle", "space", and "bound" (and variants thereof) representing the states 0, 1, and 2, respectively. States of multiple qutrits have overlapping lyrics, with one line sung and two spoken. The visual component of the piece, shown in Figure G.2, symbolizes the effect of quantum information on the world around us. I was motivated to create this project by recent results that show that, in the AdS/CFT correspondence, the operator encoding between bulk and boundary acts like a quantum error correcting code. This is why the qutrits in Figure G.2 look like gravitational objects, bending spacetime around them—the exchange of quantum information is a key part of understanding quantum gravity.

## *Dance of the Qutrits*

The state

$$\begin{aligned}|\psi\rangle = c_0\,&|\text{This web is something tangled}\rangle\\ + c_1\,&|\text{the space between my thumb and pointer finger}\rangle\\ + c_2\,&|\text{filled with unbounded halfways.}\rangle\end{aligned}$$

becomes

$$\left|\tilde{\psi}\right\rangle = c_0\,|\tilde{0}\rangle + c_1\,|\tilde{1}\rangle + c_2\,|\tilde{2}\rangle$$

with

$$\begin{aligned}|\tilde{0}\rangle = \frac{1}{\sqrt{3}}\Bigg(&\left|\begin{array}{l}\text{My bed head hair tangled and retangled but}\\ \text{untangled just yesterday and}\\ \text{now entangled, inseparable at the pillowcase edge.}\end{array}\right\rangle\\ &+\left|\begin{array}{l}\text{Or at the theory's edge, where spacetime uncurves}\\ \text{like pixels in the spaces between the letters.}\\ \text{Black space full of almost everything.}\end{array}\right\rangle\\ &+\left|\begin{array}{l}\text{Unbounded like the ocean, does it really ever meet the sky?}\\ \text{Or, my extra dimensions bound and squeezed,}\\ \text{bound to be here, there, everywhere.}\end{array}\right\rangle\Bigg),\end{aligned}$$

$$\begin{aligned}|\tilde{1}\rangle = \frac{1}{\sqrt{3}}\Bigg(&\left|\begin{array}{l}\text{Fungal lattice tangled up, the birch trees intertwined}\\ \text{talking to each other across gaps in space}\\ \text{their white bark boundaries transparent, become one.}\end{array}\right\rangle\\ &+\left|\begin{array}{l}\text{Separate beings in time and space but}\\ \text{all bound to err, correct, err again.}\\ \text{Are we really so different, tangled together like this?}\end{array}\right\rangle\\ &+\left|\begin{array}{l}\text{My boundary, my skin, a suggestion}\\ \text{entangled with the air and maybe}\\ \text{dust lost in space and sunlight streaming through fall leaves.}\end{array}\right\rangle\Bigg),\end{aligned}$$

and

$$\begin{aligned}|\tilde{2}\rangle = \frac{1}{\sqrt{3}}\Bigg(&\left|\begin{array}{l}\text{An untangled worm living locally at dawn}\\ \text{but slowly unbound, non-locally a seagull soaring}\\ \text{and maybe spatially spread into a red dwarf, the milky way,}\end{array}\right\rangle\\ &+\left|\begin{array}{l}\text{even the space inside a black hole horizon}\\ \text{tiny particle pings entangled with whoever lies outside}\\ \text{an information matrimony, forever bound}\end{array}\right\rangle\\ &+\left|\begin{array}{l}\text{and so, unbound, no longer you and me but amorphous us}\\ \text{spacetime has handed you your fate and it's}\\ \text{capital letters F-A-T-E, past and future all tangled up.}\end{array}\right\rangle\Bigg).\end{aligned}$$

Then

$$U_{12}^{\dagger} = \begin{pmatrix}\text{Spun and unspun, done and undone.}\\ \text{A hidden code in the universe, pulling apart the fabric and}\\ \text{weaving it back together,}\\ \text{a repeating message because she is clumsy, the great big sky,}\\ \text{coding and recoding and encoding and decoding.}\\ \text{Someday (I think) she'll reveal her secrets.}\end{pmatrix}$$

decodes $\left|\tilde{\psi}\right\rangle$, giving

$$\begin{aligned}U_{12}^{\dagger}\left|\tilde{\psi}\right\rangle = |\psi\rangle_1 \otimes \frac{1}{\sqrt{3}}\Bigg(&\left|\begin{array}{l}\text{This web is something tangled}\\ \text{my grandmother's quilt, why would I detangle}\end{array}\right\rangle_{23}\\ &+\left|\begin{array}{l}\text{the space between my thumb and pointer finger,}\\ \text{nothing more than spacetime herself}\end{array}\right\rangle_{23}\\ &+\left|\begin{array}{l}\text{filled with unbounded halfways}\\ \text{(as we are all bound to be)}\end{array}\right\rangle_{23}\Bigg).\end{aligned}$$

# Bibliography


[1] J. Held, M. Kaplan, D. Marolf, and J. qiang Wu, *Link-area commutators in ads$_3$ area-networks*, arXiv:2401.0248.

[2] M. Kaplan, *The action of geometric entropy in topologically massive gravity*, *Journal of High Energy Physics* **2023** (Dec., 2023) 106, [arXiv:2308.0976].

[3] M. Kaplan and D. Marolf, *The action of HRT-areas as operators in semiclassical gravity*, *Journal of High Energy Physics* **2022** (aug, 2022) [arXiv:2203.0427].

[4] M. Kaplan, D. Marolf, Z. Yu, and Y. Zhao, "De Sitter quantum gravity and the emergence of local algebras." to appear.

[5] J. Held, M. Kaplan, D. Marolf, and Z. Wang, "Do Euclidean Wormhole Saddles Contribute to the Factorization Problem?." to appear.

[6] S. W. Hawking, *Particle creation by black holes*, *Communications in Mathematical Physics* **43** (Aug., 1975) 199–220.

[7] A. Almheiri, N. Engelhardt, D. Marolf, and H. Maxfield, *The entropy of bulk quantum fields and the entanglement wedge of an evaporating black hole*, *Journal of High Energy Physics* **2019** (Dec., 2019) [arXiv:1905.0876].

[8] G. Penington, *Entanglement wedge reconstruction and the information paradox*, arXiv:1905.0825.

[9] G. Penington, S. H. Shenker, D. Stanford, and Z. Yang, *Replica wormholes and the black hole interior*, arXiv:1911.1197.

[10] T. Hertog, B. Truijen, and T. Van Riet, *Euclidean axion wormholes have multiple negative modes*, *Physical Review Letters* **123** (Aug., 2019) [arXiv:1811.1269].

[11] Z. Fu, B. Grado-White, and D. Marolf, *Traversable Asymptotically Flat Wormholes with Short Transit Times*, *Class. Quant. Grav.* **36** (2019), no. 24 245018, [arXiv:1908.0327].

[12] R. Mahajan, D. Marolf, and J. E. Santos, *The double cone geometry is stable to brane nucleation*, *Journal of High Energy Physics* **2021** (Sept., 2021) [arXiv:2104.0002].

[13] D. Marolf and J. E. Santos, *Ads euclidean wormholes*, *Classical and Quantum Gravity* **38** (Oct., 2021) 224002, [arXiv:2101.0887].

[14] D. Marolf and J. E. Santos, *The canonical ensemble reloaded: the complex-stability of euclidean quantum gravity for black holes in a box*, *Journal of High Energy Physics* **2022** (Aug., 2022) [arXiv:2202.1178].

[15] G. J. Loges, G. Shiu, and N. Sudhir, *Complex saddles and euclidean wormholes in the lorentzian path integral*, *Journal of High Energy Physics* **2022** (Aug., 2022) [arXiv:2203.0195].

[16] S. Andriolo, G. Shiu, P. Soler, and T. Van Riet, *Axion wormholes with massive dilaton*, *Class. Quant. Grav.* **39** (2022), no. 21 215014, [arXiv:2205.0111].

[17] S. E. Aguilar-Gutierrez, T. Hertog, R. Tielemans, J. P. van der Schaar, and T. Van Riet, *Axion-de Sitter wormholes*, *JHEP* **11** (2023) 225, [arXiv:2306.1395].

[18] C. Jonas, G. Lavrelashvili, and J.-L. Lehners, *Stability of axion-dilaton wormholes*, *Phys. Rev. D* **109** (2024), no. 8 086022, [arXiv:2312.0897].

[19] T. Hertog, S. Maenaut, B. Missoni, R. Tielemans, and T. Van Riet, *Stability of Axion-Saxion wormholes*, arXiv:2405.0207.

[20] T. G. Mertens and G. J. Turiaci, *Solvable models of quantum black holes: a review on Jackiw–Teitelboim gravity*, *Living Rev. Rel.* **26** (2023), no. 1 4, [arXiv:2210.1084].

[21] P. Saad, S. H. Shenker, and D. Stanford, *JT gravity as a matrix integral*, arXiv:1903.1111.

[22] D. Stanford and E. Witten, *JT gravity and the ensembles of random matrix theory*, *Adv. Theor. Math. Phys.* **24** (2020), no. 6 1475–1680, [arXiv:1907.0336].

[23] J. Maldacena, G. J. Turiaci, and Z. Yang, *Two dimensional Nearly de Sitter gravity*, *JHEP* **01** (2021) 139, [arXiv:1904.0191].

[24] J. Cotler, K. Jensen, and A. Maloney, *Low-dimensional de Sitter quantum gravity*, *JHEP* **06** (2020) 048, [arXiv:1905.0378].

[25] H. Maxfield and G. J. Turiaci, *The path integral of 3D gravity near extremality; or, JT gravity with defects as a matrix integral*, *JHEP* **01** (2021) 118, [arXiv:2006.1131].

[26] E. Witten, *Matrix Models and Deformations of JT Gravity*, *Proc. Roy. Soc. Lond. A* **476** (2020), no. 2244 20200582, [arXiv:2006.1341].

[27] S. Collier, L. Eberhardt, B. Muehlmann, and V. A. Rodriguez, *The Virasoro minimal string*, *SciPost Phys.* **16** (2024), no. 2 057, [arXiv:2309.1084].

[28] N. Bao, G. Penington, J. Sorce, and A. C. Wall, *Holographic Tensor Networks in Full AdS/CFT*, arXiv:1902.1015.

[29] C. Akers, T. Faulkner, S. Lin, and P. Rath, *Reflected entropy in random tensor networks*, *JHEP* **05** (2022) 162, [arXiv:2112.0912].

[30] X. Dong, X.-L. Qi, and M. Walter, *Holographic entanglement negativity and replica symmetry breaking*, *Journal of High Energy Physics* **2021** (June, 2021) [arXiv:2101.1102].

[31] N. Cheng, C. Lancien, G. Penington, M. Walter, and F. Witteveen, *Random Tensor Networks with Non-trivial Links*, *Annales Henri Poincare* **25** (2024), no. 4 2107–2212, [arXiv:2206.1048].

[32] A. Belin, J. de Boer, D. L. Jafferis, P. Nayak, and J. Sonner, *Approximate CFTs and Random Tensor Models*, arXiv:2308.0382.

[33] X. Dong, S. McBride, and W. W. Weng, *Holographic Tensor Networks with Bulk Gauge Symmetries*, arXiv:2309.0643.

[34] S. A. W. Leutheusser, *Emergent Times in Holographic Duality*, *Phys. Rev. D* **108** (2023), no. 8 086020, [arXiv:2112.1215].

[35] S. Leutheusser and H. Liu, *Causal connectability between quantum systems and the black hole interior in holographic duality*, *Phys. Rev. D* **108** (2023), no. 8 086019, [arXiv:2110.0549].

[36] S. Leutheusser and H. Liu, *Subalgebra-subregion duality: emergence of space and time in holography*, arXiv:2212.1326.

[37] E. Witten, *Gravity and the crossed product*, *JHEP* **10** (2022) 008, [arXiv:2112.1282].

[38] V. Chandrasekaran, G. Penington, and E. Witten, *Large N algebras and generalized entropy*, *JHEP* **04** (2023) 009, [arXiv:2209.1045].

[39] V. Chandrasekaran, R. Longo, G. Penington, and E. Witten, *An algebra of observables for de sitter space*, *Journal of High Energy Physics* **2023** (Feb., 2023) [arXiv:2206.1078].

[40] K. Jensen, J. Sorce, and A. J. Speranza, *Generalized entropy for general subregions in quantum gravity*, *JHEP* **12** (2023) 020, [arXiv:2306.0183].

[41] J. Kudler-Flam, S. Leutheusser, and G. Satishchandran, *Generalized Black Hole Entropy is von Neumann Entropy*, arXiv:2309.1589.

[42] E. Colafranceschi, D. Marolf, and Z. Wang, *A trace inequality for Euclidean gravitational path integrals (and a new positive action conjecture)*, *JHEP* **04** (2024) 140, [arXiv:2309.0249].

[43] E. Colafranceschi, X. Dong, D. Marolf, and Z. Wang, *Algebras and Hilbert spaces from gravitational path integrals: Understanding Ryu-Takayanagi/HRT as entropy without invoking holography*, arXiv:2310.0218.

[44] T. Faulkner, M. Li, and H. Wang, *A modular toolkit for bulk reconstruction*, *JHEP* **04** (2019) 119, [arXiv:1806.1056].

[45] C.-H. Chen and G. Penington, *A clock is just a way to tell the time: gravitational algebras in cosmological spacetimes*, arXiv:2406.0211.

[46] J. Kudler-Flam, S. Leutheusser, and G. Satishchandran, *Algebraic observational cosmology*, arXiv:2406.0166.

[47] J. D. Bekenstein, *Black holes and entropy*, *Phys. Rev. D* **7** (Apr, 1973) 2333–2346.

[48] C. B. Thorn, *Reformulating string theory with the 1/N expansion*, in *The First International A.D. Sakharov Conference on Physics*, 5, 1991. hep-th/9405069.

[49] G. 't Hooft, *Dimensional reduction in quantum gravity*, *Conf. Proc. C* **930308** (1993) 284–296, [gr-qc/9310026].

[50] L. Susskind, *The World as a hologram*, *J. Math. Phys.* **36** (1995) 6377–6396, [hep-th/9409089].

[51] T. Banks, W. Fischler, S. H. Shenker, and L. Susskind, *M theory as a matrix model: A conjecture*, *Phys. Rev. D* **55** (1997) 5112–5128, [hep-th/9610043].

[52] J. Maldacena, *The Large N limit of superconformal field theories and supergravity*, *International Journal of Theoretical Physics* **38** (1999), no. 4 1113–1133, [9711200].

[53] S. S. Gubser, I. R. Klebanov, and A. M. Polyakov, *Gauge theory correlators from noncritical string theory*, *Phys. Lett. B* **428** (1998) 105–114, [hep-th/9802109].

[54] E. Witten, *Anti-de Sitter space and holography*, *Adv. Theor. Math. Phys.* **2** (1998) 253–291, [hep-th/9802150].

[55] T. Banks, M. R. Douglas, G. T. Horowitz, and E. J. Martinec, *AdS dynamics from conformal field theory*, hep-th/9808016.

[56] A. Hamilton, D. N. Kabat, G. Lifschytz, and D. A. Lowe, *Holographic representation of local bulk operators*, *Phys. Rev. D* **74** (2006) 066009, [hep-th/0606141].

[57] D. Harlow and D. Stanford, *Operator Dictionaries and Wave Functions in AdS/CFT and dS/CFT*, arXiv:1104.2621.

[58] A. Almheiri, X. Dong, and D. Harlow, *Bulk Locality and Quantum Error Correction in AdS/CFT*, *JHEP* **04** (2015) 163, [arXiv:1411.7041].

[59] X. Dong, D. Harlow, and A. C. Wall, *Reconstruction of Bulk Operators within the Entanglement Wedge in Gauge-Gravity Duality*, *Phys. Rev. Lett.* **117** (2016), no. 2 021601, [arXiv:1601.0541].

[60] D. Harlow, *The Ryu–Takayanagi Formula from Quantum Error Correction*, *Commun. Math. Phys.* **354** (2017), no. 3 865–912, [arXiv:1607.0390].

[61] S. Ryu and T. Takayanagi, *Holographic derivation of entanglement entropy from AdS/CFT*, *Phys. Rev. Lett.* **96** (2006) 181602, [hep-th/0603001].

[62] S. Ryu and T. Takayanagi, *Aspects of Holographic Entanglement Entropy*, *JHEP* **08** (2006) 045, [hep-th/0605073].

[63] V. E. Hubeny, M. Rangamani, and T. Takayanagi, *A Covariant holographic entanglement entropy proposal*, *JHEP* **07** (2007) 062, [arXiv:0705.0016].

[64] A. C. Wall, *Maximin Surfaces, and the Strong Subadditivity of the Covariant Holographic Entanglement Entropy*, *Class. Quant. Grav.* **31** (2014), no. 22 225007, [arXiv:1211.3494].

[65] A. Lewkowycz and J. Maldacena, *Generalized gravitational entropy*, *JHEP* **08** (2013) 090, [arXiv:1304.4926].

[66] X. Dong, A. Lewkowycz, and M. Rangamani, *Deriving covariant holographic entanglement*, *JHEP* **11** (2016) 028, [arXiv:1607.0750].

[67] T. Faulkner, A. Lewkowycz, and J. Maldacena, *Quantum corrections to holographic entanglement entropy*, *JHEP* **11** (2013) 074, [arXiv:1307.2892].

[68] N. Engelhardt and A. C. Wall, *Quantum Extremal Surfaces: Holographic Entanglement Entropy beyond the Classical Regime*, *JHEP* **01** (2015) 073, [arXiv:1408.3203].

[69] F. Pastawski, B. Yoshida, D. Harlow, and J. Preskill, *Holographic quantum error-correcting codes: Toy models for the bulk/boundary correspondence*, *JHEP* **06** (2015) 149, [arXiv:1503.0623].

[70] A. J. Ferris and D. Poulin, *Tensor networks and quantum error correction*, *Physical Review Letters* **113** (jul, 2014) [arXiv:1312.4578].

[71] P. Hayden, S. Nezami, X.-L. Qi, N. Thomas, M. Walter, and Z. Yang, *Holographic duality from random tensor networks*, *JHEP* **11** (2016) 009, [arXiv:1601.0169].

[72] T. Kohler and T. Cubitt, *Toy models of holographic duality between local hamiltonians*, *Journal of High Energy Physics* **2019** (aug, 2019) [arXiv:1810.0899].

[73] B. Swingle, *Entanglement renormalization and holography*, *Physical Review D* **86** (sep, 2012) [arXiv:0905.1317].

[74] B. Swingle, *Constructing holographic spacetimes using entanglement renormalization*, arXiv:1209.3304.

[75] X. Dong, D. Harlow, and D. Marolf, *Flat entanglement spectra in fixed-area states of quantum gravity*, *JHEP* **10** (2019) 240, [arXiv:1811.0538].

[76] X. Dong, *Holographic entanglement entropy for general higher derivative gravity*, *Journal of High Energy Physics* **2014** (jan, 2014) [arXiv:1310.5713].

[77] X. Dong and D. Marolf, *One-loop universality of holographic codes*, *Journal of High Energy Physics* **2020** (mar, 2020) [arXiv:1910.0632].

[78] N. Bao, G. Penington, J. Sorce, and A. C. Wall, *Beyond Toy Models: Distilling Tensor Networks in Full AdS/CFT*, *JHEP* **11** (2019) 069, [arXiv:1812.0117].

[79] A. G. Riess, A. V. Filippenko, P. Challis, A. Clocchiatti, A. Diercks, P. M. Garnavich, R. L. Gilliland, C. J. Hogan, S. Jha, R. P. Kirshner, B. Leibundgut, M. M. Phillips, D. Reiss, B. P. Schmidt, R. A. Schommer, R. C. Smith, J. Spyromilio, C. Stubbs, N. B. Suntzeff, and J. Tonry, *Observational evidence from supernovae for an accelerating universe and a cosmological constant*, *The Astronomical Journal* **116** (Sept., 1998) 1009–1038, [9805201].

[80] A. Strominger, *Inflation and the dS / CFT correspondence*, *JHEP* **11** (2001) 049, [hep-th/0110087].

[81] M. Alishahiha, A. Karch, E. Silverstein, and D. Tong, *The dS/dS correspondence*, *AIP Conf. Proc.* **743** (2004), no. 1 393–409, [hep-th/0407125].

[82] B. Freivogel, Y. Sekino, L. Susskind, and C.-P. Yeh, *A Holographic framework for eternal inflation*, *Phys. Rev. D* **74** (2006) 086003, [hep-th/0606204].

[83] X. Dong, B. Horn, E. Silverstein, and G. Torroba, *Micromanaging de Sitter holography*, *Class. Quant. Grav.* **27** (2010) 245020, [arXiv:1005.5403].

[84] X. Dong, B. Horn, S. Matsuura, E. Silverstein, and G. Torroba, *FRW solutions and holography from uplifted AdS/CFT*, *Phys. Rev. D* **85** (2012) 104035, [arXiv:1108.5732].

[85] D. Anninos, S. A. Hartnoll, and D. M. Hofman, *Static Patch Solipsism: Conformal Symmetry of the de Sitter Worldline*, *Class. Quant. Grav.* **29** (2012) 075002, [arXiv:1109.4942].

[86] D. Anninos and D. M. Hofman, *Infrared Realization of $dS_2$ in $AdS_2$*, *Class. Quant. Grav.* **35** (2018), no. 8 085003, [arXiv:1703.0462].

[87] T. Banks and W. Fischler, *The holographic spacetime model of cosmology*, *Int. J. Mod. Phys. D* **27** (2018), no. 14 1846005, [arXiv:1806.0174].

[88] S. Cooper, M. Rozali, B. Swingle, M. Van Raamsdonk, C. Waddell, and D. Wakeham, *Black hole microstate cosmology*, *JHEP* **07** (2019) 065, [arXiv:1810.1060].

[89] G. B. De Luca, E. Silverstein, and G. Torroba, *Hyperbolic compactification of M-theory and de Sitter quantum gravity*, *SciPost Phys.* **12** (2022), no. 3 083, [arXiv:2104.1338].

[90] L. Susskind, *Black Holes Hint towards De Sitter Matrix Theory*, *Universe* **9** (2023), no. 8 368, [arXiv:2109.0132].

[91] L. Susskind, *Scrambling in Double-Scaled SYK and De Sitter Space*, arXiv:2205.0031.

[92] A. Sahu, P. Simidzija, and M. Van Raamsdonk, *Bubbles of cosmology in AdS/CFT*, *JHEP* **11** (2023) 010, [arXiv:2306.1314].

[93] S. Kachru, R. Kallosh, A. Linde, and S. P. Trivedi, *de sitter vacua in string theory*, *Physical Review D* **68** (Aug., 2003) [0301240].

[94] U. H. Danielsson and T. Van Riet, *What if string theory has no de Sitter vacua?*, *Int. J. Mod. Phys. D* **27** (2018), no. 12 1830007, [arXiv:1804.0112].

[95] M. Cicoli, S. De Alwis, A. Maharana, F. Muia, and F. Quevedo, *De Sitter vs Quintessence in String Theory*, *Fortsch. Phys.* **67** (2019), no. 1-2 1800079, [arXiv:1808.0896].

[96] L. McAllister, J. Moritz, R. Nally, and A. Schachner, *Candidate de Sitter Vacua*, arXiv:2406.1375.

[97] L. Boltzmann, *On certain questions of the theory of gases*, *Nature* **51** (Feb., 1895) 413–415.

[98] M. Rees, *Before The Beginning: Our Universe And Others*. Basic Books, 1997.

[99] A. Albrecht and L. Sorbo, *Can the universe afford inflation?*, *Phys. Rev. D* **70** (2004) 063528, [hep-th/0405270].

[100] D. N. Page, *Is our universe likely to decay within 20 billion years?*, *Phys. Rev. D* **78** (2008) 063535, [hep-th/0610079].

[101] S. B. Giddings, D. Marolf, and J. B. Hartle, *Observables in effective gravity*, *Physical Review D* **74** (Sept., 2006) [0512200].

[102] S. B. Giddings and D. Marolf, *A global picture of quantum de sitter space*, *Physical Review D* **76** (Sept., 2007) [arXiv:0705.1178].

[103] T. Chakraborty, J. Chakravarty, V. Godet, P. Paul, and S. Raju, *Holography of information in de Sitter space*, *JHEP* **12** (2023) 120, [arXiv:2303.1631].

[104] Y. Zou, B. Shi, J. Sorce, I. T. Lim, and I. H. Kim, *Modular commutators in conformal field theory*, *Physical Review Letters* **129** (dec, 2022) [arXiv:2206.0002].

[105] Y. Chen, X. Dong, A. Lewkowycz, and X.-L. Qi, *Modular Flow as a Disentangler*, *JHEP* **12** (2018) 083, [arXiv:1806.0962].

[106] D. Harlow, *TASI Lectures on the Emergence of Bulk Physics in AdS/CFT*, *PoS* **TASI2017** (2018) 002, [arXiv:1802.0104].

[107] R. E. Peierls, *The Commutation laws of relativistic field theory*, *Proc. Roy. Soc. Lond. A* **214** (1952) 143–157.

[108] S. Carlip and C. Teitelboim, *The Off-shell black hole*, *Class. Quant. Grav.* **12** (1995) 1699–1704, [gr-qc/9312002].

[109] T. Thiemann and H. A. Kastrup, *Canonical quantization of spherically symmetric gravity in Ashtekar's selfdual representation*, *Nucl. Phys. B* **399** (1993) 211–258, [gr-qc/9310012].

[110] H. A. Kastrup and T. Thiemann, *Spherically symmetric gravity as a completely integrable system*, *Nucl. Phys. B* **425** (1994) 665–686, [gr-qc/9401032].

[111] K. V. Kuchar, *Geometrodynamics of Schwarzschild black holes*, *Phys. Rev. D* **50** (1994) 3961–3981, [gr-qc/9403003].

[112] D. L. Jafferis and S. J. Suh, *The Gravity Duals of Modular Hamiltonians*, *JHEP* **09** (2016) 068, [arXiv:1412.8465].

[113] F. Ceyhan and T. Faulkner, *Recovering the QNEC from the ANEC*, *Commun. Math. Phys.* **377** (2020), no. 2 999–1045, [arXiv:1812.0468].

[114] R. Bousso, V. Chandrasekaran, and A. Shahbazi-Moghaddam, *From black hole entropy to energy-minimizing states in QFT*, *Phys. Rev. D* **101** (2020), no. 4 046001, [arXiv:1906.0529].

[115] R. Bousso, V. Chandrasekaran, P. Rath, and A. Shahbazi-Moghaddam, *Gravity dual of Connes cocycle flow*, *Phys. Rev. D* **102** (2020), no. 6 066008, [arXiv:2007.0023].

[116] A. Lewkowycz and O. Parrikar, *The holographic shape of entanglement and Einstein's equations*, *JHEP* **05** (2018) 147, [arXiv:1802.1010].

[117] D. L. Jafferis, A. Lewkowycz, J. Maldacena, and S. J. Suh, *Relative entropy equals bulk relative entropy*, *JHEP* **06** (2016) 004, [arXiv:1512.0643].

[118] W. Donnelly and L. Freidel, *Local subsystems in gauge theory and gravity*, *JHEP* **09** (2016) 102, [arXiv:1601.0474].

[119] A. J. Speranza, *Local phase space and edge modes for diffeomorphism-invariant theories*, *JHEP* **02** (2018) 021, [arXiv:1706.0506].

[120] V. Chandrasekaran and K. Prabhu, *Symmetries, charges and conservation laws at causal diamonds in general relativity*, *JHEP* **10** (2019) 229, [arXiv:1908.0001].

[121] M. Headrick and T. Takayanagi, *A Holographic proof of the strong subadditivity of entanglement entropy*, *Phys. Rev. D* **76** (2007) 106013, [arXiv:0704.3719].

[122] D. Marolf, M. Rangamani, and M. Van Raamsdonk, *Holographic models of de Sitter QFTs*, *Class. Quant. Grav.* **28** (2011) 105015, [arXiv:1007.3996].

[123] H. Casini, M. Huerta, and R. C. Myers, *Towards a derivation of holographic entanglement entropy*, *JHEP* **05** (2011) 036, [arXiv:1102.0440].

[124] X. Dong, D. Marolf, and P. Rath, "Geometric entropies and their geometric flow: the power of Lorentzian methods." to appear.

[125] X. Dong, D. Marolf, and P. Rath, "JLMS and the kink transform: comments and clarifications." to appear.

[126] N. Engelhardt and A. C. Wall, *Coarse Graining Holographic Black Holes*, *JHEP* **05** (2019) 160, [arXiv:1806.0128].

[127] P. Di Francesco, P. Mathieu, and D. Senechal, *Conformal Field Theory*. Graduate Texts in Contemporary Physics. Springer-Verlag, New York, 1997.

[128] I. A. Morrison and M. M. Roberts, *Mutual information between thermo-field doubles and disconnected holographic boundaries*, *Journal of High Energy Physics* **2013** (Jul, 2013).

[129] C. Akers and P. Rath, *Holographic Renyi Entropy from Quantum Error Correction*, *JHEP* **05** (2019) 052, [arXiv:1811.0517].

[130] P. Calabrese and J. Cardy, *Entanglement entropy and quantum field theory*, *Journal of Statistical Mechanics: Theory and Experiment* **2004** (jun, 2004) P06002, [0405152].

[131] A. Kitaev and J. Preskill, *Topological entanglement entropy*, *Phys. Rev. Lett.* **96** (Mar, 2006) 110404, [0510092].

[132] M. Levin and X.-G. Wen, *Detecting topological order in a ground state wave function*, *Phys. Rev. Lett.* **96** (Mar, 2006) 110405, [0510613].

[133] I. H. Kim, B. Shi, K. Kato, and V. V. Albert, *Chiral central charge from a single bulk wave function*, *Physical Review Letters* **128** (apr, 2022) [arXiv:2110.1040].

[134] I. H. Kim, B. Shi, K. Kato, and V. V. Albert, *Modular commutator in gapped quantum many-body systems*, *Physical Review B* **106** (aug, 2022) [arXiv:2110.0693].

[135] S. Deser, R. Jackiw, and S. Templeton, *Topologically massive gauge theories*, *Annals of Physics* **140** (1982), no. 2 372–411.

[136] S. Deser, R. Jackiw, and S. Templeton, *Three-dimensional massive gauge theories*, *Phys. Rev. Lett.* **48** (Apr, 1982) 975–978.

[137] S. Deser and X. Xiang, *Canonical formulations of full nonlinear topologically massive gravity*, *Physics Letters B* **263** (1991), no. 1 39–43.

[138] P. Kraus and F. Larsen, *Holographic gravitational anomalies*, *Journal of High Energy Physics* **2006** (jan, 2006) 022–022, [0508218].

[139] S. N. Solodukhin, *Holographic description of gravitational anomalies*, *Journal of High Energy Physics* **2006** (jul, 2006) 003–003, [0512216].

[140] K. Hotta, Y. Hyakutake, T. Kubota, and H. Tanida, *Brown-henneaux's canonical approach to topologically massive gravity*, *Journal of High Energy Physics* **2008** (jul, 2008) 066–066, [arXiv:0805.2005].

[141] K. Skenderis, M. Taylor, and B. C. van Rees, *Topologically massive gravity and the AdS/CFT correspondence*, *Journal of High Energy Physics* **2009** (sep, 2009) 045–045, [arXiv:0906.4926].

[142] A. Castro, S. Detournay, N. Iqbal, and E. Perlmutter, *Holographic entanglement entropy and gravitational anomalies*, *Journal of High Energy Physics* **2014** (jul, 2014) [arXiv:1405.2792].

[143] T. Azeyanagi, R. Loganayagam, and G. S. Ng, *Holographic entanglement for chern-simons terms*, arXiv:1507.0229.

[144] N. Iqbal and A. C. Wall, *Anomalies of the entanglement entropy in chiral theories*, *Journal of High Energy Physics* **2016** (oct, 2016) [arXiv:1509.0432].

[145] S. Hellerman, D. Orlando, and M. Watanabe, *Quantum information theory of the gravitational anomaly*, arXiv:2101.0332.

[146] . Radič ević, *Entanglement entropy across the lattice-continuum correspondence*, *Modern Physics Letters B* **36** (apr, 2022) [arXiv:2207.0891].

[147] R. E. Peierls, *The commutation laws of relativistic field theory*, *Proceedings of the Royal Society of London. Series A. Mathematical and Physical Sciences* **214** (1952), no. 1117 143–157.

[148] D. Harlow and J.-q. Wu, *Algebra of diffeomorphism-invariant observables in Jackiw-Teitelboim gravity*, *JHEP* **05** (2022) 097, [arXiv:2108.0484].

[149] R. L. Arnowitt, S. Deser, and C. W. Misner, *The Dynamics of general relativity*, *Gen. Rel. Grav.* **40** (2008) 1997–2027, [gr-qc/0405109].

[150] R. M. Wald, *General relativity*. Chicago Univ. Press, Chicago, IL, 1984.

[151] S. Carroll, *Spacetime and Geometry*. Cambridge University Press, sep, 2019.

[152] S. Fischetti and D. Marolf, *Flowing funnels: heat sources for field theories and the $AdS_3$ dual of $CFT_2$ Hawking radiation*, *Classical and Quantum Gravity* **29** (apr, 2012) 105004, [arXiv:1202.5069].

[153] T. Ali, S. S. Haque, and J. Murugan, *Holographic entanglement entropy for gravitational anomaly in four dimensions*, *Journal of High Energy Physics* **2017** (mar, 2017) [arXiv:1611.0341].

[154] J. Held, M. Kaplan, D. Marolf, and J. Wu, "The Action of the Entanglement Wedge Cross Section." to appear.

[155] W. Donnelly, B. Michel, D. Marolf, and J. Wien, *Living on the Edge: A Toy Model for Holographic Reconstruction of Algebras with Centers*, *JHEP* **04** (2017) 093, [arXiv:1611.0584].

[156] K. Umemoto and T. Takayanagi, *Entanglement of purification through holographic duality*, *Nature Physics* **14** (mar, 2018) 573–577, [arXiv:1708.0939].

[157] P. Nguyen, T. Devakul, M. G. Halbasch, M. P. Zaletel, and B. Swingle, *Entanglement of purification: from spin chains to holography*, *Journal of High Energy Physics* **2018** (jan, 2018) [arXiv:1709.0742].

[158] S. Dutta and T. Faulkner, *A canonical purification for the entanglement wedge cross-section*, arXiv:1905.0057.

[159] C. Akers and P. Rath, *Entanglement wedge cross sections require tripartite entanglement*, *Journal of High Energy Physics* **2020** (apr, 2020) [arXiv:1911.0785].

[160] C. Akers, T. Faulkner, S. Lin, and P. Rath, *Reflected entropy in random tensor networks*, *Journal of High Energy Physics* **2022** (may, 2022) [arXiv:2112.0912].

[161] W. Z. Chua and Y. Jiang, *Hartle-Hawking state and its factorization in 3d gravity*, arXiv:2309.0512.

[162] P. Caputa, M. Miyaji, T. Takayanagi, and K. Umemoto, *Holographic entanglement of purification from conformal field theories*, *Physical Review Letters* **122** (mar, 2019) [arXiv:1812.0526].

[163] B. S. DeWitt, *The quantization of geometry*, in *Gravitation: An introduction to current research* (L. Witten, ed.), (New York, NY), Wiley, 1962.

[164] B. S. DeWitt, *Quantum Theory of Gravity. 1. The Canonical Theory*, *Phys. Rev.* **160** (1967) 1113–1148.

[165] T. Banks, *T C P, Quantum Gravity, the Cosmological Constant and All That...*, *Nucl. Phys. B* **249** (1985) 332–360.

[166] J. B. Hartle, *Prediction in Quantum Cosmology*, *NATO Sci. Ser. B* **156** (1987) 329–360.

[167] C. Rovelli, *Quantum mechanics without time: a model*, *Phys. Rev. D* **42** (1990) 2638–2646.

[168] C. Rovelli, *Quantum reference systems*, *Class. Quant. Grav.* **8** (1991) 317–332.

[169] C. Kiefer, *The Semiclassical approximation to quantum gravity*, *Lect. Notes Phys.* **434** (1994) 170–212, [gr-qc/9312015].

[170] D. Marolf, *Almost ideal clocks in quantum cosmology: A Brief derivation of time*, *Class. Quant. Grav.* **12** (1995) 2469–2486, [gr-qc/9412016].

[171] D. Marolf, *Comments on Microcausality, Chaos, and Gravitational Observables*, *Class. Quant. Grav.* **32** (2015), no. 24 245003, [arXiv:1508.0093].

[172] G. Penington and E. Witten, *Algebras and States in JT Gravity*, arXiv:2301.0725.

[173] D. Marolf, *Quantum observables and recollapsing dynamics*, *Class. Quant. Grav.* **12** (1995) 1199–1220, [gr-qc/9404053].

[174] D. Marolf, *Observables and a Hilbert space for Bianchi IX*, *Class. Quant. Grav.* **12** (1995) 1441–1454, [gr-qc/9409049].

[175] Y. Aharonov and L. Susskind, *Charge Superselection Rule*, *Phys. Rev.* **155** (1967) 1428–1431.

[176] Y. Aharonov and T. Kaufherr, *Quantum frames of reference*, *Phys. Rev. D* **30** (1984) 368–385.

[177] L. Loveridge, T. Miyadera, and P. Busch, *Symmetry, Reference Frames, and Relational Quantities in Quantum Mechanics*, *Found. Phys.* **48** (2018), no. 2 135–198, [arXiv:1703.1043].

[178] P. A. Hoehn, A. R. H. Smith, and M. P. E. Lock, *Trinity of relational quantum dynamics*, *Phys. Rev. D* **104** (2021), no. 6 066001, [arXiv:1912.0003].

[179] C. J. Fewster, D. W. Janssen, L. D. Loveridge, K. Rejzner, and J. Waldron, *Quantum reference frames, measurement schemes and the type of local algebras in quantum field theory*, arXiv:2403.1197.

[180] J. De Vuyst, S. Eccles, P. A. Hoehn, and J. Kirklin, *Gravitational entropy is observer-dependent*, arXiv:2405.0011.

[181] A. Higuchi, *Quantum linearization instabilities of de Sitter space-time. 1*, *Class. Quant. Grav.* **8** (1991) 1961–1981.

[182] A. Higuchi, *Quantum linearization instabilities of de Sitter space-time. 2*, *Class. Quant. Grav.* **8** (1991) 1983–2004.

[183] S. Deser and D. Brill, *Instability of Closed Spaces in General Relativity*, *Commun. Math. Phys.* **32** (1973) 291.

[184] V. Moncrief, *Space-Time Symmetries and Linearization Stability of the Einstein Equations. 1.*, *J. Math. Phys.* **16** (1975) 493.

[185] V. Moncrief, *Space-Time Symmetries and Linearization Stability of the Einstein Equations. 2.*, *J. Math. Phys.* **17** (1976) 1893–1902.

[186] J. Arms, *Linearization stability of the Einstein–Maxwell system*, *J. Math. Phys.* **18** (1977) 830.

[187] J. M. Arms, *Linearization Stability of Gravitational and Gauge Fields*, *J. Math. Phys.* **20** (1979) 443–453.

[188] D. Marolf, *The Spectral analysis inner product for quantum gravity*, in *7th Marcel Grossmann Meeting on General Relativity (MG 7)*, pp. 851–853, 9, 1994. gr-qc/9409036.

[189] A. Ashtekar, J. Lewandowski, D. Marolf, J. Mourao, and T. Thiemann, *Quantization of diffeomorphism invariant theories of connections with local degrees of freedom*, *J. Math. Phys.* **36** (1995) 6456–6493, [gr-qc/9504018].

[190] D. Giulini and D. Marolf, *On the generality of refined algebraic quantization*, *Class. Quant. Grav.* **16** (1999) 2479–2488, [gr-qc/9812024].

[191] D. Marolf, *Group averaging and refined algebraic quantization: Where are we now?*, in *9th Marcel Grossmann Meeting on Recent Developments in Theoretical and Experimental General Relativity, Gravitation and Relativistic Field Theories (MG 9)*, 7, 2000. gr-qc/0011112.

[192] D. Marolf, *Path integrals and instantons in quantum gravity: Minisuperspace models*, *Phys. Rev. D* **53** (1996) 6979–6990, [gr-qc/9602019].

[193] R. F. Streater and A. S. Wightman, *PCT, spin and statistics, and all that.* 1989.

[194] N. Y. Vilenken and A. U. Klimyk, *Representations of Lie Groups and Special Functions*, vol. 1-3. Dordrecht: Kluwer Acad. Publ, 1991-1993.

[195] M. K. F. Wong, *Unitary representations of so(n,1)*, *J. Math. Phys.* **15** (1974) 25–30.

[196] Z. Sun, *A note on the representations of* $SO(1, d + 1)$, arXiv:2111.0459.

[197] D. Marolf and I. A. Morrison, *Group averaging for de sitter free fields*, *Classical and Quantum Gravity* **26** (Oct., 2009) 235003, [arXiv:0810.5163].

[198] S. Gao and R. M. Wald, *Theorems on gravitational time delay and related issues*, *Class. Quant. Grav.* **17** (2000) 4999–5008, [gr-qc/0007021].

[199] P. C. Aichelburg and R. U. Sexl, *On the Gravitational field of a massless particle*, *Gen. Rel. Grav.* **2** (1971) 303–312.

[200] J. J. Halliwell and J. B. Hartle, *Wave functions constructed from an invariant sum over histories satisfy constraints*, *Phys. Rev. D* **43** (1991) 1170–1194.

[201] M. P. Reisenberger and C. Rovelli, *'Sum over surfaces' form of loop quantum gravity*, *Phys. Rev. D* **56** (1997) 3490–3508, [gr-qc/9612035].

[202] D. Marolf and H. Maxfield, *Transcending the ensemble: baby universes, spacetime wormholes, and the order and disorder of black hole information*, *JHEP* **08** (2020) 044, [arXiv:2002.0895].

[203] A. Higuchi, D. Marolf, and I. A. Morrison, *de Sitter invariance of the dS graviton vacuum*, *Class. Quant. Grav.* **28** (2011) 245012, [arXiv:1107.2712].

[204] D. Seery, *Infrared effects in inflationary correlation functions*, *Classical and Quantum Gravity* **27** (May, 2010) 124005, [arXiv:1005.1649].

[205] A. Linde, *Particle Physics and Inflationary Cosmology*. 2005.

[206] S. B. Giddings and M. S. Sloth, *Cosmological observables, infrared growth of fluctuations, and scale-dependent anisotropies*, *Physical Review D* **84** (Sept., 2011) [arXiv:1104.0002].

[207] D. Giulini and D. Marolf, *A uniqueness theorem for constraint quantization*, *Classical and Quantum Gravity* **16** (Jan., 1999) 2489–2505, [9902045].

[208] D. Marolf and I. A. Morrison, *The IR stability of de Sitter: Loop corrections to scalar propagators*, *Phys. Rev. D* **82** (2010) 105032, [arXiv:1006.0035].

[209] D. Marolf and I. A. Morrison, *Group averaging of massless scalar fields in 1 + 1 de sitter*, *Classical and Quantum Gravity* **26** (Jan., 2009) 035001, [arXiv:0808.2174].